



# **EXTRACTION OF SULPHUR COMPOUNDS FROM MODEL FUELS WITH USE OF IONIC LIQUIDS**

By

**Marcin Hubert Durski**

(BSc. Eng. in Chemical Technology, Warsaw University of Technology,  
MSc. Eng. in Chemical Technology, Warsaw University of Technology)

**Submitted in fulfilment of the academic requirements for the degree of  
Doctor of Philosophy in Engineering to the School of Engineering, Discipline  
of Chemical Engineering**

**University of KwaZulu-Natal  
Durban**

November 2020

**Supervisor:** Prof. Paramespri Naidoo

**Co-supervisors:** Prof. Urszula Domańska-Żelazna and Prof. Deresh Ramjugernath

## PREFACE

The investigation or study presented in this thesis entitled “Extraction of sulphur compounds from model fuels with use of ionic liquids” was undertaken at the University of KwaZulu-Natal in the School of Engineering, Howard College Campus, Durban, South Africa. The duration of the study was from October 2016 to October 2020. The study was supervised by Prof. Paramespri Naidoo and co-supervised by Prof. Urszula Domańska-Żelazna and Prof. Deresh Ramjugernath.

This thesis has been submitted as the full requirement for the award of the Doctor of Philosophy (PhD) degree in Chemical Engineering. The study presented in this thesis is my original work, unless otherwise stated.

The thesis has not been submitted before for degree or examination at any other tertiary institute or university.

As the candidate’s supervisor, I, Prof. Paramespri Naidoo, agree to the submission of this thesis.

30-NOV-2020

---

Prof. Paramespri Naidoo

---

Date

As the candidate’s co-supervisor, I, Prof. Urszula Domańska-Żelazna, agree to the submission of this thesis.

30.11.2020

---

Prof. Urszula Domańska-Żelazna

---

Date

As the candidate’s co-supervisor, I, Prof. Deresh Ramjugernath, agree to the submission of this thesis.

30/11/2020

---

Prof. Deresh Ramjugernath

---

Date

## DECLARATION 1 – PLAGIARISM

I, Marcin Hubert Durski, student number 216076949 declare that:

The reported research project is my original research work.

- i. This thesis has not been submitted for any degree or examination at any other university before.
- ii. All the data such as pictures, graphs or any other information presented in this dissertation, has been acknowledged as being sourced from other persons, except in a case where it is my original work.
- iii. All the graphs, tables or text copied and pasted from the Internet, has been acknowledged, and the referenced source in this thesis is presented in detail in the References section.
- iv. All the other persons' writing in this thesis has been referenced and acknowledged.
  - a. Their words have been re-written but the general information attributed to them has been referenced.
  - b. Where their exact words have been used, then their writing has been placed in italics and inside quotation marks and referenced.

Signed:

---

Marcin Hubert Durski

27.11.2020

---

Date

## DECLARATION 2 – PUBLICATIONS

DETAILS OF CONTRIBUTION TO PUBLICATIONS that form part and/or include research presented in this thesis (include publications in preparation, submitted, in press and published and give details of the contributions of each author to the experimental work and writing of each publication).

- Publication 1. Durski, M.; Naidoo, P.; Ramjugernath, D.; Domańska, U. „Thermodynamics and Activity Coefficients at Infinite Dilution for Organic Solutes in the Ionic Liquid 1-Butyl-1-Methylpyrrolidinium Dicyanamide”. *Fluid Phase Equilib.* **2018**, 473, 175–182. <https://doi.org/10.1016/j.fluid.2018.06.013>.
- Publication 2. Durski, M.; Naidoo, P.; Ramjugernath, D.; Domańska, U. Ternary Liquid-Liquid Phase Equilibria of {Ionic Liquid + Thiophene + (Octane/Hexadecane)}. *J. Chem. Thermodyn.* **2019**, 134, 157–163. <https://doi.org/10.1016/j.jct.2019.03.017>.
- Publication 3. Durski, M.; Naidoo, P.; Ramjugernath, D.; Domańska, U. „Separation of Thiophene from Octane/Hexadecane with Ionic Liquids in Ternary Liquid-Liquid Phase Equilibrium”. *Fluid Phase Equilib.* **2020**, 509, 112467. <https://doi.org/10.1016/j.fluid.2020.112467>.

Signed:

---

Marcin Hubert Durski

27.11.2020

---

Date

# Acknowledgments

I would like to take this opportunity to acknowledge and thank the following people who have made a tremendous contribution to this work:

- My supervisors: Professor Paramespri Naidoo, Professor Urszula Domańska-Żelazna and Professor Deresh Ramjugernath for their knowledge, guidance and support during the studies.
- SASOL Ltd. and National Research Foundation (NRF) for the financial support of this project.
- The help and advice of the Thermodynamics Research Unit's laboratory technician, Mr Ayanda Khanyile was greatly appreciated.
- My mother Cecylia, for many years of wholehearted support, encouragement, love and motivation.
- Fellow colleagues from Thermodynamics Research Unit (TRU) for making me feel at home in South Africa.

# Abstract

One of the most promising applications of ionic liquids in the modern chemical industry is its use as extractants in separation methods, primarily extraction and extractive distillation. Sulphur emissions are regulated widely by governments and international organisations, to ensure the lowest possible emission of sulphur oxides to the atmosphere, with many stipulations that the amount of sulphur compounds in the fuel must not exceed 10 ppm. This study focused on the screening of the potential extractants for the desulphurisation of the fuels by performing experimental measurements for five different ionic liquids via two-phase separation techniques, namely, gas-liquid chromatography (GLC) and liquid-liquid extraction (LLE) measurements. The 1-butyl-1-methylpyrrolidinium dicyanamide [BMPYR][DCA] was used as a solvent in a packed column during gas-liquid chromatography measurements of the retention times which allowed for the calculation of activity coefficients at infinite dilution. This technique was used to ensure coverage of the whole spectrum of the experimental methods and thermodynamic principles for assessing the suitability of ILs for the intended purpose.

Four ionic liquids: dihydroxyimidazolium bis{(trifluoromethyl)sulphonyl}imide [OHOHIM][NTf<sub>2</sub>], 1-butyl-3-methylimidazolium trifluoromethanesulphonate [BMIM][OTf], 1-butyl-1-methylpiperidinium dicyanamide [BMPIP][DCA] and tri-iso-butylmethylphosphonium tosylate [P<sup>-i4,i4,i4,1</sup>][TOS], were assessed via liquid-liquid equilibria measurements for suitability as extractants. Ternary LLE measurements for the systems {IL+thiophene+hydrocarbon} were performed, and the selectivity (*S*), distribution ratio ( $\beta$ ) and performance index (PI) of the ILs investigated in this work was compared to ILs reported in the literature. The LLE tielines were modelled using the Non-Random Two Liquid (NRTL) model, which showed a satisfactory correlation of the experimental data, with a maximum absolute average deviation of 0.01 in the mole fractions.

The most promising IL determined in this study is [BMIM][OTf] with PI equal to 54.8 and 193 for octane and hexadecane systems, respectively. This conforms with the findings in literature as imidazolium ILs with relatively short alkyl substituents as reported to be the most promising extractants in terms of performance index (PI). The

least promising results were obtained for [BMPIP][DCA]. Dicyanamide anion was not strongly represented in LLE literature, yet PIs calculated using activity coefficients data for ILs with this anion provided justification for further investigations. The recommendation from this work is that laboratory-scale extraction measurements be performed to assess the viability and reuse of this IL.

# Table of Contents

<b>PREFACE</b> .....	ii
<b>DECLARATION 1 – PLAGIARISM</b> .....	iii
<b>DECLARATION 2 – PUBLICATIONS</b> .....	iv
<b>Acknowledgments</b> .....	v
<b>Abstract</b> .....	vi
<b>Table of Figures</b> .....	x
<b>Table of Tables</b> .....	xiv
<b>Nomenclature</b> .....	xvi
<b>List of the abbreviations and the names of the mentioned ionic liquids</b> .....	xix
<b>Chapter 1 Introduction</b> .....	1
<b>Chapter 2 Literature review</b> .....	4
2.1 Ionic Liquids .....	4
2.2 ILs in green chemistry processes .....	7
2.3 Sulphur separation problems .....	10
2.4 ILs in extractive desulphurisation .....	11
<b>Chapter 3 Thermodynamic principles relating to solvent extraction studies</b> ....	34
3.1 Chemical potential.....	34
3.2 Liquid-liquid equilibria .....	35
3.2.1 The equilibrium state .....	35
3.2.2 Types of phase diagrams for ternary systems.....	38
3.3 Activity coefficients .....	41
3.3.1 Activity coefficients at infinite dilution $\gamma_{13}^{\infty}$ .....	41
3.4 LLE data regression or parameter fitting .....	43
3.5 Non-random two-liquid (NRTL) model.....	44
3.6 Data regression .....	47
3.7 Gas-Liquid Chromatography technique. ....	49
3.8 $\gamma_{13}^{\infty}$ via gas-liquid chromatography .....	51
<b>Chapter 4 Experimental method</b> .....	53
4.1 Activity coefficients at infinite dilution, $\gamma_{13}^{\infty}$ .....	53
4.1.1 Review of experimental methods .....	53
4.1.2 Review of the GLC method.....	57



4.1.3 Description of the apparatus .....	57
4.1.4 Methodology used in this study.....	58
4.2 Liquid-liquid equilibria .....	61
4.2.1 Review of experimental methods .....	61
4.2.2 Review of analytical methods .....	65
4.2.3 Methodology applied in this study .....	67
4.2.4 Equipment used in this study.....	68
4.2.5 Sample withdrawal .....	69
4.2.6 GC method.....	70
4.2.7 GC detector calibrations and calculation of the mole fractions.	71
4.2.8 Gas chromatograph operation.....	75
4.3 Safety gear.....	75
<b>Chapter 5 Results &amp; discussion.....</b>	<b>77</b>
5.1 Motivation for the ILs tested.....	77
5.2 Materials.....	79
5.3 Activity coefficients at infinite dilution, $\gamma_{13}^{\infty}$ .....	83
5.4 Liquid – liquid equilibria .....	95
5.5 Laboratory scale extraction studies .....	108
5.5.1 Operating parameters for the extraction study .....	108
5.5.2 Assessing the reuse of the solvent .....	112
5.6 Perspectives of the industrial desulphurisation process using ILs ..	113
<b>Chapter 6 Conclusions .....</b>	<b>118</b>
<b>Chapter 7 Recommendations .....</b>	<b>120</b>
<b>References.....</b>	<b>121</b>
<b>Appendix A.....</b>	<b>138</b>
<b>Appendix B .....</b>	<b>139</b>
<b>Appendix C.....</b>	<b>141</b>
<b>Appendix D.....</b>	<b>143</b>

# Table of Figures

<b>Fig. 2-1</b> Examples of cations used in the synthesis of ionic liquids: Im, imidazolium, Py, pyridinium, Quin, quinolinium, Mor, morpholinium, Pip, piperidinium, Pyr, pyrrolidinium, N, ammonium, and P, phosphonium (compiled in this work).....	5
<b>Fig. 2-2</b> Examples of anions used in the synthesis of ionic liquids: bis(trifluoromethanesulphonyl)imide, trifluoromethanesulphonate, borate, tetrafluoroborate, hexafluorophosphate, dicyanamide, nitrate, chloride, methanesulphonate, tosylate, thiocyanate and methylsulphate (compiled in this work)..	6
<b>Fig. 2-3</b> Structure of the thiophene in the ionic liquid [BMIM][SCN] proposed by Revelli et al. [ <sup>119</sup> ]. .....	26
<b>Fig. 3-1</b> Graphical representation of the transition of the N-component system from the unstable initial state to the equilibrium state, associated with achieving the minimum Gibbs free energy [ <sup>160</sup> ]. .....	36
<b>Fig. 3-2</b> Classification of liquid-liquid phase diagrams in ternary systems, according to Weinstock [ <sup>162</sup> ]. Light grey and dark grey areas indicate areas of limited miscibility in a two-phase and three-phase system, respectively. ....	39
<b>Fig. 3-3</b> Example of an experimental ternary diagram with visible tie-lines [ <sup>164</sup> ]. .....	40
<b>Fig. 3-4</b> Flow diagram of the NRTL parameter fitting method. ....	48
<b>Fig. 4-1</b> Schematic representation of the NSGLC method. A is the injection port, B is the GC column, C is the TCD detector and D is a recorder [ <sup>181</sup> ]. .....	54
<b>Fig. 4-2</b> Schematic of the dilutor cell [ <sup>183</sup> ]. .....	55
<b>Fig. 4-3</b> Schematic of the Świętosławski ebulliometer. A – reflux condenser, B – dropper, C – thermometer nest, D- bubble, E – heated tank, F – drain valve [ <sup>193</sup> ]. ....	56
<b>Fig. 4-4</b> Schematic of the gas-liquid chromatography setup used for measurements. ...	58
<b>Fig. 4-5</b> Schematic of the apparatus used for mutual solubility measurements with laser-light scattering technique [ <sup>206</sup> ]. A – equilibrium cell, B – stirring element, C – light sensor, D – magnetic stirrer, E – optical system, F – thermometer, G – digital multimeter, H – computer. ....	62
<b>Fig. 4-6</b> Diagram of Ndlovu's LLE cell [ <sup>207</sup> ]. A – sample point for denser liquid phase, B – temperature sensor in a thermo-well, C – heating medium inlet, D – heating medium outlet, E – Teflon coated bar, F – sample point for lighter liquid phase, G – stirrer driven by DC motor. ....	63
<b>Fig. 4-7</b> Diagram of a single measuring 10 ccm cell with a water jacket, height of the cell is 68 mm, and the external diameter is 28 mm. ....	64
<b>Fig. 4-8</b> Diagram of modified Ndlovu's cell used in TRU by Narasigadu et al. [ <sup>209</sup> ]. A – sample point for denser liquid phase, B – temperature sensor in a thermo-well, C – heating medium inlet, D – heating medium outlet, E – Teflon coated magnetic agitator, F – sample point for the lighter liquid phase. ....	65
<b>Fig. 4-9</b> Block diagram of the HPLC apparatus with UV and refractometer detectors [ <sup>212</sup> ]. .....	66
<b>Fig. 4-10</b> Schematic of the equilibration setup used during the preparation of the LLE data samples. ....	69

<b>Fig. 4-11</b> Schematic of gas chromatography setup used for liquid-liquid equilibrium measurements.....	69
<b>Fig. 4-12</b> GC FID detector calibration curve. The ratio of ( $A_{\text{thiophene}}/A_{\text{standard}}$ ) correlated with the respective mass ratio. For each sample, three separate measurements (marked as ●, ▲ and ■, respectively) were carried out. The average value of ratios (○) for each sample was used to establish the calibration curve linear equation $y = 0.9482x$ with coefficient of determination $R^2 = 0.9997$ .....	72
<b>Fig. 4-13</b> Residuals for the calibration of the GC FID detector for thiophene calibration. The standard error for the calibration was 0.001. ....	72
<b>Fig. 4-14</b> GC FID detector calibration curve. The ratio of ( $A_{\text{octane}}/A_{\text{standard}}$ ) correlated with the respective mass ratio. For each sample, three separate measurements (marked as ●, ▲ and ■, respectively) were carried out. The average value of ratios (○) for each sample was used to establish the calibration curve linear equation $y = 0.64396x$ with coefficient of determination $R^2 = 0.99986$ . ....	73
<b>Fig. 4-15</b> Residuals for the calibration of the GC FID detector for octane calibration. The standard error for the calibration was 0.004. ....	73
<b>Fig. 4-16</b> GC FID detector calibration curve. The ratio of ( $A_{\text{hexadecane}}/A_{\text{standard}}$ ) correlated with the respective mass ratio. For each sample, three separate measurements (marked as ●, ▲ and ■, respectively) were carried out. The average value of ratios (○) for each sample was used to establish the calibration curve linear equation $y = 0.4818x$ with coefficient of determination $R^2 = 0.99980$ .....	74
<b>Fig. 4-17</b> Residuals for the calibration of the GC FID detector for hexadecane calibration. The standard error for the calibration was 0.005. ....	74
<b>Fig. 5-1</b> Plot of $\ln(\gamma_{13}^{\infty})$ for ionic liquid [BMPYR][DCA] versus $1000/T$ for the solutes: (◇) heptane; (○) octane; (+) nonane; (●) hexene; (■) cyclohexene; (▲) heptene; (◆) octene; (*) decene; (Δ) hexyne; (□) heptyne.; (×) octyne. ....	88
<b>Fig. 5-2</b> Plot of $\ln(\gamma_{13}^{\infty})$ for ionic liquid [BMPYR][DCA] versus $1000/T$ for the solutes: (●) benzene; (◆) toluene; (▲) ethylbenzene; (Δ) o-xylene; (□) m-xylene; (○) p-xylene; (×) styrene; (*) α-methylstyrene. ....	89
<b>Fig. 5-3</b> Plot of $\ln(\gamma_{13}^{\infty})$ for ionic liquid [BMPYR][DCA] versus $1000/T$ for the solutes: (●) methanol; (◆) ethanol; (▲) 1-propanol; (■) 2-propanol; (○) 1-butanol; (◇) 2-butanol; (Δ) 2-methyl-1-propanol. ....	90
<b>Fig. 5-4</b> Plot of $\ln(\gamma_{13}^{\infty})$ for ionic liquid [BMPYR][DCA] versus $1000/T$ for the solutes: (●) methyl tert-butyl ether; (■) methyl tert-propyl ether; (▲) ethyl tert-butyl ether; (○) dipropyl ether; (□) di-iso-propyl ether; (Δ) dibutyl ether. ....	91
<b>Fig. 5-5</b> Plot of $\ln(\gamma_{13}^{\infty})$ for ionic liquid [BMPYR][DCA] versus $1000/T$ for the solutes: (●) acetone; (◆) 2-pentanone; (▲) 3-pentanone; (Δ) methyl propionate; (○) methyl butyrate; (◇) ethyl acetate; (×) propionaldehyde; (*) butyraldehyde. ....	92
<b>Fig. 5-6</b> Plot of the experimental versus calculated LLE data for the ternary system {[OHOHIM][NTf <sub>2</sub> ] (1) + thiophene (2) + octane (3)} in mole fractions at $T = 308.15$ K and $P = 101$ kPa. ●, Exp: black solid lines; ▲, NRTL Model: red solid lines. ....	98

<b>Fig. 5-7</b> Plot of the experimental versus calculated LLE data for the ternary system {[BMIM][OTf] (1) + thiophene (2) + octane (3)} in mole fractions at T = 308.15 K and P = 101 kPa. ●, Exp: black solid lines; ▲, NRTL Model: red solid lines. ....	99
<b>Fig. 5-8</b> Plot of the experimental versus calculated LLE data for the ternary system {[BMPIP][DCA] (1) + thiophene (2) + octane (3)} in mole fractions at T = 308.15 K and P = 101 kPa. ●, Exp: black solid lines; ▲, NRTL Model: red solid lines. ....	100
<b>Fig. 5-9</b> Plot of the experimental versus calculated LLE data for the ternary system {[P <sub>i4,i4,i4,1</sub> ][TOS] (1) + thiophene (2) + octane (3)} in mole fractions at T = 308.15 K and P = 101 kPa. ●, Exp: black solid lines; ▲, NRTL Model: red solid lines. ....	101
<b>Fig. 5-10</b> Plot of the experimental versus calculated LLE data for the ternary system {[OHOHIM][NTf <sub>2</sub> ] (1) + thiophene (2) + hexadecane (3)} in mole fractions at T = 308.15 K and P = 101 kPa. ●, Exp: black solid lines; ▲, NRTL Model: red solid lines.....	102
<b>Fig. 5-11</b> Plot of the experimental versus calculated LLE data for the ternary system {[BMIM][OTf] (1) + thiophene (2) + hexadecane (3)} in mole fractions at T = 308.15 K and P = 101 kPa. ●, Exp: black solid lines; ▲, NRTL Model: red solid lines. ....	103
<b>Fig. 5-12</b> Plot of the experimental versus calculated LLE data for the ternary system {[BMPIP][DCA] (1) + thiophene (2) + hexadecane (3)} in mole fractions at T = 308.15 K and P = 101 kPa. ●, Exp: black solid lines; ▲, NRTL Model: red solid lines.....	104
<b>Fig. 5-13</b> Plot of the experimental versus calculated LLE data for the ternary system {[P <sub>i4,i4,i4,1</sub> ][TOS] (1) + thiophene (2) + hexadecane (3)} in mole fractions at T = 308.15 K and P = 101 kPa. ●, Exp: black solid lines; ▲, NRTL Model: red solid lines. ....	105
<b>Fig. 5-14</b> GC FID detector calibration curve. The ratio of ( $A_{\text{hexadecane}}/A_{\text{standard}}$ ) correlated with the respective mass ratio. For each sample, three separate measurements (marked as ●, ▲ and ■, respectively) were carried out. The average value of ratios (○) for each sample was used to establish the calibration curve linear equation $y = 0.4887x$ with coefficient of determination $R^2 = 0.99979$ .....	108
<b>Fig. 5-15</b> Residuals for the calibration of the GC FID detector for hexadecane calibration. The standard error for the calibration was 0.005. ....	109
<b>Fig. 5-16</b> GC FID detector calibration curve. The ratio of ( $A_{\text{thiophene}}/A_{\text{standard}}$ ) correlated with the respective mass ratio. For each sample, three separate measurements (marked as ●, ▲ and ■, respectively) were carried out. The average value of ratios (○) for each sample was used to establish the calibration curve linear equation $y = 0.96648x$ with coefficient of determination $R^2 = 0.99983$ .....	109
<b>Fig. 5-17</b> Residuals for the calibration of the GC FID detector for thiophene calibration. The standard error for the calibration was 0.003. ....	110
<b>Fig. 5-18</b> Percent removal of S-compound in laboratory-scale EDS for {[P <sub>i4,i4,i4,1</sub> ][TOS] + thiophene + hexadecane} system in the range of the temperatures and time (equal stirring and settling time); ● T = 298.15 K; ■ T = 308.15 K; ▲ T = 318.15 K.....	111
<b>Fig. 5-19</b> Graphical representation of the % removal of thiophene from hexadecane model fuel for the EDS process at T = 308.15 K and P = 101 kPa. ....	112
<b>Fig. 5-20</b> Schematic of the mixer-settler [ <sup>235</sup> ].....	115
<b>Fig. 5-21</b> Schematic of the extraction column with the light phase dispersed in heavy phase. ....	116

<b>Fig. B-1</b> Calibration curve for the temperature probe 1 used during the LLE measurements. The calibration curve linear equation is $y = 1.0021x + 0.3223$ with coefficient of determination $R^2 = 1$ .....	139
<b>Fig. B-2</b> Residuals for the calibration of the temperature probe calibration. The standard error for the calibration was 0.005.....	139
<b>Fig. B-3</b> Calibration curve for the temperature probe 2 used during the LLE measurements. The calibration curve linear equation is $y = 1.0014x + 0.234$ with coefficient of determination $R^2 = 0.9999$ .....	140
<b>Fig. B-4</b> Residuals for the calibration of the temperature probe calibration. The standard error for the calibration was 0.005.....	140
<b>Fig. C-1</b> Plot of the molar fraction of heptane ( $x_1$ ) versus T/K for {heptane (1) + methanol(2)} binary system – methanol rich phase. ● Experiment 1; ♦ Experiment 2; ▲ Matsuda [227], ■ Narasigadu [224], × Casas [225]. .....	141
<b>Fig. C-2</b> Plot of the molar fraction of heptane ( $x_1$ ) versus T/K for {heptane (1) + methanol(2)} binary system – heptane rich phase. ● Experiment 1; ♦ Experiment 2; ▲ Matsuda [227], ■ Narasigadu [224], × Casas [225]. .....	142

# Table of Tables

<b>Table 2-1</b> A summary of results from previous related literature for activity coefficient at infinite dilution systems: temperature (T), selectivity (S) and solute distribution ratio ( $\beta$ ) of thiophene and performance index (PI) calculated by the use of the literature $\gamma^\infty$ data.....	13
<b>Table 2-2</b> A summary of results from literature for {IL + thiophene + hydrocarbon} LLE systems: temperature (T), average selectivity ( $S_{Av}$ ) and average solute distribution ratio ( $\beta_{Av}$ ) of thiophene, performance index (PI), and reported standard uncertainty (u(x)). .	23
<b>Table 2-3</b> A summary of results from literature for {IL + benzothiophene + hydrocarbon} LLE systems: temperature (T), average selectivity ( $S_{Av}$ ) and average solute distribution ratio ( $\beta_{Av}$ ) of a benzothiophene, performance index (PI), and reported standard uncertainty (u(x)). .....	27
<b>Table 2-4</b> A summary of results from literature for {LLE + dibenzothiophene + hexadecane} systems: temperature (T), average selectivity ( $S_{Av}$ ) and average solute distribution ratio ( $\beta_{Av}$ ) of a dibenzothiophene, performance index (PI), and reported standard uncertainty (u(x)).....	28
<b>Table 2-5</b> A summary of laboratory-scale extraction literature data. Columns T/%, BT/% and DBT% shows the percentage of thiophene, benzothiophene and dibenzothiophene removed from the initial model fuel composition, respectively. Table sorted according to the percentage of thiophene removed. ....	30
<b>Table 4-1</b> Gas chromatograph operational conditions for compositional analysis of the equilibrium phases. ....	70
<b>Table 5-1</b> The sources and mass fraction purities of materials used during measurements of activity coefficients at infinite dilution $\gamma_{13}^\infty$ . ....	79
<b>Table 5-2</b> Properties of the ionic liquids investigated: structure, name, abbreviation of name, supplier, CAS number, molar mass (M), mass fraction purity (as stated by the supplier) and purification method. ....	81
<b>Table 5-3</b> Properties and purity of the original materials used in the LLE study. ....	82
<b>Table 5-4</b> The experimental activity coefficients at infinite dilution $\gamma_{13}^\infty$ for the solutes in ionic liquid [BMPYR][DCA] at different temperatures. ....	84
<b>Table 5-5</b> Limiting partial molar excess enthalpies $\Delta H_1^{E,\infty}$ Gibbs energies, $\Delta G_1^{E,\infty}$ , and entropies $T_{ref}\Delta S_1^{E,\infty}$ for the solutes in [BMPYR][DCA] at the reference temperature $T_{ref} = 358.15$ K. ....	86
<b>Table 5-6</b> The experimental (gas + liquid) partition coefficients, $K_L$ for the solutes in ionic liquid [BMPYR] [DCA] at different temperatures. <sup>a</sup> .....	87
<b>Table 5-7</b> Selectivities (S) and partition coefficients ( $\beta$ ) for heptane/benzene, thiophene/heptane, heptane/heptyne and .....	94
<b>Table 5-8</b> A summary of the LLE results for {IL + thiophene + hydrocarbon} systems: T is temperature, S and $\beta$ are average selectivity and average solute distribution ratio of the sulphur compound, respectively, PI is the performance index, and u(x) is reported standard uncertainties <sup>a</sup> . ....	96

<b>Table 5-9</b> Compositions of experimental tie-lines in mole fractions, selectivity, S and distribution ratios, $\beta$ for the ternary system {[OHOHIM][NTf <sub>2</sub> ] (1) + thiophene (2) + octane (3)} at T = 308.15 K and P = 101 kPa <sup>a</sup> .....	98
<b>Table 5-10</b> Compositions of experimental tie lines in mole fractions, selectivity, S and solute distribution ratios, $\beta$ for the ternary system {[BMIM][OTf] (1) + thiophene (2) + octane (3)} at T = 308.15 K and P = 101 kPa <sup>a</sup> .....	99
<b>Table 5-11</b> Compositions of experimental tie lines in mole fractions, selectivity, S and solute distribution ratios, $\beta$ for the ternary system {[BMPIP][DCA] (1) + thiophene (2) + octane (3)} at T = 308.15 K and P = 101 kPa <sup>a</sup> .....	100
<b>Table 5-12</b> Compositions of experimental tie lines in mole fractions, selectivity, S and solute distribution ratios, $\beta$ for the ternary systems {[P <sub>-i4,i4,i4,1</sub> ][TOS] (1) + thiophene (2) + octane (3)} at T = 308.15 K and P = 101 kPa <sup>a</sup> .....	101
<b>Table 5-13</b> Compositions of experimental tie lines in mole fractions, selectivity, S and solute distribution ratios, $\beta$ for the ternary system {[OHOHIM][NTf <sub>2</sub> ] (1) + thiophene (2) + hexadecane (3)} at T = 308.15 K and P = 101 kPa <sup>a</sup> .....	102
<b>Table 5-14</b> Compositions of experimental tie lines in mole fractions, selectivity, S and solute distribution ratios, $\beta$ for the ternary system {[BMIM][OTf] (1) + thiophene (2) + hexadecane (3)} at T = 308.15 K and P = 101 kPa <sup>a</sup> .....	103
<b>Table 5-15</b> Compositions of experimental tie lines in mole fractions, selectivity, S and solute distribution ratios, $\beta$ for the ternary system {[BMPIP][DCA] (1) + thiophene (2) + hexadecane (3)} at T = 308.15 K and P = 101 kPa <sup>a</sup> .....	104
<b>Table 5-16</b> Compositions of experimental tie lines in mole fractions, selectivity, S and solute distribution ratios, $\beta$ for the ternary systems {[P <sub>-i4,i4,i4,1</sub> ][TOS] (1) + thiophene (2) + hexadecane (3)} at T = 308.15 K and P = 101 kPa <sup>a</sup> .....	105
<b>Table 5-17</b> NRTL model regression results for the ternary systems {[OHOHIM][NTf <sub>2</sub> ], [BMIM][OTf], [BMPIP][DCA], [P <sub>i4,i4,i4,1</sub> ][TOS] (1) + thiophene (2) + octane/hexadecane (3)} at T= 308.15 K and P = 101 kPa.....	107
<b>Table 5-18</b> Percent removal of S-compound in laboratory-scale EDS for {[P <sub>-i4,i4,i4,1</sub> ][TOS] + thiophene + hexadecane} system in the different temperatures and time (equal stirring and settling time) <sup>a</sup> .....	110
<b>Table A-1</b> The literature and the experimental activity coefficients at infinite dilution $\gamma_{13}^{\infty}$ for the solutes in hexadecane at different temperatures - test system.....	138
<b>Table D-1</b> Standard uncertainties estimations.....	143

# Nomenclature

## Symbols

$B_{11}$	second virial coefficient/ $\text{m}^3\text{mol}^{-1}$
$B_{12}$	mixed second virial coefficient/ $\text{m}^3\text{mol}^{-1}$
$f$	fugacity
$g_{ij}$	Gibbs energy of interaction between components of the mixture
$G_i^E$	excess Gibbs energy for the component $i$
$J_2^3$	pressure correction term
$k$	number of tie-lines
$k_j^\infty$	capacity coefficient
$n$	number of experimental points
$n_3$	number of moles of the solvent
$P$	the set of parameters
$P$	pressure/kPa
$P_0$	outlet pressure/kPa
$P_{in}$	inlet pressure/kPa
$P_0 J_2^3$	mean column pressure/kPa
$P_1^*$	saturated vapour pressure of the solute/kPa
$R$	gas constant/ $\text{J K}^{-1}\text{mol}^{-1}$
$S$	selectivity
$S_{ij}^\infty$	selectivity at infinite dilution
$t_G$	retention time for an unretained gas/s
$t_R$	retention time for the solute/s



$T$	temperature
$T$	equilibrium temperature/K
$T_c$	critical temperature/K
$u(P)$	estimated error of the pressure/kPa
$u(S)$	estimated error of the selectivity
$u(T)$	estimated error of the temperature/K
$u(\beta)$	estimated error of the partition coefficient
$u(\gamma_{13}^\infty)$	estimated error of the activity coefficient at infinite dilution/%
$U_{ii}$	interaction energy between particles of this same compound for UNIFAC model
$U_{ij}$	interaction energy between particles of different compounds for UNIFAC model
$U_o$	column outlet flow rate
$V_c$	critical volume/m <sup>3</sup> mol <sup>-1</sup>
$V_N$	retention volume of the solute/m <sup>3</sup> mol <sup>-1</sup>
$V_1^*$	molar volume of the solute/m <sup>3</sup> mol <sup>-1</sup>
$V_1^\infty$	partial molar volume of the solute at infinite dilution/m <sup>3</sup> mol <sup>-1</sup>
$x$	mole fraction
$\mathbf{x}^I, \mathbf{x}^{II}$	vector of molar fractions in phase I and phase II
$\mathbf{z}$	vector of molar fractions

### **Greek letters**

$\alpha_{ij}$	non-randomness parameter of NRTL model
$\beta$	partition coefficient
$\gamma_i$	activity coefficient of $i$ -th component

$\gamma_{13}^{\infty}$	activity coefficient at infinite dilution
$\delta$	relative amount of selected phase
$\mu_i^I, \mu_i^{II}$	chemical potential of the $i$ -th component
$\hat{\mu}_i^*$	chemical potential of the $i$ -th component in the mixture
$\tau_{12}, \tau_{21}$	NRTL model binary interaction parameters
$\varphi$	fugacity coefficient

### Subscript

$i, j$	components
1, 2, 3	components of the mixture
$i, l, m$	component, phase and tie-line

### Superscript

calc	calculated value
exp	experimental value
I, II	phases
*	ideal state
o	initial state

## List of the abbreviations and the names of the mentioned ionic liquids

[(MOH) <sub>2</sub> IM][NTf <sub>2</sub> ]	1,3-di(2-methoxyhexyl)imidazolium bis{(trifluoromethyl)sulphonyl}imide
[AMIM][DCA]	1-allyl-3-methylimidazolium dicyanamide
[AMIM][NTf <sub>2</sub> ]	1-allyl-3-methylimidazolium bis{(trifluoromethyl)sulphonyl}imide
[B(CN)(3)PY][NTf <sub>2</sub> ]	1-butyl-3-cyanopyridinium bis{(trifluoromethyl)sulphonyl}imide
[B(CN)(4)PY][NTf <sub>2</sub> ]	1-butyl-4-cyanopyridinium bis{(trifluoromethyl)sulphonyl}imide
[BM(3)PY][DCA]	1-butyl-3-methylpyridinium dicyanamide
[BM(3)PY][OTf]	1-butyl-3-methylpyridinium trifluoromethanesulfonate
[BM(4)PY][DCA]	1-butyl-4-methylpyridinium dicyanamide
[BM(4)PY][NTf <sub>2</sub> ]	1-butyl-3-pyridinium bis{(trifluoromethyl)sulphonyl}imide
[BM(4)PY][SCN]	1-butyl-4-methylpyridinium thiocyanate
[BMIM][BF <sub>4</sub> ]	1-butyl-3-methylimidazolium tetrafluoroborate
[BMIM][Br]	1-butyl-3-methylimidazolium bromide
[BMIM][Cl]	1-butyl-3-methylimidazolium chloride
[BMIM][DCA]	1-butyl-3-methylimidazolium dicyanamide
[BMIM][DCNM]	1-butyl-3-methylimidazolium dicyano(nitroso)methanide
[BMIM][HSO <sub>4</sub> ]	1-butyl-3-methylimidazolium hydrosulphate
[BMIM][MeSO <sub>4</sub> ]	1-butyl-3-methylimidazolium methylsulfate

[BMIM][NO <sub>3</sub> ]	1-ethyl-3-methylimidazolium nitrate
[BMIM][NTf <sub>2</sub> ]	1-butyl-3-methylimidazolium bis{(trifluoromethyl)sulphonyl}imide
[BMIM][OAc]	1-butyl-3-methylimidazolium acetate
[BMIM][OTf]	1-butyl-3-methylimidazolium trifluoromethanesulfonate
[BMIM][PF <sub>6</sub> ]	1-butyl-3-methylimidazolium hexafluorophosphate
[BMIM][SCN]	1-butyl-3-methylimidazolium thiocyanate
[BMIM][TCM]	1-butyl-3-methylimidazolium tricyanomethanide
[BMMOR][TCM]	1-ethyl-1-methylmorpholinium tricyanomethanide
[BMPIP][DCA]	1-butyl-1-methylpiperidinium dicyanamide
[BMPIP][NTf <sub>2</sub> ]	1-butyl-1-methylpiperidinium bis{(trifluoromethyl)sulphonyl}imide
[BMPYR][BOB]	1-butyl-1-methylpyrrolidinium bis(oxalato)borate
[BMPYR][DCA]	1-butyl-1-methylpyrrolidinium dicyanamide
[BMPYR][DCNM]	1-butyl-1-methylpyrrolidinium dicyano(nitroso)methanide
[BMPYR][FAP]	1-butyl-1-methylpyrrolidinium trifluorotris(perfluoroethyl)phosphate
[BMPYR][FSI]	1-butyl-1-methylpyrrolidinium bis(fluorosulfonyl)imide
[BMPYR][HSO <sub>4</sub> ]	1-butyl-1-methylpyrrolidinium hydrosulphate
[BMPYR][NTf <sub>2</sub> ]	1-butyl-1-methylpyrrolidinium bis{(trifluoromethyl)sulphonyl}imide
[BMPYR][OTf]	1-butyl-1-methylpyrrolidinium trifluoromethanesulfonate

[BMPYR][SCN]	1-butyl-1-methylpyrrolidinium thiocyanate
[BMPYR][TCB]	1-butyl-1-methylpyrrolidinium tetracyanoborate
[BMPYR][TCM]	1-butyl-1-methylpyrrolidinium tricyanomethanide
[BPY][NO <sub>3</sub> ]	1-butylpyridinium nitrate
[BzMIM][NTf <sub>2</sub> ]	1-benzyl-3-methylimidazolium bis{(trifluoromethyl)sulphonyl}imide
[DMMIM][NTf <sub>2</sub> ]	1-decyl-2,3-dimethylimidazolium bis{(trifluoromethyl)sulphonyl}imide
[DoMIM][NTf <sub>2</sub> ]	1-dodecyl-3-methylimidazolium bis{(trifluoromethyl)sulphonyl}imide
[E(OH)MIM][FAP]	1-(2-hydroxyethyl)-3-methylimidazolium trifluorotris(perfluoroethyl)phosphate
[E(OH)MIM][FAP]	1-(2-hydroxyethyl)-3-methylimidazolium trifluorotris(perfluoroethyl)phosphate
[EMIM][DCA]	1-ethyl-3-methylimidazolium dicyanamide
[EMIM][DCNM]	1-ethyl-3-methylimidazolium dicyano(nitroso)methanide
[EMIM][DEP]	1-ethyl-3-methylimidazolium diethylphosphate
[EMIM][EtSO <sub>4</sub> ]	1-ethyl-3-methylimidazolium ethylsulfate
[EMIM][FAP]	1-ethyl-3-methylimidazolium trifluorotris(perfluoroethyl)phosphate
[EMIM][MDEGSO <sub>4</sub> ]	1-ethyl-3-methylimidazolium 2-(2-methoxyethoxy)ethylsulfate
[EMIM][MeSO <sub>3</sub> ]	1-ethyl-3-methylimidazolium methanesulfonate
[EMIM][MeSO <sub>4</sub> ]	1-ethyl-3-methylimidazolium methylsulfate
[EMIM][MP]	1-ethyl-3-methylimidazolium methylphosphonate
[EMIM][NO <sub>3</sub> ]	1-ethyl-3-methylimidazolium nitrate

[EMIM][NTf <sub>2</sub> ]	1-ethyl-3-methylimidazolium bis{(trifluoromethyl)sulphonyl}imide
[EMIM][OAc]	1-ethyl-3-methylimidazolium acetate
[EMIM][OTf]	1-ethyl-3-methylimidazolium trifluoromethanesulfonate
[EMIM][SCN]	1-ethyl-3-methylimidazolium thiocyanate
[EMIM][TCB]	1-ethyl-3-methylimidazolium tetracyanoborate
[EMIM][TCM]	1-ethyl-3-methylimidazolium tricyanomethanide
[EMIM][TFA]	1-ethyl-3-methylimidazolium trifluoroacetate
[EMMOR][DCA]	1-ethyl-1-methylmorpholinium dicyanamide
[EMPYR][DCNM]	1-ethyl-1-methylpyrrolidinium dicyano(nitroso)methanide
[EMPYR][LAC]	1-ethyl-1-methylpyrrolidinium lactate
[H(CN)(4)PY][NTf <sub>2</sub> ]	1-hexyl-4-cyanopyridinium bis{(trifluoromethyl)sulphonyl}imide
[HMIM][NTf <sub>2</sub> ]	1-hexyl-3-methylimidazolium bis{(trifluoromethyl)sulphonyl}imide
[HMIM][OAc]	1-hexyl-3-methylimidazolium acetate
[HMIM][PF <sub>6</sub> )]	1-hexyl-3-methylimidazolium hexafluorophosphate
[HMIM][SCN]	1-hexyl-3-methylimidazolium thiocyanate
[HMIM][TCB]	1-hexyl-3-methylimidazolium tetracyanoborate
[HMMPY][NTf <sub>2</sub> ]	1-hexyl-3,5-dimethylpyridinium bis{(trifluoromethyl)sulphonyl}imide
[HMPIP][NTf <sub>2</sub> ]	1-hexyl-1-methylpiperidinium bis{(trifluoromethyl)sulphonyl}imide
[HMPYR][NTf <sub>2</sub> ]	1-hexyl-1-methylpyrrolidinium bis{(trifluoromethyl)sulphonyl}imide

[HpMMIM][NTf <sub>2</sub> ]	1-heptyl-2,3-dimethylimidazolium bis{(trifluoromethyl)sulphonyl}imide
[HQUIN][NTf <sub>2</sub> ]	1-hexylquinuclidinium bis{(trifluoromethyl)sulphonyl}imide
[MMIM][MP]	1,3-dimethylimidazolium methylphosphonate
[MMP][DMP]	1,1-dimethylpyrrolidonium dimethylphosphate
[MOEMIM][FAP]	1-(2-methoxyethyl)-3-methylimidazolium trifluorotris(perfluoroethyl)phosphate
[MOEMMOR][FAP]	4-(2-methoxyethyl)-4-methylmorpholinium trifluorotris(perfluoroethyl)phosphate
[MOEMMOR][NTf <sub>2</sub> ]	4-(2-methoxyethyl)-4-methylmorpholinium bis{(trifluoromethyl)sulphonyl}imide
[MOEMPIP][FAP]	1-(2-methoxyethyl)-1-methylpiperidinium trifluorotris(perfluoroethyl)phosphate
[MOEMPIP][NTf <sub>2</sub> ]	1-(2-methoxyethyl)-1-methylpiperidinium bis{(trifluoromethyl)sulphonyl}imide
[MOEMPYR][FAP]	1-(2-methoxyethyl)-1-methylpyrrolidinium trifluorotris(perfluoroethyl)phosphate
[MOEMPYR][NTf <sub>2</sub> ]	1-(2-methoxyethyl)-1-methylpyrrolidinium bis{(trifluoromethyl)sulphonyl}imide
[MOHMIM][NTf <sub>2</sub> ]	1-(6-methoxyhexyl)-3-methylimidazolium bis{(trifluoromethyl)sulphonyl}imide
[MTBDH][BETI]	1,3,4,6,7,8-hexahydro-1-methyl-2H-pyrimido[1,2-a]pyrimidine bis (pentafluoroethyl)sulfonylimide
[N- <sub>2</sub> O <sub>1,2,1,1</sub> ][FAP]	N,N-diethyl-N-methyl-N-(2-methoxy-ethyl)ammonium trifluorotris(perfluoroethyl)phosphate
[N- <sub>2</sub> O <sub>1,2,2,1</sub> ][FAP]	N,N-diethyl-N-methyl-N-(2-methoxy-ethyl)ammonium trifluorotris(perfluoroethyl)phosphate
[N- <sub>2</sub> O <sub>1,2,2,1</sub> ][NTf <sub>2</sub> ]	N,N-diethyl-N-methyl-N-(2-methoxy-ethyl)ammonium bis{(trifluoromethyl)sulphonyl}imide
[N- <sub>2</sub> OH <sub>1,1,1,1</sub> ][NTf <sub>2</sub> ]	N,N,N-trimethyl-N-(2-methoxy-ethyl)ammonium bis{(trifluoromethyl)sulphonyl}imide
[N- <sub>2</sub> OH][LAC]	2-hydroxyethanaminium lactate
[N- <sub>2</sub> OH][OAc]	2-hydroxyethanaminium acetate

[N-2OH][OFo]	2-hydroxyethanaminium formate
[N-2OH][OPr]	2-hydroxyethanaminium propionate
[N-2OPh,12,1,1][NTf <sub>2</sub> ]	N,N-dimethyl-N-dodecyl-N-(2-phenoxyethyl)ammonium bis{(trifluoromethyl)sulphonyl}imide
[N-8,2,2,2][FSI]	N-triethyl-N-octylammonium bis(fluorosulfonyl)imide
[OHOHIM][NTf <sub>2</sub> ]	1,3-dihydroxyimidazolium bis{(trifluoromethyl)sulphonyl}imide
[OMIM][BF <sub>4</sub> ]	1-octyl-3-methylimidazolium tetrafluoroborate
[OMIM][Cl]	1-octyl-3-methylimidazolium chloride
[OMIM][HSO <sub>4</sub> ]	1-octyl-3-methylimidazolium hydrosulphate
[OMIM][NTf <sub>2</sub> ]	1-octyl-3-methylimidazolium bis{(trifluoromethyl)sulphonyl}imide
[OMIM][OAc]	1-octyl-3-methylimidazolium acetate
[OMIM][SCN]	1-octyl-3-methylimidazolium thiocyanate
[OPY][NO <sub>3</sub> ]	1-octylpyridinium nitrate
[OQUIN][NTf <sub>2</sub> ]	1-octyl-1-methylpiperidinium bis{(trifluoromethyl)sulphonyl}imide
[P(OH)MIM][DCA]	1-(3-hydroxypropyl)-3-methylimidazolium dicyanamide
[P(OH)MMOR][NTf <sub>2</sub> ]	4-(3-hydroxypropyl)-4-methylmorpholinium bis{(trifluoromethyl)sulphonyl}imide
[P(OH)PY][DCA]	1-(3-hydroxypropyl)pyridinium dicyanamide
[P(OH)PY][NTf <sub>2</sub> ]	1-(3-hydroxypropyl)pyridinium bis{(trifluoromethyl)sulphonyl}imide
[P-14,6,6,6][PF <sub>6</sub> ]	trihexyltetradecylphosphonium hexafluorophosphate
[P-14,6,6,6][TCM]	trihexyltetradecylphosphonium tricyanomethanide



[P-14,6,6,6][TMPP]	trihexyltetradecylphosphonium bis(2,4,4,-trimethylpentyl)phosphinate
[P-4,4,4,2(O)OH][Br]	tributyl(carboxymethyl)phosphonium bromide
[P-4,4,4,2][DEP]	tributylethylphosphonium diethylphosphate
[P-4,4,4,2] <sub>2</sub> [DTMN]	tributylethylphosphonium dithiomaleonitrile
[P-4,4,4,2OH][Br]	tributyl-(2-hydroxyethyl)phosphonium bromide
[P-4,4,4,4][MeSO <sub>3</sub> ]	tetrabutylphosphonium methanesulfonate
[P-8,8,8,8][NTf <sub>2</sub> ]	tetraoctylphosphonium bis(trifluoromethylsulfonyl)imide
[PeMPIP][NTf <sub>2</sub> ]	1-pentyl-1-methylpiperidinium bis{(trifluoromethyl)sulphonyl}imide
[P-i4,i4,i4,1][TOS]	tri-iso-butylmethylphosphonium tosylate
[PMIM][NTf <sub>2</sub> ]	1-propyl-3-methylimidazolium bis{(trifluoromethyl)sulphonyl}imide
[PMPiP][NTf <sub>2</sub> ]	1-propyl-1-methylpiperidinium bis{(trifluoromethyl)sulphonyl}imide
[S-2,2,2][NTf <sub>2</sub> ]	triethylsulphonium bis{(trifluoromethyl)sulphonyl}imide
[TEMA][MeSO <sub>4</sub> ]	tris-(2-hydroxyethyl)-methylanmonium methylsulfate

# Chapter 1 Introduction

The intensity in the search for new solutions in many scientific, engineering and technology developments in recent years, has been devoted to "green chemistry" and sustainable processing [<sup>1</sup>]. Major challenges still exist for the modern chemical industry to provide solutions that allow for the production of materials in a sustainable manner, minimising the negative influence of the industry on the environment and society. Green chemistry summarises the most important principles and directions of research into new materials and processes.

There are 12 Principles of Green Chemistry [<sup>1</sup>]. The relevant principle to this work is principle 5, "green" processes in which the use of solvents is minimised. In practice, it is difficult to imagine such a process. The vast majority of chemical reactions (in both organic and inorganic chemistry) occur in a solvent environment. This also extends to different types of purification or separation methods, such as extraction. Therefore, the direction of the development of "green chemistry" is in search of new solvents.

In addition, goal 12 of #Envision2030 Agenda adopted in 2015 by the United Nations [<sup>2</sup>] which is to ensure sustainable consumption and production of goods, is one of the most important goals to achieve before 2030. Use of ionic liquids (ILs) in chemical processes is one way of achieving these goals since due to their properties ILs can be recycled multiple times [<sup>3</sup>], which enables to minimise waste production.

The existence of modern civilisation is highly dependent on fossil fuels even if circumstances are changing. In many countries, the transport of people and goods require huge volumes of petrol. According to the U.S. Energy Information Administration, 98.76 million barrels of oil (including crude oil, products of distillation and biofuels) were used per day in 2017, and 100.63 million barrels were produced per day in 2019 [<sup>4</sup>]. Emission products generated during the consumption of crude oil products are carbon oxides, nitrogen oxides and sulphur oxides. The need to separate sulphur compounds from fuel mixtures is dictated by concern for the natural environment. Restrictive sulphur content standards in fuels that are petroleum processing products make it impossible to use some of the deposits of this raw material without proper treatment. In the United States of America and the European Union, liquid fuel products cannot contain more than 10 ppm of sulphur compounds such as thiophene, dibenzothiophene or thioethers [<sup>5,6</sup>]. In South Africa, sulphur limits in gasoline and diesel fuel were not so restrictive, which changed

over the years. In 2006 Clean Fuels (CF1) Regulations were implemented, which forced the decrease of the sulphur content from 3000 ppm to 500 ppm and introduction of the niche grade of 50 ppm which became the most popular type of fuel in South Africa [7]. Since July 2017 CF1 should be replaced by the Clean Fuels 2 (CF2) Regulations, which has been delayed indefinitely due to financial reasons. CF2 would force the petroleum industry to decrease the concentration of tS-compounds in fuels to below 10 ppm, which agrees with the European Union standard EURO 5 [8]. The main disadvantage of hydrodesulphurization (HDS) processes widely used in petrol industry is the complicated and intricate steps necessary to achieve the desired specifications. Additionally, HDS processes demand high energy requirements to provide proper conditions for hydrogen – sulphur compound reaction on cobalt and molybdenum catalyst, as it requires temperatures in the range of 300 to 400°C and pressures of 30 to 130 bar, which also generates the highly toxic hydrogen sulphide as one of the products of the process [9].

The approach proposed by many other researchers and supported in this study would allow for relatively cheap and safe sulphur removal from the products of oil distillation by the use of a simpler method of extraction. The main objective of this work is to investigate prospective ionic liquids (ILs) for this purpose and to benchmark the performance of the IL solvents to those in literature. This would enable a simpler and more efficient process than HDS to meet reduced energy consumption and environmental regulations, as ionic liquids can be reused after purification.

The objectives of this study were to:

- I. Undertake a literature review of the extractive desulphurisation (EDS) process.
- II. Determine the most suitable ILs from screening techniques, including Gas - Liquid Chromatography (GLC) and Liquid - Liquid Equilibria (LLE) measurements.
- III. Benchmark the performance of suitable solvents to current commercial and patented solvents.
- IV. Summarise the state of knowledge about EDS with the use of ILs.

This thesis is presented in 7 chapters. Chapter 2 provides a brief overview of ionic liquids as chemical compounds, their structures and properties. This chapter also

describes their potential usage for various applications and summarises data about the potential use of ILs in the desulphurisation process.

Chapter 3 explains the theory behind the experimental methods used in obtaining the thermodynamic phase equilibrium and solubility data.

Chapter 4 describes methods of gas chromatography and extraction and how they were translated to the language of chemical thermodynamics and phase separation.

Chapter 5 presents the results obtained during this work and offers a discussion with respect to the literature data presented in Chapter 2. This chapter also contains a graphical representation of the results.

Chapter 6 summarises conclusions drawn from this work.

Chapter 7 presents recommendations for the further work related to the extractive desulphurisation process.

## Chapter 2 Literature review

This chapter provides information about ionic liquids as chemical compounds and their possible applications in modern chemical industrial processes. Furthermore, knowledge about the potential use of ionic liquids as extractants in desulphurisation processes is discussed, and a summary of the extracting capabilities, as reported in the literature is presented.

### 2.1 Ionic Liquids

Ionic liquids have been considered potential solvents for "green chemistry" since the beginning of the 1990s [10]. Ionic liquids are organic salts having a sizeable organic cation in their structure. It is conventionally assumed that an ionic liquid is an organic salt whose solid-liquid phase transition temperature is lower than the standard boiling point of water, i.e. 100°C. Numerous literature reports show that ionic liquids are characterised by many interesting properties for both laboratory chemistry (synthesis, analytical chemistry) and applied chemistry (separation processes) [11–18].

Examples of cation structures are shown in Figure 2.1. These cations are derivatives of quaternary organic bases such as imidazoles, pyridines, piperidines, amines, and phosphines.

Anions, as shown in Fig. 2-2, in ionic liquids are usually smaller. They also often have axial or planar symmetry.

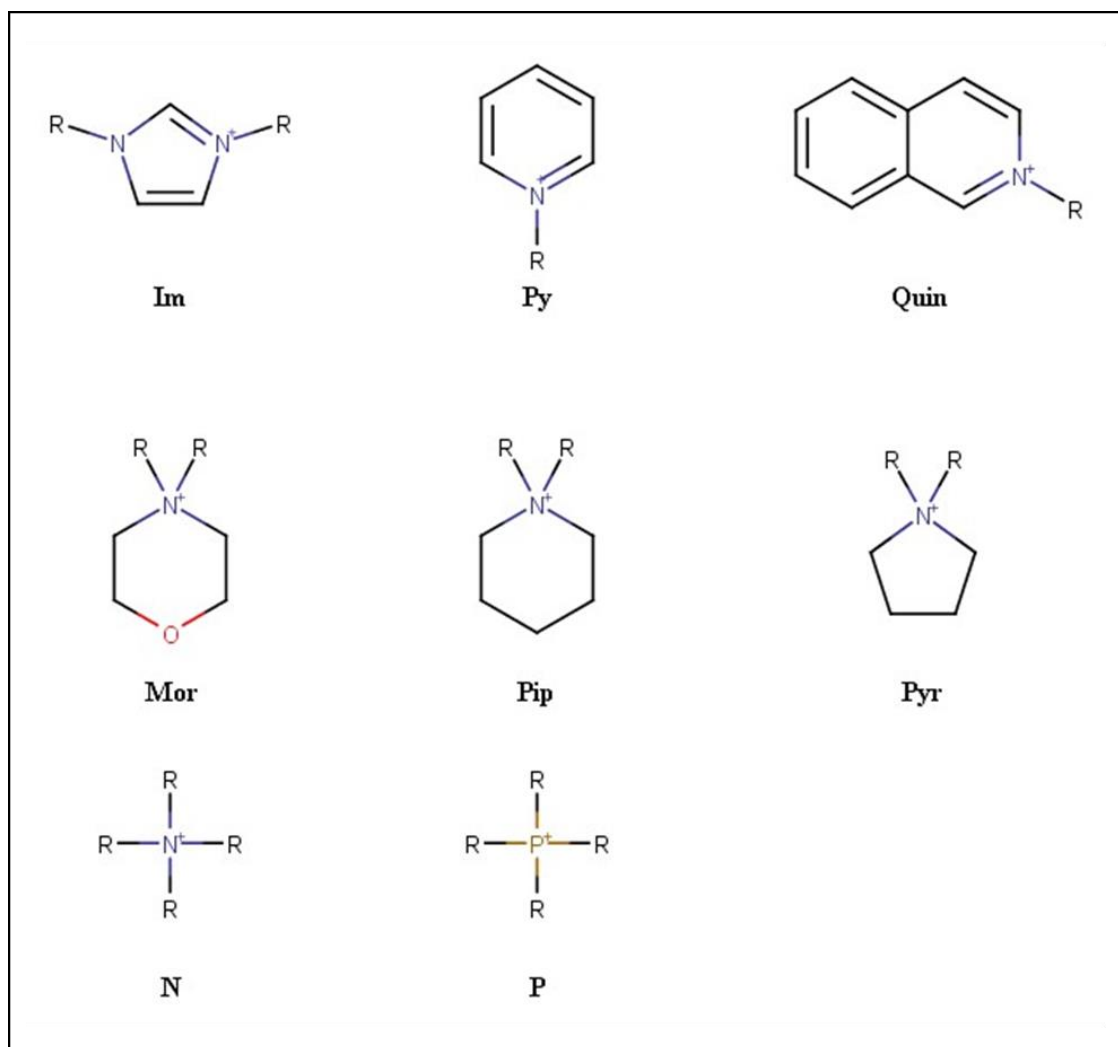


**Fig. 2-1** Examples of cations used in the synthesis of ionic liquids: Im, imidazolium, Py, pyridinium, Quin, quinolinium, Mor, morpholinium, Pip, piperidinium, Pyr, pyrrolidinium, N, ammonium, and P, phosphonium (compiled in this work).

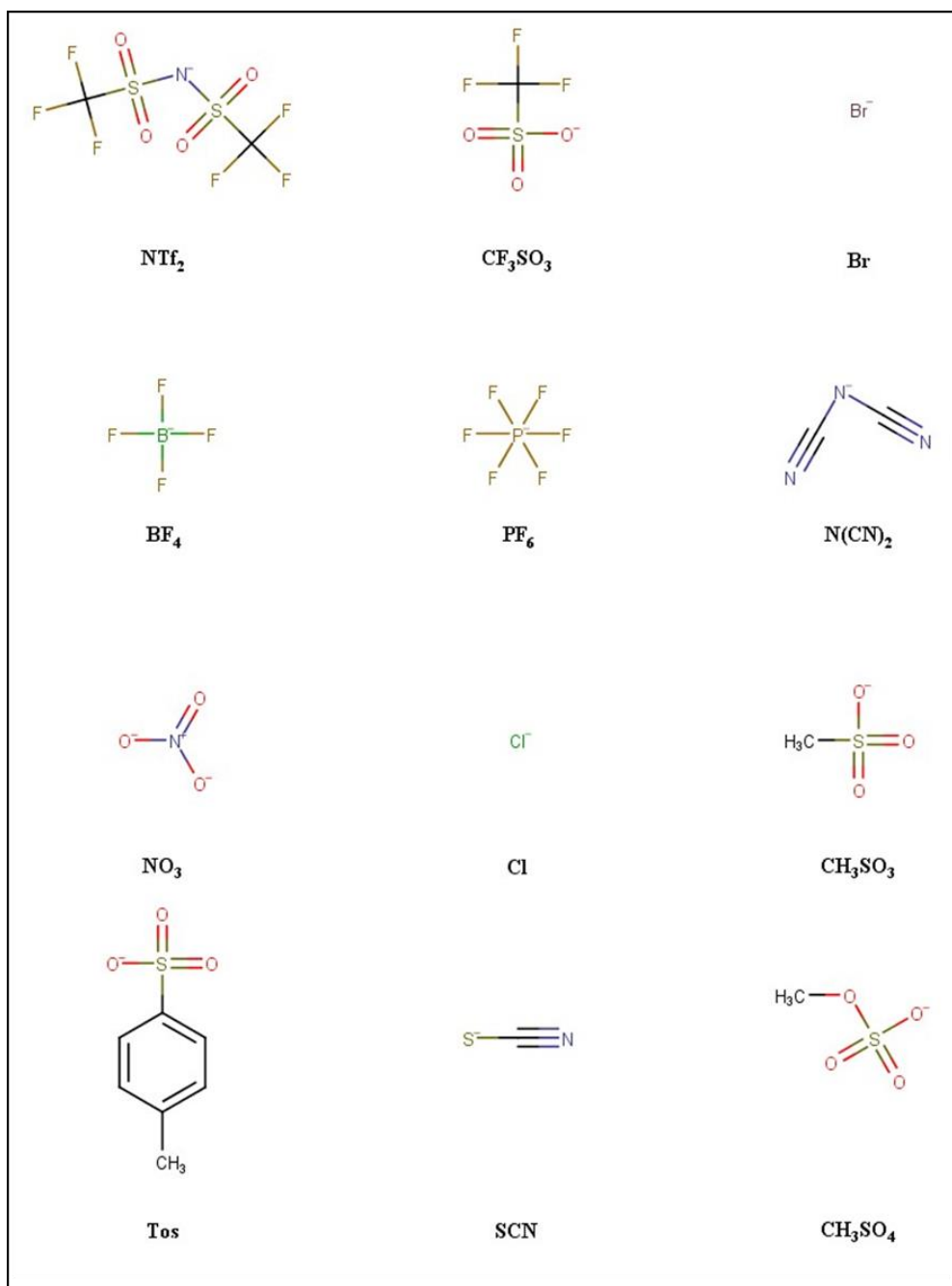


**Fig. 2-2** Examples of anions used in the synthesis of ionic liquids: bis(trifluoromethanesulphonyl)imide, trifluoromethanesulphonate, borate, tetrafluoroborate, hexafluorophosphate, dicyanamide, nitrate, chloride, methanesulphonate, tosylate, thiocyanate and methylsulphate (compiled in this work).

Significant differences in the size and symmetry of the counter-ions lead to a significant reduction in the energy of the salt crystal lattice. This effect helps to create a liquid phase at a temperature much lower than that of typical inorganic salts. Indeed, in the case of ionic liquids, the melting point is much lower [19].

Properties of particular importance for applications are excellent thermal and chemical stability of ionic liquids and their extremely low saturated vapour pressure, even at elevated temperatures as opposed to organic solvents which are toxic and volatile. Ionic liquids also have a wide temperature range of liquid phase stability, compared to organic and inorganic solvents. These green solvents also display a wide range of physicochemical (density, viscosity, surface tension, refractive index, boiling point, melting point, thermal stability) and thermodynamic (miscibility, solubility, the heat of mixing, vapour pressure, heat capacity, thermal conductivity) properties, which can be modified in a controlled manner by modifying the structure of ions or substituents present in cations or anions in the IL. This is achieved by changing the substituent length or introducing different functional groups. Therefore, in the literature, ionic liquids are often referred to as tunable solvents or designer solvents [10]. For more information on the classification, properties and synthesis of ILs, the reader is referred to the following books: “An Introduction to Ionic Liquids” [20], “Ionic Liquids: Physicochemical Properties” [21], “Ionic Liquids in Separation Technology” [22] and “Ionic Liquids in Synthesis” [23].

## 2.2 ILs in green chemistry processes

Research on the use of ionic liquids in liquid-liquid extraction processes began in 2001 [24] with systems in which one of the phases was water and the other the ionic liquids: 1-butyl-3-methylimidazolium hexafluorophosphate ([BMIM][PF<sub>6</sub>]) or 1-hexyl-3-methylimidazolium hexafluorophosphate ([HMIM][PF<sub>6</sub>]). Researchers reported on the so-called partition coefficient, which is a ratio of the concentration of a solute in a mixture of two immiscible solvents. Comparison of the partition coefficients for the ionic liquid/water with the octanol/water for alcohols, aromatic carboxylic acids, and common organic solvents showed a linear relationship between the ionic liquid/water and



octanol/water partition coefficients. Armstrong [25] determined the partition coefficients [BMIM][PF<sub>6</sub>] / water for nearly 40 organic compounds from various groups, which included acids, bases, and amino acids. Differences between ionic liquid/water and octanol/water partition coefficients were noted for individual groups of compounds in relation to their acid-base properties. For compounds with acidic properties, much lower values of partition coefficients in the ionic liquid/water system were noted, while for amino acids, the value of this coefficient increased. It was concluded that this was due to the lower alkalinity of the ionic liquid [BMIM][PF<sub>6</sub>] compared to octanol.

Another application of ionic liquids with the anion [PF<sub>6</sub>] is the extraction of organic impurities and metal compounds (including heavy metals) from environmental samples. Ionic liquids were also used to study the concentration of 18 polycyclic aromatic hydrocarbons [26] as well as nickel and lead compounds [27] in water samples from various environments. In addition, the content of zinc compounds in water and milk were tested [28]. Another example of the use of ionic liquids is the isolation of alkaloids and other compounds from plant material, e.g. white pepper piperine [29].

Over the past years, summaries of the collective findings and uses of the ILs have been reported. A review published by Cevasco and Chiappe in 2014 [30] summarises potential uses of ILs in green chemistry processes. According to the data gathered by the authors, ionic liquids are very potent solvents in the field of reusable materials like cellulose and chitin, which are naturally occurred polymers. Updated research confirms pieces of information gathered and published earlier in 2006 by Zhu et al. [31] This may lead to many interesting ways of wood and paper recycling products, especially since it is possible to reconstruct cellulose from the solution. This method still has some limitations, as not all of the described ILs allow for receiving reconstruction products with these same properties as the dissolved material. Another interesting usage of the cellulose dissolved in ILs is dissolution combined with hydrolysis, which could be used in the production of biofuels. According to the authors, ILs that shows acidic properties can compete with fungal biorefinery processes or novel bioengineered enzymes in terms of the process complexity. According to Cevasco, ILs can be also used for the dissolution of the largest biopolymers as keratin, chitin or silk with similar results. Another interesting use of the ILs described by the Cevasco and Chiappe is depolymerisation of the human-made polymers. Authors referred to the depolymerisation of nylon-6, rubber tires and fibre reinforced plastics [30].

Interesting usage of the ILs in the pilot-scale operation is mercury removal from the natural gas streams described by Abai et al. [32]. According to authors ionic liquids mixed with copper chloride are suitable for mercury vapour extraction. It was proven that this process may be upscaled without loss of the removal efficiency, which was established as 20 wt% of the mercury vapours.

The last described usage of the ILs in the article published by Cevasco et al. [30] is removal of the gasses from the industrial streams, i.e. CO<sub>2</sub> capture, which is currently one of the biggest environmental challenges. Authors states that ILs have the potential to be an alternative for currently used CO<sub>2</sub> capture technologies. However, the capacity of the ILs based carbon dioxide filters is directly proportional to the system pressure, which creates problems for applications in atmospheric pressure. Another disadvantage to the use of ionic liquids is their high viscosity, which gets even higher for the CO<sub>2</sub> + IL adducts, as those two compounds create hard to remove tars. Additional work to find the most suitable ILs for CO<sub>2</sub> capture has to be made. According to the authors, the most promising ILs for this purpose are those prepared with the use of the weak proton donors neutralised with phosphonium hydroxide or superbases neutralised with weak bases. These observations confirm the data gathered and published by the Karadas et al. in 2010 [33]. The mentioned work delivers valuable information about the use of the ILs in carbon dioxide process. Capturing of CO<sub>2</sub> was also summarised in 2018 by Aghaie et al.[34]. In this review, authors analysed not only the possibilities of the carbon dioxide adsorption by the ILs but additionally put the data into an economic context. All of the mentioned authors agree that ILs are prospective adsorbents for CO<sub>2</sub> removal from industrial streams, which finds confirmation in the pilot-scale CO<sub>2</sub> capturing plant described by Valencia-Marquez et al. [35,36].

Karadas et al. [33] present data gathered for the H<sub>2</sub>S adsorption by use of the ILs. Hydrogen sulphide is a highly toxic and corrosive gas present in many reservoirs of the natural gas, commonly removed is ammino-based process [37]. According to Karadas et al. [33] the most popular ILs based on the imidazolium cation are not suitable for this process and the most efficient H<sub>2</sub>S capture study was carried out with [BMIM][MeSO<sub>4</sub>] with the H<sub>2</sub>S/CO<sub>2</sub> selectivity equal to 13.5.

For more information on the application and uses of ILs, the reader is referred to the referenced articles [33–38], which show possible uses of the ionic liquids in the catalysis and electrochemistry.

## 2.3 Sulphur separation problems

Over the years, different methods of desulphurisation were developed. According to the published review papers [<sup>44-47</sup>], there are at least four alternate methods for desulphurisation except for the HDS process mentioned in the introduction to this thesis. The first one is bio-desulphurisation (BDS). In this method, microorganisms metabolising organic sulphur compounds in one of two possible ways, the so-called Kodama pathway and 4S pathway, which are characterised by different mechanisms of the reaction [<sup>47</sup>]. The highest potential advantages of this method are low greenhouse gases emissions and enzyme specificity, which allows for the selective removal of the S-compound. Major drawbacks prevent this method from being industrialised. The biggest disadvantages of the BDS process is the duration of the process, a high amount of the living biomass to obtain satisfying efficiency of the process and specific conditions in which microorganisms remain alive and active. This means that very strict temperature, pH, concentration of the oxygen control must be maintained [<sup>45</sup>]. Additionally, microorganisms potentially decrease the energy content of the fuels as some of the biochemical processes may inhibit the hydrocarbons during the process. Last of the mentioned disadvantages are related to the separation of the biomass from the fuel and toxicity of the by-product of the BDS process – 2-hydroxybiphenyl [<sup>46</sup>].

Another method of sulphur removal mentioned by the authors [<sup>46,47</sup>] is adsorptive desulphurisation (ADS). In this method, sulphur compounds are adsorbed on the surface of the so-called active phase placed on the porous, chemically inert material, which helps to develop a surface area of the active phase. According to Abro et al. [<sup>45</sup>], different adsorbents were tested, i.e. zeolites, alumina, zirconia, and silica gel. The best results were obtained for activated carbon. According to the authors, activated carbon was able to remove up to 95% of the dibenzothiophene and up to 88% of the thiophene from model complex fuel. Cu-zirconia was able to remove up to 99% of thiophene from octane and gallium + Y-zeolite removed up to 97% of dibenzothiophene from nonane. The worst efficiency of sulphur removal was noted for alumina (only 30% of dibenzothiophene was removed from the model fuel). Ionic liquids were tested in the role of the active phase placed on different supports [<sup>48-50</sup>]. Advantages of this method are a relatively low temperature of the process and lack of emissions of any pollutant. The biggest drawbacks are low selectivity of sulphur compounds, and low capacities of the adsorbents, which requires multiple large beds to fulfil efficiency requirements [<sup>47</sup>].

An alternative to the mentioned methods is oxidative desulphurisation (ODS). In this process, S-compounds are treated by the addition of the oxidative agents (i.e.  $\text{NO}_2$  or  $\text{H}_2\text{O}_2$  [45]) which oxidises sulphides into sulfoxides and sulfones. Those compounds are removed from the fuel by use of the extraction. Bhutto et al. published a review focused on the ILs in the ODS process [51], which shows that ionic liquids may be an interesting choice for this type of the desulphurisation process. According to their findings, ILs may be recognised as double role solvents for oxidation and extraction. The advantages of the ODS method are summarised as clean, energetically efficient and complementary to the HDS method as hydrodesulphurisation uses reductive reactions. The major drawbacks of this method are unwanted side reactions leading to less energetic fuel and highly toxic, potentially harmful catalytic systems [47].

## 2.4 ILs in extractive desulphurisation

One of the most important potential applications of ionic liquids in the modern chemical industry is their use as extractants in separation methods, primarily extraction and extractive distillation [52]. The extraction process involves the diffusive separation of the components of the mixture between the so-called raffinate, i.e., a primary solvent that is free of some components of the initial mixture and an extract containing components that were selectively separated from the primary mixture and dissolved in the secondary solvent (extractant). This process is carried out in the concentration range of the miscible region between the primary and secondary solvent, creating a two-phase system. Such a system can be separated using appropriate tools such as separation funnels or industrial separators after reaching equilibrium. The separated component is thereafter recovered from the separated extract, e.g., by distillation methods [53].

The separation efficiency in extraction processes is affected by factors such as the type of solvent (extractant), temperature, time and intensity of mixing that affect the development of the interface [54]. Since the exchange of species in the mixture can only take place at the interface, the development of the interface is one of the most important factors limiting the overall efficiency of the process.

Extractive distillation involves the process of distilling the components of a mixture with the addition of a so-called separating agent, which aims to increase the

volatility ratio of the components of the mixture. It thus facilitates or even allows the separation of components, e.g., azeotropic mixtures. A well-chosen separating agent, used during extraction distillation, is characterised by low volatility and leaves the distillation system as one of the components of the residue (components of the mixture with lower volatility). Due to the significant volatility difference between the components of the residue and the separating agent, it is possible to recover it, e.g., via simple distillation [53].

The most critical parameters to determine the legitimacy of the use of a given compound as an extractant or separation agent in separation processes such as extraction of a mixture with components  $i$  and  $j$  are the partition coefficient  $\beta$ , and selectivity  $S$ . The partition coefficient indicates the distribution of a given component between the phases of the system and is defined as:

$$\beta_i = \frac{x_i^{extract}}{x_i^{raffinate}} \quad (2 - 1)$$

$$\beta_j = \frac{x_j^{extract}}{x_j^{raffinate}} \quad (2 - 2)$$

where  $x$  is the mole fraction of the substance in each of the phases. These values can be read from phase equilibrium diagrams for binary or ternary systems. On the other hand, selectivity is a measure of the efficiency of a given solvent in isolating one of the components of a mixture and is defined by the formula:

$$S = \frac{\beta_i}{\beta_j} \quad (2 - 3)$$

The tables which follow summarises results of relevant literature on ionic liquids tested for this sole purpose. The test components used as a fuel basis for the measurements were hexane, heptane, octane, decane, dodecane, hexadecane, cyclohexane, methylcyclohexane and toluene. These compounds represent the variation of components in fuels. Thiophene, benzothiophene and dibenzothiophene were used as model sulphur compounds to study the extraction of compounds of varying complexity.

While the performance and ranking of solvents are based on the selectivity and distribution ratio, the Performance Index ( $PI = S \times \beta$ ) has been reported by Kumar &

Banerjee [55] The information presented in tables 2-1 to 2-4 are listed in order of decreasing PI.

Table 2-1 lists selectivities, partition coefficients and performance indices gathered from the activity coefficient at infinite dilution literature for thiophene and hydrocarbons. Values of selectivity  $S$  were calculated using equation 2-3, while  $\beta$  is equal to the inverse of the activity coefficient at infinite dilution for thiophene in the studied IL.

**Table 2-1** A summary of results from previous related literature for activity coefficient at infinite dilution systems: temperature (T), selectivity (S) and solute distribution ratio ( $\beta$ ) of thiophene and performance index (PI) calculated by the use of the literature  $\gamma^\infty$  data.

IL	T/K	$S$	$\beta$	PI	Ref.
Hexane					
[BMIM][SCN]	308.15	152.297	0.806	122.721	56
[BM(4)PY][SCN]	308.15	97.053	1.016	98.631	57
[EMMOR][DCA]	318.15	215.179	0.446	96.062	58
[BM(4)PY][DCA]	308.15	68.248	1.217	83.027	59
[EMPYR][LAC]	318.15	96.899	0.775	75.116	60
[AMIM][DCA]	308.15	84.706	0.588	49.827	61
[BMIM][DCA]	318.15	54.035	0.877	47.399	62
[BMPYR][OTf]	308.15	48.654	0.962	46.783	63
[BMPYR][TCM]	318.15	33.004	1.410	46.550	64
[P-i4,i4,i4,1][TOS]	308.15	37.972	1.179	44.778	65
[P(OH)PY][DCA]	318.15	113.846	0.385	43.787	66
[P(OH)MMOR][NTf <sub>2</sub> ]	318.15	81.481	0.529	43.112	67
[EMIM][TCM]	318.15	48.333	0.877	42.398	68
[BMIM][TCM]	318.15	35.912	1.105	39.681	69
[BMPYR][FSI]	318.15	33.294	1.185	39.448	70
[B(CN)(4)PY][NTf <sub>2</sub> ]	308.15	36.026	1.092	39.330	71
[BMPYR][TCB]	318.15	24.886	1.517	37.764	72
[BMPY][NTf <sub>2</sub> ]	308.15	23.237	1.603	37.239	73
[PMPIP][NTf <sub>2</sub> ]	308.15	28.677	1.236	35.448	74
[EMIM][TCB]	308.15	32.350	1.054	34.088	75
[MOEMMOR][FAP]	318.15	26.357	1.292	34.052	76

**Table 2-1** cont.

IL	T/K	<i>S</i>	$\beta$	PI	Ref.
[MOEMMOR][NTf <sub>2</sub> ]	318.15	33.119	0.917	30.385	77
[N- <sub>8,2,2,2</sub> ][FSI]	318.15	16.440	1.835	30.166	70
[MOEMPIP][FAP]	318.15	17.173	1.745	29.970	78
[S- <sub>2,2,2</sub> ][NTf <sub>2</sub> ]	308.15	28.021	1.070	29.969	79
[HMIM][TCB]	318.15	18.553	1.572	29.172	80
[P(OH)PY][NTf <sub>2</sub> ]	318.15	36.772	0.787	28.954	81
[BMIM][OTf]	308.15	33.130	0.870	28.809	82
[BM(3)PY][OTf]	318.15	25.835	1.114	28.770	83
[MOEMPIP][NTf <sub>2</sub> ]	318.15	21.474	1.271	27.286	84
[MOEMIM][FAP]	318.15	29.369	0.901	26.459	85
[MOEMPYR][FAP]	318.15	16.590	1.536	25.484	86
[MTBDH][BETI]	308.15	19.216	1.307	25.119	87
[BMPIP][NTf <sub>2</sub> ]	308.15	17.942	1.391	24.954	88
[MOEMPYR][NTf <sub>2</sub> ]	318.15	21.469	1.130	24.259	89
[PeMPIP][NTf <sub>2</sub> ]	308.15	15.325	1.548	23.723	90
[N- <sub>201,2,2,1</sub> ][FAP]	318.15	18.340	1.239	22.726	91
[EMIM][FAP]	318.15	19.244	1.181	22.721	92
[N- <sub>201,2,2,1</sub> ][NTf <sub>2</sub> ]	318.15	20.088	1.104	22.173	93
[HQUIN][NTf <sub>2</sub> ]	313.15	12.732	1.718	21.876	94
[HMPIP][NTf <sub>2</sub> ]	308.15	12.492	1.629	20.345	90
[AMIM][NTf <sub>2</sub> ]	318.15	20.962	0.962	20.155	95
[OQUIN][NTf <sub>2</sub> ]	313.15	8.579	1.988	17.055	94
[N- <sub>2OH,1,1,1</sub> ][NTf <sub>2</sub> ]	318.15	33.500	0.500	16.750	96
[MOHMIM][NTf <sub>2</sub> ]	308.15	10.699	1.344	14.380	97
[N- <sub>2OPh,12,1,1</sub> ][NTf <sub>2</sub> ]	318.15	5.449	1.873	10.205	98
[DoMIM][NTf <sub>2</sub> ]	318.15	5.295	1.789	9.473	99
[(MOH) <sub>2</sub> IM][NTf <sub>2</sub> ]	308.15	5.443	1.739	9.467	97
[P- <sub>8,8,8,8</sub> ][NTf <sub>2</sub> ]	318.15	2.874	2.375	6.827	100
Heptane					
[EMIM][NO <sub>3</sub> ]	318.15	333.813	0.719	240.153	101
[BMIM][SCN]	308.15	197.421	0.806	159.083	56
[EMIM][MeSO <sub>3</sub> ]	318.15	312.255	0.490	153.066	102

**Table 2-1** cont.

IL	T/K	<i>S</i>	$\beta$	PI	Ref.
[BMPYR][SCN]	308.15	157.692	0.962	151.627	57
[EMMOR][DCA]	318.15	325.446	0.446	145.289	58
[BMPY][SCN]	308.15	132.114	1.016	134.262	57
[BM(4)PY][DCA]	308.15	100.730	1.217	122.542	59
[EMPYR][LAC]	318.15	151.938	0.775	117.781	60
[EMIM][OTf]	308.15	202.139	0.535	108.096	103
[BMPYR][DCA]	318.15	89.307	1.175	104.943	104
[BMPYR][BOB]	318.15	55.664	1.468	81.738	105
[AMIM][DCA]	308.15	138.824	0.588	81.661	61
[P(OH)PY][DCA]	318.15	185.000	0.385	71.154	66
[BMIM][DCA]	318.15	79.825	0.877	70.022	62
[BMPYR][TCM]	318.15	47.532	1.410	67.041	64
[EMIM][TCM]	318.15	75.088	0.877	65.866	68
[P(OH)MMOR][NTf <sub>2</sub> ]	318.15	117.989	0.529	62.428	67
[BMPYR][OTf]	308.15	62.212	0.962	59.819	63
[BMIM][TCM]	318.15	52.265	1.105	57.752	69
[BMPYR][FSI]	318.15	47.986	1.185	56.855	70
[B(CN)(4)PY][NTf <sub>2</sub> ]	308.15	50.000	1.092	54.585	71
[E(OH)MIM][FAP]	318.15	57.703	0.934	53.878	106
[EMIM][TCB]	308.15	50.474	1.054	53.187	75
[BMPYR][TCB]	318.15	34.901	1.517	52.961	72
[MOEMMOR][FAP]	318.15	39.018	1.292	50.411	76
[BMPYR][TCB]	318.15	34.068	1.468	50.026	105
[BMPY][NTf <sub>2</sub> ]	308.15	30.288	1.603	48.539	73
[EMIM][TCB]	318.15	45.011	1.062	47.782	107
[MOEMMOR][NTf <sub>2</sub> ]	318.15	49.908	0.917	45.787	77
[P(OH)PY][NTf <sub>2</sub> ]	318.15	58.110	0.787	45.756	81
[PMPIP][NTf <sub>2</sub> ]	308.15	36.465	1.236	45.074	74
[S- <sub>2,2,2</sub> ][NTf <sub>2</sub> ]	308.15	39.465	1.070	42.209	79
[MOEMPIP][FAP]	318.15	24.084	1.745	42.031	78
[MOEMIM][FAP]	318.15	46.306	0.901	41.717	85
[HMIM][TCB]	318.15	25.943	1.572	40.792	80



**Table 2-1** cont.

IL	T/K	<i>S</i>	$\beta$	PI	Ref.
[BM(3)PY][OTf]	318.15	36.414	1.114	40.550	83
[MOEMPYR][FAP]	318.15	26.453	1.529	40.447	106
[MOEMPIP][NTf <sub>2</sub> ]	318.15	31.131	1.271	39.556	84
[BMIM][OTf]	308.15	44.522	0.870	38.715	82
[N <sup>-</sup> <sub>8,2,2,2</sub> ][FSI]	318.15	20.917	1.835	38.381	70
MOEMPYR][FAP]	318.15	24.117	1.536	37.046	86
[P <sup>-</sup> <sub>i4,i4,i4,1</sub> ][TOS]	308.15	31.132	1.179	36.712	65
[MOEMPYR][NTf <sub>2</sub> ]	318.15	31.638	1.130	35.750	89
[BMPIP][NTf <sub>2</sub> ]	308.15	25.313	1.391	35.206	88
[EMIM][FAP]	318.15	28.689	1.181	33.872	92
[N <sup>-</sup> <sub>2O1,2,2,1</sub> ][FAP]	318.15	27.014	1.239	33.474	91
[MTBDH][BETI]	308.15	25.229	1.307	32.979	87
[PeMPIP][NTf <sub>2</sub> ]	308.15	21.053	1.548	32.589	90
[N <sup>-</sup> <sub>2O1,2,2,1</sub> ][NTf <sub>2</sub> ]	318.15	29.139	1.104	32.162	93
[AMIM][NTf <sub>2</sub> ]	318.15	31.154	0.962	29.956	95
[HQUIN][NTf <sub>2</sub> ]	313.15	16.514	1.718	28.374	94
[HMPIP][NTf <sub>2</sub> ]	308.15	16.612	1.629	27.056	90
[N <sup>-</sup> <sub>2OH,1,1,1</sub> ][NTf <sub>2</sub> ]	318.15	53.000	0.500	26.500	96
[EMIM][NTf <sub>2</sub> ]	313.15	27.579	0.935	25.775	108
[OQUIN][NTf <sub>2</sub> ]	313.15	10.887	1.988	21.643	94
[BMIM][PF <sub>6</sub> ]	313.15	26.569	0.730	19.394	108
[MOHMIM][NTf <sub>2</sub> ]	308.15	13.441	1.344	18.066	97
[N <sup>-</sup> <sub>2OPh,12,1,1</sub> ][NTf <sub>2</sub> ]	318.15	6.442	1.873	12.064	98
[(MOH) <sub>2</sub> IM][NTf <sub>2</sub> ]	308.15	6.626	1.739	11.524	97
[DoMIM][NTf <sub>2</sub> ]	318.15	6.351	1.789	11.361	99
[OMIM][Cl]	313.15	13.598	0.758	10.302	108
[P <sup>-</sup> <sub>8,8,8,8</sub> ][NTf <sub>2</sub> ]	318.15	3.325	2.375	7.899	100
Octane					
[EMIM][NO <sub>3</sub> ]	318.15	461.151	0.719	331.763	101
[EMIM][MeSO <sub>3</sub> ]	318.15	498.039	0.490	244.137	102
[EMMOR][DCA]	318.15	506.250	0.446	226.004	58
[BMPYR][SCN]	308.15	233.654	0.962	224.667	57

**Table 2-1** cont.

IL	T/K	<i>S</i>	$\beta$	PI	Ref.
[BMIM][SCN]	308.15	250.604	0.806	201.937	56
[BMPY][SCN]	308.15	196.138	1.016	199.327	57
[EMPYR][LAC]	318.15	237.984	0.775	184.484	60
[BM(4)PY][DCA]	308.15	149.635	1.217	182.038	59
[EMIM][OTf]	308.15	319.251	0.535	170.723	103
[BMPYR][DCA]	318.15	135.135	1.175	158.796	104
[AMIM][DCA]	308.15	224.706	0.588	132.180	61
[EMIM][MP]	313.15	231.658	0.503	116.411	109
[BMPYR][BOB]	318.15	78.584	1.468	115.395	105
[P(OH)PY][DCA]	318.15	296.923	0.385	114.201	66
[BMIM][DCA]	318.15	120.175	0.877	105.417	62
[EMIM][TCM]	318.15	114.912	0.877	100.800	68
[BMPYR][TCM]	318.15	67.842	1.410	95.687	64
[P(OH)MMOR][NTf <sub>2</sub> ]	318.15	166.667	0.529	88.183	67
[BMIM][TCM]	318.15	75.801	1.105	83.758	69
[E(OH)MIM][FAP]	318.15	87.862	0.934	82.037	106
[EMIM][TCB]	308.15	77.555	1.054	81.723	75
[BMPYR][OTf]	308.15	83.558	0.962	80.344	63
[BMPYR][FSI]	318.15	65.640	1.185	77.772	70
[B(CN)(4)PY][NTf <sub>2</sub> ]	308.15	70.961	1.092	77.468	71
[BMPYR][TCB]	318.15	49.469	1.517	75.067	72
[MOEMMOR][FAP]	318.15	56.848	1.292	73.446	76
[EMIM][TCB]	318.15	68.153	1.062	72.349	107
[P(OH)PY][NTf <sub>2</sub> ]	318.15	91.339	0.787	71.920	81
[BMPYR][TCB]	318.15	48.752	1.468	71.589	105
[MOEMMOR][NTf <sub>2</sub> ]	318.15	75.321	0.917	69.102	77
[BMPY][NTf <sub>2</sub> ]	308.15	41.346	1.603	66.260	73
[MOEMIM][FAP]	318.15	71.261	0.901	64.199	85
[S- <sub>2,2,2</sub> ][NTf <sub>2</sub> ]	308.15	57.005	1.070	60.968	79
[PMPIP][NTf <sub>2</sub> ]	308.15	47.837	1.236	59.131	74
[MOEMPIP][FAP]	318.15	33.682	1.745	58.783	78
[MOEMPYR][FAP]	319.15	38.226	1.529	58.450	106

**Table 2-1** cont.

IL	T/K	<i>S</i>	$\beta$	PI	Ref.
[BM(3)PY][OTf]	318.15	51.559	1.114	57.415	83
[MOEMPIP][NTf <sub>2</sub> ]	318.15	44.981	1.271	57.155	84
[HMIM][TCB]	318.15	35.849	1.572	56.366	80
[BMIM][PF <sub>6</sub> ]	313.15	74.912	0.730	54.681	108
[BMIM][OTf]	308.15	62.435	0.870	54.291	82
[MOEMPYR][FAP]	318.15	33.948	1.536	52.147	86
[MOEMPYR][NTf <sub>2</sub> ]	318.15	45.763	1.130	51.709	89
[EMIM][FAP]	318.15	42.621	1.181	50.320	92
[N- <sub>8,2,2,2</sub> ][FSI]	318.15	26.972	1.835	49.491	70
[N- <sub>201,2,2,1</sub> ][FAP]	318.15	39.901	1.239	49.443	91
[BMPIP][NTf <sub>2</sub> ]	308.15	35.466	1.391	49.327	88
[N- <sub>201,2,2,1</sub> ][NTf <sub>2</sub> ]	318.15	42.274	1.104	46.660	93
[MTBDH][BETI]	308.15	35.556	1.307	46.478	87
[AMIM][NTf <sub>2</sub> ]	318.15	46.827	0.962	45.026	95
[PeMPIP][NTf <sub>2</sub> ]	308.15	28.173	1.548	43.612	90
[EMIM][NTf <sub>2</sub> ]	313.15	44.916	0.935	41.977	108
[N- <sub>20H,1,1,1</sub> ][NTf <sub>2</sub> ]	318.15	81.000	0.500	40.500	96
[P- <sub>i4,i4,i4,1</sub> ][TOS]	308.15	30.425	1.179	35.878	65
[HQUIN][NTf <sub>2</sub> ]	313.15	19.921	1.718	34.228	94
[HMPIP][NTf <sub>2</sub> ]	308.15	21.010	1.629	34.218	90
[OQUIN][NTf <sub>2</sub> ]	313.15	13.726	1.988	27.288	94
[MOHMIM][NTf <sub>2</sub> ]	308.15	17.204	1.344	23.124	97
[N- <sub>20Ph,12,1,1</sub> ][NTf <sub>2</sub> ]	318.15	7.584	1.873	14.203	98
[(MOH) <sub>2</sub> IM][NTf <sub>2</sub> ]	308.15	8.035	1.739	13.974	97
[DoMIM][NTf <sub>2</sub> ]	318.15	7.460	1.789	13.345	99
[OMIM][Cl]	313.15	16.576	0.758	12.557	108
[P- <sub>8,8,8,8</sub> ][NTf <sub>2</sub> ]	318.15	3.777	2.375	8.971	100
Nonane					
[BMPY][SCN]	308.15	338.415	1.016	343.917	57
[BMPYR][SCN]	308.15	349.038	0.962	335.614	57
[EMMOR][DCA]	318.15	688.393	0.446	307.318	58
[EMPYR][LAC]	318.15	367.442	0.775	284.839	60

**Table 2-1** cont.

IL	T/K	<i>S</i>	$\beta$	PI	Ref.
[BM(4)PY][DCA]	308.15	221.411	1.217	269.357	59
[BMIM][SCN]	308.15	333.602	0.806	268.817	56
[EMIM][OTf]	308.15	487.166	0.535	260.516	103
[AMIM][DCA]	308.15	355.294	0.588	208.997	61
[MMIM][MP]	313.15	432.389	0.405	175.056	109
[P(OH)PY][DCA]	318.15	453.846	0.385	174.556	66
[BMIM][DCA]	318.15	181.579	0.877	159.280	62
[EMIM][MP]	313.15	310.050	0.503	155.804	109
[EMIM][TCM]	318.15	172.807	0.877	151.585	68
[EMIM][TCB]	308.15	138.040	1.054	145.458	75
[BMPYR][TCM]	318.15	97.038	1.410	136.866	64
[P(OH)MMOR][NTf <sub>2</sub> ]	318.15	235.450	0.529	124.577	67
[BMIM][TCM]	318.15	108.287	1.105	119.654	69
[BMPYR][OTf]	308.15	117.308	0.962	112.796	63
[P(OH)PY][NTf <sub>2</sub> ]	318.15	142.520	0.787	112.220	81
[BMPYR][FSI]	318.15	93.957	1.185	111.324	70
[B(CN)(4)PY][NTf <sub>2</sub> ]	308.15	101.419	1.092	110.720	71
[MOEMMOR][FAP]	318.15	82.817	1.292	106.998	76
[BMPYR][TCB]	318.15	70.106	1.517	106.383	72
[MOEMMOR][NTf <sub>2</sub> ]	318.15	114.679	0.917	105.210	77
[MOEMIM][FAP]	318.15	109.009	0.901	98.206	85
[BMPY][NTf <sub>2</sub> ]	308.15	56.891	1.603	91.172	73
[S- <sub>2,2,2</sub> ][NTf <sub>2</sub> ]	308.15	82.995	1.070	88.764	79
[MOEMPIP][NTf <sub>2</sub> ]	318.15	64.549	1.271	82.019	84
[BM(3)PY][OTf]	318.15	73.385	1.114	81.721	83
[MOEMPIP][FAP]	318.15	46.597	1.745	81.321	78
[PMPIP][NTf <sub>2</sub> ]	308.15	65.513	1.236	80.980	74
[BMIM][PF <sub>6</sub> ]	313.15	109.182	0.730	79.695	108
[HMIM][TCB]	318.15	49.371	1.572	77.627	80
[BMIM][OTf]	308.15	88.696	0.870	77.127	82
[EMIM][FAP]	318.15	63.164	1.181	74.574	92
[MOEMPYR][FAP]	318.15	48.541	1.536	74.563	86

**Table 2-1** cont.

IL	T/K	<i>S</i>	$\beta$	PI	Ref.
[MOEMPYR][NTf <sub>2</sub> ]	318.15	65.650	1.130	74.180	89
[N- <sub>20</sub> 1,2,2,1][FAP]	318.15	57.745	1.239	71.555	91
[BMPIP][NTf <sub>2</sub> ]	308.15	49.513	1.391	68.864	88
[N- <sub>20</sub> 1,2,2,1][NTf <sub>2</sub> ]	318.15	61.479	1.104	67.858	93
[AMIM][NTf <sub>2</sub> ]	318.15	69.423	0.962	66.753	95
[N- <sub>8,2,2,2</sub> ][FSI]	318.15	34.679	1.835	63.631	70
[MTBDH][BETI]	308.15	48.627	1.307	63.565	87
[N- <sub>20</sub> H,1,1,1][NTf <sub>2</sub> ]	318.15	124.500	0.500	62.250	96
[EMIM][NTf <sub>2</sub> ]	313.15	63.757	0.935	59.586	108
[PeMPIP][NTf <sub>2</sub> ]	308.15	37.461	1.548	57.990	90
[HQUIN][NTf <sub>2</sub> ]	313.15	29.141	1.718	50.070	94
[HMPIP][NTf <sub>2</sub> ]	308.15	27.524	1.629	44.828	90
[OQUIN][NTf <sub>2</sub> ]	313.15	19.149	1.988	38.070	94
[P- <sub>i4,i4,i4,1</sub> ][TOS]	308.15	29.127	1.179	34.348	65
[MOHMIM][NTf <sub>2</sub> ]	308.15	22.312	1.344	29.989	97
[(MOH) <sub>2</sub> IM][NTf <sub>2</sub> ]	308.15	9.861	1.739	17.149	97
[N- <sub>20</sub> Ph,12,1,1][NTf <sub>2</sub> ]	318.15	8.933	1.873	16.728	98
[DoMIM][NTf <sub>2</sub> ]	318.15	8.801	1.789	15.745	99
[OMIM][Cl]	313.15	19.053	0.758	14.434	108
[P- <sub>8,8,8,8</sub> ][NTf <sub>2</sub> ]	318.15	4.371	2.375	10.381	100
Decane					
[BMPYR][SCN]	308.15	522.115	0.962	502.034	57
[BMPY][SCN]	308.15	470.528	1.016	478.179	57
[EMMOR][DCA]	318.15	994.196	0.446	443.838	58
[EMPYR][LAC]	318.15	562.016	0.775	435.671	60
[BM(4)PY][DCA]	308.15	334.550	1.217	406.995	59
[BMIM][SCN]	308.15	468.171	0.806	377.253	56
[EMIM][OTf]	308.15	703.209	0.535	376.047	103
[AMIM][DCA]	308.15	547.647	0.588	322.145	61
[P(OH)PY][DCA]	318.15	663.846	0.385	255.325	66
[BMIM][DCA]	318.15	275.439	0.877	241.613	62
[EMIM][TCM]	318.15	268.421	0.877	235.457	68

**Table 2-1** cont.

IL	T/K	<i>S</i>	$\beta$	PI	Ref.
[EMIM][TCB]	308.15	213.909	1.054	225.405	75
[EMIM][MP]	313.15	443.216	0.503	222.722	109
[MMIM][MP]	313.15	493.927	0.405	199.970	109
[BMPYR][TCM]	318.15	139.915	1.410	197.342	64
[P(OH)PY][NTf <sub>2</sub> ]	318.15	223.622	0.787	176.080	81
[P(OH)MMOR][NTf <sub>2</sub> ]	318.15	330.159	0.529	174.687	67
[BMIM][TCM]	318.15	158.011	1.105	174.598	69
[MOEMMOR][NTF <sub>2</sub> ]	318.15	176.147	0.917	161.603	77
[BMPYR][OTf]	308.15	167.308	0.962	160.873	63
[MOEMMOR][FAP]	318.15	120.801	1.292	156.074	76
[BMPYR][TCB]	318.15	99.697	1.517	151.285	72
[BMPYR][FSI]	318.15	126.777	1.185	150.210	70
[MOEMIM][FAP]	318.15	165.766	0.901	149.339	85
[B(CN)(4)PY][NTf <sub>2</sub> ]	308.15	135.371	1.092	147.785	71
[S- <sub>2,2,2</sub> ][NTf <sub>2</sub> ]	308.15	121.925	1.070	130.401	79
[BMPY][NTf <sub>2</sub> ]	308.15	79.006	1.603	126.613	73
[MOEMPIP][NTf <sub>2</sub> ]	318.15	93.901	1.271	119.315	84
[BM(3)PY][OTf]	318.15	105.679	1.114	117.683	83
[MOEMPIP][FAP]	318.15	64.747	1.745	112.996	78
[PMPIP][NTf <sub>2</sub> ]	308.15	91.100	1.236	112.608	74
[BMIM][OTf]	308.15	128.696	0.870	111.909	82
[EMIM][FAP]	318.15	94.097	1.181	111.094	92
[HMIM][TCB]	318.15	68.553	1.572	107.788	80
[MOEMPYR][FAP]	318.15	69.278	1.536	106.418	86
[N- <sub>201,2,2,1</sub> ][FAP]	318.15	85.874	1.239	106.411	91
[MOEMPYR][NTf <sub>2</sub> ]	318.15	93.898	1.130	106.100	89
[N- <sub>201,2,2,1</sub> ][NTf <sub>2</sub> ]	318.15	90.508	1.104	99.898	93
[AMIM][NTf <sub>2</sub> ]	318.15	103.846	0.962	99.852	95
[BMPIP][NTf <sub>2</sub> ]	308.15	69.402	1.391	96.526	88
[N- <sub>2OH,1,1,1</sub> ][NTf <sub>2</sub> ]	318.15	183.500	0.500	91.750	96
[MTBDH][BETI]	308.15	67.059	1.307	87.659	87
[N- <sub>8,2,2,2</sub> ][FSI]	318.15	44.404	1.835	81.475	70

**Table 2-1** cont.

IL	T/K	$S$	$\beta$	PI	Ref.
[PeMPIP][NTf <sub>2</sub> ]	308.15	49.381	1.548	76.441	90
[HMPIP][NTf <sub>2</sub> ]	308.15	38.274	1.629	62.335	90
[HQUIN][NTf <sub>2</sub> ]	313.15	32.885	1.718	56.503	94
[OQUIN][NTf <sub>2</sub> ]	313.15	21.660	1.988	43.062	94
[P-i <sub>4</sub> ,i <sub>4</sub> ,i <sub>4</sub> ,1][TOS]	308.15	34.434	1.179	40.606	65
[MOHMIM][NTf <sub>2</sub> ]	308.15	29.167	1.344	39.203	97
[(MOH) <sub>2</sub> IM][NTf <sub>2</sub> ]	308.15	12.174	1.739	21.172	97
[N-2OPh,12,1,1][NTf <sub>2</sub> ]	318.15	10.712	1.873	20.059	92
[DoMIM][NTf <sub>2</sub> ]	318.15	10.411	1.789	18.625	99
[P-8,8,8,8][NTf <sub>2</sub> ]	318.15	4.964	2.375	11.792	100
Undecane					
[EMIM][MP]	313.15	674.372	0.503	338.880	109
[MMIM][MP]	313.15	619.433	0.405	250.783	109
[HQUIN][NTf <sub>2</sub> ]	313.15	42.522	1.718	73.062	94
Dodecane					
[EMIM][MP]	313.15	876.884	0.503	440.645	109
[MMIM][MP]	313.15	953.036	0.405	385.845	109
Tridecane					
[EMIM][MP]	313.15	1288.442	0.503	647.458	109
[MMIM][MP]	313.15	963.563	0.405	390.106	109
Tetradecane					
[EMIM][MP]	313.15	1755.276	0.503	882.048	109
[MMIM][MP]	313.15	1441.296	0.405	583.520	109
$S = \beta_i/\beta_j; \beta_i = 1/\gamma_{1i}^\infty; \text{PI} = S \times \beta_i$					

It can be observed from the tables that the highest PI for systems with thiophene is achieved by imidazolium ILs with relatively short alkyl substituents, which does not create a spatial hindrance. An interesting fact is that ILs with anions based on the sulphur compounds as [SCN] or [TOS] also present relatively high values of the performance index. Those factors were taken under consideration during the ILs selection process in this study.

Very high values of selectivities and PIs for alkanes longer than ten carbon atoms may be explained by extremely high values of  $\gamma^\infty$  for the systems of ILs with hydrocarbons, which increase with the increase of the alkyl chain length. This behaviour shows that interactions of listed ILs with long-chain alkanes are negligible. At this same time  $\gamma^\infty$  values for thiophene are relatively low (between 0.5 to 3.0). Since selectivity is calculated by dividing these two values, high values for higher C- alkanes is expected.

Table 2-2 summarises the data obtained from LLE measurements. Values of the average selectivity and the average distribution ratio were calculated as an average of the values for all tie-lines in the given {IL + thiophene + hydrocarbon} system.

**Table 2-2** A summary of results from literature for {IL + thiophene + hydrocarbon} LLE systems: temperature (T), average selectivity ( $S_{Av}$ ) and average solute distribution ratio ( $\beta_{Av}$ ) of thiophene, performance index (PI), and reported standard uncertainty ( $u(x)$ ).

IL	T/K	$S_{Av}$	$\beta_{Av}$	PI	$u(x) <$	Ref.
Hexane						
[BMIM][SCN]	298.15	119.8	1.75	210	0.002	110
[HMIM][SCN]	298.15	42.7	1.74	74.3	0.003	111
[EMIM][EtSO <sub>4</sub> ]	298.15	52.8	0.91	48.0	0.006	112
[EMIM][OAc]	298.15	45.7	0.87	39.8	0.007	113
[EMIM][DEP]	298.15	19.7	1.45	28.6	0.007	113
[OMIM][SCN]	298.15	14.2	2.00	28.4	0.003	111
[EMIM][NTf <sub>2</sub> ]	298.15	21.2	1.19	25.2	0.005	114
[HMMPY][NTf <sub>2</sub> ]	298.15	6.89	1.58	10.9	0.003	115
[OMIM][BF <sub>4</sub> ]	298.15	5.73	1.28	7.33	0.0005	116
[OMIM][NTf <sub>2</sub> ]	298.15	3.30	1.22	4.03	0.0006	117
Heptane						
[EMIM][SCN]	298.15	653	0.69	451	0.001	118
[MMIM][MP]	298.15	606	0.51	309	0.0001	119
[EMIM][OAc]	298.15	183	1.28	234	0.005	120
[MMIM][MP]	298.15	534	0.37	198	0.001	118
[BMIM][BF <sub>4</sub> ]	298.15	133	1.36	181	0.0001	119
[BMIM][SCN]	298.15	114	1.44	164	0.0001	119
[EMIM][TCM]	298.15	82.8	1.34	111	0.003	121
[BMPYR][TCM]	298.15	50.7	1.76	89.2	0.003	122
[E(OH)MIM][FAP]	298.15	63.2	1.39	87.8	0.002	123



**Table 2-2** cont.

IL	T/K	$S_{Av}$	$\beta_{Av}$	PI	$u(x) <$	Ref.
[BMIM][OAc]	298.15	57.1	1.53	87.4	0.005	120
[N-2O1,2,1,1][FAP]	298.15	39	2.08	81.1	0.002	123
[EMIM][FAP]	298.15	40.9	1.94	79.3	0.002	123
[EMIM][TCM]	308.15	60.7	1.25	75.9	0.003	121
[MOEMMOR][FAP]	298.15	36.8	1.46	53.7	0.002	124
[BMPYR][TCB]	298.15	30.5	1.67	50.9	0.003	122
[MOEMMOR][NTf <sub>2</sub> ]	298.15	38.7	1.12	43.3	0.002	125
[MOEMPYR][FAP]	298.15	24.6	1.71	42.1	0.002	124
[HMIM][OAc]	298.15	23.1	1.80	41.6	0.005	120
[BMIM][NTf <sub>2</sub> ]	298.15	24.3	1.69	41.1	0.003	126
[BMPYR][FAP]	298.15	21.7	1.89	41.0	0.003	122
[EMIM][EtSO <sub>4</sub> ]	298.15	38.0	0.89	33.8	0.006	112
[BMPYR][CF <sub>3</sub> SO <sub>3</sub> ]	308.15	29.3	1.14	33.4	0.005	127
[MOEMPIP][FAP]	298.15	19.2	1.71	32.8	0.002	124
[MOEMPYR][NTf <sub>2</sub> ]	298.15	23.9	1.31	31.3	0.002	125
[MOEMPIP][NTf <sub>2</sub> ]	298.15	22.2	1.39	30.9	0.002	125
[HMIM][TCB]	308.15	18.9	1.47	27.8	0.005	127
[BMIM][OTf]	298.15	21.1	1.14	24.1	0.001	128
[HMIM][NTf <sub>2</sub> ]	298.15	13.9	1.72	23.9	0.003	126
[B(CN)(4)PY][NTf <sub>2</sub> ]	308.15	21.6	1.07	23.1	0.003	129
[B(CN)(3)PY][NTf <sub>2</sub> ]	308.15	22.1	1.01	22.3	0.003	129
[H(CN)(4)PY][NTf <sub>2</sub> ]	308.15	13.6	1.37	18.6	0.003	129
[PMPIP][NTf <sub>2</sub> ]	308.15	11.8	1.40	16.5	0.003	130
[OMIM][OAc]	298.15	7.26	1.86	13.5	0.005	120
[HMMPY][NTf <sub>2</sub> ]	298.15	7.30	1.43	10.4	0.007	131
[P-4,4,4,2][DEP]	308.15	3.50	1.87	6.55	0.003	130
[OMIM][NTf <sub>2</sub> ]	298.15	3.93	1.27	4.99	0.0006	117
[OMIM][BF <sub>4</sub> ]	298.15	3.28	0.97	3.18	0.007	132
[TEMA][MeSO <sub>4</sub> ]	298.15	33.5	0.07	2.35	0.001	118
Octane						
[BMIM][SCN]	298.15	289	1.44	416	0.002	110
[HMIM][SCN]	298.15	80.2	1.83	147	0.003	111
[OMIM][SCN]	298.15	20.1	1.85	37.2	0.003	111
[HMMPY][NTf <sub>2</sub> ]	298.15	6.66	1.33	8.86	0.007	131
[EMIM][OAc]	298.15	4.08	1.01	4.12	-	133
[BMIM][SCN]	298.15	549	1.31	719	0.002	110

**Table 2-2** cont.

IL	T/K	$S_{Av}$	$\beta_{Av}$	PI	$u(x) <$	Ref.
Decane						
[HMIM][SCN]	298.15	136	1.56	212	0.003	111
[OMIM][SCN]	298.15	28.8	1.56	44.9	0.003	111
Dodecane						
[EMIM][MeSO <sub>4</sub> ]	298.15	146	0.47	68.6	0.005	134
[OMIM][NTf <sub>2</sub> ]	298.15	5.57	1.04	5.79	0.0002	135
[HMMPY][NTf <sub>2</sub> ]	298.15	6.88	0.82	5.64	0.003	136
[OMIM][BF <sub>4</sub> ]	298.15	5.17	0.83	4.29	0.007	132
Hexadecane						
[HMMPY][NTf <sub>2</sub> ]	298.15	11.7	0.84	9.83	0.003	136
[OMIM][BF <sub>4</sub> ]	298.15	6.84	0.70	4.79	0.007	132
[OMIM][NTf <sub>2</sub> ]	298.15	4.96	0.76	3.77	0.0006	117

$$S = \beta_i / \beta_j; \beta_i = 1 / \gamma_{1i}^{\infty}; PI = S \times \beta_i$$

There are three main factors that can be used to analyse the potential of ILs as extractants for the extractive desulphurisation of the fuels. The influence of the length of the alkyl chain of hydrocarbons in model fuels, the influence of cation and the influence of anion will be discussed. According to data gathered in Table 2-2, the highest PI is observed for imidazolium ionic liquids with relatively short substituent chains. Good examples of this behaviour are imidazolium ILs with thiocyanate anion ([BMIM][SCN], [HMIM][SCN] and [OMIM][SCN]). This same correlation is observed for systems of heptane and imidazolium ILs with acetate anion ([EMIM][OAc], [BMIM][OAc], [HMIM][OAc] and [OMIM][OAc]). For each of the studied fuels, the highest reported PI was achieved using an IL with the shortest substituent chain. Song et al. [120] showed that this behaviour might be observed for the ILs with small anions, which show hydrogen bond acceptor properties. In relation to this statement, results published by Wlazło et al. [126] for a series of piperidinium ILs with bis(trifluoromethanesulphonyl)imide anion [NTf<sub>2</sub>] showed similar behaviour for the more complex anion, yet, the authors did not offer any explanation for this phenomenon.

The influence of the anion is also studied. For all of the listed hydrocarbon systems average  $S$  and PI decreases in direct proportion to the size and branching of the anion. Relatively small anions with an easily accessible centre of negative charge are more favourable in the thiophene extraction than big, widely branched anions such as

tetracyanoborate [TCB], which creates huge spatial hindered, that prevents the creation of the intermolecular bonds between ions and thiophene particles. Revelli et al. [<sup>119</sup>] proposed spatial structure of interactions between thiophene and the [BMIM][SCN] molecules based on <sup>1</sup>H NMR. Figure 2-3 shows the molecular structure of the thiophene surrounding the [SCN] anion of the mentioned IL. In this model sulphur atoms (yellow) of thiophene point to the anion while the cation is located in the shielding cone of thiophene due to the upfield chemical shift effect observed with protons of the [BMIM] cation.

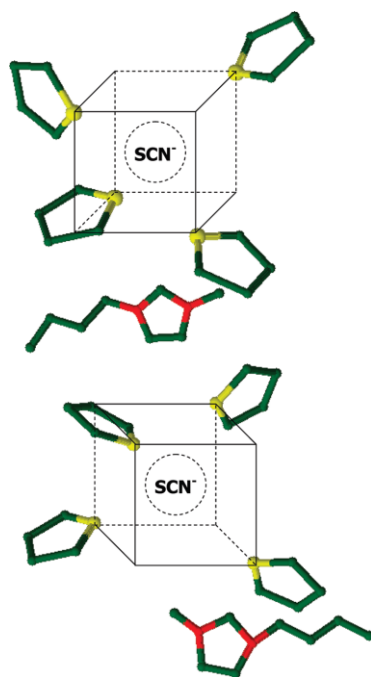


**Fig. 2-3** Structure of the thiophene in the ionic liquid [BMIM][SCN] proposed by Revelli et al. [<sup>119</sup>].

Another factor that could be considered is the length of the model fuel alkyl chain. For the series of the imidazolium ionic liquids with [SCN] anion, the selectivity and PI increase with the length of the model fuel alkyl chain. An interesting fact is that the partition coefficient decreases, though not enough to compensate for rising values of selectivity. This behaviour may be related to decreasing solubility of the ionic liquid in the longer hydrocarbons.

The imidazolium-based ILs are the most popular, as observed by the number of IL studied. This is related to the highly accessible chemicals and its relatively low prices, which makes them a good choice for the laboratory-scale study. IoLiTec Ionic Liquids Technologies GmbH, offers 208 ILs based on the imidazolium cation [137], while 30 of each ammonium, pyrrolidinium and pyridinium-based ILs, 25 phosphonium-based and 17 piperidinium-based ILs.

**Table 2-3** A summary of results from literature for {IL + benzothiophene + hydrocarbon} LLE systems: temperature (T), average selectivity ( $S_{Av}$ ) and average solute distribution ratio ( $\beta_{Av}$ ) of a benzothiophene, performance index (PI), and reported standard uncertainty ( $u(x)$ ).

IL	T/K	$S_{Av}$	$\beta_{Av}$	PI	$u(x) <$	Ref.
Heptane						
[BMPYR][TCM]	308.15	58.2	2.4	140	0.005	127
[HMIM][TCB]	308.15	38.3	2.77	106	0.005	127
[BMPYR][OTf]	308.15	38.2	1.64	62.6	0.005	127
[B(CN)(4)PY][NTf <sub>2</sub> ]	308.15	34.2	1.53	52.3	0.003	129
[PMIM][NTf <sub>2</sub> ]	308.15	23.7	2.16	51.2	0.003	126
[H(CN)(4)PY][NTf <sub>2</sub> ]	308.15	22.3	2.04	45.5	0.003	129
[PMPIP][NTf <sub>2</sub> ]	308.15	19.3	2.22	42.8	0.003	130
[N-2O1,2,1,1][FAP]	308.15	20.3	1.95	39.6	0.002	138
[MOEMMOR][FAP]	308.15	17	1.67	28.4	0.002	138
[E(OH)MIM][FAP]	308.15	20.5	1.21	24.8	0.002	138
[P-4,4,4,2][DEP]	308.15	5.64	2.66	15.0	0.003	130
Hexadecane						
[HMPYR][NTf <sub>2</sub> ]	303.15	466	2.79	1300	0.0001	139
[P-i4,i4,i4,1][TOS]	303.15	82.9	2.56	212	0.0001	139
[BMPYR][NTf <sub>2</sub> ]	303.15	91.3	2.32	212	0.0001	139
[P-4,4,4,4][MeSO <sub>3</sub> ]	333.15	33.1	2.34	77.5	0.0001	139

$$S = \beta_i / \beta_j ; \beta_i = 1 / \gamma_{1i}^{\infty} ; PI = S \times \beta_i$$

Table 2-3 shows data gathered for systems with benzothiophene. In contrast to thiophene, benzothiophene is an aromatic compound. This means that besides the intermolecular interactions between the sulphur atom and anion, the aromaticity of the benzene ring must be taken under consideration. Six delocalised electrons from double-

bonded carbon atoms create a circular  $\pi$ -bond which providing chemical stability of the aromatic ring and also adding a partial negative charge to the ring. In relation to the bigger size of the particle, it is clear that ILs with small cations of short alkyl chains substituents and small anions are not preferred, since higher selectivities and PI were obtained for ILs with more branched anions.

**Table 2-4** A summary of results from literature for {LLE + dibenzothiophene + hexadecane} systems: temperature (T), average selectivity ( $S_{Av}$ ) and average solute distribution ratio ( $\beta_{Av}$ ) of a dibenzothiophene, performance index (PI), and reported standard uncertainty (u(x)).

IL	T/K	$S_{Av}$	$\beta_{Av}$	PI	u(x) <	Ref.
[P- <sub>4,4,4,4</sub> ][MeSO <sub>3</sub> ]	333.15	53.6	3.83	205	0.0001	<sup>139</sup>
[HMPYR][NTf <sub>2</sub> ]	303.15	49.8	2.64	131	0.0001	<sup>139</sup>
[P- <sub>i4,i4,i4,1</sub> ][TOS]	303.15	43.3	2.52	109	0.0001	<sup>139</sup>
[BMPYR][NTf <sub>2</sub> ]	303.15	25.1	1.81	45.4	0.0001	<sup>139</sup>

$$S = \beta_i / \beta_j ; \beta_i = 1 / \gamma_{1i}^{\infty} ; PI = S \times \beta_i$$

Table 2-4 presents data obtained for systems of {IL + dibenzothiophene + hexadecane}. This same author [<sup>139</sup>] published data for exactly this same ILs with benzothiophene (as shown in Table 2-3). An interesting fact is that the overall PI decreased significantly for mixtures with dibenzothiophene, which mentioned earlier is related to the spatial hindrance as dibenzothiophene is a bigger particle than the listed cations and anions. Another interesting fact is the IL which performs the worst in the system with benzothiophene has the highest selectivity and performance index in the dibenzothiophene system. Unfortunately the authors did not provide an explanation for this behaviour.

The differences in PI values shown in the tables obtained by limiting activity coefficients (Table 2-1) and LLE measurements (Table 2-2) may vary because of temperature differences and the fact that the values presented in Table 2-1 are calculated by use of specific values of activity coefficients at infinite dilution. The values listed in tables 2-2 to 2-4 are averaged from the whole spectrum of selectivities obtained for each tie-line separately.

Table 2-5 lists reported laboratory-scale extractive desulphurisation experiments, the maximum percentage of removed sulphur compounds and model fuel composition.

Two kinds of model fuel can be distinguished in Table 2-5. The first is based on the single hydrocarbon as a base with the addition of the sulphur compound. In contrast, the second approach uses a mixture of different chemicals to simulate the composition of crude oil. The scale of the experiments did not exceed 100 ml. Some of the research groups studied multiple IL : fuel ratios [<sup>140–146</sup>]. Their findings show that with a higher amount of IL, better results in the desulphurisation process are achieved. Sulphur concentration was measured with the use of different techniques. X-ray fluorescence (XRF), gas chromatography (GC) and high-pressure liquid chromatography (HPLC) were the most popular analysis methods used by different research groups. A brief description of these methods may be found in section 4.2.1.

**Table 2-5** A summary of laboratory-scale extraction literature data. Columns T/%, BT/% and DBT% shows the percentage of thiophene, benzothiophene and dibenzothiophene removed from the initial model fuel composition, respectively. Table sorted according to the percentage of thiophene removed.

IL	T/%	BT/%	DBT/%	Model fuel composition	Ref.
[BM(3)PY][DCA]	78.0		86.0	0.5% T, 0.5% BT, 2% DBT, 5% Toluene, 28% Tetraline, 64% Heptane	147
[BMIM][TCM]	77.0		86.0	0.5% T, 0.5% BT, 2% DBT, 5% Toluene, 28% Tetraline, 64% Heptane	147
[BM(4)PY][DCA]	76.0		85.0	0.5% T, 0.5% BT, 2% DBT, 5% Toluene, 28% Tetraline, 64% Heptane	147
[N-2OH,1,1,1][OAc]	72.1			1000 ppm of S-compound in hexane and xylene (1:1)	148
[MMPYR][DMP]	70.9	76.9	87.5	500 ppm of S-compound in n-octane	149
[BM(4)PY][SCN]	70.0		84.0	0.5% T, 0.5% BT, 2% DBT, 5% Toluene, 28% Tetraline, 64% Heptane	147
[BMPYR][TCM]	70.0	72.0	73.0	0.5% T, 0.5% BT, 2% DBT, 5% Toluene, 28% Tetraline, 64% Heptane	150
[N-2OH,1,1,1][OOx]	69.1			1000 ppm of S-compound in hexane and xylene (1:1)	148
[N-2OH,1,1,1][OPr]	68.9			1000 ppm of S-compound in hexane and xylene (1:1)	148
[N-2OH,1,1,1][OFo]	68.4			1000 ppm of S-compound in hexane and xylene (1:1)	148
[BMIM][TCM]	68.0	68.0	69.0	0.5% T, 0.5% BT, 2% DBT, 5% Toluene, 28% Tetraline, 64% Heptane	150
[BMPYR][TCB]	68.0	70.0	56.0	0.5% T, 0.5% BT, 2% DBT, 5% Toluene, 28% Tetraline, 64% Heptane	150
[BM(4)PY][DCA]	66.0	76.0	78.0	0.5% T, 0.5% BT, 2% DBT, 5% Toluene, 28% Tetraline, 64% Heptane	150
[P-14,6,6,6][TMPP]	66.0	69.3	74.5	500ppm of S-compound in Dodecane	140
[BMMOR][TCM]	66.0	62.0	57.0	0.5% T, 0.5% BT, 2% DBT, 5% Toluene, 28% Tetraline, 64% Heptane	150
[HMPIP][NTf <sub>2</sub> ]	64.0	68.0	68.0	0.5% T, 0.5% BT, 2% DBT, 5% Toluene, 28% Tetraline, 64% Heptane	150
[BMPYR][DCA]	64.0	64.0	64.0	0.5% T, 0.5% BT, 2% DBT, 5% Toluene, 28% Tetraline, 64% Heptane	150
[MOEMPIP][FAP]	64.0	66.0	60.0	0.5% T, 0.5% BT, 2% DBT, 5% Toluene, 28% Tetraline, 64% Heptane	150
[PMPIP][NTf <sub>2</sub> ]	64.0	64.0	56.0	0.5% T, 0.5% BT, 2% DBT, 5% Toluene, 28% Tetraline, 64% Heptane	150
[COC <sub>2</sub> MPYR][FAP]	64.0	60.0	54.0	0.5% T, 0.5% BT, 2% DBT, 5% Toluene, 28% Tetraline, 64% Heptane	150
[BMPYR][OTf]	64.0	62.0	52.0	0.5% T, 0.5% BT, 2% DBT, 5% Toluene, 28% Tetraline, 64% Heptane	150
[BMIM][BF <sub>4</sub> ]	62.2	73.7	79.0	500 ppm of S-compound in Dodecane	141
[BMIM][DCA]	62.0		77.0	0.5% T, 0.5% BT, 2% DBT, 5% Toluene, 28% Tetraline, 64% Heptane	147
[MOEMPYR][NTf <sub>2</sub> ]	60.0	58.0	58.0	0.5% T, 0.5% BT, 2% DBT, 5% Toluene, 28% Tetraline, 64% Heptane	150

**Table 2-5** A summary of laboratory-scale extraction literature data. Columns T/%, BT/% and DBT% shows the percentage of thiophene, benzothiophene and dibenzothiophene removed from the initial model fuel composition, respectively. Table sorted according to the percentage of thiophene removed.

IL	T/%	BT/%	DBT/%	Model fuel composition	Ref.
[BMPiP][NTf <sub>2</sub> ]	60.0	64.0	58.0	0.5% T, 0.5% BT, 2% DBT, 5% Toluene, 28% Tetraline, 64% Heptane	150
[BMIM][Cl]	58.0	70.0	75.4	500ppm of S-compound in Dodecane	142
[N-201,1,1,2][FAP]	58.0	48.0	38.0	0.5% T, 0.5% BT, 2% DBT, 5% Toluene, 28% Tetraline, 64% Heptane	150
[BMIM][Br]	57.8	60.0	63.1	500ppm of S-compound in Dodecane	143
[BMIM][BF <sub>6</sub> ]	56.2	67.1	74.0	500ppm of S-compound Dodecane	141
[P-14,6,6,6][TCM]	56.0	56.0	73.0	0.5% T, 0.5% BT, 2% DBT, 5% Toluene, 28% Tetraline, 64% Heptane	150
[MOEPYR][NTf <sub>2</sub> ]	56.0	54.0	47.0	0.5% T, 0.5% BT, 2% DBT, 5% Toluene, 28% Tetraline, 64% Heptane	150
[BMIM][OTf]	56.0	56.0	45.0	0.5% T, 0.5% BT, 2% DBT, 5% Toluene, 28% Tetraline, 64% Heptane	150
[EMIM][FAP]	56.0	46.0	43.0	0.5% T, 0.5% BT, 2% DBT, 5% Toluene, 28% Tetraline, 64% Heptane	150
[BMIM][SCN]	55.6	66.4	77.3	2536,8 ppm of S-compound in Octane	144
[EMIM][TFA]	54.0	44.0	26.0	0.5% T, 0.5% BT, 2% DBT, 5% Toluene, 28% Tetraline, 64% Heptane	150
[BMIM][BF <sub>4</sub> ]	53.8	63.9	66.0	500ppm of S-compound in Dodecane	141
[OMIM][OAc]	53.7	60.9	71.0	498 ppm of S-compound in Dodecane	151
[BMIM][DCNM]	53.0		66.0	500 ppm of S-compounds in Hexane and Toluene(0,85w/0,15w)	152
[BMPYR][DCNM]	52.2		57.1	500 ppm of S-compounds in Hexane and Toluene(0,85w/0,15w)	152
[DMMIM][NTf <sub>2</sub> ]	50.8		67.1	26% Hexane, 6% T, 26% i-Octane, 25% Heptane, 6% Pyridine, 10% Toluene	145
[OMIM][HSO <sub>4</sub> ]	50.7	52.0	58.0	498 ppm of S-compound in Dodecane	151
[E(OH)MIM][FAP]	50.0	38.0	23.0	0.5% T, 0.5% BT, 2% DBT, 5% Toluene, 28% Tetraline, 64% Heptane	150
[EMIM][DCNM]	44.7		52.0	500 ppm of S-compounds in Hexane and Toluene(0,85w/0,15w)	152
[P(OH)MMOR][NTf <sub>2</sub> ]	44.0	34.0	17.0	0.5% T, 0.5% BT, 2% DBT, 5% Toluene, 28% Tetraline, 64% Heptane	150
[BzMIM][NTf <sub>2</sub> ]	43.9		48.3	26% Hexane, 6% T, 26% i-Octane, 25% Heptane, 6% Pyridine, 10% Toluene	145
[EMPYR][DCNM]	43.5		48.3	500 ppm of S-compounds in hexane and toluene(0,85w/0,15w)	152
[BMIM][SCN]	42.0		70.0	0.5% T, 0.5% BT, 2% DBT, 5% Toluene, 28% Tetraline, 64% Heptane	147



**Table 2-5** A summary of laboratory-scale extraction literature data. Columns T/%, BT/% and DBT% shows the percentage of thiophene, benzothiophene and dibenzothiophene removed from the initial model fuel composition, respectively. Table sorted according to the percentage of thiophene removed.

IL	T/%	BT/%	DBT/%	Model fuel composition	Ref.
[EMIM][EtSO <sub>4</sub> ]	40.3		37.8	26% Hexane, 6% T, 26% i-Octane, 25% Heptane, 6% Pyridine, 10% Toluene	145
[BMPYR][HSO <sub>4</sub> ]	28.5		30.6	Hexane, Toluene	153
[HpMMIM][NTf <sub>2</sub> ]	21.4		33.7	26% Hexane, 6% T, 26% i-Octane, 25% Heptane, 6% Pyridine, 10% Toluene	145
[OPY][NO <sub>3</sub> ]			74.7	500 ppm of S-compound in Decane	154
[BMIM][NO <sub>3</sub> ]			74.1	500 ppm of S-compound in Decane	154
[P-2(O)OH,4,4,4][Br]		53.0	70.0	500 ppm of S-compound in Heptane	146
[BPY][NO <sub>3</sub> ]			68.2	500 ppm of S-compound in Decane	154
[P-4,4,4,2OH][Br]		56.0	68.0	500ppm of S-compound in Heptane	155
[BMIM][Cl]			61.5	500ppm of S-compound in Dodecane	143
[BMIM][BF <sub>4</sub> ]			60.3	500ppm of S-compound in Dodecane	143
[BMIM][PF <sub>6</sub> ]			58.1	500ppm of S-compound in Dodecane	143
[BMIM][HSO <sub>4</sub> ]			48.0	1000 ppm of S-compound in Octane	156
[BMIM][BF <sub>4</sub> ]			35.9	160 ppm of S-compound in Octane	157
[BMIM][PF <sub>6</sub> ]			32.9	160 ppm of S-compound in Octane	157

Ionic liquids with high selectivities and PI indices were able to extract more of the sulphur compounds from the model fuels, as expected. At this same time, an example of the [BMIM][SCN], [EMIM][FAP] or [BMIM][BF<sub>4</sub>] shows that some of the ILs studied for the {thiophene + hydrocarbon} system may be less efficient in the complex model fuel systems, which is related to the reasons mentioned above.

Recycling studies were also performed. Bui et al. [<sup>151</sup>] used cyclohexane and ethyl acetate to extract S-compounds from the [OMIM][OAc], and then recover the IL via distillation. According to their findings, the recycled ionic liquid showed a slightly lower efficiency of for the desulphurisation. Only one cycle was studied. A series of papers published by Dharaskar et al. [<sup>140–143</sup>] presented an interesting approach to the reuse of the ILs in which the same batch of ILs was used without removal of the sulphur compounds. This process was repeated for four to five cycles. The efficiency of the desulphurisation decreased with each cycle, i.e., in the first cycle results show the [BMIM][Br] was able to remove 67.4% of S-compounds while after the fourth cycle only 44.8% of sulphur was removed [<sup>143</sup>]. This approach gives interesting feedback from the economic point of view, as it may be a good way for the process optimisation.

In summary, according to the gathered data, ILs with relatively small cations and anions are the most suitable for thiophene extraction. For benzothiophene, this statement is not fully supported because the size of the benzothiophene particles allows them to fit better between more branched ions. In general, an increase in selectivities and PIs with the increase in the length of the model fuel alkyl chain is observed. It is related to decreasing interactions between IL and hydrocarbons, which leads to a conclusion that, in theory, extractive desulphurisation may be easier for heavier fractions obtained during the distillation of the crude oil.

## Chapter 3 Thermodynamic principles relating to solvent extraction studies

This chapter summarises the theoretical background, starting with the thermodynamic description of liquid-liquid equilibria in a ternary system, followed by an explanation about activity coefficients at infinite dilution. The section which follows summarises knowledge about chromatography as an analytical method used to obtain activity coefficients at infinite dilution  $\gamma_{13}^{\infty}$ , liquid-liquid equilibria data and thermodynamic modelling of LLE data.

### 3.1 Chemical potential

The field of physical chemistry, which gives a simple and universal interpretation of multicomponent mixtures, is classical chemical thermodynamics. In particular, it defines a system called the ideal mixture. This definition is based on providing the expression for free molecular chemistry (the so-called chemical potential) of the  $i$ -th component of the mixture.

The expression for chemical potential is [<sup>158</sup>]:

$$\hat{\mu}_i^*(T, P, \mathbf{z}) = \hat{\mu}_i^*(T, P) + RT \ln x_i \quad (3 - 1)$$

where  $T$  and  $P$  denote system temperature and pressure, respectively, and  $\mathbf{z}$  is a vector of molar fractions of all components of the mixture. The superscript "\*" indicates properties describing the ideal system. The circumflex " $\wedge$ " refers to the component in the mixture, and its absence means that the symbol is assigned to the properties of a pure substance. Chemical potential is calculated as a derivative of internal energy, enthalpy, free enthalpy, or free energy, depending on the number of moles of molecules of a given component, with fixed values of constraints adequate for the selected thermodynamic potential. Chemical potential plays an essential role in chemical thermodynamics. In particular, this concept is the basis for the definition of thermodynamic activity (appearing in the criteria and conditions of phase and chemical equilibria).

Real solutions (especially those of practical importance, e.g., mixtures of polar and associative compounds, aqueous solutions of electrolytes) usually show significant deviations from ideal behaviour. These deviations can be both positive and negative. It depends on the composition of the mixture, but most of all, the chemical nature of all its components is essential, in particular, the type and strength of intermolecular interactions.

## 3.2 Liquid-liquid equilibria

### 3.2.1 The equilibrium state

The theoretical tool that allows for the description of intermolecular interactions and their translation into macroscopic systems is *phase equilibrium thermodynamics*, which describes the so-called deviations from perfection or ideality. In addition, phase equilibrium diagrams described and explained by this tool enable the design and optimisation of separation processes. When considering any phase equilibrium, a system consisting of  $N$  components forming a multiphase system in equilibrium is generally studied. Assuming chemical inertia of the mixture components (no reactions occurring in the discussed system), at constant temperature  $T$  and pressure  $P$ , it can be seen that the initial state of this system is presented in the form of a homogeneous mixture with mole fractions of individual components expressed by the vector  $\mathbf{z} = [z_1, \dots, z_N]$ , where  $z_i \geq 0$  and  $\sum_{i=1}^N z_i = 1$ . If the system is thermodynamically unstable, then as a result of the spontaneous pursuit of the system to the minimum of thermodynamic potential (for  $T, P = \text{constant}$  equal to Gibbs free energy) equilibrium state in which two phases, I and II, coexist with the compositions expressed by the vectors  $\mathbf{x}^I = [x_1^I, \dots, x_N^I]$  and  $\mathbf{x}^{II} = [x_1^{II}, \dots, x_N^{II}]$  is reached. For the general case, it is assumed that  $\mathbf{x}^I \neq \mathbf{x}^{II} \neq \mathbf{z}$ . This process is shown in Figure 3-1. The difficulty in phase equilibria is the calculation of  $\mathbf{x}^I$  and  $\mathbf{x}^{II}$  as functions of  $T$  and  $P$ . To present the described phenomena in a way that is most clearly understood from a mathematical point of view, it was assumed that the components of the mixture do not enter the gas phase. It means that no additional pressure is exerted in the system under consideration. The reader is referred to “Molecular Thermodynamics of Fluid-Phase Equilibria” by Prausnitz, Lichtenthaler and de Azevedo [159].

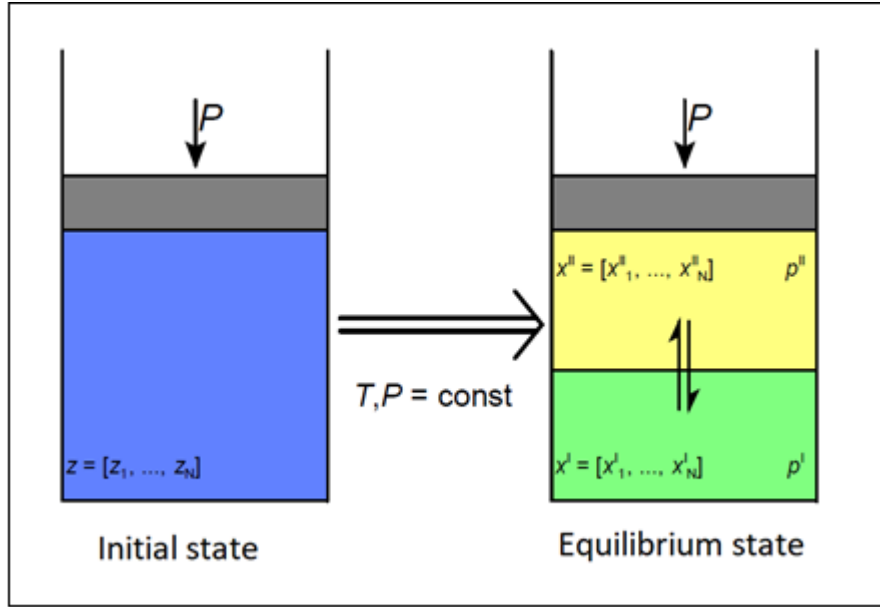


**Fig. 3-1** Graphical representation of the transition of the N-component system from the unstable initial state to the equilibrium state, associated with achieving the minimum Gibbs free energy [160].

The primary condition for the existence of equilibrium in the system described by chemical thermodynamics is the equality of chemical potentials:

$$\mu_i^I(T, P, \mathbf{x}^I) = \mu_i^{II}(T, P, \mathbf{x}^{II}) \quad i = 1, \dots, N \quad (3-2)$$

Assuming that for an ideal gas, the expression on the derivative of the chemical potential with respect to pressure ( $T = \text{const}$ ) can be expressed by the formula:

$$\left( \frac{\partial \mu_i}{\partial P} \right)_T = \frac{RT}{P} \quad i = 1, \dots, N \quad (3-3)$$

where  $\mu_i$  is the chemical potential of the pure substance, then after integration in terms of constant temperature, this expression will take the form:

$$\mu_i - \mu_i^0 = RT \ln \frac{P}{P^0} \quad i = 1, \dots, N \quad (3-4)$$

Equation 3-4 represents the change in chemical potential during the isothermal change in system pressure from pressure  $P^0$  to pressure  $P$ . According to the definition of fugacity by Lewis [161], this can be described by transforming equation 3-3 and is given by the formula:

$$\mu_i - \mu_i^0 = RT \ln \frac{f_i}{f_i^0} \quad i = 1, \dots, N \quad (3-5)$$

$\mu_i^0$  and  $f_i^0$  are selected in such a way that, assuming the value of one of these parameters, which specifies a reference state, the value of the other is chosen so that the equation is satisfied. For a system consisting of phases I and II, it is possible to write a system of equations:

$$\mu_i^I - \mu_i^{0I} = RT \ln \frac{f_i^I}{f_i^{0I}} \quad i = 1, \dots, N \quad (3-6)$$

$$\mu_i^{II} - \mu_i^{0II} = RT \ln \frac{f_i^{II}}{f_i^{0II}} \quad i = 1, \dots, N \quad (3-7)$$

After substituting into equation 3-2, representing the condition of equilibrium in the system, then equating equations 3-6 and 3-7, the following relationship is obtained:

$$\mu_i^{0I} + RT \ln \frac{f_i^I}{f_i^{0I}} = \mu_i^{0II} + RT \ln \frac{f_i^{II}}{f_i^{0II}} \quad i = 1, \dots, N \quad (3-8)$$

Assuming that  $\mu_i^{0I} = \mu_i^{0II}$  and  $f_i^{0I} = f_i^{0II}$ , the state of diffusion equilibrium can be described by the equation:

$$f_i^I(T, P, \mathbf{x}^I) = f_i^{II}(T, P, \mathbf{x}^{II}) \quad i = 1, \dots, N \quad (3-9)$$

where  $f$  is fugacity (with units of pressure). A more common record due to practical applications is:

$$\varphi^I x_i^I(T, P, \mathbf{x}^I) = \varphi^{II} x_i^{II}(T, P, \mathbf{x}^{II}) \quad i = 1, \dots, N \quad (3-10)$$

where  $\varphi$  is the so-called coefficient of fugacity or fugacity coefficient described by the equation [159]:

$$\varphi_i(T, P, \mathbf{x}) \equiv \frac{f_i(T, P, \mathbf{x})}{x_i P} \quad i = 1, \dots, N \quad (3-11)$$

Equation 3-11, however, has one very significant drawback. The number of variables ( $\mathbf{x}^I, \mathbf{x}^{II}$ ) twice exceeds the number of equations for the  $N$ -component system, which requires additional material balance equations to be included:

$$\delta x_i^I + (1 - \delta) x_i^{II} = n_i \quad i = 1, \dots, N \quad (3-12)$$

where  $\delta$  describes the relative amount of selected phase I ( $0 \leq \delta \leq 1$ ) and the balance of mole fractions for both phases:

$$\sum_{i=1}^N x_i^I = \sum_{i=1}^N x_i^{II} = 1 \quad x_i^I, x_i^{II} \geq 0; i = 1, \dots, N \quad (3-13)$$

The balance equations allow for a system of  $2N + 1$  equations with  $2N + 1$  unknowns ( $x_i^I; x_i^{II}; \delta$ ), which can then be solved by numerical methods taking into account the model describing the relationship  $\varphi_i = \varphi_i(T, P, \mathbf{x})$ .

Fugacity in gaseous systems corresponds directly to activity in liquid mixtures. The equality of fugacities in each phase allows for the creation of mathematic models, which helps to find promising solutions for equilibria problems.

### 3.2.2 Types of phase diagrams for ternary systems

According to the division proposed by Weinstock in 1952 [162], three main types of phase diagrams for liquid-liquid equilibria in ternary systems can be distinguished. These are shown in Figure 3-2:

- I. An area of limited miscibility exists for one of the pairs of compounds
- II. An area of limited miscibility exists for two pairs of compounds
- III. An area of limited miscibility exists for three pairs of compounds

An example, the first type is observed for the mixture consisting of water, benzene and ethanol. A characteristic feature of this type of system is the existence of one critical point of miscibility, in which both phases have identical composition.

For the second type of system, it is possible to distinguish two different cases. In the first, there is no critical point of miscibility. An example of this type of mixture is a system consisting of heptane, hexane, and methanol. In the second case (2a), the areas of limited miscibility do not merge, resulting in two separate miscibility gaps, each with its miscibility critical point. An example of such a system is a mixture of ionic liquid 1-butyl-3-methylimidazolium hexafluorophosphate with water and ethanol. According to Swatloski et al. [163], this behaviour may be caused by the creation of so-called clusters. It means that in systems with lower concentrations of ethanol, functional groups of alcohol create hydrophobic, hydrogen-bonded, structures in the presence of the IL. 1-butyl-3-methylimidazolium hexafluorophosphate is hydrophobic, yet with increasing

ethanol concentration bonding sites open to create “sandwich-like” molecular structures, which allows water to bond in void spaces of the structure.

The third type of system distinguished by Weinstock can be divided into three categories. In the first, at certain concentrations, a three-phase system is formed (the darker triangle in Fig. 3-2). An exemplary mixture of this type consists of water, oil, and a surfactant. In the second case (3a), for two substance pairs, a joint miscibility gap without a critical point is created, while for the remaining pair, a miscible gap with a critical point is created. An example of such a system is a mixture of water, 1-butanol, and polymer. In the last case (3b), three separate areas of limited miscibility are formed in the system. This type of system is a theoretically postulated system.

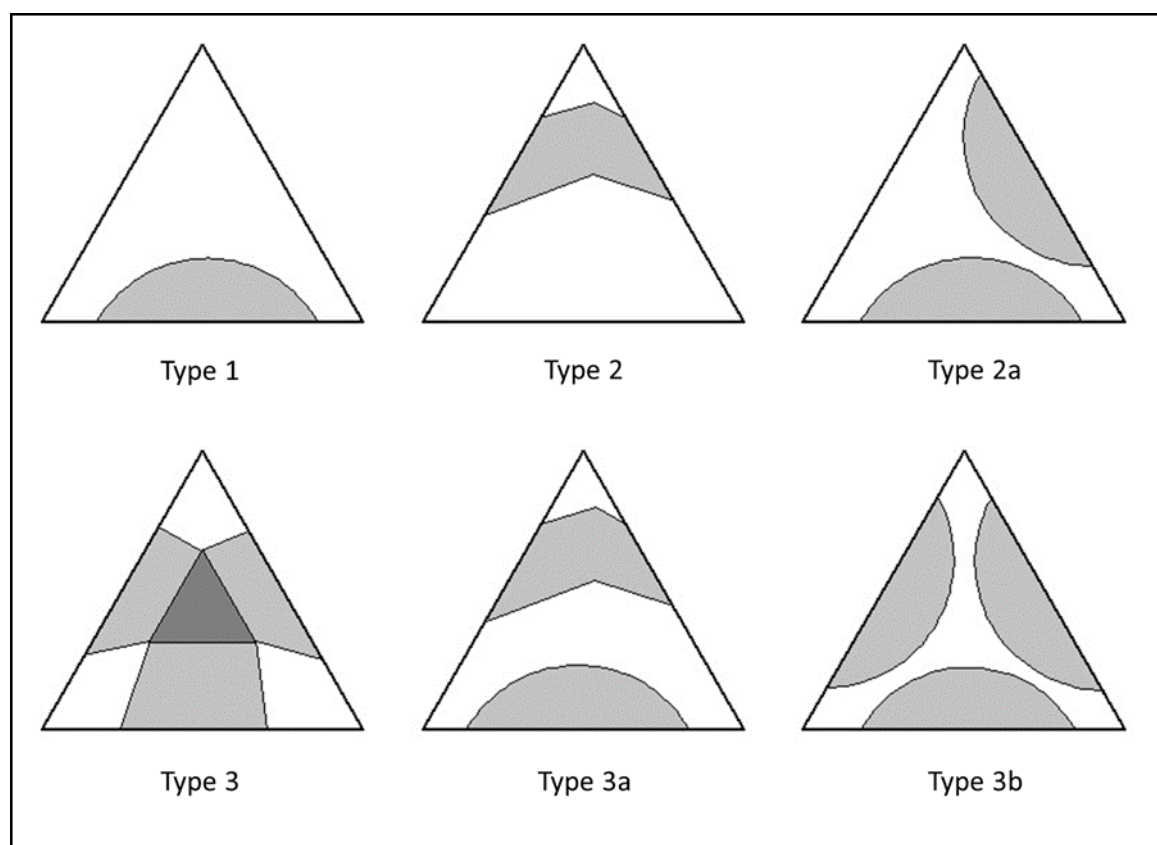


**Fig. 3-2** Classification of liquid-liquid phase diagrams in ternary systems, according to Weinstock [<sup>162</sup>]. Light grey and dark grey areas indicate areas of limited miscibility in a two-phase and three-phase system, respectively.



Fig. 3-3 shows an example of a ternary equilibrium diagram for {IL + thiophene + octane} system. Each tie-line connects two points that represent concentrations of the mixture components for both phases. The area between those points shows a so-called miscibility gap, which means that all of the ternary mixtures with composition within the miscibility region will split into two phases.

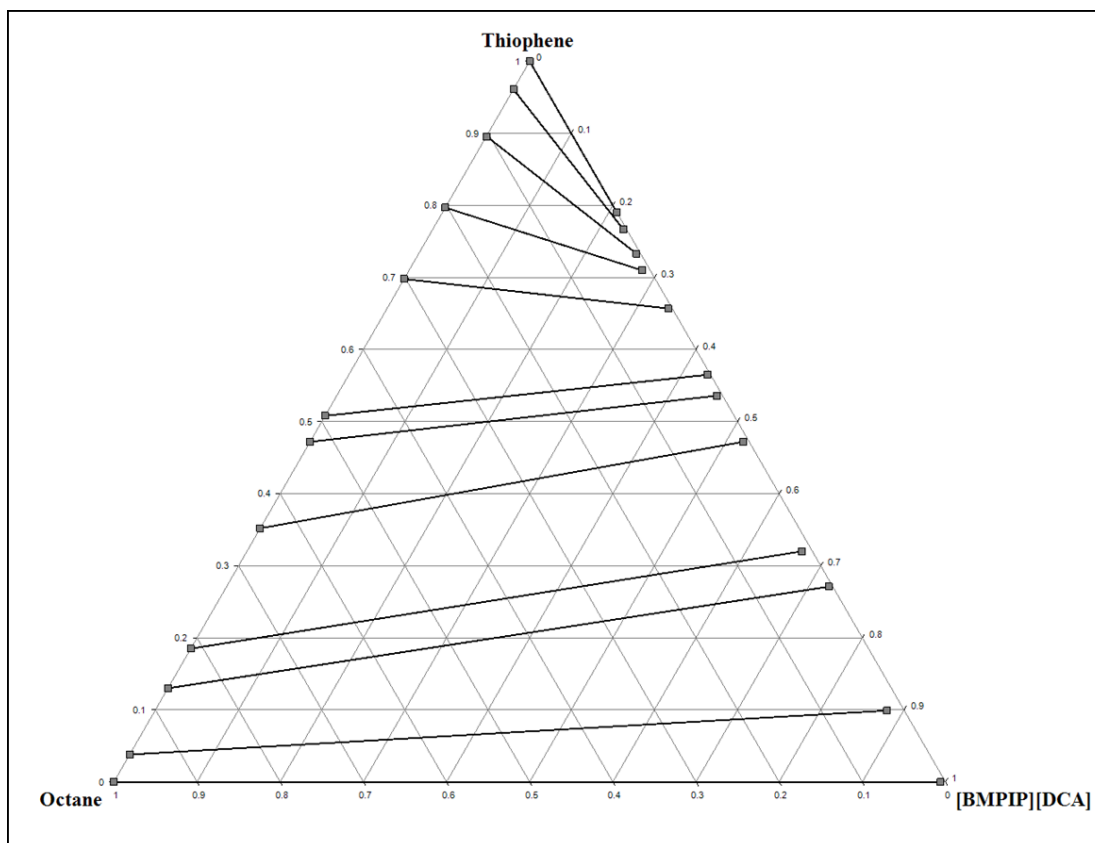


**Fig. 3-3** Example of an experimental ternary diagram with visible tie-lines [<sup>164</sup>].

### 3.3 Activity coefficients

In classical thermodynamics, it is not possible to give a general expression on the chemical potential of a component in a real mixture, analogous to equation (3-1), because this domain does not describe the effect of microscopic properties of the system on its macroscopic properties. However, it is possible to derive some values that describe only the deviations of the mixture properties from the properties of the selected reference system. A system of the ideal mixture is defined by equation (3-1), and the measure of deviation is the so-called activity coefficient,  $\gamma$ . According to the definition [158]:

$$\ln \gamma_i(T, P, \mathbf{x}) \equiv \frac{\hat{\mu}_i(T, P, \mathbf{x}) - \hat{\mu}_i^*(T, P, \mathbf{x})}{RT} \quad (3 - 14)$$

where  $T$  and  $P$  denote system temperature and pressure, respectively, and  $\mathbf{x}$  is a vector of molar fractions of all components of the mixture. The superscript "\*" indicates properties describing the ideal system. The circumflex "^" refers to the component in the mixture, and its absence means that the symbol is assigned to the properties of a pure substance.

Equation 3-14 may also be shown in the form:

$$\ln \gamma_i(T, P, \mathbf{x}) = \frac{G_i^E}{RT} \quad (3 - 15)$$

where  $G_i^E$  is excess Gibbs energy for the component  $i$ . Excess Gibbs energy models are described in the sections which follow. Calculation of the Gibbs free energy values enables the remaining thermodynamic functions as internal energy, enthalpy, or entropy to be evaluated.

#### 3.3.1 Activity coefficients at infinite dilution $\gamma_{13}^\infty$

Infinite dilution is defined as a state of the solution that contains so much solvent in comparison to solute that when more solvent is added to the mixture, there is no real change in concentration of solvent. It means that the properties of the solute are constant.

In binary systems, the activity coefficient of component "2" in the solvent "1" at infinite dilution is defined by the equation:

$$\gamma_{12}^\infty = \lim_{x_2 \rightarrow 0} \gamma_1 \quad (3 - 16)$$

The value of  $\gamma_{12}^{\infty}$  is a source of information on the mutual affinity between the solvent and solute molecules. If  $\gamma_{12}^{\infty} \ll 1$ , affinity is strong (1-2 interactions are stronger than 1-1), whereas if  $\gamma_{12}^{\infty} \gg 1$  affinity is weak (1-2 interactions are weaker than 1-1). However, if  $\gamma_{12}^{\infty} \approx 1$ , the system is close to perfection, which means that the interaction of the molecules in the mixture has a force comparable to the action of the molecules of the same component. In addition to purely cognitive significance,  $\gamma_{12}^{\infty}$  values can also have practical significance. By use of the  $\gamma_{12}^{\infty}$  value, it is possible, for example, to calculate the activity coefficients of two-component mixtures with any concentration of solute or solvent [165]. This type of calculation can be made with an appropriate thermodynamic model giving the relationship of excess free enthalpy of mixing. In such models, there are usually some parameters that can be adjusted to the  $\gamma_{12}^{\infty}$  data. The knowledge of these parameters is particularly important because they allow for the calculation of many interesting thermodynamic properties of mixtures, such as liquid-vapour, liquid-liquid, solid-liquid phase diagrams, or excess enthalpies and thermal capacities of mixing.

From the  $\gamma_{12}^{\infty}$  data, it is also possible to calculate various types of parameters determining the suitability of a given solvent (e.g., ionic liquid) in selected extraction processes. An example of such a parameter is the selectivity  $S_{ij}^{\infty(1)}$  defined as:

$$S_{ij}^{\infty(1)} = \frac{\gamma_{1i}^{\infty}}{\gamma_{1j}^{\infty}} \quad (3 - 17)$$

where the symbols  $i$  and  $j$  indicate the indices assigned to the components, in relation to which the selectivity is calculated.

Values of  $S_{ij}^{\infty(1)} \gg 1$  indicate that the solvent "1" can be regarded as a suitable medium for separating the component from the component  $j$ . In the literature, particular attention was paid to the capacity of ionic liquids for the extraction separation of aliphatic and aromatic hydrocarbons [166], sulphur compounds (for example thiophene or benzothiophene) from light gasoline fractions (model systems for processes of extractive desulphurization of fuels) [136], or butanol from aqueous solutions [167].

Activity coefficients at infinite dilution can only be used to determine the degree of the substance's impact on the natural environment [168]. This is due to the fact that  $\gamma_{12}^{\infty}$  can be associated with different types of partition coefficients for selected substances, e.g., between an aquatic environment or air and soil. Experimental  $\gamma_{12}^{\infty}$  values are usually determined by direct phase equilibrium measurements (e.g., vapour-liquid equilibria,

ebulliometry) in diluted solutions or also from chromatographic measurements. The former are generally time-consuming and not very accurate if extrapolated from vapour liquid equilibria at concentrated regions. In addition, they require large amounts of test substances, which is why they are relatively expensive. Therefore, the methods based on the use of chromatography are preferred. This method is limited only to systems with a non-volatile solvent. Therefore, they are used, among others for determining  $\gamma_{12}^{\infty}$  in polymers and ionic liquids. [169]

### 3.4 LLE data regression or parameter fitting

Some popular Gibbs excess free enthalpy models, such as the Universal QUasi Chemical (UNIQUAC), UNIQUAC Functional group Activity Coefficients (UNIFAC) and Non-Random Two-Liquid (NRTL) are discussed briefly. The basic concept of these models is based on the Wilson hypothesis assuming that the local concentration around the molecule is not the same as the concentration in the entire volume of the solution.

The models mentioned are most often used to describe liquid-liquid and liquid-vapour equilibria for the mixtures of electrolytes which show large deviations from the ideality. For a description of the liquid equilibria in a ternary system, the parameters of the model must be determined based on the experimental data obtained for two-component mixtures. For the needs of models based on the Wilson equation, ILs are considered as electrically neutral ionic pairs.

The NRTL model correlates activity coefficients  $\gamma_i$  with mole fractions  $x_i$  in the liquid phase. The idea behind this model is based on Wilson's hypothesis that bulk phase concentration is different from local concentration at the microscale, which is related to different values of the interaction energy between particles of this same compound  $U_{ii}$  and particles of different chemical individuals  $U_{ij}$ .

The UNIQUAC model is considered as a second-generation activity coefficient model. It is related to the modified excess Gibbs energy equation, which consists not only an enthalpy term but also adds entropy under consideration. The entropic term is responsible for the description of deviation from ideality, and it is called combinatorial contribution, while the enthalpic correction or so-called residual contribution describes the correction based on intermolecular interactions. Due to its versatility, UNIQUAC is

considered as one of the best correlative models but, the mathematical complexity and not always satisfying results in UNIFAC is a modification of the previously mentioned UNIQUAC model. The biggest change in comparison with the previous model is the introduction of the group contribution method, which could deliver more accurate results of correlation but also increase the level of the algebraic complexity.

### 3.5 Non-random two-liquid (NRTL) model

The non-random two-liquid model (NRTL) was used to calculate predicted compositions at the end of the tie-lines. The NRTL equation was derived by Renon & Prausnitz in 1968 [170]. This model is widely used [110–119,121–136,138,139] to correlate liquid-liquid equilibria in the systems with ionic liquids is well-known, easy to use and versatile. It allows for correlating ternary data with satisfying accuracy, but without overcomplicating the calculations.

In 1985 Walas proposed application of NRTL to LLE data correlation [171], which was adopted in this study. The NRTL model equations are presented as:

$$\frac{G^E}{RT} = x_1 x_2 \left[ \frac{\tau_{21} G_{21}}{x_1 + x_2 G_{21}} + \frac{\tau_{12} G_{12}}{x_2 + x_1 G_{12}} \right] \quad (3 - 18)$$

where:

$$\tau_{12} = \frac{g_{12} - g_{22}}{RT} \quad (3 - 19)$$

$$\tau_{21} = \frac{g_{12} - g_{11}}{RT} \quad (3 - 20)$$

$$G_{12} = \exp(-\alpha_{12} \tau_{12}) \quad (3 - 21)$$

$$G_{21} = \exp(-\alpha_{12} \tau_{21}) \quad (3 - 22)$$

where  $x_1$  and  $x_2$  are molar fractions of the components,  $g_{11}$  and  $g_{22}$  are the Gibbs energies of the pure substances,  $g_{12}$  is Gibbs energy of the interaction between components of the mixture and  $\tau_{12}$ ,  $\tau_{21}$  and  $\alpha_{12}$  are independent parameters. Parameter  $\alpha_{12}$ , the non-randomness parameter, is an interesting case because it is the only parameter that must be provided and tested by the researcher. Renon and Prausnitz suggested values from the range 0.2 – 0.47.

For most of the datasets listed in tables 2-2 to 2-3 the value of the non-randomness parameter,  $\alpha_{12}$ , used for NRTL correlation was 0.3, which allowed to achieve the lowest root mean standard deviation (RMSD) values. In seven of the listed articles the value of  $\alpha_{12}$  parameter was equal to 0.2, while three papers [112,113,115] reported correlated data for sets of non-randomness parameters from 0.1 to 0.3. In this work, the non-randomness parameter was set to a value 0.3 for three of the four studied systems. For [BMIM][OTf], the value of  $\alpha_{12}$  set equal to 0.1 resulted in the correlation most consistent with the experimental data.

Analysis of the gathered literature shows that in most of the listed articles, the NRTL model was used to correlate results. Numerous literature data support the NRTL model as a very versatile tool, which allows to achieve very good correlation with RMSD values equal or lower than 0.01 for most of the {IL + thiophene + hydrocarbon} systems. For example, values of RMSD for correlations performed by Domańska et al. [122] for series of [BMPYR] ILs with different anions are very low, in the range of 0.0076, 0.0030 and 0.0036 for [FAP],[TCB] and [TCM] anions, respectively. Ahmed et al. [139] published a series of LLE data for {IL + benzothiophene/dibenzothiophene + hexadecane}. Correlation results obtained for dibenzothiophene were in the range from 0.005 to 0.0131. RMSD results published by Ahmed et al. for benzothiophene were slightly lower and were in the range from 0.009 to 0.0233.

The UNIQUAC model was also used to correlate LLE data in ten of the mentioned articles [112–115,118,119,131,133,134,136]. In comparison to the NRTL model, the UNIQUAC model is more complex and data demanding, while it does not offer a significant increase of the obtained data quality. Cheruku et al. [133] showed that for systems with [EMIM][OAc] the NRTL equations provided a better correlation than the UNIQUAC model. RMSDs for {IL + thiophene + *i*-octane} system calculated for the NRTL model and for the UNIQUAC model were equal to 0.0082 and 0.0147, respectively. Interesting data was published by Kędra-Królik et al. [118]. Two {IL + thiophene + heptane} and two {IL + thiophene + pyridine} systems with two ILs were studied. According to published data NRTL has better consistency for {[MMIM][MP] + pyridine + heptane} and {[BMIM][SCN] + thiophene + heptane} systems (RMSD = 0.0005 and 0.0056, respectively), while RMSDs for UNIQUAC were slightly better for {[BMIM][SCN] + pyridine + heptane} and {[MMIM][MP] + thiophene + heptane} (RMSD = 0.0117 and 0.0055, respectively). The fifth system with tris-(2-hydroxyethyl)-methylammonium methylsulfate [TEMA][MeSO<sub>4</sub>] published by the authors was

correlated only by use of the NRTL model, which was related to lack of the UNIQUAC equations parameters required for correlation. In the equivalent number of cases, the UNIQUAC model shows slightly lower RMSD. Arce et al. [131] published correlation results for {[HMMPY][NTf<sub>2</sub>] + thiophene + heptane} systems, where the RMSD for the NRTL model was equal to 0.0063 while the RMSD for the UNIQUAC model was equal to 0.0041.

The NRTL model is a versatile tool which allows one to achieve very good correlation without over-complication of the calculations and easily accessible parameters. Correlation consistency tests show clearly that a complicated tool as the UNIQUAC model is not generally superior in comparison to the NRTL model and, in relation to missing literature data, may not be possible to apply for some systems with ILs. In comparison, the NRTL model requires only experimental data and temperature to correlate data with very good consistency.

Song et al. [120] followed a novel approach and used the CONductor like Screening Model for Real Solvents (COSMO-RS) predictive model [172] to obtain theoretical tie-lines, which were compared to experimental data and NRTL correlation. The COSMO-RS method is based on data obtained with the help of quantum-mechanical calculations that allow a virtual area of segments to be spread around a particle. This area determines the distribution of shielding charge density at each segment and the formation of this area is described by parameters such as surface area and charge density  $\sigma$ . According to COSMO-RS theory, liquids are considered as closely packed and thoroughly surrounded by other molecules in the mixture. At the point of contact of segments belonging to two molecules, it is possible to determine the resultant value of the density of shielding charges of both molecules,  $\sigma$  and  $\sigma'$ , respectively, which in COSMO-RS theory is responsible for the description of electrostatic interactions between liquids.

Data published by Song et al. show that the RMSD obtained for the series of imidazolium ILs with the increasing length of substituent chain [C<sub>n</sub>MIM][OAc] (n = 2, 4, 6, 8) were correlated very precisely by use of the NRTL model (0.0022, 0.0034, 0.0068, 0.0035, respectively). The consistency of the COSMO-RS predictions was lower than the NRTL model (0.0247, 0.0107, 0.0222 and 0.1026, respectively), which is visible for the [OMIM][OAc] predictions. Nevertheless, predictive models open interesting opportunities. COSMO-RS predictions are based on the molecular structures of the

chemical compounds, which makes them easy to use for novel and structurally complex particles such as ILs. The COSMO model is available as a commercial product with a relatively expensive license.

### 3.6 Data regression

In correlating the LLE data, i.e., to minimize the difference between the experimental and calculated values of the endpoint on the tie-lines, the following objective function was used:

$$F(P) = \sum_{i=1}^n [x_2^{I exp} - x_2^{I calc}(PT)]^2 + [x_3^{I exp} - x_3^{I calc}(PT)]^2 + [x_2^{II exp} - x_2^{II calc}(PT)]^2 + [x_3^{II exp} - x_3^{II calc}(PT)]^2 \quad (3 - 23)$$

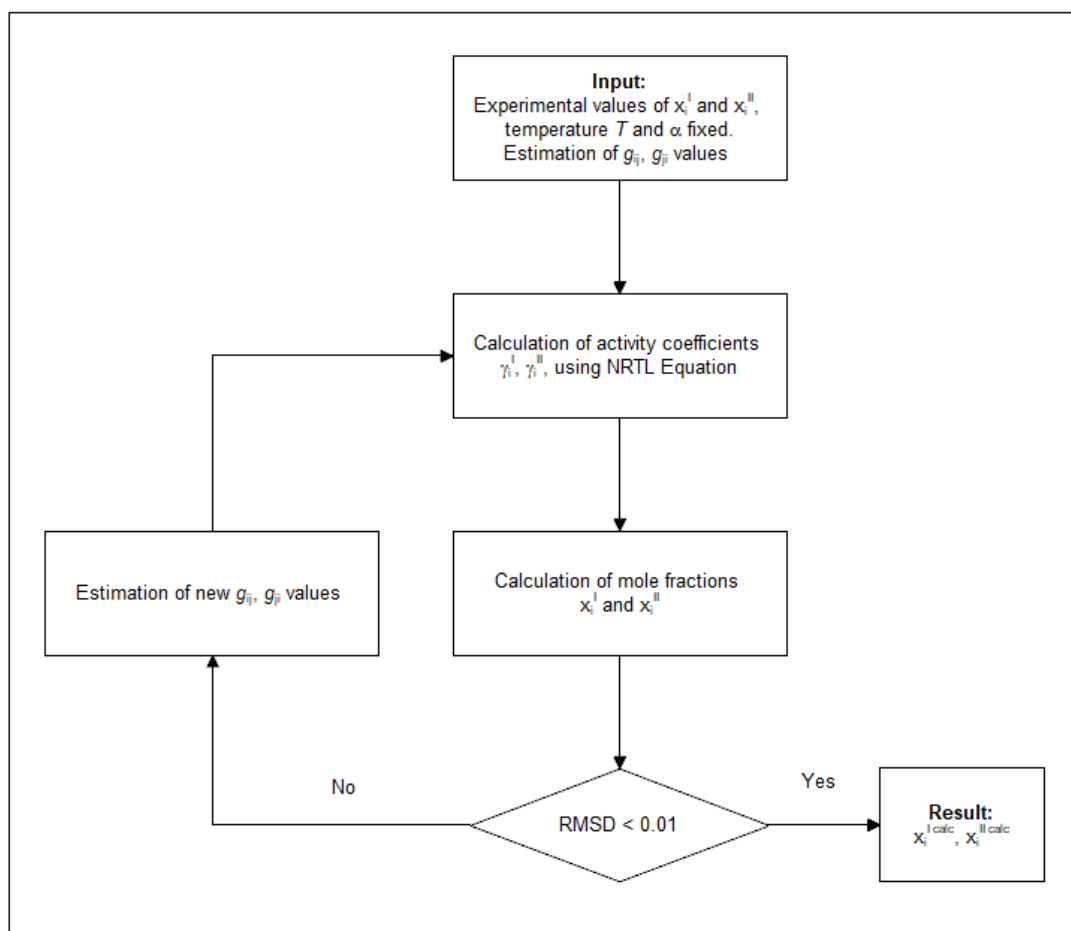
where  $P$  is the set of parameters vector,  $n$  is the number of experimental tie-lines,  $x_2^{I exp}$ ,  $x_3^{I exp}$  and,  $x_2^{I calc}(PT)$ ,  $x_3^{I calc}(PT)$  are the experimental and calculated mole fractions of one phase and  $x_2^{II exp}$ ,  $x_3^{II exp}$  and  $x_2^{II calc}(PT)$ ,  $x_3^{II calc}(PT)$  are the experimental and calculated mole fractions of the second phase.

Figure 3-4 shows the block flow diagram of the NRTL parameter fitting software operation. The first step of this procedure was the preparation of the file with experimental LLE data. This was followed by the system properties in which temperature and the value of the dimensionless independent parameter  $\alpha$  are introduced. Thereafter the fitting of the binary parameters was initialized. The main factor taken into account to determine the closeness of the correlation fit was the root mean standard deviation shown by:

$$RMSD = \left( \sum_i \sum_l \sum_m [x_{ilm}^{exp} - x_{ilm}^{calc}]^2 / 6k \right)^{1/2} \quad (3 - 24)$$

where  $x$  is the mole fraction, the subscript  $i$ ,  $l$ , and  $m$  are component, phase and tie-line, respectively, and  $k$  is the number of the tie-lines. If the root mean standard deviation (RMSD) was lower than 0.01, then correlation results were accepted. If the RMSD was far above 0.01, then the process was repeated by adjusting input values of Gibbs energy of the interaction between components parameters until the satisfactory results were achieved.





**Fig. 3-4** Flow diagram of the NRTL parameter fitting method.

### 3.7 Gas-Liquid chromatography technique

In general, chromatography is a technique that allows for the separation of the mixture components. Gas chromatography is a common method among analytical and physical chemists. The characteristic of this method is the use of an inert gas as the mobile phase, which is called the carrier gas. It allows for the separation of compounds that can be vaporized without decomposition easily. A very small amount of studied mixture is injected through a heated injection port, where components evaporate and are moved into the gas stream that continually flows through the stationary phase, locked in the form of so-called columns in the form of long tubes made of chemically inert non-adsorbent materials like steel or fused silica. The column is placed in an oven, which allows to control the temperature of the measurement.

The studied mixture is dissolved in the mobile phase, which acts as a carrier for the mixture components that go through the stationary phase. The stationary phase is chosen in the way that allows to achieve disparity of strength of interactions between different components and the stationary phase. Differentiation of the interactions allows for the separation of the mixture into individual components [<sup>173</sup>].

Two types of columns can be used in this method: packed and capillary. Packed columns, in most cases, are relatively short (the length does not extend beyond 2 meters) and have approximately 2 to 5 mm of inner diameter. This type of column can be made easily from stainless steel tubing and prepared in the laboratory by the use of fine porous material as solid support for the stationary phase [<sup>158</sup>]. Packed columns were used during measurements for this work to obtain data of activity coefficients at infinite dilution.

Capillary columns are the second type of column used in gas chromatography. These columns are characterized by the length that could reach even 100 meters and very small diameters in the order of fractions of a millimetre. This type of column allows for the separation of very complex mixtures that contain many components. Capillary columns are more expensive than packed ones, but they can offer a higher resolution of data gathered by their usage [<sup>174</sup>]. In this work, the capillary column was used in determining the sample compositions during liquid-liquid equilibria measurements.

The difference in the strength of interactions between various components and the stationary phase enables the separation of the components of the initial mixture which

reach the end of the column with different so-called retention times, measured by the detector at the end of the chromatographic line. Besides the retention time, separated vapours of mixture ingredients, which reach the detector produce "peaks" on chromatograms (charts produced by chromatograph software). Peaks show the response of the detector as a function of time and provide useful information about interactions between mixture components and stationary phase and amounts of those components in the sample.

There are several types of detectors. The most popular and also used during this work is the thermal conductivity detector (TCD) and a flame ionization detector (FID). The TCD also called a katharometer, is designed to sense changes in the thermal conductivity of the effluent. Considering the thermal conductivity of the carrier gas stream as a reference value, then any additional chemical compound in the stream will change the thermal conductivity of effluent. This change causes the change of the temperature of the tungsten-rhodium filament, an increase of filament temperature, and fluctuations of the voltage, which produces the signal. As long as the thermal conductivity of the studied substance is lower than the thermal conductivity of carrier gas, the TCD will produce a signal. Helium, hydrogen, or nitrogen can be used as a carrier gas and is versatile for a wide range of systems. It is related to relatively high values of thermal conductivity of the mentioned gases [<sup>173</sup>].

The FID is not universal as the TCD, but it offers higher resolution and increased sensitivity of signal, especially for carbon compounds. Molecules of organic compounds are combusted in the hydrogen flame, and then newly created ions are detected by two electrodes. A positively charged electrode also plays the role of a nozzle, whereby the flame combusts the effluent, while a tubular-shaped negatively charged electrode (also known as the collector plate) is placed above the flame. Positively charged ions are attracted to the collector plate and induce the current in contact with the surface of the electrode. A high impedance picoammeter detects current changes and feeds this to the integrator, which summarizes and processes the data to be displayed. The measured current is proportional to the number of carbon atoms reduced in the hydrogen flame, which allows the gathered data to be used to calculate concentrations of components in the initial mixture [<sup>173</sup>].

### 3.8 $\gamma_{13}^{\infty}$ via gas-liquid chromatography

The most common measurement method of activity coefficients at infinite dilution is gas chromatography. Everett's equation developed in 1965 [175] and expanded in 1966 by Cruickshank et al. [176] has been used to calculate values of  $\gamma^{\infty}$  by various researchers since 2001. Previously this methodology was assumed only for ideal carrier gases. Still, Cruickshank's extension enabled its use to non-ideal carrier gases, which was possible by application of virial coefficients as a way to estimate molar vapour volumes for the imperfect gas mixture. The equation developed by Everett is:

$$\ln(\gamma_{13}^{\infty}) = \ln \frac{n_3 RT}{V_N P_1^0} - \frac{(B_{11} - v_1^*) P_1^0}{RT} + \frac{(2B_{12} - v_1^{\infty}) J_2^3 P_0}{RT} \quad (3 - 25)$$

where indices 1, 2 and 3 are solute, carrier gas and solvent respectively and  $B_{11}$  and  $B_{12}$  are second virial coefficients for pure solute and for pure solute and carrier gas, respectively. The equation for the solute retention volume was given by Letcher in 2001[177]:

$$V_N = \frac{q_{ov}(t_R - t_G)}{J_2^3} \quad (3 - 26)$$

$t_R$  and  $t_G$  are retention times of solute and inert gas (air), respectively. The increase in the measured retention time is strongly correlated with the decrease in the value of the limiting activity coefficient, which is responsible for the increase of the strength of the interaction between solute and the IL.

The pressure correction term is given by the equation:

$$J_2^3 = \frac{2}{3} \left[ \frac{\left(\frac{P_{in}}{P_0}\right)^3 - 1}{\left(\frac{P_{in}}{P_0}\right)^2 - 1} \right] \quad (3 - 27)$$

where  $P_{in}$  and  $P_0$  are the column inlet and atmospheric pressure, respectively.

The parameter  $q_{ov}$  is the correction value for the flow obtained generally by the use of a bubble flow meter. This parameter allows for the change in water vapour pressure

as dependence on atmospheric pressure and temperature. The equation for  $q_{ov}$  is presented as:

$$q_{vo} = q_v \left( 1 - \frac{P_w^0}{P_o} \right) \frac{T}{T_s} \quad (3 - 28)$$

$q_v$  is flow reported on the gas chromatograph,  $P_w^0$  is the saturated pressure for water at surrounding temperature  $T_s$ ,  $P_o$  is atmospheric pressure, and  $T$  is column temperature.

Equation (3-21) shows that the activity coefficients at infinite dilution can be used to calculate the partial molar excess thermodynamic functions:

$$\ln \gamma_{13}^\infty = \frac{\Delta H_1^{E,\infty}}{RT} - \frac{\Delta S_1^{E,\infty}}{R} \quad (3 - 29)$$

Short-range temperature dependence may be shown in the form of the linear van't Hoff relation:

$$\ln \gamma_{13}^\infty = a/T + b \quad (3 - 30)$$

where the partial molar excess enthalpy,  $\Delta H_1^{E,\infty} = Ra$ , and entropy  $\Delta S_1^{E,\infty}$  at infinite dilution can be obtained from the slope and intercept. The expression for the excess Gibbs energy at infinite dilution is given by the formula:

$$\Delta G_1^{E,\infty} = \Delta H_1^{E,\infty} - T \Delta S_1^{E,\infty} \quad (3 - 31)$$

The gas (G) - liquid (L) partition coefficient shown by equation  $K_L = (c_1^L/c_1^G)$  where  $c_1^L$  and  $c_1^G$  represent the equilibrium solute concentration in the liquid and the vapour phase, respectively, describes a solute partitioning between a carrier gas and the stationary phase and can be calculated from the solute retention [<sup>96</sup>]:

$$\ln(K_L) = \ln \left( \frac{V_N \rho_3}{m_3} \right) - \frac{P_o J_2^3 (2B_{12} - V_1^\infty)}{RT} \quad (3 - 32)$$

where  $\rho_3$  is the density of the IL,  $m_3$  is the mass of the IL and  $V_1^\infty$  is the partial molar volume of the solute at infinite dilution in the solvent.

## Chapter 4 Experimental method

This chapter presents the literature review of the equipment and techniques used for the measurement of activity coefficients at infinite dilution  $\gamma_{13}^{\infty}$  and liquid-liquid equilibria. In addition, the precise description of the methodology used for the measurements of systems with ILs selected in this study is also explained. The first section describes the equipment, column preparation and methodology of  $\gamma_{13}^{\infty}$  measurements. The second section describes the LLE measurements, preparation of calibration curves, mixing procedure and analysis of separated phases used to obtain tie-line data for different concentrations of the components in the ternary systems.

### 4.1 Activity coefficients at infinite dilution, $\gamma_{13}^{\infty}$

#### 4.1.1 Review of experimental methods

To obtain retention data and calculate the activity coefficients at infinite dilution, two types of methods can be used. These are the direct experimental approach and indirect extrapolations. Direct methods are based on the inert carrier gas flow or the measurements of differential vapour-liquid equilibrium in the dilute concentration range. The first of these approaches gathers different chromatography techniques as Gas-Liquid Chromatography (GLC) described in this work, Non-Steady-State GLC (NSGLC), and Gas Stripping.

Non –Steady-State GLC method was developed and described in 1972 by Belfer [178]. The major difference between GLC and NSGLC methods is the preparation of the column. In the GLC method solvent is dispersed evenly on the chemically inert porous material during the preparation of the column before the experiment, while in the NSGLC method the column is filled with the inert porous material and a solvent is injected on the head of the column during the measurement. A solvent is slowly removed from the column while the solute is rapidly injected on the head of the column, which results with a decreasing retention time of the solute. The value of  $\gamma^{\infty}$  is related to the solvent and the solute vapour pressures ratio and the decrease of the solute retention time. Fig. 4-1 shows a schematic representation of this method. The following steps of the measurement procedure are:

- 1 Injection of the solvent into the injection port. Vaporised solvent fills the column.
- 2 Condensation of the solvent vapours on the walls of the column and the solid support. Start of the elution.
- 3, 4 Continuous elution of the solvent and saturation of the carrier gas. In these steps, solutes are injected into the injection port.
- 5 All of the solvent eluted from the column.

Belfer et al. used the described method in 1984 [<sup>179</sup>] to calculate activity coefficients at infinite dilution for the series of compounds in acetonitrile at 298.15 K, series of solutes in octane at 313.15 K and 333.15 K and benzene and heptane in octadecane at 333.15 K. This work was continued in 1990 and 1991 by Belfer and his associates [<sup>180,181</sup>]. The latest article which used this method was published in 2005 by Dohnal et al. [<sup>182</sup>]. In this work, the NSGLC method was used to calculate limiting activity coefficients of a series of short-chained alcohols in water.

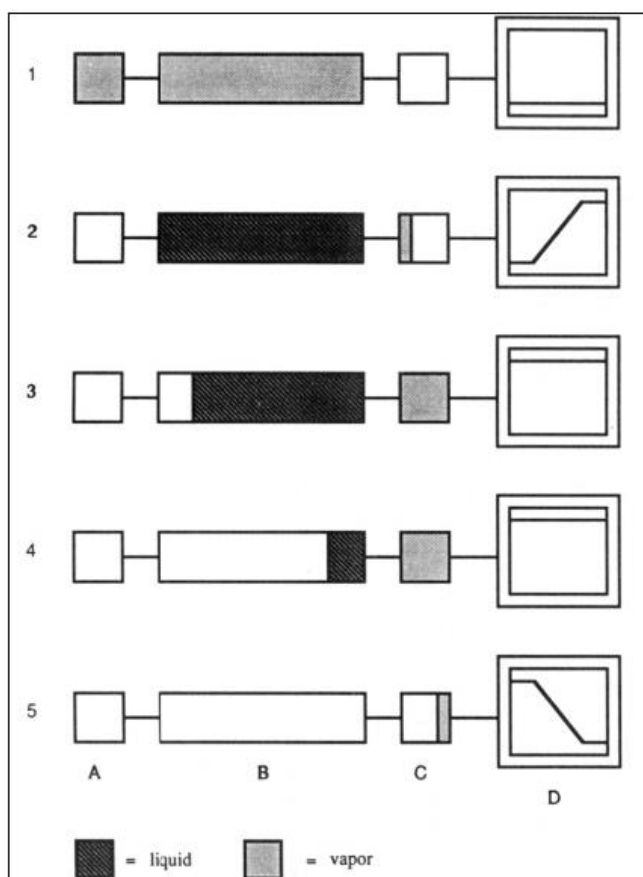


**Fig. 4-1** Schematic representation of the NSGLC method. A is the injection port, B is the GC column, C is the TCD detector and D is a recorder [<sup>181</sup>].

The gas stripping or so-called dilutor technique is another direct experimental technique of the activity coefficients at infinite dilution measurement. This method is based on the removal of the highly diluted solute by a constant stream of inert gas at isothermal conditions. To obtain values of the  $\gamma^\infty$  the change of the composition of the vapour phase in time measured by the gas chromatograph is used. Very important for this method is strict control of the system equilibrium to ensure the correctness of the results [183]. The first use of this method was published in 1962 by Fowles and Scott [184]. In their work dilutor was used for calibration of the macro-argon detector which contained radioactive strontium-90. The dilutor technique was used for the first time to calculate activity coefficients at infinite dilution in 1977 by Lerol et al. [185]. In their work values of the  $\gamma^\infty$  were measured for the series of solutes in two solvents: hexane and benzene. Fig 4-2 shows a schematic diagram of the dilutor cell used by Krummen et al. [183]. One of the greatest advantages of the gas stripping method is the possibility of using it for the determination of the limiting activity coefficients not only for pure components but also for the mixtures of solvents, i.e., N-methyl-2-pyrrolidone and N-formylmorpholine with water [186]. According to Kojima et al. [187], the dilutor method is a very good method for measurements of the systems with high values of  $\gamma^\infty$ . The main drawback of this method is its limitation to volatile solutes [188,189].

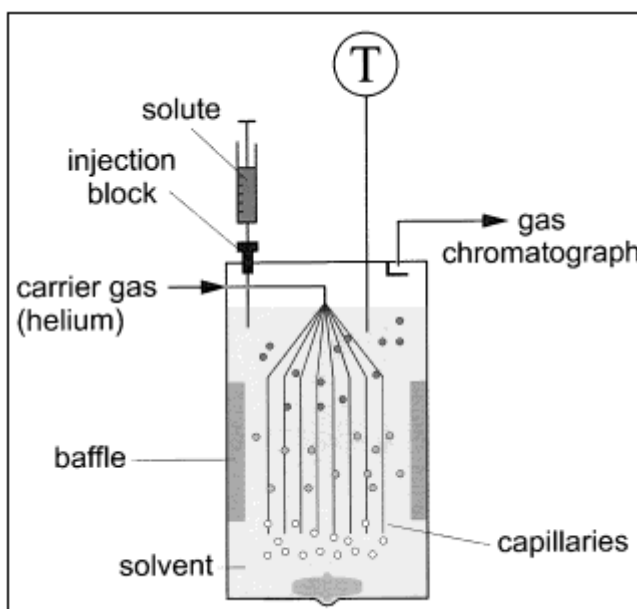


**Fig. 4-2** Schematic of the dilutor cell [183].



The second approach to the measurement of activity coefficients at infinite dilution is the usage of the differential vapour-liquid equilibrium. The most popular method based on this idea is differential ebulliometry, which may be defined as a measurement of the differences between boiling points of the pure solvent and solvent with highly diluted solute measured under isobaric conditions. Unfortunately, the accuracy of this method for high viscosity solvents, i.e. ionic liquids or systems with high relative volatility is questionable [187]. The beginning of differential ebulliometry dates back to 1925. Świątosławski designed the first ebulliometer based on the Cottrell pump and published his work in 1945 [190]. The first values of activity coefficients at infinity dilution obtained with the use of this method were published in 1955 by Gautreaux and Coates [191]. During the 20<sup>th</sup> century, ebulliometers were modified in many ways, mostly by adding insulation to minimize the temperature fluctuations and by changes to the heater design [169]. The most significant modification of Świątosławski's ebulliometer was presented by Scott in 1986 [192] who reinvented Świątosławski's idea, by resigning from Cottrell pump in favour of a very well stirred 500 ml round bottom flask which allowed the reduction of temperature fluctuations. An additional advantage of the new ebulliometer design was the possibility of usage of higher amounts of the solvent, which allowed for the reduction of the composition errors.

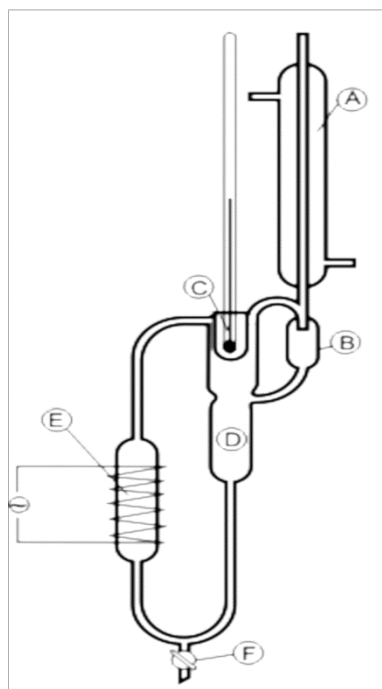


**Fig. 4-3** Schematic of the Świątosławski ebulliometer. A – reflux condenser, B – dropper, C – thermometer nest, D- bubble, E – heated tank, F – drain valve [193].

Vapour-liquid ebulliometry is still a popular technique for the measurement of limiting activity coefficients. In recent years, the methods described in the literature focus mostly on values of activity coefficients at infinite dilution for mixtures of volatile compounds such as alcohols, i.e., in recent years data for mixtures of dichloromethane and 1-alkanols [<sup>194</sup>], polystyrene and butan-2-one [<sup>195</sup>], water and oxygenated solvents (alcohols, ketones, ethers, etc.) [<sup>196</sup>] and alcohols with octane, ethyl acetate and butan-2-one [<sup>197</sup>] have been published.

#### 4.1.2 Review of the GLC method

The fundamentals of the gas-liquid chromatography (GLC) method used in this study are described in sections 3.7 and 3.8. While the former shows a general idea of chromatography as an analytic method, the latter discusses physicochemical principles of this method and the direct way to obtain activity coefficients at infinite dilution data by use of chromatography.

The GLC method is widely recognized as a convenient method for  $\gamma_{13}^{\infty}$  measurement. This statement is substantiated by the fact that all of the literature data gathered and presented in table 2-1 were measured via this technique. The references are available in the last column of the mentioned table.

The Thermodynamics Research Unit at the University of KwaZulu-Natal has successfully used the described technique in previous years [<sup>177,198,199</sup>]. The GLC method was used to establish values of the activity coefficients at infinity dilution for 28 solutes in 1-ethyl-3-methylimidazolium 2-(2-methoxyethoxy)ethylsulfate [EMIM][MDEGSO<sub>4</sub>] [<sup>200</sup>] and the limiting activity coefficients for 31 solutes in trihexyltetradecylphosphonium hexafluorophosphate [<sup>201</sup>].

#### 4.1.3 Description of the apparatus

Measurements of retention times required for calculations of the activity coefficients at infinite dilution,  $\gamma_{13}^{\infty}$ , were made with the use of a Shimadzu GC-2014 Gas Chromatograph, with helium as a carrier gas and equipped with thermal conductivity

detector (TCD). The oven was modified and fitted with a steel column of 1 m length and 4.52 mm inner diameter. The column was filled with a stationary phase dispersed on a solid support (Chromosorb W\_HP 100/120 mesh). The stability of the flow rate was checked on an ongoing basis using a bubble flow meter. A 10 $\mu$ l SGE Analytical Science microsyringe was used to inject solutes into the injector port. A schematic of the gas-liquid chromatography setup used for this work is presented in Fig. 4-4.

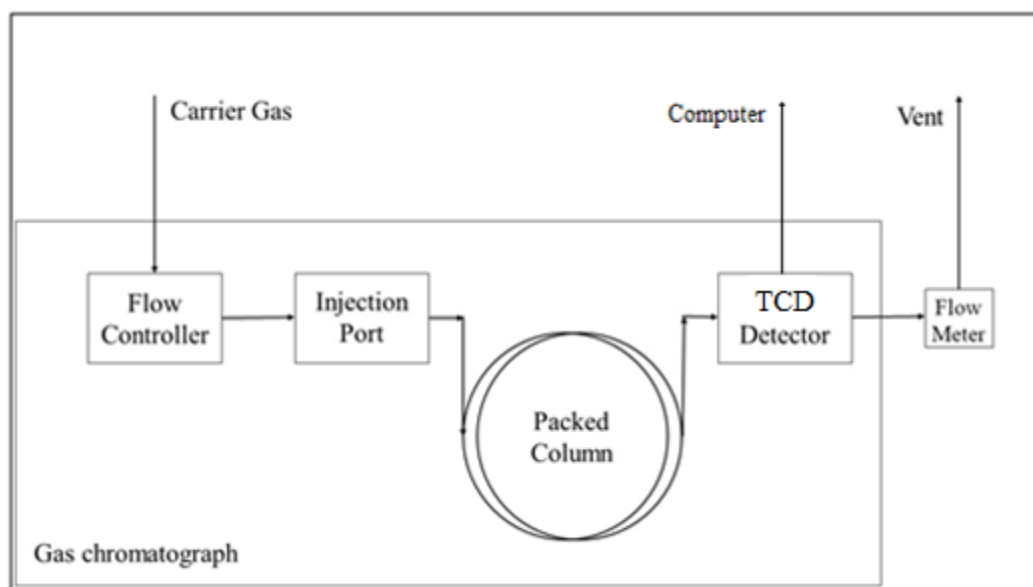


**Fig. 4-4** Schematic of the gas-liquid chromatography setup used for measurements.

#### 4.1.4 Methodology used in this study

The water content was analysed by the Karl-Fischer Moisture Titrator MKS 500. The sample of ionic liquid was dried for 72 h at a temperature of 353 K under lower pressure ( $\sim 0.35$  atm.), to remove volatile impurities and trace amounts of water. During this time, two stainless steel columns were thoroughly washed and dried. Known amounts of solid support and ionic liquid (stationary phase) were added into a 250 ml round bottom flask with the addition of 50 ml of dichloromethane (DCM), which was used as a low boiling solvent, allowing the stationary phase to be evenly dispersed on the solid support. The contents were dried for additional time to make sure that the mass of the flask reached the same mass as before the addition of dichloromethane. The masses of the stationary phase and solid support were weighed using an Ohaus PR Series analytical balance with a precision  $\pm 0.0001$  g. Two columns were prepared with approximately 30% and 40%

mass per cent of ionic liquid, respectively. The relatively high percentage of the stationary phase was used to prevent the possibility of the residual adsorption of the solutes onto the chromosorb, which could increase the retention time for the long-chain hydrocarbons and significantly influence the results. Repeatability of retention times for multiple runs and symmetrical peak shapes proved that chosen loading percentages provided proper coverage of the surface of the chromosorb. Two separate columns with a different mass ratio of the IL to the chromosorb were prepared to ensure consistency of the results obtained by the use of this method [<sup>202</sup>].

The stationary phase was then transferred into the 1 m length and 4.52 mm inner diameter stainless steel column by the use of the funnel. The most important part of this procedure was to be certain that the chromosorb with adsorbed ionic liquid was packed well without any empty spaces inside the column, as this could influence the results of the measurements with a faster retention time of solutes. Consistency of the column filling process was achieved by blocking one end of the column followed by slow addition and tapping of the stationary phase inside the column. Thereafter, the previously straight column was bent to the shape of the spiral such that this could be fitted into the GC oven. Once installed, the column was left in the heated GC oven, where it was flushed with carrier gas for at least 1 hour. This process, called conditioning, allows removing any traces of water or impurities from the air that could create interferences during the measurements, as a baseline noise.

A stable carrier gas flow is very important for achieving accurate results. To ensure a constant flow rate, three measurements were performed hourly using a bubble flow meter, followed by averaging to minimise human error. Using equation (3-27), readings from the bubble flow meter were corrected to account for the influence of atmospheric pressure and ambient temperature on the bubble behaviour.

The following steps were performed for the measurement of activity coefficients at infinite dilution:

- I. The chromatograph was switched on. The flow of the carrier gas was set. Temperatures of the oven, detector, and injector of the GC were set as well. The injector port and the detector temperatures were set to 523.15 K. The oven temperature ranged from 323.15 K to 373.15 K depending on the measurement settings.

- II. The GC was left to heat up upon which the detector was then switched. The system was left for a further 30 min to ensure that the baseline was stable and the apparatus was ready.
- III. After equilibration of the GC detector baseline, the flow rate was measured using a bubble flow meter. This was repeated hourly. Thereafter, 1  $\mu$ l of the solute and 9  $\mu$ l of the air were injected through the injection port. Air peaks retention times were used as a reference for calculation of the net retention time of the solutes. This procedure was repeated for all solutes listed in the Table 5-1 at a given temperature. Addition of air peak allowed to marginalise errors, which are created by delayed retention times. This means that retention time is extended by so-called dead time, in which solutes evaporate in the injection port before they reach the top of the column. Each solute was tested three times.
- IV. Once measurements were completed for the entire temperature range, the GC detector was switched off. The temperature settings were then set to 25°C, and the unit was left to cool.
- V. When the temperature of the detector was below 50°C, this was deemed safe to switch off the carrier gas flow.
- VI. After each day of measurements the column was weighed using an Ohaus PR Series analytical balance with a precision  $\pm 0.0001$  g, to ensure stability, and no change in the mass of ionic liquid. If there was a change in the mass of stationary phase, then the column had to be prepared again.

The temperature of the injection port was set to ensure that the solutes were in the gaseous phase before they reached the column. Each solute was studied at five different temperatures. To ensure that the results obtained with the method described were correct, a second column with a higher stationary phase concentration was installed. Therefore, the results obtained with the use of both columns were compared. The autosampler was not used. It was not possible to run the sample injections using the autosampler since the retention times of the solutes varied significantly, and it was more efficient in terms of time and carrier gas consumed to follow the baseline on an ongoing basis and respond to emerging peaks.

The final uncertainty of the results was estimated at  $\pm 5\%$ , taking into account the possible uncertainties in determining the column loading ( $\pm 0.1\%$ ), the retention times ( $\pm 0.1\text{s}$ ), and solute vapour pressure ( $\pm 1\text{ Pa}$ ).

## 4.2 Liquid-liquid equilibria

### 4.2.1 Review of experimental methods

Liquid-liquid equilibrium experiments can be performed by the use of the three main methods: the titration, the laser-light scattering or through the direct analytical method.

The titration method is based on the principle of continuous addition of the solvent to the known amount of the mixture comprising components miscible without limits. The equilibrium point is determined by the appearance or disappearance of turbidity (so-called cloud point). The knowledge about the amount of the individual components in the equilibrium point allows for the construction of the binodal curve. To determine experimental tie-lines, additional analytical techniques must be used. More detailed information about this technique can be found in the literature [<sup>203–205</sup>].

The laser-light scattering technique is used as an improvement of the titration method. The exact determination of the turbidity change may be a cause of the discussion as it depends on the researcher perception. In 1993 Benjamin et al. [<sup>206</sup>] developed an apparatus shown in fig. 4-5. The sensor detects a change of the scattered light intensity and the experimental cloud point is determined by the use of the plot of scattered light intensity versus temperature.

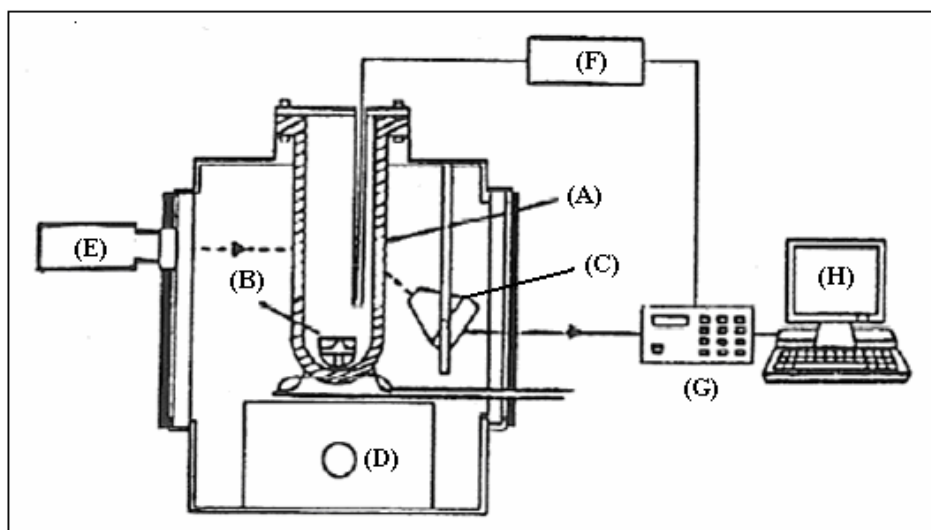


**Fig. 4-5** Schematic of the apparatus used for mutual solubility measurements with laser-light scattering technique [206]. A – equilibrium cell, B – stirring element, C – light sensor, D – magnetic stirrer, E – optical system, F – thermometer, G – digital multimeter, H – computer.

The last of the mentioned methods of LLE study is the direct analytical method used in this work and is described step by step in the following sections. In this method, the isothermal cell is filled with two immiscible phases. The content of the cell is stirred for a given time to ensure that equilibrium is established and then the cell is left for a sufficient time to allow for proper separation of both phases. Samples of both phases are withdrawn, and then concentrations of the components are analysed by the use of methods mentioned in the following section.

The design of the equilibrium cells is very important for the proper performance of the direct analysis method. A variety of design solutions must be taken into consideration. One of the most important concerns is to provide isothermal conditions. This may be achieved in two ways. The first is the use of cells without a jacket, which must be fully submerged in the thermo-controlled bath to ensure the stable temperature of the experiment. In contrast, the second type has a jacket, which allows for a flow of the heating or cooling medium around the equilibrium cell.

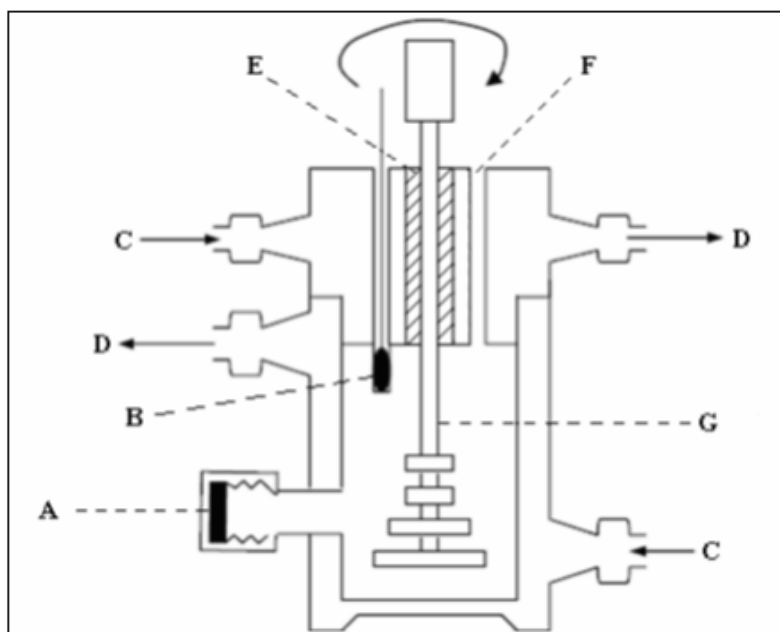


**Fig. 4-6** Diagram of Ndlovu's LLE cell <sup>[207]</sup>. A – sample point for denser liquid phase, B – temperature sensor in a thermo-well, C – heating medium inlet, D – heating medium outlet, E – Teflon coated bar, F – sample point for lighter liquid phase, G – stirrer driven by DC motor.

Stirring is another very important factor, which is responsible for the proper distribution of both phases and the development of the interface area. The well-developed interface is crucial for the efficiency of the extraction process. Design of the cell published by Raal and Brouckaert <sup>[208]</sup> was modified by Ndlovu <sup>[207]</sup>. Modified cell is shown in the fig. 4-6 uses a mechanical stirrer which ensures proper mixing of both phases, especially in the cells of higher volume. An additional advantage of this type of mixing is better agitation of the more viscous liquids. Another popular solution of the stirring problem, useful mostly for the smaller cells is the usage of the Teflon coated agitators and magnetic stirrers. The schematic of the cell used in this work is shown in the fig. 4-7. This relatively small cell contains 10 ccm of the liquid, and its sizes are 68 mm of height and 28 mm of the external diameter. Small sizes of this vessel allow to use one agitator, which will mix the liquid in the whole volume of the cell.

The biggest disadvantage of the cell shown in figure 4-7 is the lack of probing point for the temperature sensor. This generates additional problems, as the exact temperature of the mixture in the cell cannot be determined. To solve this problem, two separate thermocouples were used. The first one measured temperature of the heated bath, while the second one measured the temperature in between four cells clipped together to



create a cuboid cluster. This method also allowed to save space in the laboratory as one magnetic stirrer was able to mix four independent samples at this same time.

The last factor that should be taken into consideration is sample withdrawal. In the design of the cell shown in Ndlovu's work two separate sampling points are available, one for each phase. This solution is convenient and does not require any additional equipment. Design of the cell used in this work has only one point of entry, which is septum placed in the cup of the cell. It requires longer needles to withdraw a sample from the bottom phase.

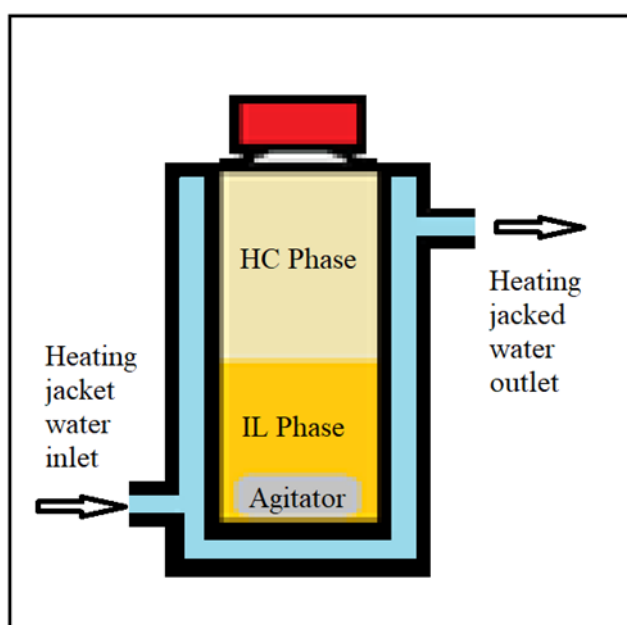


**Fig. 4-7** Diagram of a single measuring 10 ccm cell with a water jacket, height of the cell is 68 mm, and the external diameter is 28 mm.

Further modifications of the Raal and Brouckaert's cell lead to the vessel shown in figure 4-8. In this case, the mechanical stirrer was replaced by Teflon coated magnetic agitator. Cells of this design were used at Thermodynamics Research Unit in earlier years by Narasigadu et al. [209] and Mungar Ram et al. [210]. The biggest disadvantage of this cell is its size. The bulky jacket creates additional issues to gain proper access to both phases and the proper submersion of the temperature probe. Dedicated sampling ports and thermo-well must be introduced during the manufacturing process, which makes this process more complicated. To decrease consumption of the ILs and therefore costs of the measurements cell design presented in fig. 4-7 was chosen.

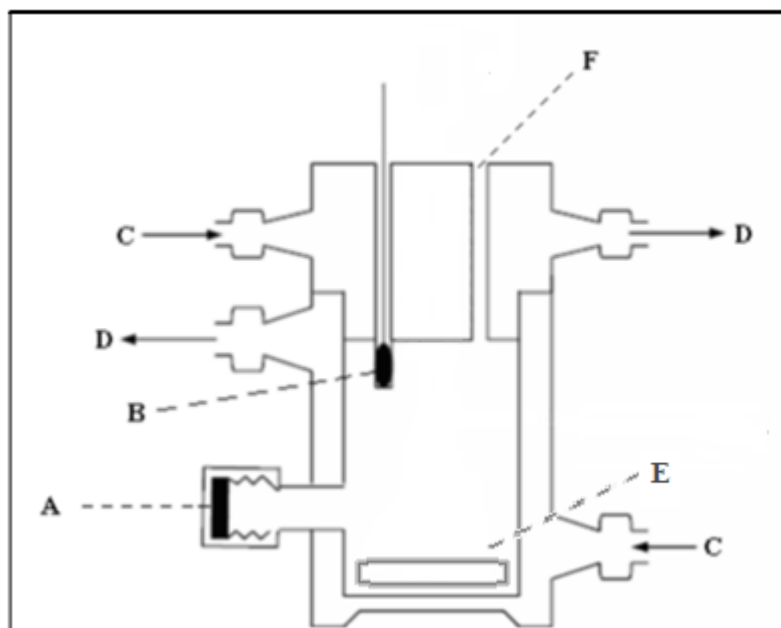


**Fig. 4-8** Diagram of modified Ndlovu's cell used in TRU by Narasigadu et al. [209]. A – sample point for denser liquid phase, B – temperature sensor in a thermo-well, C – heating medium inlet, D – heating medium outlet, E – Teflon coated magnetic agitator, F – sample point for the lighter liquid phase.

#### 4.2.2 Review of analytical methods

To determine concentrations at the ends of the experimental tie-lines, a variety of 3 to 4 of methods are commonly used. One of the most popular and versatile methods, used in this work is the usage of the internal standard and co-solvent described in the following sections. Different techniques may then be used to analyse mixtures obtained after mixing and equilibration processes. The most popular methods are Gas Chromatography (GC) described in this work, High-Performance Liquid Chromatography (HPLC) and X-Ray Fluorescence Spectrometry (XRF).

HPLC is relatively similar to the GC method. The difference between these two techniques is the use of liquid as a mobile phase. A sample is dissolved in the HPLC grade solvent, i.e., methanol, DMSO or tetrachloromethane and then injected to the pressurised stream of the mobile phase. Differences of the intermolecular strength between column filling and the components of the mixture are responsible for the separation of the mixture. The column filling is in the form of the granular porous material with developed surface

area (i.e. silica or polymer). Then separated compounds are directed to the detector as in the GC method. According to Dong [211], HPLC is less efficient and more difficult for an unexperienced user than gas chromatography.

High-Performance liquid chromatography is derived, and it is an extension of the liquid chromatography (LC), and its origins date back to the '60s. The development of this technique is inextricably linked with the development of biotechnology, as LC analysis was time-consuming and separations of more complex mixtures took many hours or even day and methods of the gas chromatography were not suitable for the study of the high mass, polarised particles of the biopolymers [212].

Over the years, this method has been used in many areas. HPLC allowed biotechnologists to study the exact composition of the DNA bases [213] or to separate enantiomers of the chiral compounds [214]. Geologists adapted HPLC to study traces of amino acids [215] and fullerenes [216] in the geological samples.

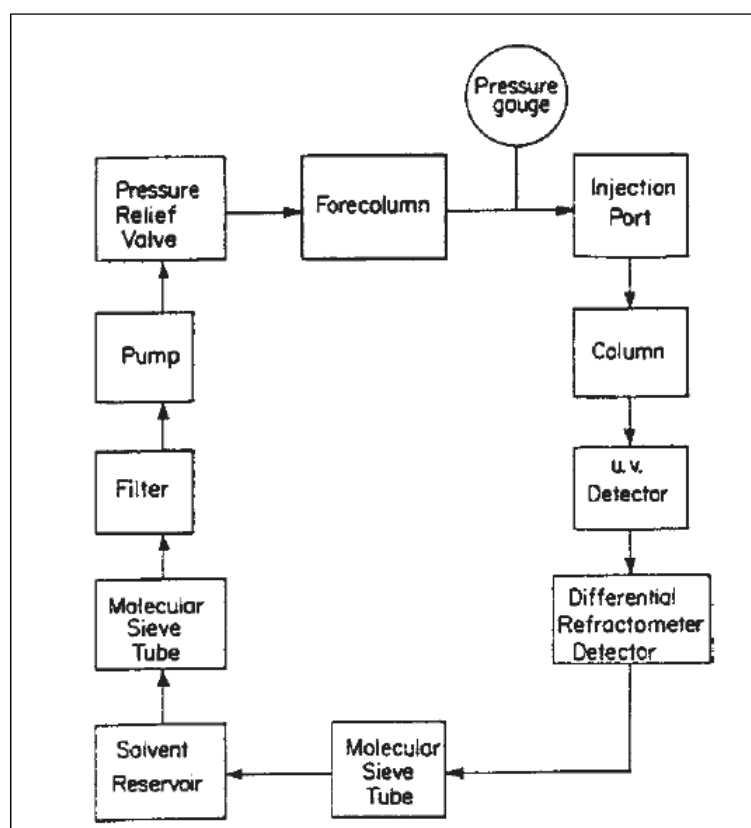


**Fig. 4-9** Block diagram of the HPLC apparatus with UV and refractometer detectors [212].

X-Ray Fluorescence Spectrometry, unlike the methods mentioned before, is not based on the separation of the mixture by use of a chromatographic column. In the case of XFR analysis is based on the detection of the characteristic, so-called fluorescent radiation of the material bombarded with high-energy gamma rays. Atoms are excited by the X-ray spectrum radiation, which means that electrons from the inner orbitals may be expelled. This causes instability of the electron's structure of the atom. An electron from the higher orbital "falls" to the lower one to ensure a more stable electron's structure. This process releases a photon of the energy equal to the difference between higher and lower orbitals. Each element has different characteristic energy of the electron "fall", which is base of the analysis of the samples. For more detailed information reader is referred to the literature [217].

According to Wobrauschek [218], XRF Spectrometry is used in many fields of science. Environmental study, i.e. water, air, soil and organic material such as food or plant material, can be conducted by the use of this technique. Mineralogy and medicine also use XRF for the sample analysis. Oyedotun [219] published a review paper about the use of XRF in geological studies. In this work, the method mentioned was used to establish amounts of the different elements in the sediments from South West England.

Gas Chromatography is widely used to analyse LLE data for the ILs containing systems. As a versatile, relatively simple method with good repeatability, this technique is used worldwide. The internal standard method, described in this work, was successfully used by many scientists [100,115,115,122,129,132,135].

In the previous years, the Thermodynamic Research Unit of the University of KwaZulu-Natal published papers, where GC was used to obtain data for the LLE systems such as short-chained alcohols + water + dodecane [220], short-chained alcohols + water + acetonitrile [209] or alkylsulfate-based ILs + ethanol + dodecane [210].

#### 4.2.3 Methodology applied in this study

LLE measurements for two-phase mixtures containing hydrocarbon, thiophene, and IL were carried out using glass cells, fitted with heating jackets each with a capacity of 10 cm<sup>3</sup> and equipped with the polymer-coated magnetic stirring element. Size of the agitator and stirring speed were chosen to provide proper mixing of both phases. The cells designs used were that reported by Ndlovu [207] though the volumes were reduced due to

the quantities of available ILs. The jacketed cells were connected to a thermostatic water bath (PolyScience temperature controller) to maintain a constant temperature  $T = 308.15$  K ( $\pm 0.1$ ). Analysis of the phases was performed using a Shimadzu GC-2010 gas chromatograph equipped with an FID detector and Elite-5MS Perkin Elmer capillary column. Nitrogen was used as a carrier gas, hydrogen and air were supplied to provide stable operation of the detector.

#### 4.2.4 Equipment used in this study

Four jacketed equilibrium cells, connected to PolyScience Temperature Controller and water bath and equipped with polymer-coated magnetic stirring elements were placed on the stirring plate and filled with 2 ml of IL. To two of them, thiophene was added. The remaining two were filled with octane and hexadecane, respectively. Each sample was agitated for 6 h and allowed to settle down for another 12 hours at a constant temperature to ensure complete mixing of both phases and then their complete separation in isothermal conditions. After the withdrawal of the samples from each cell, an additional amount of chemicals were added. Both vessels with hydrocarbons were supplemented with small doses of thiophene, while one of the cells containing thiophene was replenished with octane and another one with hexadecane. This approach a series of balance chords to be obtained, starting with binary mixtures. The vessels were sealed with septa to prevent moisture and other possible impurities from the atmosphere entering the cell and to prevent losses of mixtures components by evaporation. Two calibrated temperature sensors were used to control the thermal stability of the setup. Both sensors were submerged in the WIKA CTB9100 micro calibration bath, and their readings were compared with the certified thermometer WIKA CTH6500. Calibration curves charts and linear equations used to obtain real values of the temperature are presented in Appendix B. One of the thermocouples was placed in the water bath to control the temperature of the water, which goes into cells jackets. The second thermocouple was attached to the last cell, to control the temperature of the water at the end of the cells line. The temperature was controlled to ensure that all mixtures were mixed at this same conditions. Results were obtained at 35°C. Figure 4-10 shows a schematic diagram of the equilibrium setup used during this study.

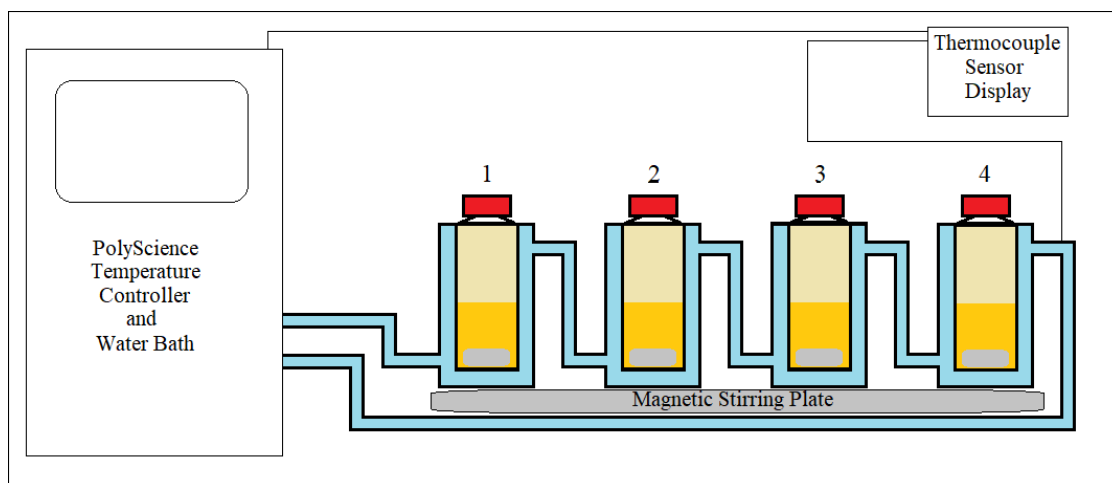


**Fig. 4-10** Schematic of the equilibration setup used during the preparation of the LLE data samples.

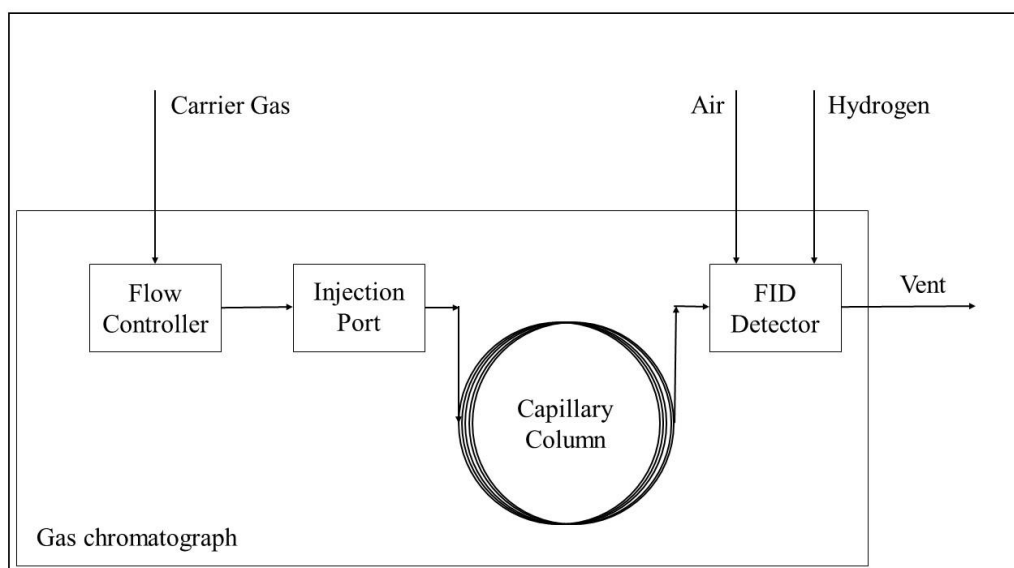


**Fig. 4-11** Schematic of gas chromatography setup used for liquid-liquid equilibrium measurements.

#### 4.2.5 Sample withdrawal

For the preparation of the samples for analysis via chromatography, 0.1-0.3 cm<sup>3</sup> of each phase were withdrawn by the use of disposable plastic syringes and placed in separate 2 cm<sup>3</sup> glass vials of known masses, sealed with a septum. Each vial with the sample was weighed with the precision of  $\pm 0.0001$  g, and to each one of them, 1 cm<sup>3</sup> of

an internal standard prepared by mixing of 5 ml of chosen standard and 95 ml of co-solvent, were added. 2-pentanone was used as a standard, while 1-propanol served as co-solvent. Both chemicals were used because of their retention times and lack of peak overlapping with the components of the studied mixtures. The addition of the internal standard provided reference compound for chromatography measurements and also prevented the mixture from separating, acting as a co-solvent. Vials with samples of the phases and standard mixture were weighed again. Differences of masses between each step were used to calculate molar fractions of components of the samples, which allowed to obtain tie-lines data for the liquid-liquid equilibria.

#### 4.2.6 GC method

Table 4-1 shows the column and method used during LLE measurements. An Elite-5MS capillary column supplied by Perkin Elmer was used as the most suitable column. It allowed for the analyses of all components for both the octane and hexadecane systems, as well as the good separation of the peaks for all of the mixture components.

**Table 4-1** Gas chromatograph operational conditions for compositional analysis of the equilibrium phases.

Element	Characteristic	Description
Column	Type	Elite-5MS Perkin Elmer (1,4-bis(dimethylsiloxy)phenylene dimethylpolysiloxane), length 30 m, inner diameter 0.25 mm, film thickness $\mu\text{m}$
	Flow	$1 \text{ mL} \cdot \text{min}^{-1}$
	Carrier gas	Nitrogen
Oven	Temperature	323.15 K
Injector	Injection volume	$0.5 \mu\text{L}$
	Split ratio	75:1
	Temperature	573 K
Detector	Type	Flame ionisation detector (FID)
	Temperature	573 K

#### 4.2.7 GC detector calibrations and calculation of the mole fractions

Calibration of the GC FID was conducted by use of the internal standard method. Preparation of each sample required weighing a set mass of one of the components. Then a known mass of the internal standard was added to the prepared vessel. The use of a known mass for both compounds - the sample and the standard allowed the use of the method consisting in correlating the mass ratio of both components with the peak area ratio. For each sample, three separate measurements were carried out to check the repeatability of the detector and minimise possible errors. The average value of ratios for each sample was used to establish the calibration curve linear equation. This method allowed the calculation of the molar fraction of ionic liquid, which was retained in the chromatograph response factor. Figures 4-12 to 4-17 shows the calibration curves obtained for thiophene, octane and hexadecane, respectively.

A sample from each phase was withdrawn from the equilibrium cell and was prepared as described in the section 4.2.5. From this prepared sample three GC samples were injected to ensure minimisation of errors. by adding a known amount of internal standard, the mass of this known variable was used to determine the remaining unknowns via the peaks area ratios obtained from the GC injections. Two other unknowns which are peak areas for the standard and for the studied compound, i.e., thiophene were obtained by the use of the GC. The last unknown, i.e., the mass of the studied compound was calculated by the use of the linear equation (eqn. 4 - 1) obtained during the calibration process.

$$y = ax + b \quad (4 - 1)$$

where:

$$y = \frac{m_{thiophene}}{m_{standard}} \quad (4 - 2)$$

$$x = \frac{A_{thiophene}}{A_{standard}} \quad (4 - 3)$$

The value of the slope  $a$  is obtained from the calibration curve, with the intercept  $b$  equal to 0.

These calculations were performed for the S-compound and hydrocarbon in the sample, which yielded the masses of both compounds. The IL was prevented from



entering the GC column via a liner placed in the injection port. However the mass of the ionic liquid is calculated by the reduction of the initial sample mass (withdrawn sample) by the mass of the S-compound and hydrocarbon. This allows for the calculation of all the component molar fractions in the sample.

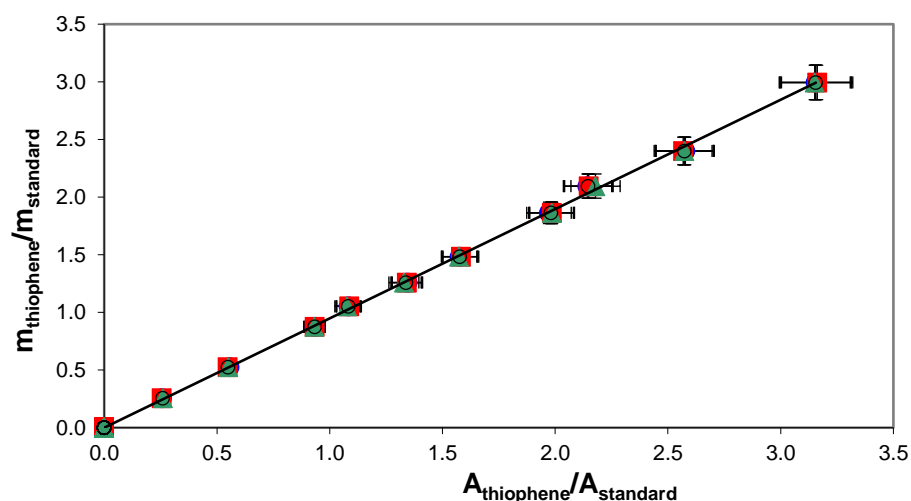


**Fig. 4-12** GC FID detector calibration curve. The ratio of ( $A_{\text{thiophene}}/A_{\text{standard}}$ ) correlated with the respective mass ratio. For each sample, three separate measurements (marked as  $\bullet$ ,  $\blacktriangle$  and  $\blacksquare$ , respectively) were carried out. The average value of ratios ( $\circ$ ) for each sample was used to establish the calibration curve linear equation  $y = 0.9482x$  with coefficient of determination  $R^2 = 0.9997$ .

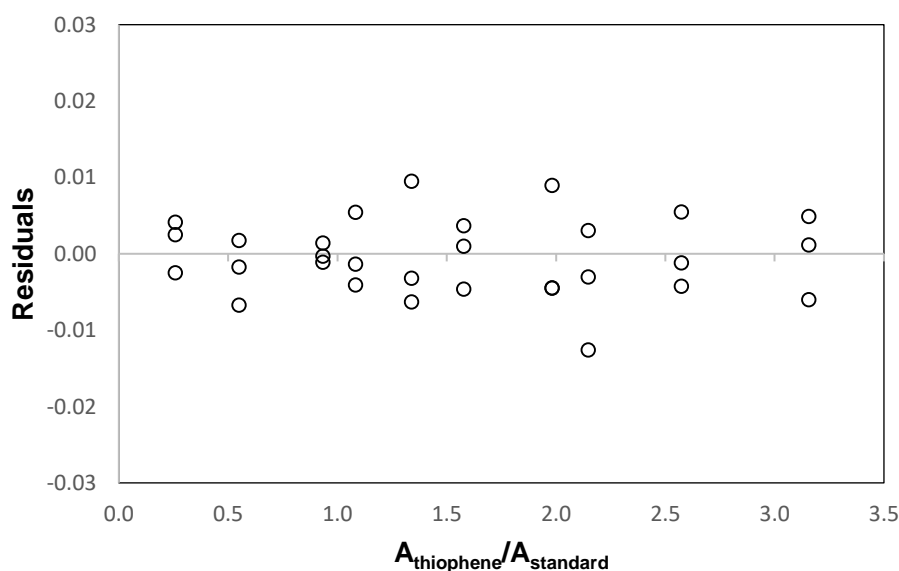


**Fig. 4-13** Residuals for the calibration of the GC FID detector for thiophene calibration. The standard error for the calibration was 0.001.

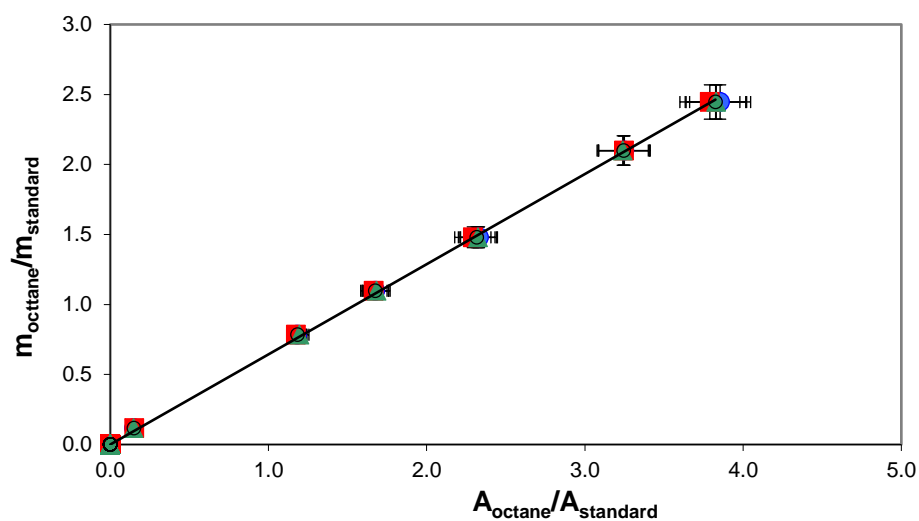


**Fig. 4-14** GC FID detector calibration curve. The ratio of ( $A_{\text{octane}}/A_{\text{standard}}$ ) correlated with the respective mass ratio. For each sample, three separate measurements (marked as ●, ▲ and ■, respectively) were carried out. The average value of ratios (○) for each sample was used to establish the calibration curve linear equation  $y = 0.64396x$  with coefficient of determination  $R^2 = 0.99986$ .

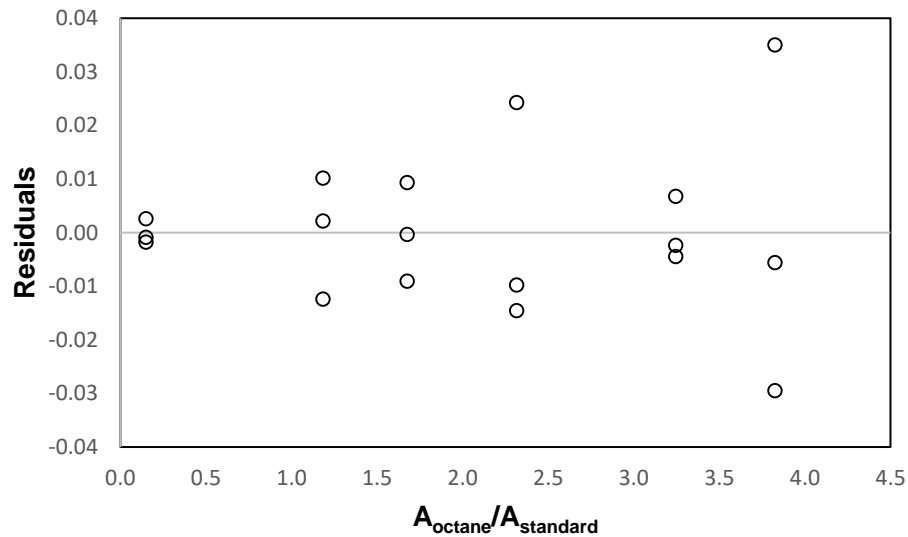


**Fig. 4-15** Residuals for the calibration of the GC FID detector for octane calibration. The standard error for the calibration was 0.004.

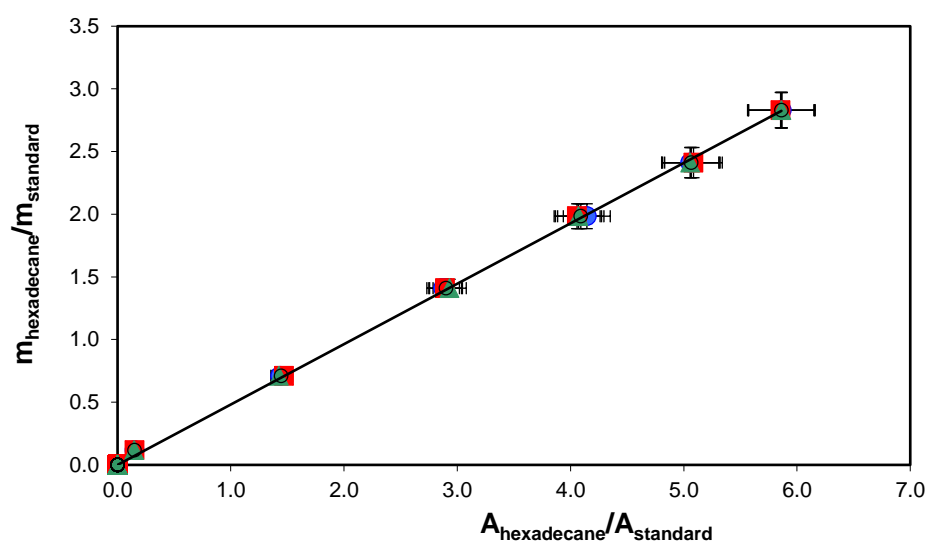


**Fig. 4-16** GC FID detector calibration curve. The ratio of ( $A_{\text{hexadecane}}/A_{\text{standard}}$ ) correlated with the respective mass ratio. For each sample, three separate measurements (marked as ●, ▲ and ■, respectively) were carried out. The average value of ratios (○) for each sample was used to establish the calibration curve linear equation  $y = 0.4818x$  with coefficient of determination  $R^2 = 0.99980$ .

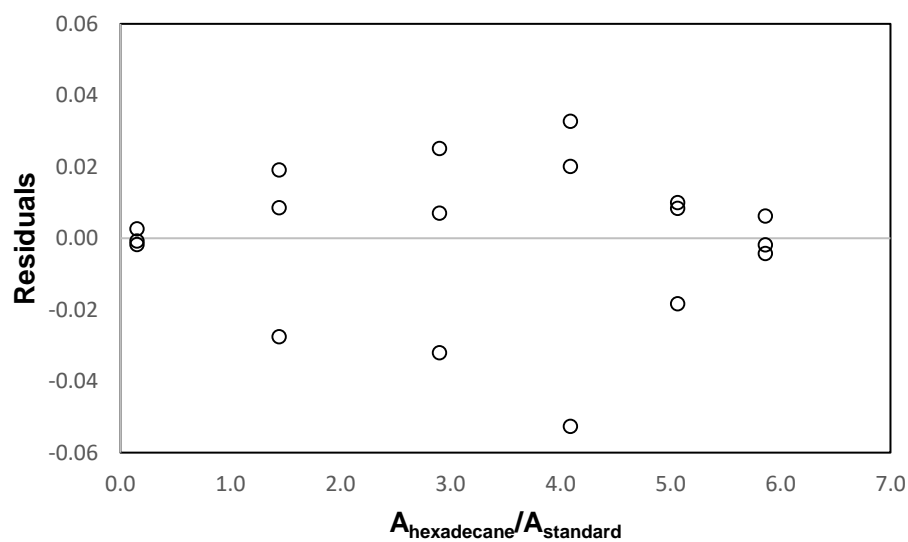


**Fig. 4-17** Residuals for the calibration of the GC FID detector for hexadecane calibration. The standard error for the calibration was 0.005.

#### 4.2.8 Gas chromatograph operation

- I. The inner lining of the injector port was removed, cleaned and supplied with a small piece of the glass wool to prevent non-volatile ionic liquids from blocking the column during the measurements. This was cleaned weekly.
- II. The Shimadzu GC-2010 was switched on, gas valves on cylinders were opened, and GC operating parameters were set on the monitor.
- III. The system was left to stabilise for at least an hour.
- IV. Samples were injected into the injector port. Each sample was injected three times, then ratios of the peak areas between individual components of the mixture and internal standard from three runs were averaged.
- V. After completion of analyses, the GC detector was switched off while the temperature settings were set to 25°C. These allowed the unit to cool down. Gas flow was kept unchanged to the moment when the detector reached 50°C. This was deemed safe to turn off the apparatus.
- VI. The gas cylinder valves were closed, and the GC was turned off.

### 4.3 Safety gear

Safety in the laboratory is always a priority. During both experimental procedures, standard protective equipment was used. This includes a laboratory coat, latex/nitrile gloves and goggles. Work with potentially dangerous or odorous, and volatile compounds was conducted in a fume cupboard as a workstation. Due to the nature of sample preparation, mixing took place outside working hours, so that analyses could be performed during normal working hours. The magnetic stirrer was connected using a control device, and the current was switched off to stop stirring after 6 hours.

Chemicals were stored in two ways. Small vials and bottles of highly volatile compounds were kept in the refrigeration unit at a temperature of about 3-4°C to ensure proper storage conditions. Bottles with non-volatile chemical compounds were kept in chemical storage. Used chemicals were placed in properly labelled bottles. Each bottle's

label contained the name of the chemists, list of the compounds and approximate concentration of the chemicals in the mixture. Filled bottles were disposed of safely by the laboratory technician.

## Chapter 5 Results & discussion

This chapter summarizes the results obtained from the experimental work and undertakes a discussion to draw conclusions about the collected data. The first part summarizes the results of the limiting activity coefficients calculations, while the second part focuses on the liquid-liquid equilibrium data and the results of the NRTL modelling. The third part of this chapter presents a possible design of the EDS processes with the use of ILs. The chapter concludes with an assessment of the viability of the proposed process.

### 5.1 Motivation for the ILs tested

The choice of ionic liquids was a very important part of this work. Few steps were taken into consideration during this process. The first step of the potential IL screening was related to the data presented in Chapter 2. In this step, ionic liquids used in this work were chosen by comparison of the performance index values, which helped to choose few potential groups of the solvents, i.e. imidazolium-based ILs with short alkyl chain or ILs with dicyanamide [DCA] anion which showed high values of the PI obtained from the literature. Crucial information was obtained by calculation of the selectivities, partition coefficients and performance indices from activity coefficients at infinite dilution. In the next step, the proposed systems were compared with the literature data, to check which of these had been studied and published. The final step of the IL screening procedure was the availability of the ILs.

1,3-Dihydroxyimidazolium bis{(trifluoromethyl)sulphonyl}imide [OHOHIM][NTf<sub>2</sub>] represents the family of the imidazolium ILs with short substituent chains. The imidazolium-based and short-chained ILs are known as a promising extractant for extractive desulphurization process, as shown in Table 2-1. This IL was also interesting because it consists of two hydroxyl groups instead of alkyl chains as substituents, which have not been widely studied as a potential extractant for the desulphurisation process.

1-Butyl-1-methylpiperidinium dicyanamide [BMPIP][DCA] was chosen because of the interesting anion. In general, ILs with the dicyanamide anion presents high values of selectivity and performance indices. At the time of the experimental

measurements for this work, the amount of studied piperidinium ILs was relatively low, which was an additional motivation, to study this particular ionic liquid.

Tri-*iso*-butylmethylphosphonium tosylate [P<sub>-i4,i4,i4,1</sub>][TOS] was chosen because of promising results obtained for benzo- and dibenzothiophene LLE systems. There currently exists no published results for LLE systems with this IL and thiophene. At this same time, values of the Performance Indices obtained by the use of activity coefficients at infinite dilution data published for shorter chain alkanes stood in contradiction to the published LLE data.

1-Butyl-3-methylimidazolium trifluoromethanesulphonate [BMIM][OTf] was chosen in a similar way to the [P<sub>-i4,i4,i4,1</sub>][TOS], as not many systems with this IL was published, especially for the systems with longer alkyl chain model fuels.

1-Butyl-1-methylpyrrolidinium dicyanamide [BMPYR][DCA] was used in the activity coefficients at infinite dilution study as an important step, to ensure coverage of the whole spectrum of the experimental methods and thermodynamic principles, which leads to the extractive desulphurisation process. Without this measurement, this thesis would not be complete, as the  $\gamma^\infty$  values are crucial for the development of the extractive desulphurisation.

The following ionic liquids were used in LLE measurements with both octane and hexadecane:

- I. 1,3-dihydroxyimidazolium bis{(trifluoromethyl)sulphonyl}imide  
([OHOHIM][NTf<sub>2</sub>])
- II. 1-butyl-3-methylimidazolium trifluoromethanesulphonate  
([BMIM][OTf])
- III. 1-butyl-1-methylpiperidinium dicyanamide ([BMPIP][DCA])
- IV. Tri-*iso*-butylmethylphosphonium tosylate ([P<sub>-i4,i4,i4,1</sub>][TOS])

## 5.2 Materials

Tables 5-1 to 5-3 lists the chemical compounds used during this study. Table 5-1 shows information about chemicals used for GLC measurements. Table 5-2 summarizes the properties and purities of ILs used, while table 5-3 lists chemical compounds used during LLE measurements.

**Table 5-1** The sources and mass fraction purities of materials used during measurements of activity coefficients at infinite dilution  $\gamma_{13}^{\infty}$ .

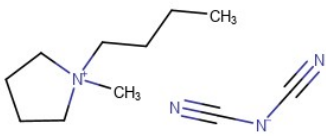
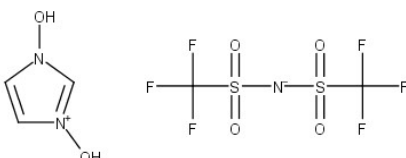
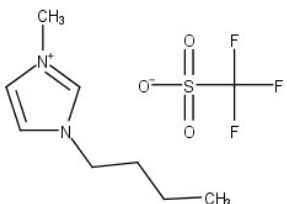
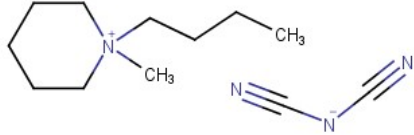
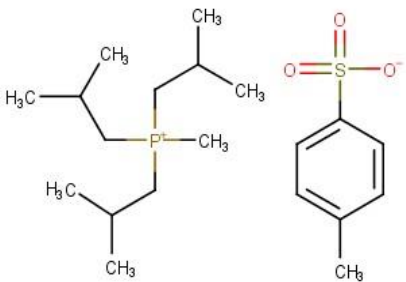
Chemical name	Source	Initial mass fraction purity
n-heptane	Saarchem	$\geq 0.99$
n-octane	Merck	$\geq 0.99$
n-nonane	Merck	$\geq 0.99$
1-hexene	Merck	$\geq 0.96$
cyclohexene	Aldrich	$\geq 0.999$
1-heptene	Aldrich	$\geq 0.97$
1-octene	Aldrich	$\geq 0.98$
1-decene	Aldrich	$\geq 0.94$
1-hexyne	Aldrich	$\geq 0.97$
1-heptyne	Aldrich	$\geq 0.98$
1-octyne	Aldrich	$\geq 0.97$
benzene	Aldrich	$\geq 0.99$
toluene	Aldrich	$\geq 0.999$
ethylbenzene	Aldrich	$\geq 0.998$
<i>o</i> -xylene	Aldrich	$\geq 0.99$
<i>m</i> -xylene	Aldrich	$\geq 0.99$
<i>p</i> -xylene	Aldrich	$\geq 0.99$
styrene	Aldrich	$\geq 0.99$
<i>alpha</i> -methylstyrene	Aldrich	$\geq 0.99$
methanol	Merck	$\geq 0.995$
ethanol	Aldrich	$\geq 0.998$
1-propanol	Aldrich	$\geq 0.999$
2-propanol	Aldrich	$\geq 0.995$
1-butanol	Aldrich	$\geq 0.998$
2-butanol	Aldrich	$\geq 0.995$
2-methyl-1-propanol	Aldrich	$\geq 0.99$
thiophene	Aldrich	$\geq 0.99$
tetrahydrofuran	Aldrich	$\geq 0.999$
1,4-dioxane	Aldrich	$\geq 0.998$
<i>tert</i> -butyl ethyl ether	Aldrich	$\geq 0.99$
<i>tert</i> -butyl methyl ether	Aldrich	$\geq 0.998$
<i>tert</i> -pentyl methyl ether	Aldrich	$\geq 0.97$
di- <i>n</i> -propyl ether	Aldrich	$\geq 0.99$



**Table 5-1** The sources and mass fraction purities of materials used during measurements of activity coefficients at infinite dilution  $\gamma_{13}^{\infty}$ .

Chemical name	Source	Initial mass fraction purity
di- <i>iso</i> -propyl ether	Fluka	$\geq 0.98$
di- <i>n</i> -butyl ether	Aldrich	$\geq 0.99$
acetone	Merck	$\geq 0.98$
2-pentanone	Aldrich	$\geq 0.995$
3-pentanone	Aldrich	$\geq 0.99$
methyl propionate	Aldrich	$\geq 0.99$
methyl butyrate	Aldrich	$\geq 0.99$
ethyl acetate	Aldrich	$\geq 0.997$
propionaldehyde	Merck	$\geq 0.98$
butyraldehyde	Aldrich	$\geq 0.99$
acetonitrile	Fluka	$\geq 0.999$
pyridine	Merck	$\geq 0.99$
1-nitropropane	Aldrich	$\geq 0.985$

**Table 5-2** Properties of the ionic liquids investigated: structure, name, abbreviation of name, supplier, CAS number, molar mass (M), mass fraction purity (as stated by the supplier) and purification method.

Structure	Name, abbreviation, supplier, CAS	M/ (g·mol <sup>-1</sup> )	Mass fraction purity /maximum water content (mass fraction) <sup>a</sup>
	1-Butyl-1-methylpyrrolidinium dicyanamide, [BMPYR][DCA], Io-Li-Tec, CAS: 370865-80-8	208.30	>0.980/ <500x10 <sup>-6</sup>
	1,3-Dihydroxyimidazolium bis((trifluoromethyl)sulfonyl)imide, [OHOHIM][NTf2], Sigma Aldrich, CAS: 951021-12-8	381.23	>0.980/ <500x10 <sup>-6</sup>
	1-Butyl-3-methylimidazolium trifluoromethanesulphonate, [BMIM][OTf], Sigma Aldrich, CAS: 174899-66-2	264.30	>0.980/ <500x10 <sup>-6</sup>
	1-Butyl-1-methylpiperidinium dicyanamide, [BMPIP][DCA], Io-li-tec, CAS: 827033-52-3	222.34	>0.970/ <500x10 <sup>-6</sup>
	Tri(isobutyl)methylphosphonium tosylate, [P-i4,i4,i4,1][TOS], Io-li-tec, CAS: 374683-35-9	388.55	>0.950/ <500x10 <sup>-6</sup>

**Table 5-3** Properties and purity of the original materials used in the LLE study.

Compound	Supplier	Mass fraction purity	Maximum water content (mass fraction) <sup>a</sup>	Analysis method	CAS number
Octane	Merck	0.990	$<1000 \times 10^{-6}$	GC	111-65-9
Hexadecane	Sigma Aldrich	0.990	$<1000 \times 10^{-6}$	GC	544-76-3
Thiophene	Sigma Aldrich	0.990	$<1000 \times 10^{-6}$	GC	110-02-1
2-pentanone	Sigma Aldrich	0.995	$<1000 \times 10^{-6}$	GC	107-87-9
1-propanol	Sigma Aldrich	0.990	$<1000 \times 10^{-6}$	GC	71-23-8
Methanol	Sigma Aldrich	0.990	$<1000 \times 10^{-6}$	Karl Fisher	67-56-1

<sup>a</sup> Purification method: molecular sieves

To remove volatile impurities and trace amounts of water samples the ILs were dried for 72 h at  $T = 353$  K under pressure  $P = 0.33$  atm. Thiophene, octane and hexadecane used for LLE measurements were stored over freshly activated 0.3 nm molecular sieves supplied by Merck. The water content was checked by the use of the Karl-Fischer Moisture Titrator MKS 500. Samples of ILs or solvents were dissolved in methanol and titrated in steps of  $0.005 \text{ cm}^3$ . The error in the water content was  $\pm 10 \times 10^{-6}$  in mass fraction. The water content in the IL used during limiting activity coefficients calculations was less than  $500 \times 10^{-6}$  in mass fraction, while the water content of the ILs used during the LLE measurements were less than  $1000 \times 10^{-6}$  in mass fraction.

### 5.3 Activity coefficients at infinite dilution, $\gamma_{13}^{\infty}$

Few trial injections of the hexane, 1-hexene, cyclohexane benzene and toluene were made to prove that the apparatus was setup correctly, leak-free and the experimental method was correct. As a test system, hexadecane was chosen. Results obtained during the test system measurements were satisfying in comparison with the literature data, values were in the range of  $\pm 2.5\%$ , and the slopes of the data sets agreed. This proved a proper preparation of the experimental setup and allowed for the continuation of the experimental work.

Two columns were prepared according to the procedure described in section 4.1.2. Columns contained 27.26% and 44.16% of hexadecane adsorbed on the solid support, respectively. Experimental results were compared to the literature data [221] and are presented in Appendix A.

Table 5-4 shows the values of  $\gamma_{13}^{\infty}$  for 46 solutes in [BMPYR][DCA], obtained at five different temperatures. Figures 5-1 to 5-5 show a graphical representation of the trends for individual groups of compounds in relation to temperature. The value of  $\gamma_{13}^{\infty}$  is used to describe an existing interaction between a solute and the solvent at the infinite dilution. The strongest interactions are with [BMPYR][DCA] and the lowest values of the  $\gamma_{13}^{\infty}$  values for all of the temperatures were obtained for alcohols such as methanol, ethanol or 1-propanol, respectively ( $\gamma_{13}^{\infty} = 0.333$ ,  $\gamma_{13}^{\infty} = 0.525$  and  $\gamma_{13}^{\infty} = 0.645$ ) at  $T = 323.15$  K. Strong interaction was observed also for acetonitrile ( $\gamma_{13}^{\infty} = 0.668$ ), 2-propanol ( $\gamma_{13}^{\infty} = 0.719$ ), 1-nitropropane ( $\gamma_{13}^{\infty} = 0.740$ ), 2-methyl-1-propanol ( $\gamma_{13}^{\infty} = 0.835$ ), thiophene ( $\gamma_{13}^{\infty} = 0.845$ ), 1-butanol ( $\gamma_{13}^{\infty} = 0.873$ ), 2-butanol ( $\gamma_{13}^{\infty} = 0.888$ ), and acetone ( $\gamma_{13}^{\infty} = 0.910$ ) at  $T = 323.15$  K. The highly polar dicyanamide anion ([DCA]) is responsible for strong interactions with polar solutes. In contrast, non-polar solvents, such as alkanes reveal high values of  $\gamma_{13}^{\infty}$ , e.g., for alkanes ( $\gamma_{13}^{\infty} = 74$  to  $154$  at  $T = 323.15$  K), alkenes ( $\gamma_{13}^{\infty} = 20.3$  to  $98.2$  at  $T = 323.15$  K), and alkynes ( $\gamma_{13}^{\infty} = 3.98$  to  $9.03$  at  $T = 323.15$  K) for 1-butyl-1-methylpyrrolidinium dicyanamide, [BMPYR][DCA].

**Table 5-4** The experimental activity coefficients at infinite dilution  $\gamma_{13}^{\infty}$  for the solutes in ionic liquid [BMPYR][DCA] at different temperatures.

Solute	T/K				
	313.15	323.15	343.15	363.15	373.15
n-heptane	79.1	74.6	66.5	60.2	53.6
n-octane	119	111	96.0	86.0	81.0
n-nonane	172	154	133	120	114
1-hexene	21.0	20.3	19.3	18.4	18.6
cyclohexene	9.06	8.78	8.65	8.48	8.26
1-heptene	31.5	30.4	29.2	27.8	27.7
1-octene	47.8	46.3	42.8	40.3	39.0
1-decene	104	98.2	89.4	83.7	78.7
1-hexyne	3.81	3.98	4.32	4.61	4.77
1-heptyne	5.76	5.95	6.39	6.76	6.92
1-octyne	8.87	9.03	9.41	9.79	9.87
benzene	1.38	1.40	1.49	1.60	1.62
toluene	2.07	2.14	2.30	2.43	2.48
ethylbenzene	3.32	3.43	3.52	3.70	3.77
o-xylene	2.69	2.75	2.91	3.10	3.18
m-xylene	3.36	3.47	3.58	3.74	3.81
p-xylene	3.24	3.24	3.47	3.63	3.73
styrene	1.49	1.54	1.70	1.80	1.90
alpha-methylstyrene	2.20	2.37	2.67	2.89	3.02
methanol	0.336	0.333	0.339	0.348	0.353
ethanol	0.533	0.525	0.520	0.519	0.521
1-propanol	0.649	0.645	0.648	0.665	0.638
2-propanol	0.744	0.719	0.714	0.711	0.696
1-butanol	0.897	0.873	0.844	0.836	0.814
2-butanol	0.875	0.888	0.859	0.869	0.881
2-methyl-1-propanol	0.872	0.835	0.785	0.786	0.764
thiophene	0.807	0.845	0.929	1.01	1.05
tetrahydrofuran	1.34	1.39	1.48	1.56	1.60
1,4-dioxane	0.909	0.962	1.05	1.13	1.17
methyl tert-butyl ether	6.25	6.32	6.55	6.92	7.15
methyl tert-pentyl ether	9.56	9.39	9.65	9.77	9.93
ethyl tert-butyl ether	17.2	16.9	16.9	16.7	16.1
di-n-propyl ether	17.9	17.0	16.8	16.6	16.6
di-iso-propyl ether	19.4	18.8	19.1	18.6	18.3
di-n-butyl ether	40.2	38.8	36.2	33.9	32.9
acetone	0.907	0.910	0.978	1.04	1.06
2-pentanone	1.73	1.79	1.89	1.96	2.02
3-pentanone	1.70	1.76	1.90	1.99	2.04
methyl propionate	2.07	2.09	2.22	2.33	2.40
methyl butyrate	2.92	3.00	3.16	3.25	3.34
ethyl acetate	2.35	2.36	2.48	2.57	2.61
propionaldehyde	1.04	1.05	1.10	1.16	1.21
butyraldehyde	1.40	1.46	1.53	1.62	1.67
1-nitropropane	0.721	0.740	0.789	0.827	0.838
pyridine	1.02	1.05	1.07	1.11	1.13
acetonitrile	0.659	0.668	0.693	0.720	0.728

<sup>a</sup> Standard uncertainties  $u$  are  $u(\gamma_{13}^{\infty}) = \pm 5\%$ ,  $u(T) = 0.01\text{ K}$ ,  $u(P) = \pm 1\text{ kPa}$ .

High values of the  $\gamma_{13}^{\infty}$  for alkanes represent relatively weak interactions of this class of solutes with the studied IL. The existence of a double bond in the studied alkenes increases the strength of interactions between this class of the compounds and the polar ionic liquid, as observed by the lower values of  $\gamma_{13}^{\infty}$  for alkenes than alkanes with the same carbon number. Similar behaviour can be observed for alkynes, as the slightly acidic properties of the hydrogen atom and the presence of  $\pi$  electrons of the triple bond are responsible for even stronger interactions of alkynes and polar ionic liquid. Consequently, alkynes have lower values of  $\gamma_{13}^{\infty}$  than corresponding alkanes and alkenes.

The  $\gamma_{13}^{\infty}$  values usually show two gradients of a slope for different groups of solutes, correlated to endothermic and exothermic effects during the interaction of solutes with the IL. The temperature dependence of  $\gamma_{13}^{\infty}$  for different solutes are presented in Figs 5-1 to 5-5. Diagrams present the plot of  $\ln \gamma_{13}^{\infty}$  as a function of  $1/T$  for all investigated solutes. In this study alkynes, aromatics and esters show a different temperature dependence. The  $\gamma_{13}^{\infty}$  values decrease with an increase in temperature for alkanes, alkenes, cycloalkanes, alcohols and, long-chain ethers. The opposite can be observed for alkynes, aromatic hydrocarbons, short-chain ethers, esters, and ketones. Very low influence of temperature is noted for most of the solutes, except alkanes.

Table 5-5 lists the values of the partial molar excess enthalpies at infinite dilution,  $\Delta H_1^{E,\infty}$ , partial molar excess Gibbs energies at infinite dilution,  $\Delta G_1^{E,\infty}$ , and the partial molar excess entropies at infinite dilution,  $T_{\text{ref}}\Delta S_1^{E,\infty}$ , for all examined solutes in IL at a reference temperature  $T = 323.15$  K. These thermodynamic functions provide crucial data about the interactions between the particles of solute and IL. The  $\Delta G_1^{E,\infty}$  was calculated with the use of the temperature dependence of  $\gamma_{13}^{\infty}$ . The values of  $\Delta G_1^{E,\infty}$  are negative only for polar solutes. The infinite dilution activity coefficients are smaller than one for these solutes, i.e.,  $\gamma_{13}^{\infty} < 1$ , which could be described as a negative deviation from Raoult's law. High positive values of  $\Delta G_1^{E,\infty}$  (positive deviations from Raoult's law) were observed for alkanes, i.e., n-nonane ( $\Delta G_1^{E,\infty} = 14.33$  kJ $\times$ mol $^{-1}$ ), n-octane ( $\Delta G_1^{E,\infty} = 13.34$  kJ $\times$ mol $^{-1}$ ), alkenes, i.e., 1-decene ( $\Delta G_1^{E,\infty} = 13.20$  kJ $\times$ mol $^{-1}$ ), 1-octene ( $\Delta G_1^{E,\infty} = 11.05$  kJ $\times$ mol $^{-1}$ ) and ethers, i.e., di-n-butyl ether ( $\Delta G_1^{E,\infty} = 10.54$  kJ $\times$ mol $^{-1}$ ). The partial excess molar enthalpies at infinite dilution,  $\Delta H_1^{E,\infty}$ , calculated by use of the Gibbs-Helmholtz equation shows negative values for most of the solutes with exception of alkanes, alkenes,

long chain ethers, and alcohols except methanol ( $\Delta H_1^{E,\infty} = -0.870 \text{ kJ}\times\text{mol}^{-1}$ ) and 1-propanol ( $\Delta H_1^{E,\infty} = -0.044 \text{ kJ}\times\text{mol}^{-1}$ ).

**Table 5-5** Limiting partial molar excess enthalpies  $\Delta H_1^{E,\infty}$  Gibbs energies,  $\Delta G_1^{E,\infty}$ , and entropies  $T_{\text{ref}}\Delta S_1^{E,\infty}$  for the solutes in [BMPYR][DCA] at the reference temperature  $T_{\text{ref}} = 358.15 \text{ K}$ .

Solute	$\Delta H_1^{E,\infty} / (\text{kJ}\times\text{mol}^{-1})$	$\Delta G_1^{E,\infty} / (\text{kJ}\times\text{mol}^{-1})$	$T_{\text{ref}}\Delta S_1^{E,\infty}$
n-heptane	5.943	12.20	-6.252
n-octane	6.229	13.34	-7.108
n-nonane	6.508	14.33	-7.826
1-hexene	2.112	8.742	-6.630
cyclohexene	1.297	6.359	-5.062
1-heptene	2.119	9.953	-7.835
1-octene	3.321	11.05	-7.726
1-decene	4.323	13.20	-8.878
1-hexyne	-3.624	4.506	-8.130
1-heptyne	-3.017	5.645	-8.662
1-octyne	-1.805	6.755	-8.559
benzene	-2.791	1.332	-4.123
toluene	-2.984	2.596	-5.580
ethylbenzene	-1.989	3.864	-5.853
o-xylene	-2.766	3.324	-6.090
m-xylene	-1.970	3.900	-5.870
p-xylene	-2.422	3.810	-6.231
styrene	-3.891	1.731	-5.623
alpha-methylstyrene	-5.055	3.103	-8.158
methanol	-0.870	-3.155	2.286
ethanol	0.351	-1.944	2.295
1-propanol	-0.044	-1.285	1.241
2-propanol	0.838	-1.033	1.870
1-butanol	1.419	-0.544	1.963
2-butanol	0.097	-0.405	0.501
2-methyl-1-propanol	1.958	-0.731	2.689
thiophene	-4.287	-0.030	-4.257
tetrahydrofuran	-2.856	1.287	-4.143
1,4-dioxane	-4.043	0.311	-4.354
tert-butyl ethyl ether	-2.170	5.737	-7.907
methyl tert-butyl ether	-0.711	6.787	-7.499
methyl tert-pentyl ether	0.819	8.354	-7.535
di-n-propyl ether	1.044	8.381	-7.337
di-iso-propyl ether	0.729	8.707	-7.978
di-n-butyl ether	3.257	10.54	-7.281
acetone	-2.739	0.063	-2.802
2-pentanone	-2.421	1.989	-4.410
3-pentanone	-2.972	2.013	-4.985
methyl propionate	-2.464	2.491	-4.955
methyl butyrate	-2.110	3.500	-5.610
propionaldehyde	-1.811	2.782	-4.593
butyraldehyde	-2.425	0.428	-2.853
acetonitrile	-2.754	1.405	-4.159
pyridine	-2.525	-0.612	-1.913
1-nitropropane	-1.562	0.292	-1.854

The negative values of  $\Delta H_1^{E,\infty}$  can be described as relatively strong energetic interactions between particles of solute and molecules of solvent. The exothermic dissolution results from the hydrogen bond between the solute and IL. The partial excess molar entropies at infinite dilution,  $T_{\text{ref}}\Delta S_1^{E,\infty}$ , are negative for all solutes, excluding alcohols. The loss of entropy for most of the solutes in [BMPYR][DCA] at a reference temperature  $T = 323.15$  K suggest a formation of an organized structure with particles of IL.

Table 5-6 presents the (gas + liquid) partition coefficients,  $K_L$  for organic solutes in [BMPYR][DCA]. The highest values are observed for alpha-methylstyrene,  $K_L = 3708$  and the lowest for 1-hexene,  $K_L = 8.65$ , at  $T = 323.15$  K. The typical trends that is decreasing  $K_L$  with the increase of the temperature and increase  $K_L$  values with the increase of the alkyl chain length in the solute are observed.

**Table 5-6** The experimental (gas + liquid) partition coefficients,  $K_L$  for the solutes in ionic liquid [BMPYR] [DCA] at different temperatures.<sup>a</sup>

Solute	T/K				
	313.15	323.15	343.15	363.15	373.15
n-heptane	13.1	9.5	5.26	3.15	2.57
n-octane	25.6	17.5	9.14	5.11	3.97
n-nonane	50.9	34.7	16.3	8.32	6.18
1-hexene	13.9	8.65	6.00	3.78	2.98
cyclohexene	62.0	44.6	23.9	14.1	11.3
1-heptene	27.1	19.1	10.1	5.91	4.58
1-octene	53.1	35.2	17.3	9.40	7.20
1-decene	197	121	50.7	23.4	17.1
1-hexyne	101	68.3	33.9	18.6	14.2
1-heptyne	195	126	57.5	29.3	21.7
1-octyne	366	229	96.8	46.1	33.4
benzene	381	253	128	68.5	52.5
toluene	776	501	222	111	82.0
ethylbenzene	1320	806	340	161	115
o-xylene	2290	1160	559	251	175
m-xylene	1480	899	382	177	125
p-xylene	1480	923	379	176	125
styrene	4430	2620	997	445	302
alpha-methylstyrene	6650	3710	1320	548	365
methanol	1080	711	333	170	125
ethanol	1340	851	373	182	131
1-propanol	2800	1670	681	292	214
2-propanol	1220	765	324	153	112
1-butanol	5680	2870	1210	509	355
2-butanol	2380	1360	548	243	169
2-methyl-1-propanol	3780	2220	854	364	254
thiophene	764	495	234	121	90.8
tetrahydrofuran	238	163	82.7	46.1	35.5



**Table 5-6** The experimental (gas + liquid) partition coefficients,  $K_L$  for the solutes in ionic liquid [BMPYR] [DCA] at different temperatures.<sup>a</sup>

Solute	T/K				
	313.15	323.15	343.15	363.15	373.15
1,4-dioxane	1350	847	374	185	135
tert-butyl ethyl ether	23.5	16.8	9.06	5.39	4.36
methyl tert-butyl ether	34.8	25.0	13.6	8.07	6.32
methyl tert-pentyl ether	69.2	48.0	24.2	13.6	10.4
di-n-propyl ether	43.0	30.6	15.7	8.9	6.86
di-iso-propyl ether	18.0	13.2	7.07	4.29	3.44
di-n-butyl ether	158	99.6	44.1	22.0	16.1
acetone	255	182	93.4	52.7	41.1
2-pentanone	743	472	213	109	79.5
3-pentanone	733	470	211	106	78.1
methyl propionate	272	182	86.6	45.8	34.4
methyl butyrate	474	300	133	67.0	48.8
ethyl acetate	220	149	71.8	38.7	29.4
propionaldehyde	166	120	64.3	37.9	29.4
butyraldehyde	320	214	108	58.8	44.6
acetonitrile	864	597	302	166	128
pyridine	2930	1830	787	382	278
1-nitropropane	4050	2460	1040	485	344

<sup>a</sup> Standard uncertainties  $u$  are  $u(K_L) = \pm 5\%$ ,  $u(T) = 0.01\text{ K}$ ,  $u(P) = \pm 1\text{ kPa}$ .

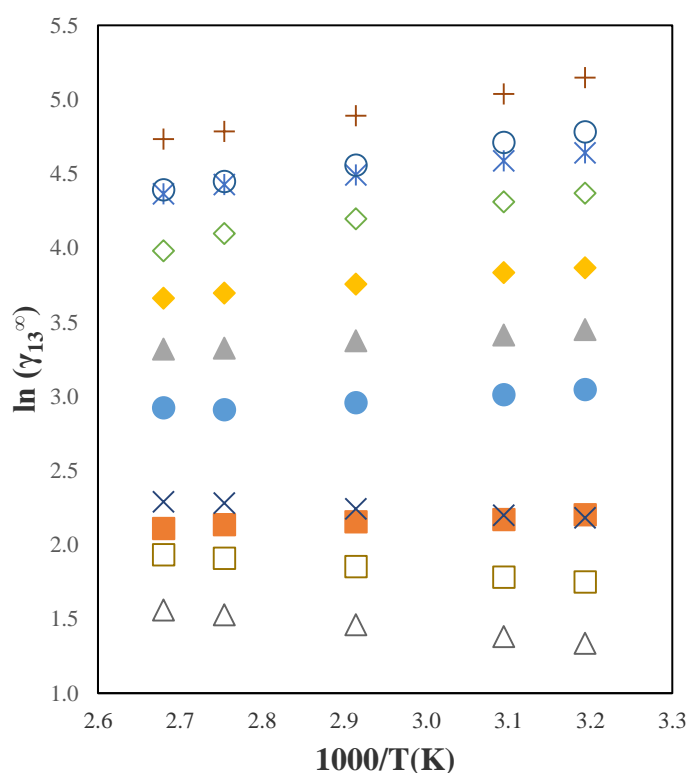


**Fig. 5-1** Plot of  $\ln(\gamma_{13}^{\infty})$  for ionic liquid [BMPYR][DCA] versus  $1000/T$  for the solutes: ( $\diamond$ ) heptane; ( $\circ$ ) octane; (+) nonane; ( $\bullet$ ) hexene; ( $\blacksquare$ ) cyclohexene; ( $\blacktriangle$ ) heptene; ( $\blacklozenge$ ) octene; ( $\star$ ) decene; ( $\triangle$ ) hexyne; ( $\square$ ) heptyne; ( $\times$ ) octyne.

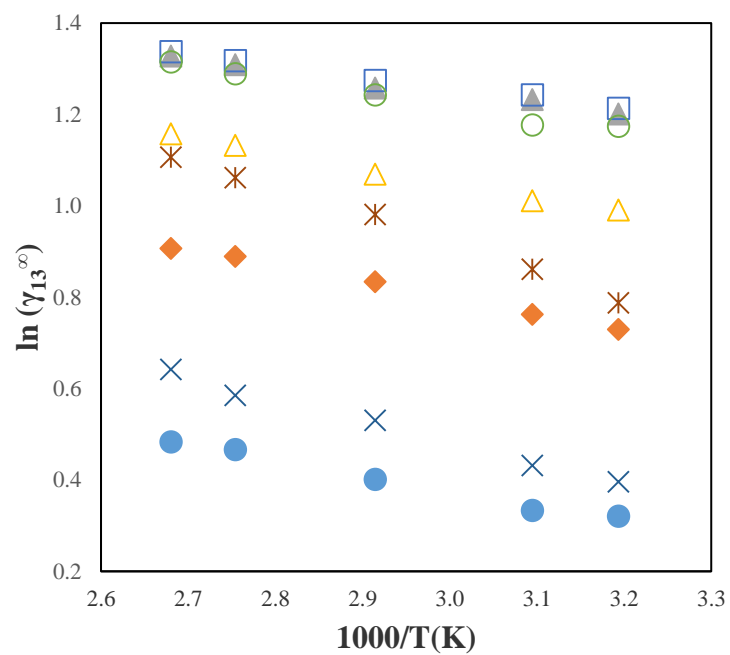


**Fig. 5-2** Plot of  $\ln(\gamma_{13}^{\infty})$  for ionic liquid [BMPYR][DCA] versus  $1000/T$  for the solutes: (●) benzene; (◆) toluene; (▲) ethylbenzene; (△) o-xylene; (◻) m-xylene; (○) p-xylene; (×) styrene; (✱) α-methylstyrene.

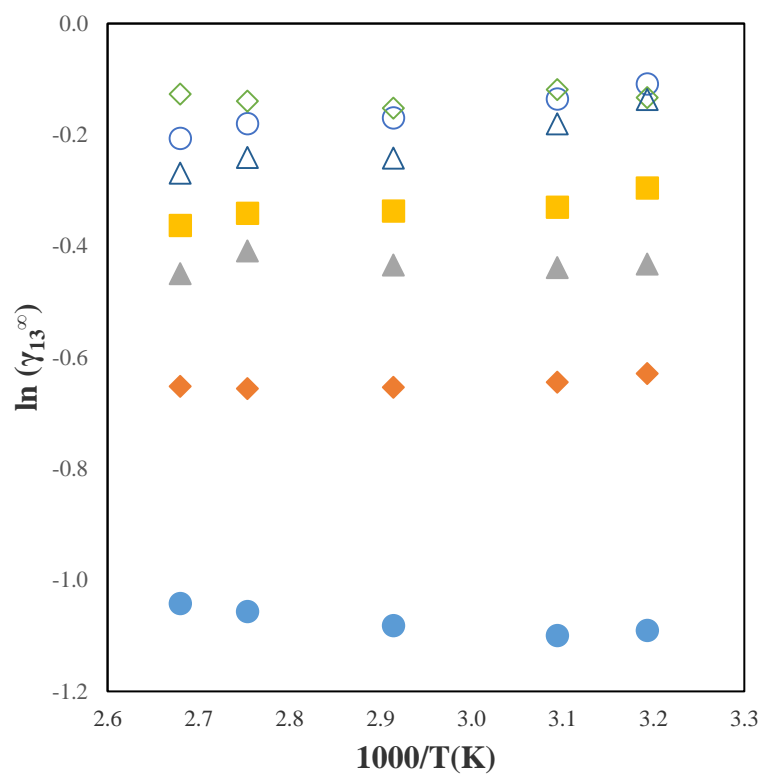


**Fig. 5-3** Plot of  $\ln(\gamma_{13}^{\infty})$  for ionic liquid [BMPYR][DCA] versus  $1000/T$  for the solutes: (●) methanol; (◆) ethanol; (▲) 1-propanol; (■) 2-propanol; (○) 1-butanol; (◇) 2-butanol; (△) 2-methyl-1-propanol.

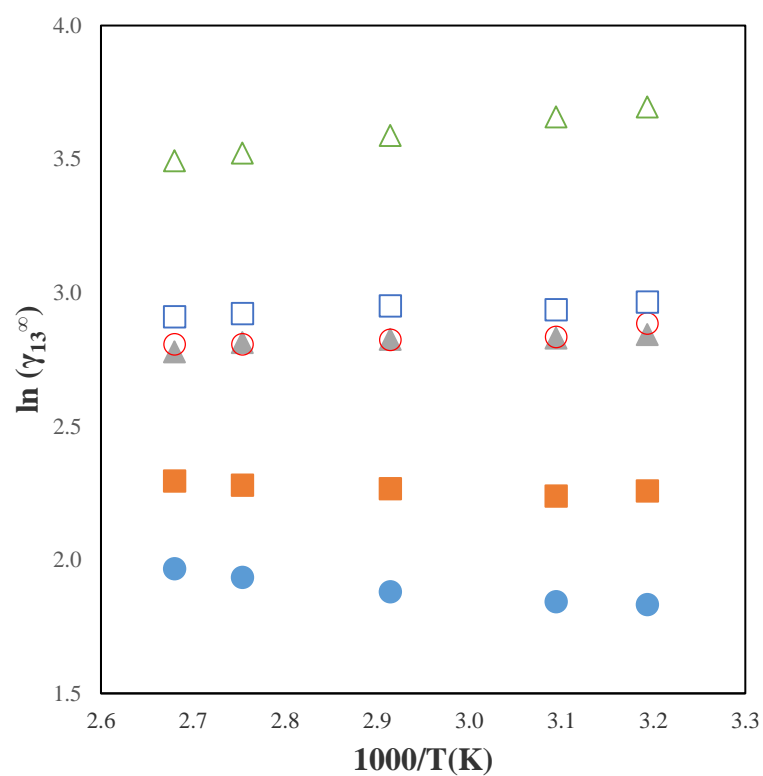


**Fig. 5-4** Plot of  $\ln(\gamma_{13}^{\infty})$  for ionic liquid [BMPYR][DCA] versus  $1000/T$  for the solutes: (●) methyl tert-butyl ether; (■) methyl tert-propyl ether; (▲) ethyl tert-butyl ether; (○) dipropyl ether; (□) di-iso-propyl ether; (△) dibutyl ether.

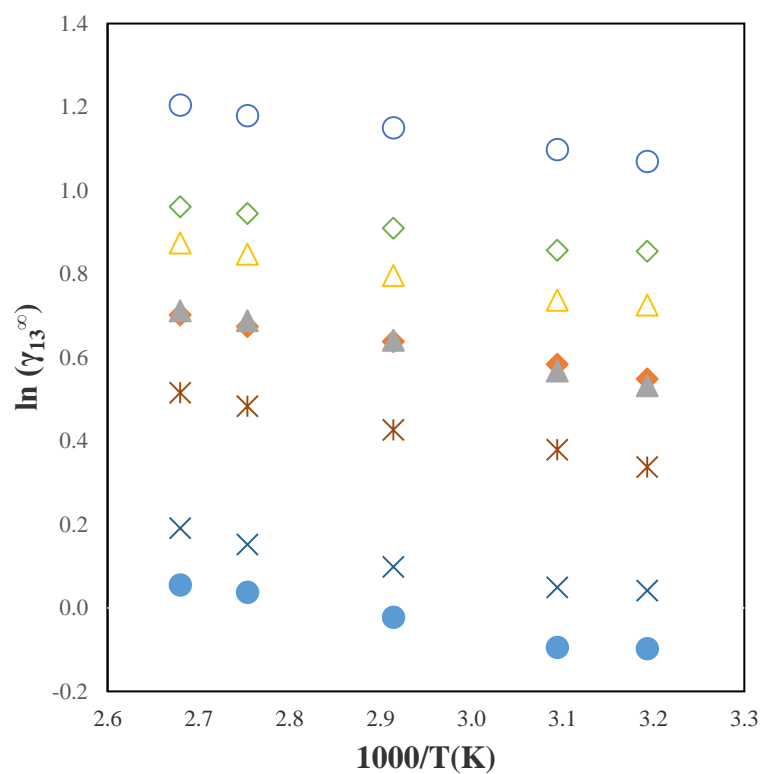


**Fig. 5-5** Plot of  $\ln(\gamma_{13}^{\infty})$  for ionic liquid [BMPYR][DCA] versus  $1000/T$  for the solutes: (●) acetone; (◆) 2-pentanone; (▲) 3-pentanone; (△) methyl propionate; (○) methyl butyrate; (◇) ethyl acetate; (×) propionaldehyde; (✱) butyraldehyde.

Equation 3-17 states that selectivity is the result of the division of activity coefficients at infinite dilution obtained for two solutes in this same solvent. This allows to estimate potential usefulness of solvent in different extraction processes. Thiophene/hydrocarbon is only one of the studied problems. Other interesting systems are aliphatic/aromatic hydrocarbons separation, alkanes/alkynes and ethylbenzene/styrene separation problems. Table 5-7 lists selectivity ( $S$ ) and partition coefficient ( $\beta$ ) literature data at  $T = 328.15$  K for mentioned systems for ILs with the [DCA] anion and [BMPYR] cation in literature [<sup>57–59,61–64,66,72,222,223</sup>].

The selectivities for all of the considered systems: heptane/benzene ( $S = 53.3$ ), heptane/thiophene ( $S = 88.3$ ), heptane/heptyne ( $S = 12.0$ ) and ethylbenzene/styrene ( $S = 2.23$ ) are higher for [BMPYR][DCA] than for other [BMPYR]-based ILs. It can be concluded that the [DCA] anion has a stronger influence on compounds such as benzene, thiophene or styrene than other studied anions.

In relation to the [DCA]-based ILs, the most interesting are high selectivities calculated for [EMMOR][DCA]. This behaviour is related to the additional interaction of the lone electron pairs on the oxygen atom in the morpholinium ring and the solute. Similar interactions were expected for the hydroxyl group, which allowed [P(OH)MIM][DCA] and [P(OH)PY][DCA] ILs to achieve high selectivities. [EMIM][DCA] and [AMIM][DCA] also show higher values of selectivity for the {heptane + benzene + IL} and {heptane + thiophene + IL} systems. This may be related to the small size of the cation particle and short alkyl substituent chains, which was discussed in the literature review.

**Table 5-7** Selectivities ( $S$ ) and partition coefficients ( $\beta$ ) for heptane/benzene, thiophene/heptane, heptane/heptyne and ethylbenzene/styrene separation problems for selected ionic liquids at  $T = 328.15$  K.<sup>a</sup>

IL	$S$				$\beta$				Ref.
	heptane/ benzene	heptane/ thiophene	heptane/ 1-heptyne	ethylbenzene/ styrene	benzene	thiophene	1-heptyne	styrene	
[BMPYR][DCA]	53.3	88.3	12.0	2.18	0.71	1.18	0.17	0.63	This work
[EMMOR][DCA]	140	273	13.9	2.32	0.22	0.42	0.02	0.15	58
[EMIM][DCA]	66.2	109	-	-	0.39	0.64	-	-	222
[AMIM][DCA]	64.1	107	11.1	2.19	0.32	0.53	0.05	0.24	61
[BMIM][DCA]	44.7	71.5	10.1	2.14	0.51	0.82	0.12	0.44	62
[P(OH)MIM][DCA]	76.5	138	-	-	0.22	0.41	-	-	223
[BM(4)PY][DCA]	50.6	80.5	11.0	2.31	0.72	1.15	0.16	0.72	59
[P(OH)PY][DCA]	85.1	163	11.5	2.27	0.19	0.37	0.03	0.14	66
[BMPYR][SCN]	28.4	48.8	6.26	-	0.52	0.9	0.12		57
[BMPYR][TCM]	30.6	43.6	7.66	1.85	0.96	1.37	0.24	0.86	64
[BMPYR][OTf]	36.6	50.2	9.91	-	0.68	0.93	0.18	-	63
[BMPYR][TCB]	26.3	32.4	6.14	-	1.23	1.51	0.29	-	72

<sup>a</sup> Standard uncertainties  $u$  are  $u(S, \beta) = 5\%$ ,  $u(T) = 0.01$  K,  $u(P) = \pm 1$  kPa

## 5.4 Liquid – liquid equilibria

To verify the LLE method measurements of the test system of heptane and methanol were performed in the  $T = 298.15$  K to  $T = 323.15$  K temperature range. The experimental results were compared with literature data [224–228]. Results are presented in the form of charts C-1 and C-2 in Appendix C.

Eight ternary systems {IL (1) + thiophene (2) + octane, or hexadecane (3)} at  $T = 308.15$  K and  $P = 101$  kPa were measured.

The following ionic liquids were used in systems with both octane and hexadecane:

- I. 1,3-dihydroxyimidazolium bis{(trifluoromethyl)sulphonyl}imide  
([OHOHIM][NTf<sub>2</sub>])
- II. 1-butyl-3-methylimidazolium trifluoromethanesulphonate  
([BMIM][OTf])
- III. 1-butyl-1-methylpiperidinium dicyanamide ([BMPIP][DCA])
- IV. Tri-*iso*-butylmethylphosphonium tosylate ([P<sub>-i4,i4,i4,1</sub>][TOS])

During the experimental analysis of the withdrawn sample, the mass balances calculated by the use of method calibrations presented in section 4.2.5 showed negligibly small traces of the IL in the hydrocarbon phase. This is important for industrial applications, as it allows for less costly methods of extraction and solvent recovery. In the binary {IL (1) + octane (3)} system, the complete liquid miscibility (solubility of octane in the IL) was up to mole fraction of octane  $x_3^{\text{IL}} = 0.008, 0.025, 0.006$  and  $0.048$  for the ILs [OHOHIM][NTf<sub>2</sub>], [BMIM][OTf], [BMPIP][DCA] and [P<sub>i4,i4,i4,1</sub>][TOS], respectively. For hexadecane, the mole fractions were,  $x_3^{\text{IL}} = 0.004, 0.019, 0.008$  and  $0.040$  for the [OHOHIM][NTf<sub>2</sub>], [BMIM][OTf], [BMPIP][DCA] and [P<sub>-i4,i4,i4,1</sub>][TOS] ILs, respectively.

The solubility of thiophene in the IL should be as high as possible, in contrary to the solubility in hydrocarbons. In the binary {IL(1) + thiophene(2)} system the complete liquid miscibility is up to mole fraction of thiophene  $x_2^{\text{IL}} = 0.473, 0.828, 0.790$



and, 0.770 for the [OHOHIM][NTf<sub>2</sub>], [BMIM][OTf], [BMPIP][DCA] and [P-i<sub>4</sub>,i<sub>4</sub>,i<sub>4</sub>,1][TOS] ILs, respectively.

Table 5-8 shows the results obtained during this work. In terms of the performance index, the ionic liquids tested in this work were not the best choice for the systems of {IL + thiophene + octane} in comparison with ILs listed in Table 2-1. [BMPIP][DCA] and [BMIM][OTf] show relatively good performance. On the contrary, three of four studied ILs in systems with hexadecane show very high values of the performance index. Especially [BMIM][OTf] and [BMPIP][DCA], with PI values of 193 and 122, respectively. This allow chosen ILs to be deemed as promising extractants for desulphurization of heavier fractions of crude oil.

**Table 5-8** A summary of the LLE results for {IL + thiophene + hydrocarbon} systems:  $T$  is temperature,  $S$  and  $\beta$  are average selectivity and average solute distribution ratio of the sulphur compound, respectively, PI is the performance index, and  $u(x)$  is reported standard uncertainties<sup>a</sup>.

IL	T/K	$S_{Av}$	$\beta_{Av}$	PI
Octane				
[BMPIP][DCA]	308.15	103	1.30	134
[BMIM][OTf]	308.15	43.9	1.25	54.8
[OHOHIM][NTf <sub>2</sub> ]	308.15	40.3	0.50	20.1
[P-i <sub>4</sub> ,i <sub>4</sub> ,i <sub>4</sub> ,1][TOS]	308.15	12.4	1.27	15.7
Hexadecane				
[BMIM][OTf]	308.15	209	0.93	193
[BMPIP][DCA]	308.15	123	0.90	122
[P-i <sub>4</sub> ,i <sub>4</sub> ,i <sub>4</sub> ,1][TOS]	308.15	110	0.99	108
[OHOHIM][NTf <sub>2</sub> ]	308.15	63.2	0.40	25.3

<sup>a</sup> Standard uncertainties  $u(S, \beta) = 0.005$

Tables 5-9 to 5-16 report the equilibrium compositions in mole fractions of the experimental tie-line endpoints for the measured systems at  $T = 308.15$  K, and pressure  $P = 101$  kPa, as well as the selectivity and distribution ratios for the studied ionic liquids. Figures 5-6 to 5-13 show a graphical representation of the tie-lines for the measured systems at  $T = 308.15$  K, and  $P = 101$  kPa. The NRTL model results are presented along

with the experimental tie-lines in figures 5-6 to 5-13. Table 5-17 reports the NRTL model parameters used to correlate the measured data. It is noticeable that the region of immiscibility is similar for all studied ILs. The desulphurization process takes place in the region with a low concentration of thiophene, which is at the lower part of the diagram.

**Table 5-9** Compositions of experimental tie-lines in mole fractions, selectivity,  $S$  and distribution ratios,  $\beta$  for the ternary system {[OHOHIM][NTf<sub>2</sub>] (1) + thiophene (2) + octane (3)} at  $T = 308.15$  K and  $P = 101$  kPa<sup>a</sup>.

Hydrocarbon - rich phase		IL - rich phase		$S$	$\beta$
$x_1^{\text{HC}}$	$x_2^{\text{HC}}$	$x_1^{\text{IL}}$	$x_2^{\text{IL}}$		
0.000	0.000	0.992	0.000	-	-
0.000	0.033	0.971	0.018	48.0	0.55
0.000	0.152	0.906	0.086	60.0	0.57
0.000	0.255	0.858	0.137	66.7	0.54
0.000	0.369	0.781	0.213	60.7	0.58
0.000	0.454	0.772	0.221	38.0	0.49
0.000	0.511	0.752	0.242	33.1	0.47
0.000	0.574	0.728	0.266	39.5	0.46
0.000	0.617	0.697	0.296	26.2	0.48
0.000	0.759	0.666	0.328	20.8	0.43
0.000	0.883	0.597	0.397	10.5	0.45
0.000	1.000	0.527	0.473	-	0.47

<sup>a</sup> Standard uncertainties are:  $u(x) = \pm 0.005$ ;  $u(T) = \pm 0.1$  K;  $u(P) = \pm 1$  kPa.

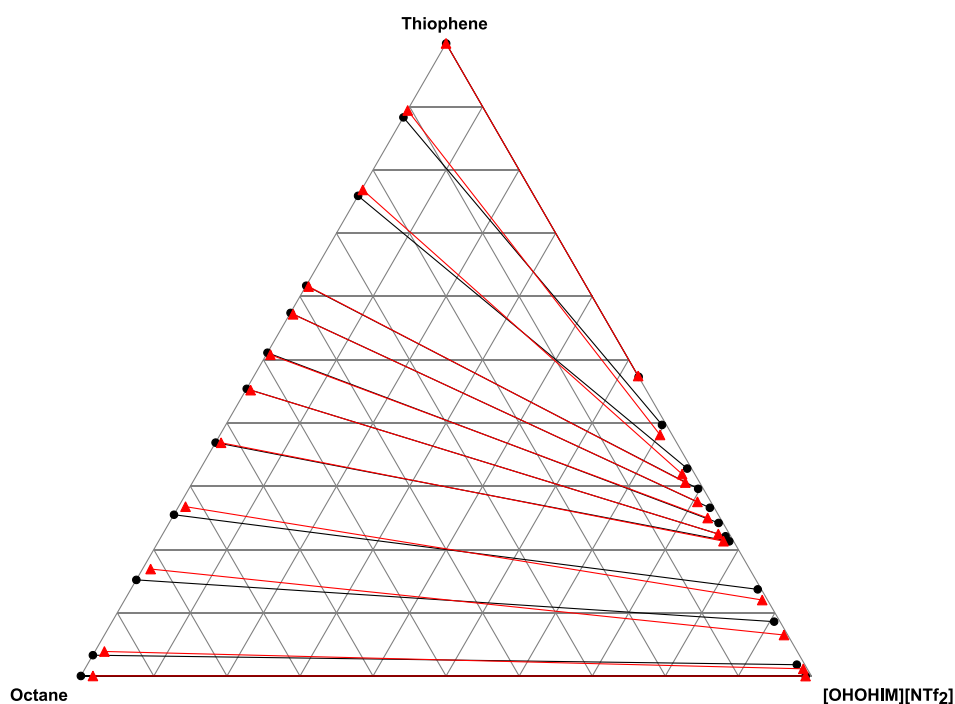


**Fig. 5-6** Plot of the experimental versus calculated LLE data for the ternary system {[OHOHIM][NTf<sub>2</sub>] (1) + thiophene (2) + octane (3)} in mole fractions at  $T = 308.15$  K and  $P = 101$  kPa. ●, Exp: black solid lines; ▲, NRTL Model: red solid lines.

**Table 5-10** Compositions of experimental tie lines in mole fractions, selectivity,  $S$  and solute distribution ratios,  $\beta$  for the ternary system {[BMIM][OTf] (1) + thiophene (2) + octane (3)} at  $T = 308.15$  K and  $P = 101$  kPa<sup>a</sup>.

Hydrocarbon - rich phase		IL - rich phase		$S$	$\beta$
$x_1^{\text{HC}}$	$x_2^{\text{HC}}$	$x_1^{\text{IL}}$	$x_2^{\text{IL}}$		
0.000	0.000	0.975	0.000	-	-
0.000	0.008	0.956	0.020	133	1.88
0.000	0.070	0.817	0.158	84.0	2.26
0.000	0.201	0.642	0.337	63.6	1.67
0.000	0.323	0.509	0.471	49.4	1.46
0.000	0.458	0.505	0.480	37.9	1.05
0.000	0.536	0.436	0.545	25.1	1.03
0.000	0.609	0.427	0.555	19.8	0.91
0.000	0.776	0.324	0.659	11.2	0.85
0.000	0.815	0.245	0.737	9.28	0.90
0.000	0.916	0.175	0.812	5.73	0.89
0.000	1.000	0.172	0.828	-	0.83

<sup>a</sup> Standard uncertainties are:  $u(x) = \pm 0.005$ ;  $u(T) = \pm 0.1$  K;  $u(P) = \pm 1$  kPa.

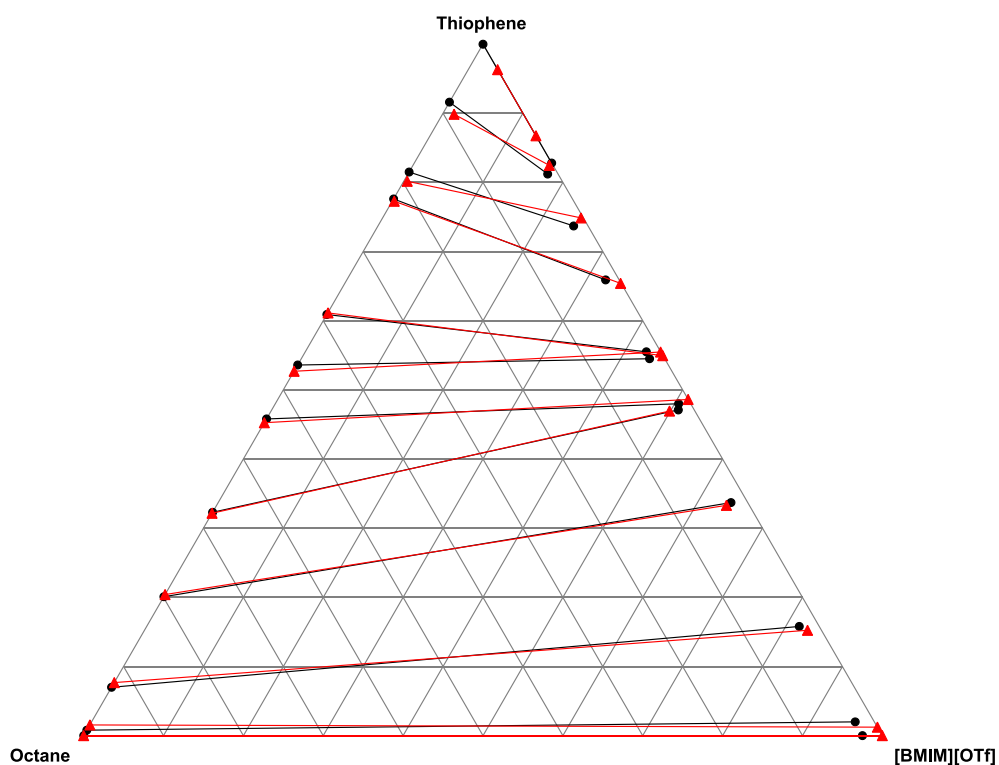


**Fig. 5-7** Plot of the experimental versus calculated LLE data for the ternary system {[BMIM][OTf] (1) + thiophene (2) + octane (3)} in mole fractions at  $T = 308.15$  K and  $P = 101$  kPa. ●, Exp: black solid lines; ▲, NRTL Model: red solid lines.

**Table 5-11** Compositions of experimental tie lines in mole fractions, selectivity,  $S$  and solute distribution ratios,  $\beta$  for the ternary system {[BMPIP][DCA] (1) + thiophene (2) + octane (3)} at  $T = 308.15$  K and  $P = 101$  kPa<sup>a</sup>.

Hydrocarbon - rich phase		IL - rich phase		$S$	$\beta$
$x_1^{\text{HC}}$	$x_2^{\text{HC}}$	$x_1^{\text{IL}}$	$x_2^{\text{IL}}$		
0.000	0.000	0.994	0.000	-	-
0.000	0.038	0.880	0.099	119	2.61
0.000	0.130	0.724	0.271	363	2.08
0.000	0.185	0.667	0.320	108	1.73
0.000	0.352	0.521	0.472	145	1.34
0.000	0.472	0.457	0.536	85.7	1.14
0.000	0.508	0.431	0.565	109	1.11
0.000	0.698	0.338	0.657	56.9	0.94
0.000	0.797	0.280	0.710	18.1	0.89
0.000	0.896	0.262	0.733	17.0	0.82
0.000	0.961	0.229	0.767	10.4	0.80
0.000	1.000	0.210	0.790	-	0.79

<sup>a</sup> Standard uncertainties are:  $u(x) = \pm 0.005$ ;  $u(T) = \pm 0.1$  K;  $u(P) = \pm 1$  kPa.

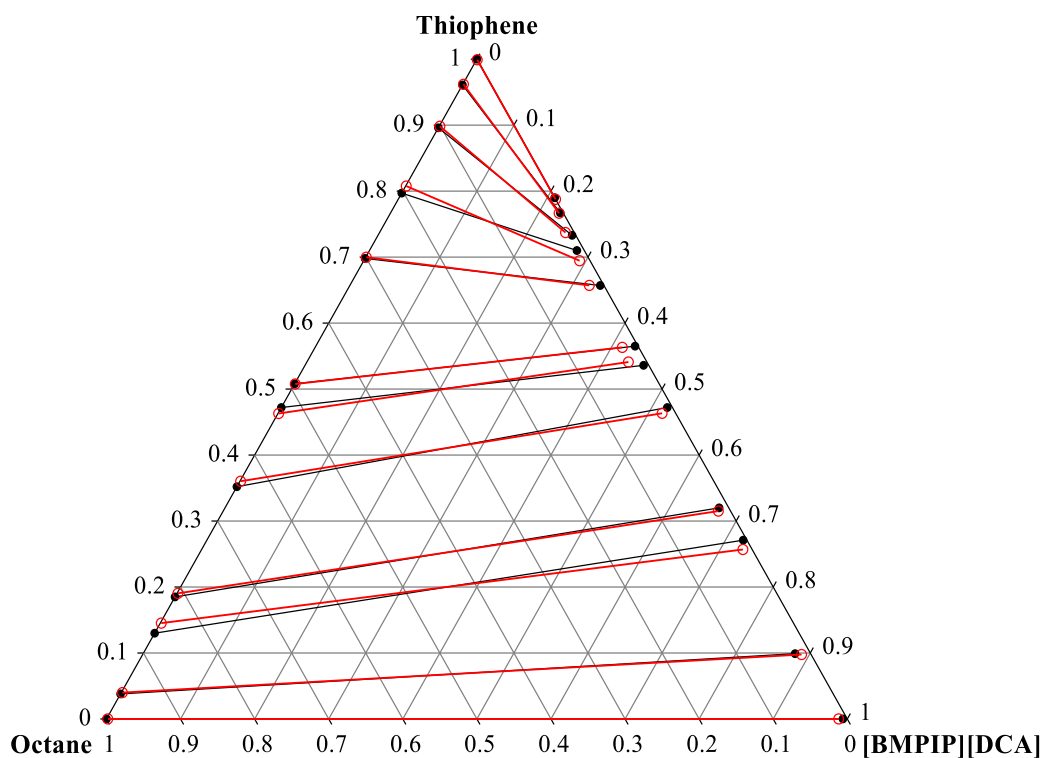


**Fig. 5-8** Plot of the experimental versus calculated LLE data for the ternary system {[BMPIP][DCA] (1) + thiophene (2) + octane (3)} in mole fractions at  $T = 308.15$  K and  $P = 101$  kPa. ●, Exp: black solid lines; ▲, NRTL Model: red solid lines.

**Table 5-12** Compositions of experimental tie lines in mole fractions, selectivity,  $S$  and solute distribution ratios,  $\beta$  for the ternary systems {[P-i4,i4,i4,1][TOS] (1) + thiophene (2) + octane (3)} at  $T = 308.15$  K and  $P = 101$  kPa<sup>a</sup>.

Hydrocarbon - rich phase		IL - rich phase		$S$	$\beta$
$x_1^{\text{HC}}$	$x_2^{\text{HC}}$	$x_1^{\text{IL}}$	$x_2^{\text{IL}}$		
0.000	0.000	0.952	0.000	-	-
0.000	0.101	0.762	0.174	24.2	1.72
0.000	0.138	0.685	0.243	21.4	1.76
0.000	0.166	0.650	0.290	24.3	1.75
0.000	0.221	0.581	0.361	22.3	1.63
0.000	0.337	0.495	0.453	16.8	1.34
0.000	0.348	0.474	0.468	15.1	1.34
0.000	0.405	0.399	0.533	11.3	1.32
0.000	0.474	0.324	0.604	9.31	1.27
0.000	0.571	0.278	0.653	7.11	1.14
0.000	0.674	0.229	0.689	4.11	1.02
0.000	0.775	0.144	0.770	2.6	0.99

<sup>a</sup> Standard uncertainties are:  $u(x) = \pm 0.005$ ;  $u(T) = \pm 0.1$  K;  $u(P) = \pm 1$  kPa.

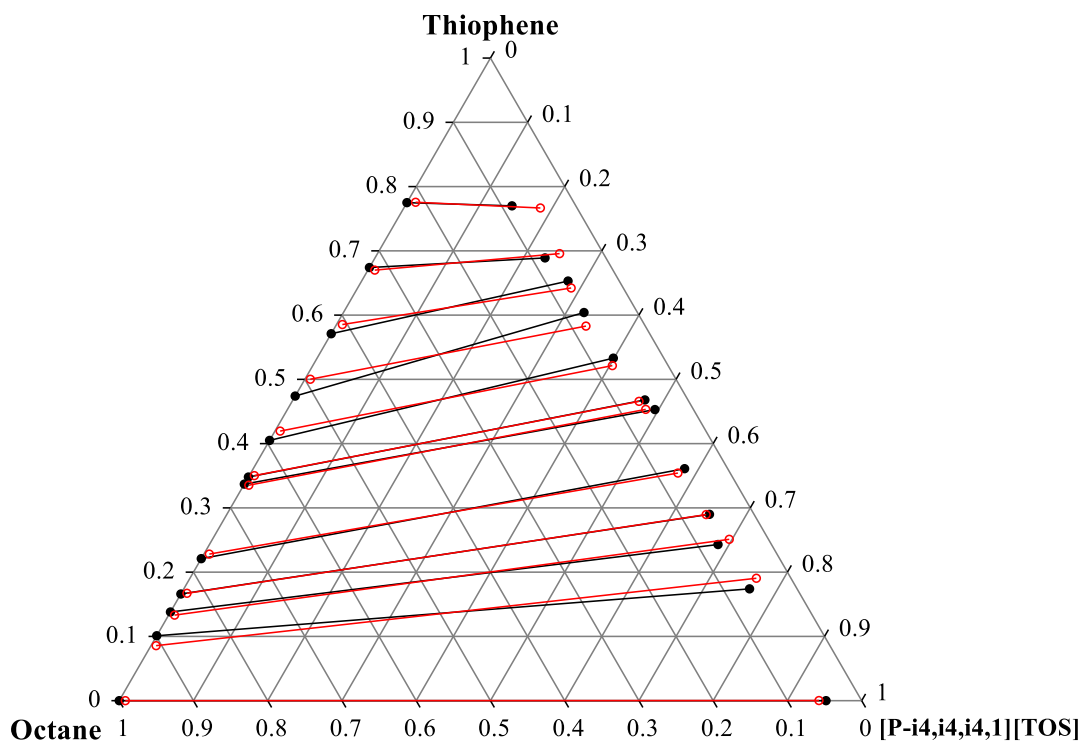


**Fig. 5-9** Plot of the experimental versus calculated LLE data for the ternary system {[P-i4,i4,i4,1][TOS] (1) + thiophene (2) + octane (3)} in mole fractions at  $T = 308.15$  K and  $P = 101$  kPa. ●, Exp: black solid lines; ▲, NRTL Model: red solid lines.

**Table 5-13** Compositions of experimental tie lines in mole fractions, selectivity,  $S$  and solute distribution ratios,  $\beta$  for the ternary system {[OHOHIM][NTf<sub>2</sub>] (1) + thiophene (2) + hexadecane (3)} at  $T = 308.15$  K and  $P = 101$  kPa<sup>a</sup>.

Hydrocarbon - rich phase		IL - rich phase		$S$	$\beta$
$x_1^{\text{HC}}$	$x_2^{\text{HC}}$	$x_1^{\text{IL}}$	$x_2^{\text{IL}}$		
0.000	0.000	0.996	0.000	-	-
0.000	0.094	0.966	0.027	37.2	0.29
0.000	0.139	0.941	0.053	54.7	0.38
0.000	0.233	0.902	0.088	29.0	0.38
0.000	0.287	0.874	0.123	102	0.43
0.000	0.385	0.845	0.153	122	0.40
0.000	0.549	0.780	0.215	35.3	0.39
0.000	0.695	0.732	0.267	117	0.38
0.000	0.758	0.699	0.299	47.7	0.39
0.000	0.781	0.651	0.348	48.8	0.45
0.000	0.912	0.599	0.400	38.6	0.44
0.000	1.000	0.527	0.473	-	0.47

<sup>a</sup> Standard uncertainties are:  $u(x) = \pm 0.005$ ;  $u(T) = \pm 0.1$  K;  $u(P) = \pm 1$  kPa.

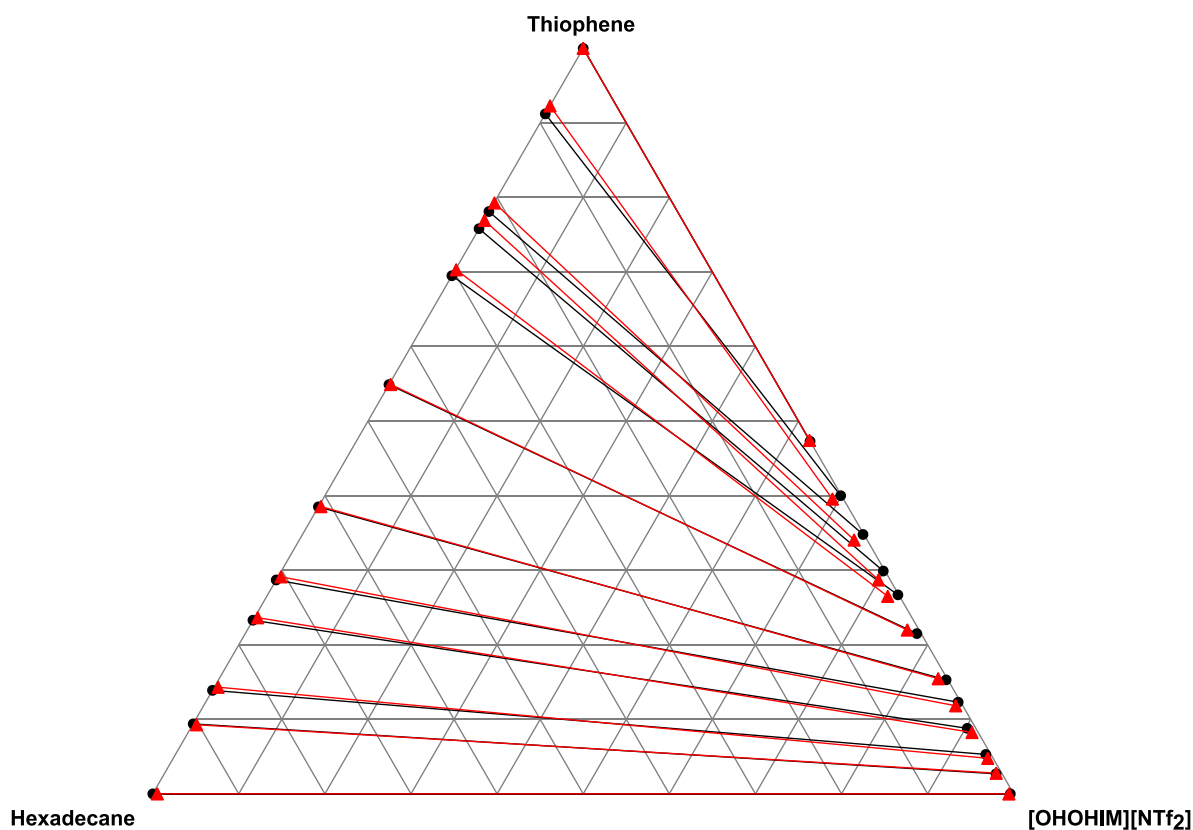


**Fig. 5-10** Plot of the experimental versus calculated LLE data for the ternary system {[OHOHIM][NTf<sub>2</sub>] (1) + thiophene (2) + hexadecane (3)} in mole fractions at  $T = 308.15$  K and  $P = 101$  kPa. ●, Exp: black solid lines; ▲, NRTL Model: red solid lines.

**Table 5-14** Compositions of experimental tie lines in mole fractions, selectivity,  $S$  and solute distribution ratios,  $\beta$  for the ternary system {[BMIM][OTf] (1) + thiophene (2) + hexadecane (3)} at  $T = 308.15$  K and  $P = 101$  kPa<sup>a</sup>.

Hydrocarbon - rich phase		IL - rich phase		$S$	$\beta$
$x_1^{\text{HC}}$	$x_2^{\text{HC}}$	$x_1^{\text{IL}}$	$x_2^{\text{IL}}$		
0.000	0.000	0.981	0.000	-	-
0.000	0.065	0.916	0.082	590	1.26
0.000	0.114	0.884	0.107	92.4	0.94
0.000	0.184	0.782	0.211	134	1.15
0.000	0.265	0.722	0.276	370	1.00
0.000	0.319	0.731	0.267	295	0.87
0.000	0.419	0.639	0.359	249	0.86
0.000	0.525	0.580	0.416	125	0.79
0.000	0.600	0.446	0.551	122	0.92
0.000	0.767	0.369	0.629	63.7	0.82
0.000	0.876	0.318	0.681	48.2	0.78
0.000	1.000	0.172	0.828	-	0.83

<sup>a</sup> Standard uncertainties are:  $u(x) = \pm 0.005$ ;  $u(T) = \pm 0.1$  K;  $u(P) = \pm 1$  kPa.

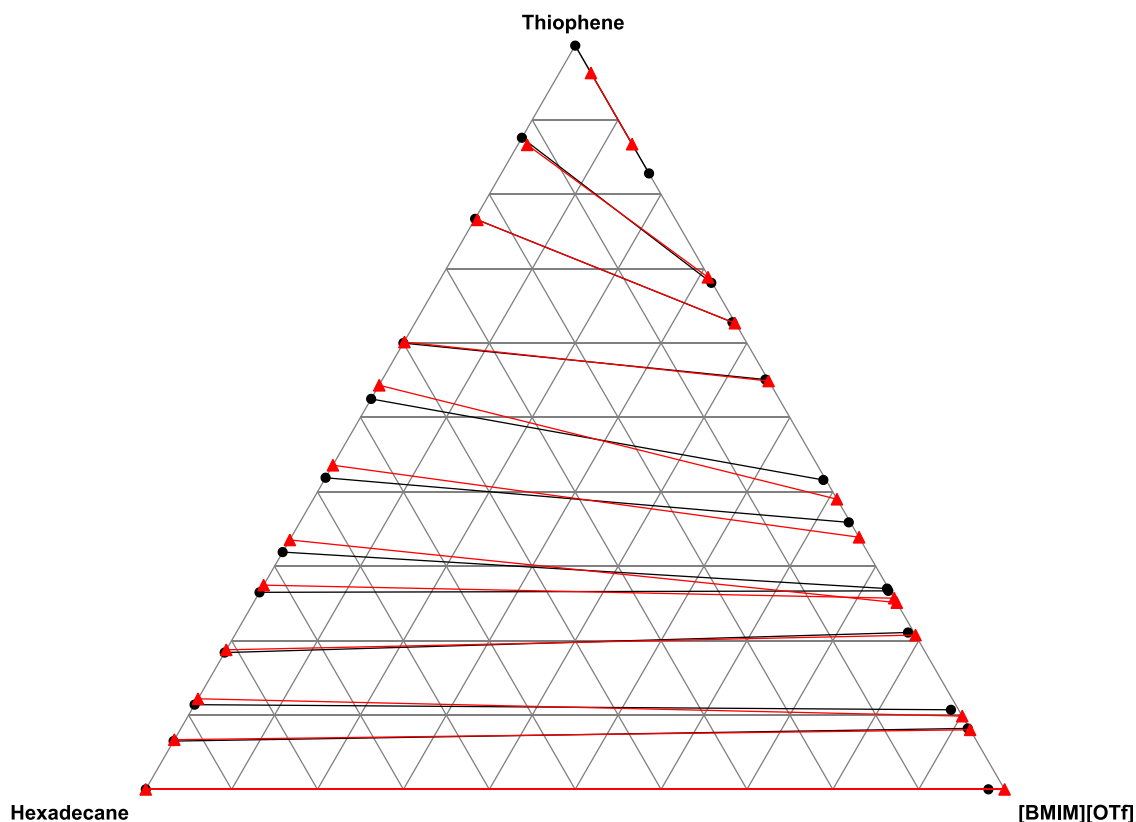


**Fig. 5-11** Plot of the experimental versus calculated LLE data for the ternary system {[BMIM][OTf] (1) + thiophene (2) + hexadecane (3)} in mole fractions at  $T = 308.15$  K and  $P = 101$  kPa. ●, Exp: black solid lines; ▲, NRTL Model: red solid lines.



**Table 5-15** Compositions of experimental tie lines in mole fractions, selectivity,  $S$  and solute distribution ratios,  $\beta$  for the ternary system {[BMPIP][DCA] (1) + thiophene (2) + hexadecane (3)} at  $T = 308.15$  K and  $P = 101$  kPa<sup>a</sup>.

Hydrocarbon - rich phase		IL - rich phase		$S$	$\beta$
$x_1^{\text{HC}}$	$x_2^{\text{HC}}$	$x_1^{\text{IL}}$	$x_2^{\text{IL}}$		
0.000	0.000	0.992	0.000	-	-
0.000	0.115	0.923	0.074	190	0.64
0.000	0.222	0.695	0.298	149	1.34
0.000	0.293	0.639	0.359	43.3	1.23
0.000	0.402	0.542	0.452	134	1.12
0.000	0.466	0.521	0.477	273	1.02
0.000	0.564	0.379	0.615	69.8	1.12
0.000	0.604	0.351	0.647	212	1.07
0.000	0.680	0.317	0.678	79.8	1.00
0.000	0.794	0.303	0.696	181	0.88
0.000	0.905	0.258	0.737	15.5	0.81
0.000	0.946	0.235	0.759	7.22	0.80
0.000	1.000	0.210	0.790	-	0.79

<sup>a</sup> Standard uncertainties are:  $u(x) = \pm 0.005$ ;  $u(T) = \pm 0.1$  K;  $u(P) = \pm 1$  kPa.

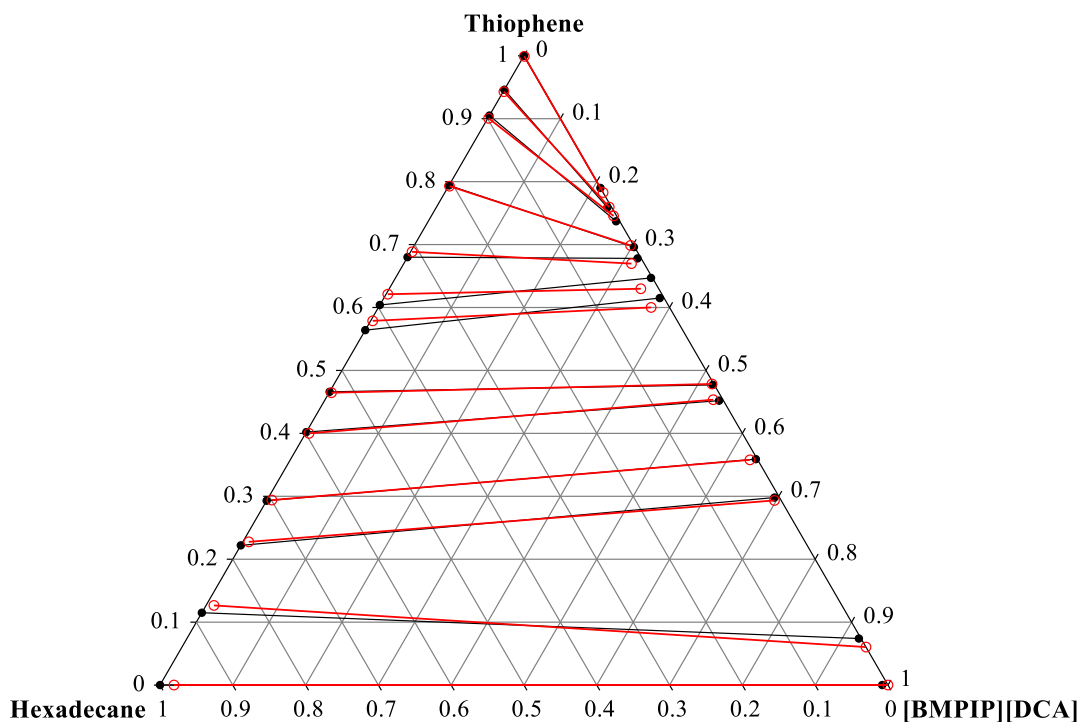


**Fig. 5-12** Plot of the experimental versus calculated LLE data for the ternary system {[BMPIP][DCA] (1) + thiophene (2) + hexadecane (3)} in mole fractions at  $T = 308.15$  K and  $P = 101$  kPa. ●, Exp: black solid lines; ▲, NRTL Model: red solid lines.

**Table 5-16** Compositions of experimental tie lines in mole fractions, selectivity,  $S$  and solute distribution ratios,  $\beta$  for the ternary systems  $\{[P_{-i4,i4,i4,1}][TOS] (1) + \text{thiophene} (2) + \text{hexadecane} (3)\}$  at  $T = 308.15 \text{ K}$  and  $P = 101 \text{ kPa}$ <sup>a</sup>.

Hydrocarbon - rich phase		IL - rich phase		$S$	$\beta$
$x_1^{\text{HC}}$	$x_2^{\text{HC}}$	$x_1^{\text{IL}}$	$x_2^{\text{IL}}$		
0.000	0.000	0.960	0.000	-	-
0.000	0.116	0.872	0.120	114	1.03
0.000	0.129	0.852	0.141	136	1.09
0.000	0.165	0.828	0.166	140	1.01
0.000	0.214	0.803	0.186	62.1	0.87
0.000	0.261	0.758	0.230	54.3	0.88
0.000	0.381	0.584	0.408	82.9	1.07
0.000	0.419	0.508	0.480	55.5	1.15
0.000	0.520	0.437	0.548	33.7	1.05
0.000	0.587	0.396	0.594	41.8	1.01
0.000	0.661	0.367	0.627	53.6	0.95
0.000	0.709	0.299	0.692	31.6	0.98
0.000	0.777	0.252	0.736	17.6	0.95
0.000	0.853	0.203	0.778	7.06	0.91
0.000	0.906	0.146	0.835	4.56	0.92

<sup>a</sup> Standard uncertainties are:  $u(x) = \pm 0.005$ ;  $u(T) = \pm 0.1 \text{ K}$ ;  $u(P) = \pm 1 \text{ kPa}$ .

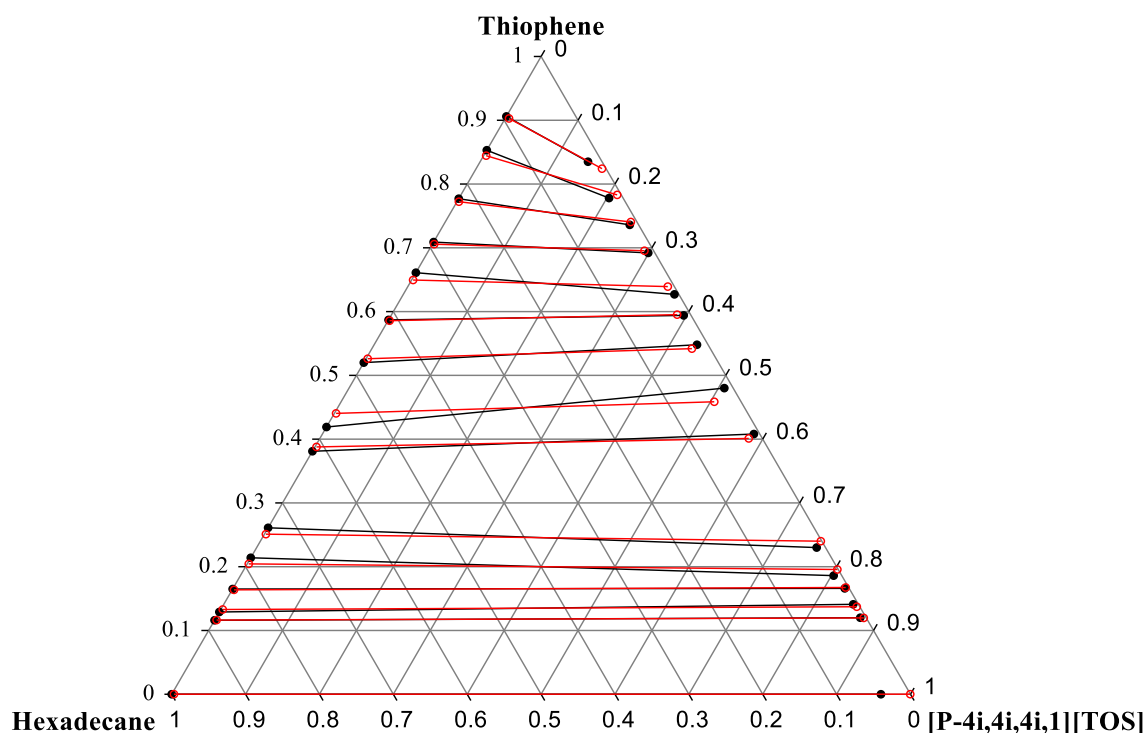


**Fig. 5-13** Plot of the experimental versus calculated LLE data for the ternary system  $\{[P_{i4,i4,i4,1}][TOS] (1) + \text{thiophene} (2) + \text{hexadecane} (3)\}$  in mole fractions at  $T = 308.15 \text{ K}$  and  $P = 101 \text{ kPa}$ . ●, Exp: black solid lines; ▲, NRTL Model: red solid lines.

For most of the listed ternary diagrams, immiscibility regions take almost the entire area of the diagram. It means that ILs and octane/hexadecane do not mix, except for very small, barely traceable amounts. This property is important when selecting extractants, as this allows to prevent raffinate losses during the process of extraction. Only [P<sub>-i4,i4,i4,1</sub>][TOS] shows a slightly higher affinity to octane than other studied ILs. This issue does not occur with the hexadecane system.

Other interesting parameters that can be taken to consideration are tie-line slopes. Positive slopes mean that IL is more suitable for extraction purposes, as more thiophene transfers from the hydrocarbon phase to the IL rich phase. The most important tie-lines for the extractive desulphurisation process are those at the bottom of the Gibbs triangle chart, as they represent mixtures with the lowest concentration of the sulphur compound as the main interest of the desulphurisation process is to decrease S-compounds concentration to below 10 ppm according to the European Union standards [5]. In this work, for the systems with octane all of the ILs, except [OHOHIM][NTf<sub>2</sub>] show a positive slope in the range of interest. For hexadecane systems, slightly positive slopes may be observed for [BMIM][OTf] and [P<sub>-i4,i4,i4,1</sub>][TOS], which corresponds to the higher values of *S* and PI obtained.

The modelling results presented in the table 5-17 show that not all of the systems were calculated with this same precision. Systems containing [BMIM][OTf] showed the highest standard deviations 0.014 and 0.013 for octane and hexadecane, respectively. NRTL model correlations in the upper parts of the Gibbs triangle charts are not well fitted for the binary mixtures of the IL and the thiophene, as shown in figures 5-7 and 5-11. The non-randomness parameter for both systems with [BMIM][OTf] was set equal to 0.1 unlike the other systems, as correlations with value  $\alpha = 0.3$  showed standard deviations above 0.025 which was unacceptable.

**Table 5-17** NRTL model regression results for the ternary systems {[OHOHIM][NTf<sub>2</sub>], [BMIM][OTf], [BMPIP][DCA], [P<sub>i4,i4,i4,1</sub>][TOS] (1) + thiophene (2) + octane/hexadecane (3)} at T= 308.15 K and *P* = 101 kPa.

IL	ij	$g_{ij}/\text{J}\cdot\text{mol}^{-1}$	$g_{ji}/\text{J}\cdot\text{mol}^{-1}$	$\alpha_{ij}$	$\sigma_x$
octane					
[OHOHIM][NTf <sub>2</sub> ]	12	7595.44	25626.75	0.3	0.011
	13	9487.91	7913.27		
	23	5650.20	2730.30		
[BMIM][OTf]	12	-6932.36	14638.14	0.1	0.014
	13	50848.03	40539.05		
	23	10580.27	-4709.30		
[BMPIP][DCA]	12	-4470.01	19493.46	0.3	0.008
	13	9130.96	13221.44		
	23	5505.10	-2659.85		
[P <sub>-i4,i4,i4,1</sub> ][TOS]	12	-5639.80	13207.06	0.3	0.012
	13	29139.08	11553.98		
	23	4974.70	-3164.41		
hexadecane					
[OHOHIM][NTf <sub>2</sub> ]	12	7595.44	25626.75	0.3	0.006
	13	10230.26	10280.69		
	23	5623.93	2891.84		
[BMIM][OTf]	12	-6932.36	14638.14	0.1	0.013
	13	62984.93	26433.90		
	23	10595.30	-4715.20		
[BMPIP][DCA]	12	-4372.69	19355.21	0.3	0.009
	13	24668.42	9868.71		
	23	9646.41	-4530.85		
[P <sub>-i4,i4,i4,1</sub> ][TOS]	12	-5039.03	14339.31	0.3	0.009
	13	18308.80	13051.45		
	23	11480.12	-5607.23		

## 5.5 Laboratory scale extraction studies

### 5.5.1 Operating parameters for the extraction study

The system of {[P-<sub>i4,i4,i4,1</sub>][TOS] + thiophene + hexadecane} was chosen for further investigation to assess the optimal parameters and reuse of the solvent.

Model fuel containing approximately 1500 ppm of thiophene dissolved in hexadecane was prepared by the mixing 0.45 g of thiophene with 109.82 g of hexadecane. The influence of time and temperature were studied.

GC FID detector was recalibrated by the use of the method described in section 4.2.7. Results and the scatter of the data are shown in the form of charts presented in figures 5-14 – 5-17.

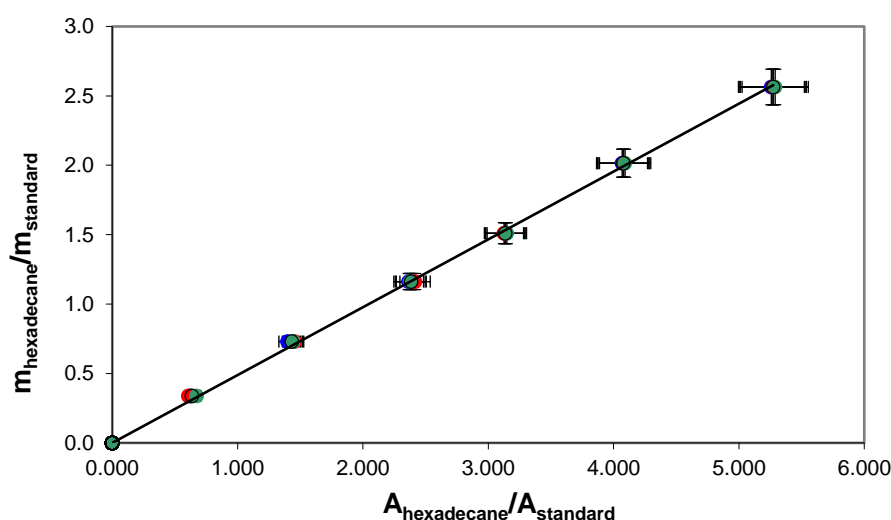


**Fig. 5-14** GC FID detector calibration curve. The ratio of ( $A_{\text{hexadecane}}/A_{\text{standard}}$ ) correlated with the respective mass ratio. For each sample, three separate measurements (marked as ●, ▲ and ■, respectively) were carried out. The average value of ratios (○) for each sample was used to establish the calibration curve linear equation  $y = 0.4887x$  with coefficient of determination  $R^2 = 0.99979$ .

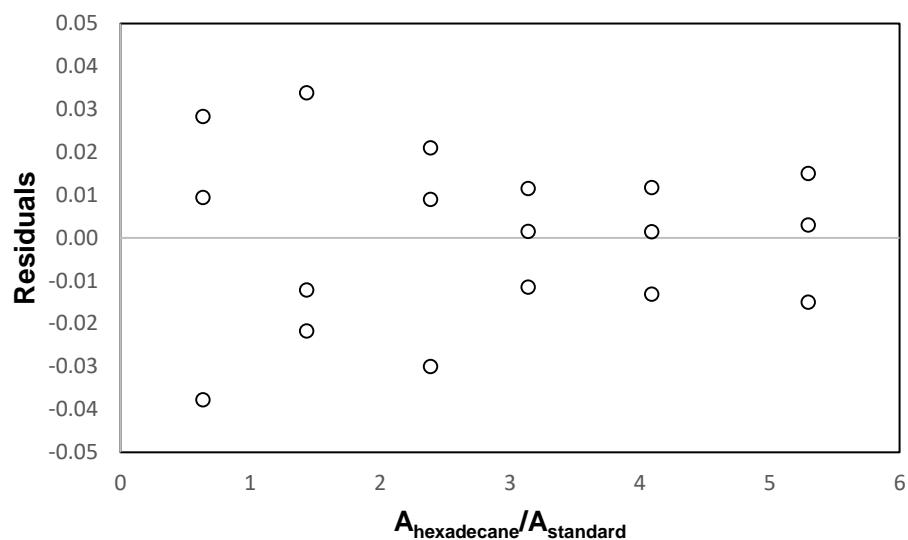


**Fig. 5-15** Residuals for the calibration of the GC FID detector for hexadecane calibration. The standard error for the calibration was 0.005.

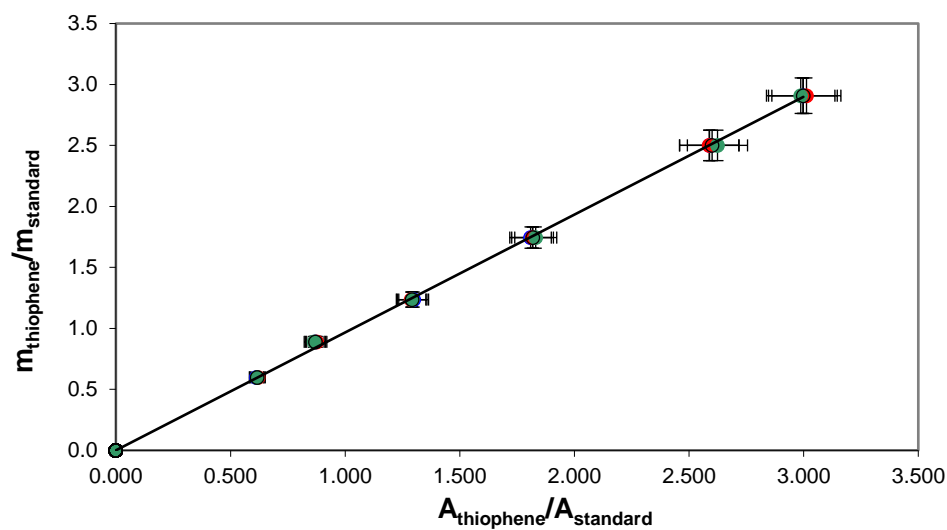


**Fig. 5-16** GC FID detector calibration curve. The ratio of ( $A_{\text{thiophene}}/A_{\text{standard}}$ ) correlated with the respective mass ratio. For each sample, three separate measurements (marked as ●, ▲ and ■, respectively) were carried out. The average value of ratios (○) for each sample was used to establish the calibration curve linear equation  $y = 0.96648x$  with coefficient of determination  $R^2 = 0.99983$ .

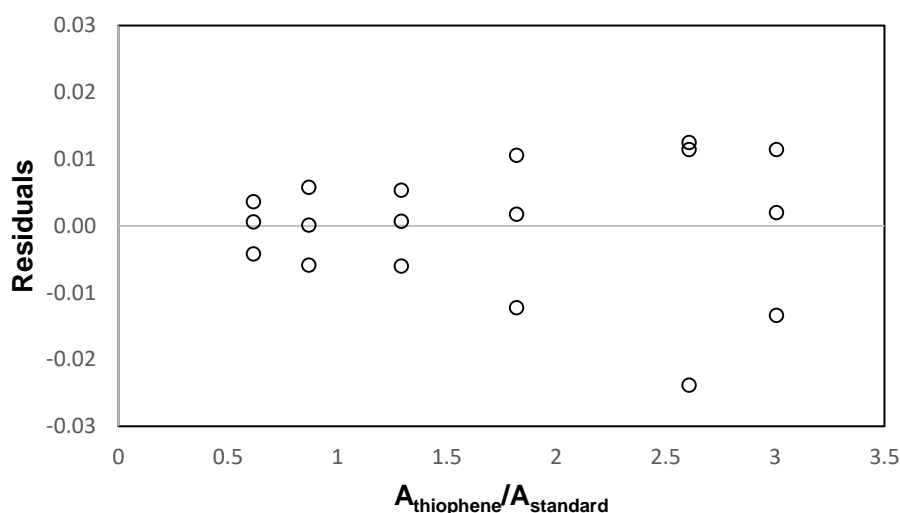


**Fig. 5-17** Residuals for the calibration of the GC FID detector for thiophene calibration. The standard error for the calibration was 0.003.

Four jacketed LLE cells of 10 ccm were filled with 3 ml of IL and 3 ml of the model fuel. Each cell was then sealed and agitated for a given amount of time. The content of the first cell was stirred with the maximum available speed (~2000 rpm) for 0.5 h, the second for 1.0 h, the third for 1.5 h and the last one for 2.0 h. The settling time for each sample was equal to the stirring time. This procedure was repeated for each of the temperatures from range  $T = 298.15$  K,  $T = 308.15$  K and  $T = 318.15$  K; furthermore, the experiments were repeated three times to ensure reproducibility of the results. Samples of the hydrocarbon phase were withdrawn and analysed in the manner discussed in section 4.2. Results of this study are presented in table 5-18 and figure 5-18.

**Table 5-18** Percent removal of S-compound in laboratory-scale EDS for {[P-<sub>i4,i4,i4,1</sub>][TOS] + thiophene + hexadecane} system in the different temperatures and time (equal stirring and settling time)<sup>a</sup>.

t/h	T/K		
	298.15	308.15	318.15
0.5	30.07	44.21	53.15
1.0	38.18	49.89	55.43
1.5	39.15	50.63	56.21
2.0	39.86	51.12	57.35

<sup>a</sup>standard uncertainties are:  $u(x) = \pm 0.5$  %;  $u(T) = \pm 0.1$  K;  $u(P) = \pm 1$  kPa

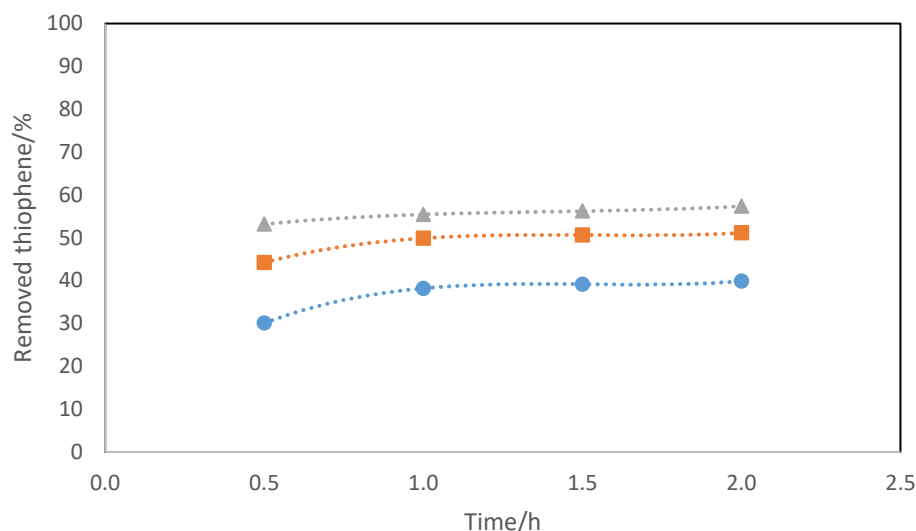


**Fig. 5-18** Percent removal of S-compound in laboratory-scale EDS for {[P-<sub>i4,i4,i4,1</sub>][TOS] + thiophene + hexadecane} system in the range of the temperatures and time (equal stirring and settling time); ● T = 298.15 K; ■ T = 308.15 K; ▲ T = 318.15 K.

The lowest amount of the removed sulphur may be observed for the shortest mixing and settling time in the lower temperature, which may be related to the high viscosity of the [P-<sub>i4,i4,i4,1</sub>][TOS], which does not allow for the proper development of the interphase surface, a factor crucial for efficient extraction. Thermal dependence of the viscosity of the IL makes temperature the most significant property during the EDS process. The stirring and settling time has a lower impact on the EDS process efficiency for the studied system. The measured data shows that stirring time longer than 1 hour has a very low impact on the efficiency of the EDS process. This tendency agrees with the previously published papers. Safa et al. [154] reported results for four ILs based on nitric anion measured in  $T = 298.15$  K, which shows that after 45 minutes of mixing the efficiency of sulphur compound removed does not increase. [OPY][NO<sub>3</sub>], [OMIM][NO<sub>3</sub>], [BMIM][NO<sub>3</sub>] and [BPY][NO<sub>3</sub>] showed approximately 95%, 70%, 70% and 65% overall efficiency of the EDS process, respectively. Taib et al. [148] published data, which show that for 2-hydroxyethanaminium acetate [N-<sub>2OH</sub>][OAc] maximum efficiency of the extraction was achieved after 30 minutes of mixing in  $T = 298.15$  K and it was equal to 59.7%.



### 5.5.2 Assessing the reuse of the solvent

The influence of recycling the solvent on the performance of the IL was studied as well. A jacketed cell was filled with 3 cm<sup>3</sup> of the [P<sub>-i4,i4,i4,1</sub>][TOS] and 3 cm<sup>3</sup> of the hexadecane-based model fuel. Both phases were stirred for 8 hours in  $T = 308.15$  K, and after 12 hours of settling in the same temperature, samples were withdrawn and analysed by the use of the internal standard method mentioned previously. The remaining fuel was decanted from the cell, and IL was reused at the same conditions but with the addition of 3 cm<sup>3</sup> of the fresh fuel. Time of the mixing and settling was exactly this same as in the previous measurement (12 hours each).

After the withdrawal of the sample from the second run IL, the used fuel was removed from the cell, and IL was transferred to the rotavap. It was treated for 24 hours at a temperature  $T = 373.15$  K and  $P = 33$  kPa. The rotavap was fitted with vent to exhaust any traces of the thiophene and other volatile impurities. IL was tested by the use of the GC. The analysis showed traces of the thiophene in the regenerated bath of the ionic liquid. The amount of IL after the treatment was placed in the cell together with 3 cm<sup>3</sup> of the fresh fuel, and the process was repeated in the same conditions as previous runs. Results showing the efficiency of the EDS process are presented in figure 5-19.

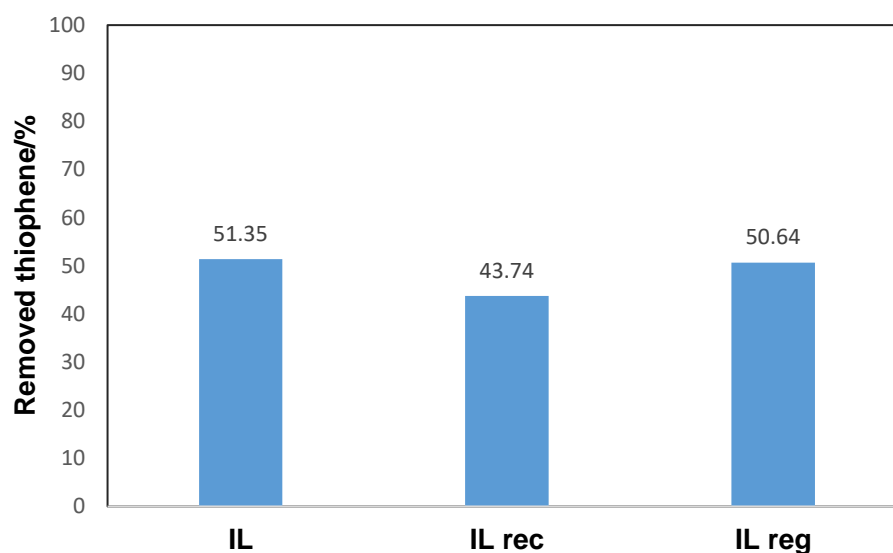


**Fig. 5-19** Graphical representation of the % removal of thiophene from hexadecane model fuel for the EDS process at  $T = 308.15$  K and  $P = 101$  kPa.

Recycled [P<sub>-i4,i4,i4,1</sub>][TOS] shows a deviation from the pure solvent used during the first measurement. In the first run, 51.35% of the thiophene was removed from the

fuel, while the recycled IL achieve only 43.74% of the S-compound removal efficiency. According to the Moghadam et al. [155] and Kianpour et al. [146], it is related to the saturation of the IL with S-compounds. It leads to the inefficient extractions after 3-4 runs, eventually.

To regenerate the IL by the removal of thiophene and other possible volatile impurities a rotavap was used. The regeneration step followed the same method as the purification of ILs before use for experiments as has been explained in Section 4.1.4. The efficiency of the EDS process with the use of the regenerated IL was negligibly lower than the efficiency of the initial measurement and is reported as 50.64% of the removed thiophene. This shows an approximate 98.5 % efficiency in the removal rate. These findings show that ionic liquids can be reused with satisfying efficiency of the extraction process for the limited number of runs and can be regenerated for reuse when the S-compound concentration in the solvent will make process suboptimal. The study conducted by Moghadam [155] shows that the extraction efficiency of the tributyl-(2-hydroxyethyl)phosphonium bromide [P-4,4,4,2OH][Br] after the regeneration process decreased from approximately 70% to 60%. Regeneration was performed by the use of the water dilution technique. Lui et al. [149] used this same method of regeneration as the previously mentioned authors. The 1,1-dimethylpyrrolidonium dimethylphosphate [MMP][DMP] showed a very low decrease of the overall extraction efficiency. Published data shows that EDS efficiency decreased from 70.9 % to 70.7 % after the first run of regeneration and 66.1 % of the efficiency after five runs.

## 5.6 Perspectives of the industrial desulphurisation process using ILs

Extractive desulphurisation is an interesting choice from the point of view of green chemistry and sustainable processes. Ionic liquids provide relatively clean, reusable extractants, which also has the possibility to reduce energy costs in comparison to the traditional treatment of the petrol industry products. As listed in tables 2-1 to 2-5, many of the ILs were studied as potential extractants for the EDS process. Those with the highest values of performance index may be considered as a potential choice for the upscaling from the laboratory scale to the pilot plant scale, and then further to the industrial-scale plant.

In comparison to the other processes alternative to the hydrodesulphurisation mentioned in the literature review, EDS has a relatively small amount of disadvantages, which require additional research. Tunability of the ILs is one of the greatest advantages of this class of compounds [10,229,230]. A virtually infinite number of the ions combinations allows for the best possible extractant not only for the EDS process but also for the different green chemistry processes.

Unfortunately, one of the biggest issues related to the use of ionic liquids is the physical properties of these compounds. The high viscosity of the ionic liquids (from 5.54 mPa for [EMIM][TCM] up to 16150 mPa for [P-4,4,4,2]<sub>2</sub>[DTMN] in temperature  $T = 293.15\text{ K}$  [231]) is one of the most serious issues of this class of compounds which has crucial influence in the bigger scale projects. The major issue is related to the mixing in the reactor or extraction column, as it requires a lot of energy to ensure turbulent flow in the whole volume of the apparatus [232]. Slow mixing will lead to the laminar flow and poorly developed interfacial surface, which will affect the efficiency of the process significantly, as the extraction is possible only in the interphase area. This issue will require additional study in two different fields.

The focus should be on decreasing the viscosity of IL solvents by mixing them with other solvents, i.e. *N,N*-dimethylacetamide, *N,N*-dimethylformamide or tetramethylene, which were studied as successful extractants for EDS process [233]. This may be an interesting way to decrease the viscosity of the IL without losing its extractive properties. The lower viscosity of the extractant ensures easier and more thorough mixing of both phases during the extraction process [234]. Additional experimental work is recommended to study the solubility of the possible co-solvents with ionic liquids, the efficiency of the mixtures and recycling of the solvents.

Another field that should be studied is a design of the modified extraction column to ensure turbulent flow during the mixing of the IL and fuel. There are two main possibilities to carry out an industrial separation process: batch and flow processes. In the first one extraction vessel is filled with both phases, then liquid inside the vessel is mixed and left to separate. The main advantage of this type of process is that a proper design of the agitators allows to ensure good mixing of the entire contents of the reactor and development of the proper interfacial surface. A good example of this type of apparatus is mixer – settler shown in fig. 5-20 and described by Tang et al. [235]. Both phases are delivered in a co-current and are mixed well by the agitators to achieve the smallest

possible size of the droplets and good dispersion of them in the volume of mixed liquid. Well-mixed phases are then moved to the settler part of the apparatus, where the separation occurs. To improve the efficiency of the separation processes with the use of mixers – settlers cascades of few combined units are used. Optimization of this process was described by Diab et al. [236].

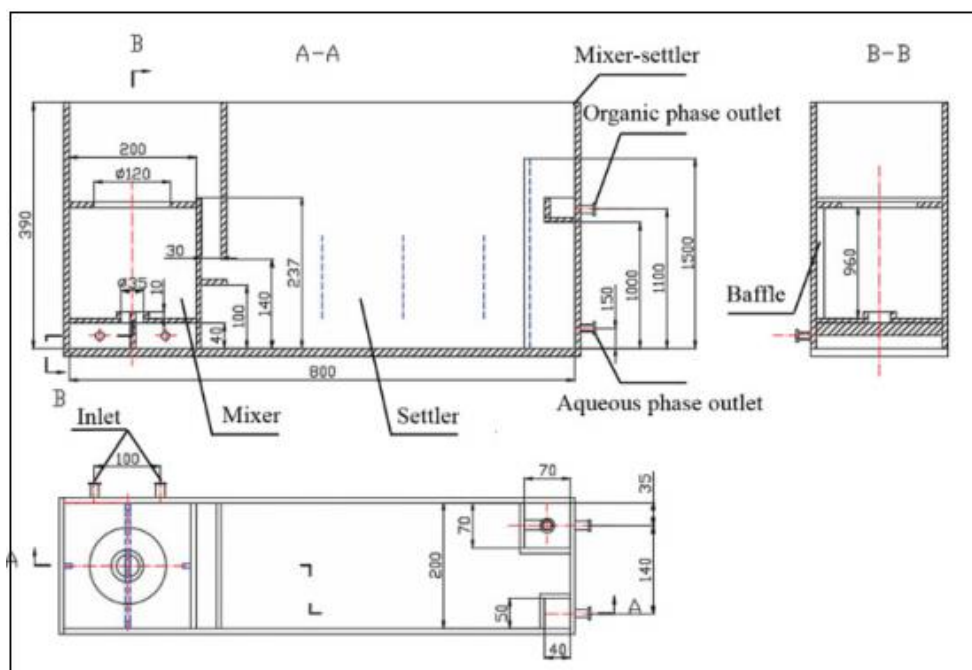


**Fig. 5-20** Schematic of the mixer-settler [235].

The second process, more suitable for the industrial-scale operations is flow extraction carried out with extraction column. In this method, both phases are in constant counter-flow. The heavier phase is introduced to the column from the top, while the lighter one is introduced from the bottom. Figure 5-16 shows a schematic of this type of column. The inlet of the light phase should be designed to ensure proper dispersion of the liquid in the mixture, and creation of the small droplets to increase the surface area of the interface. In combination with the slow counter flow of both phases, this should ensure proper efficiency of the separation process. For the case under consideration, the viscosity of the ionic liquid is a major problem as it may cause clogging of the column packing or insufficient dispersion of the hydrocarbon phase in the volume of IL. Co-solvents mentioned previously could be a solution to this issue. More investigations are required.

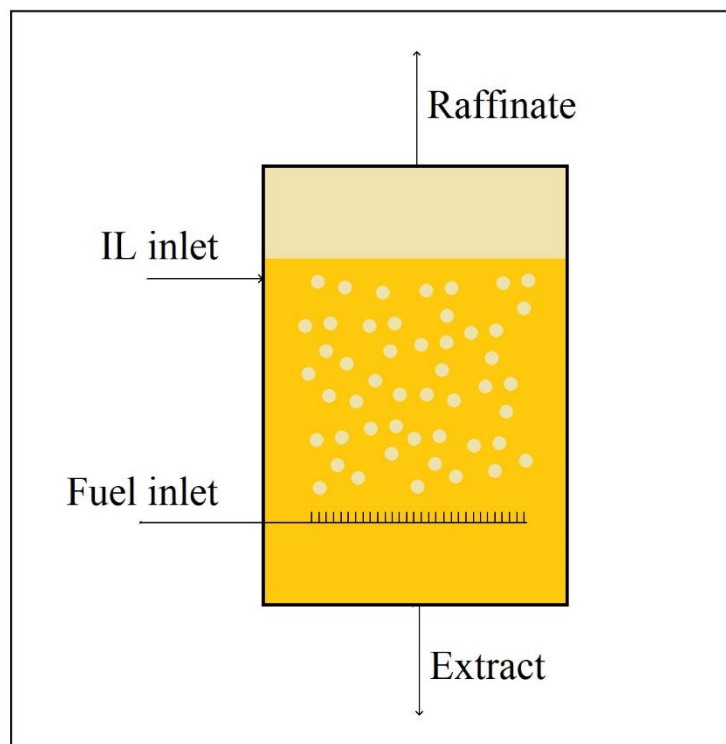


**Fig. 5-21** Schematic of the extraction column with the light phase dispersed in heavy phase.

The biggest issue related to the usage of the ionic liquids in the full-scale industry are the prices of this group of compounds. Sigma Aldrich, one of the biggest suppliers for the chemical industry offers mostly 5g or 50g packages of the ionic liquids from the ammonium-, imidazolium-, pyridinium-, pyrrolidinium-, sulfonium-, and phosphonium-based families of the ionic liquids. Prices of the available ILs are listed in South African Rand. For ammonium-based ILs prices are in the range from 628 ZAR for 25 g of the tetramethylammonium hydroxide pentahydrate  $[N_{-1,1,1,1}][OH] \cdot 5H_2O$ , (which is characterised by the relatively low complexity, and it requires additional of treatment to remove excess water) up to 7049 ZAR for 25g of tetrahexylammonium hydrogensulfate

$[N_{-6,6,6,6}][HSO_4]$  <sup>[237]</sup>. Pyridinium-based ILs are expensive as well <sup>[238]</sup>. One gram of the 1-butyl-3-methylpyridinium bis(trifluoromethylsulfonyl)imide  $[BM(3)PY][NTf_2]$  costs 2713 ZAR. This is related to the position of methyl substituent in the ortho-position, as pyridinium-based ILs without methyl substituent or with methyl substituent in para-position substituent are relatively cheaper, due to the method of synthesis. The cheapest pyridinium-based IL, 1-butyl-4-methylpyridinium iodide  $[BM(4)PY][I]$  costs 4012 ZAR

for 50g while the most expensive, 1-ethylpyridinium tetrafluoroborate [EPY][BF<sub>4</sub>] costs 6836 ZAR per 50g container.

To compare how expensive ILs are, the prices of the traditional solvents in the purity grade >99% offered by Sigma Aldrich [<sup>239</sup>] was made. In the price range of the mentioned 50g of the ILs, the following items can be purchased: an 18 litres container of the 2-propanol, 18 litres container of acetone, 18 litres of methanol, 20 litres container of the 1-octanol, two 4 litre containers of the acetonitrile, 18-litre container of the ethyl acetate, twelve 500 ml bottles of the hexane, or two 5 litre bottles of *N,N*-dimethylformamide.

IoLiTec - Ionic Liquid Technology GmbH, also offers a wide range of the available ionic liquids [<sup>240</sup>]. A query for three ILs, [P<sub>-i4,i4,i4,1</sub>][TOS], [BMPYR][DCA], and [BMIM][OTf], each in quantities of 50g and 1kg was received in which it was stated that [P<sub>-i4,i4,i4,1</sub>][TOS] was discontinued, at the time, and prices for the [BMIM][OTf] and the [BMPYR][DCA] were in the range of approximately 1500 – 2600 ZAR for 50g containers, and 16500 – 22000 ZAR for 1kg containers. Those prices do not include costs of shipment from Germany to South Africa.

South African supplier of chemicals, DLD Scientific [<sup>241</sup>] was quoted for exactly this same items as IoLiTec. The [P<sub>-i4,i4,i4,1</sub>][TOS] was unavailable at the time of quotation. Prices of the [BMIM][OTf] were 3772 ZAR for 50 g container and 18279.25 ZAR for 1 kg of the IL. Prices of the [BMPYR][DCA] offered by the DLD Scientific were 14530.25 ZAR for 50 g and 73680.50 ZAR for 1 kg container of the IL.

This case shows an additional problem, which is the availability of the ILs on the market. Less popular or more complex ILs are discontinued and removed from stock, which may have a negative impact on the progress of experimental research studies.

## Chapter 6 Conclusions

GLC and LLE measurements were performed for the investigation of suitable extractants for extractive desulphurisation processes (EDS). The following ionic liquids were used in LLE measurements with either octane and hexadecane: 1,3-dihydroxyimidazolium bis{(trifluoromethyl)sulphonyl}imide ([OHOHIM][NTf<sub>2</sub>]), 1-butyl-3-methylimidazolium trifluoromethanesulphonate ([BMIM][OTf]), 1-butyl-1-methylpiperidinium dicyanamide ([BMPIP][DCA]), and tri-iso-butylmethylphosphonium tosylate ([P-i4,i4,i4,1][TOS])

Activity coefficients at infinite dilution are important parameters for the design of separation process. The IL 1-butyl-1-methylpyrrolidinium dicyanamide [BMPYR][DCA] studied in this work showed promising results for the application in separation. The selectivities for systems from the point of liquid-liquid extraction: heptane/benzene ( $S = 53.3$ ), heptane/thiophene ( $S = 88.3$ ), heptane/heptyne ( $S = 12.0$ ) and ethylbenzene/styrene ( $S = 2.23$ ) are higher for [BMPYR][DCA] than for other [BMPYR]-based ILs. This shows that [DCA] anion has a stronger influence on the particles such as benzene, thiophene or styrene than other studied anions.

In terms of the performance index, LLE data gathered for the [IL + thiophene + hydrocarbon] obtained during this work are not the best choice for the systems of {IL + thiophene + octane} in comparison with ILs reviewed. [BMPIP][DCA] and [BMIM][OTf] show relatively good performance with PI = 134 and 54.8, respectively. On the contrary, three of four studied ILs in systems with hexadecane show very high values of the performance index. Especially [BMIM][OTf] and [BMPIP][DCA], with PI values of 193 and 122, respectively. This allows the chosen ILs to be deemed as promising extractants for desulphurization of heavier fractions of crude oil.

Recycled [P-i4,i4,i4,1][TOS] shows a deviation from the pure solvent used during the first measurement. In the first run, 51.35% of the thiophene was removed from the fuel, while the recycled IL achieve only 43.74% of the S-compound removal efficiency. The efficiency of the EDS process with the use of the regenerated IL was negligibly lower than the efficiency of the initial measurement and is reported as 50.64% of the removed thiophene. This shows an approximately 98.5 % efficiency in the removal rate, as a slight amount of the thiophene, was detected after the regeneration process. Ionic

liquids can be recycled for the limited number of the cycles. The efficiency of the extractive desulphurisation process decreases with each run as IL saturates with the removed S-compounds.

One of the biggest disadvantages of ILs is their price. The only possibility to change this is via the implementation of ionic liquids into more branches of the chemical industry, which increases market demand for this class of compounds and provides investments into new synthesis plants.



## Chapter 7 Recommendations

Continuation of the work in the form of small scale extraction of the S-compounds from the more complex model fuels (preferable samples from the refinery) with the chosen ILs is recommended. A small volume setup would be profitable to study the behaviour of ionic liquids. This will allow to prepare a list of the ionic liquids with the highest performance index values and the highest capability for recycling. The most prospective solvents should be studied on a larger scale, which would provide more details about the real-life behaviour of the systems. Upscaling of the process would allow to increase the state of knowledge about this class of compounds and possibilities of their industrial applications. From an engineering point of view, it would be interesting to design a pilot-scale installation for EDS process to minimize or at least decrease the influence of the high density and viscosity of the ILs, which are the biggest flaw of this class of chemical compounds which may be used in this technology.

High PI values obtained for [BMPIP][DCA] and [BMIM][OTf] systems with hexadecane shows great potential and should be investigated in the future as promising compounds for the heavy fuels EDS process upscaling. However, for the systems with lighter fuels, different ILs than studied should be selected. According to the data gathered in Tables 2-1 and 2-2, the best choice for the light fuels desulphurisation would be ILs based on cations with relatively short and straight alkyl chains substituent chains as 1-ethyl-3-methylimidazolium, 1-butyl-3-methylimidazolium or 1-ethyl-1-methylmorpholinium cations.

To establish the highest efficiency of the EDS process an optimization study for the most promising ionic liquids should be made. This includes the examination of the impact of the temperature, number of the runs for each batch of the fuel, number of reuse of the solvent, and regeneration of the IL used in the EDS process.

## References

- (1) Anastas, P. T.; Warner, J. P. *Green Chemistry: Theory and Practise*. *Oxf. Univ. Press* **1998**.
- (2) #Envision2030 Goal 12: Responsible Consumption and Production | United Nations Enable <https://www.un.org/development/desa/disabilities/envision2030-goal12.html> (accessed Mar 13, 2020).
- (3) Abu-Eishah, S. I. Ionic Liquids Recycling for Reuse. *Ion. Liq.* **36**.
- (4) What countries are the top producers and consumers of oil? - FAQ - U.S. Energy Information Administration (EIA) <https://www.eia.gov/tools/faqs/faq.php?id=709&t=6> (accessed Mar 13, 2020).
- (5) Directive of the European Parliament and of the Council, Brussels COM (11.05.2001) 241 Final (BS EN 590-2004/DIN EN 590-2004), Automotive Fuels, Diesel, Requirements and Test Methods; and 2003/17/EC OJ L 76, 22.3.2003, p. 10.
- (6) Regulatory Impact Analysis of the United States Environmental Protection Agency EPA420-R00-026.
- (7) SAPIA - South African Petroleum Industry Association > Key Issues > Cleaner fuels II <https://www.sapia.org.za/Key-Issues/Cleaner-fuels-II> (accessed Nov 9, 2020).
- (8) Refining: Uncertainty grips South Africa's Clean Fuels Program <https://www.hydrocarbonprocessing.com/magazine/2017/april-2017/columns/refining-uncertainty-grips-south-africa-s-clean-fuels-program> (accessed Nov 9, 2020).
- (9) Grange, P. Catalytic Hydrodesulfurization. *Catal. Rev.* **1980**, *21* (1), 135–181. <https://doi.org/10.1080/03602458008068062>.
- (10) Earle, M. J.; Seddon, K. R. Ionic Liquids. Green Solvents for the Future. *Pure Appl. Chem.* **2000**, *8*.
- (11) Chiappe, C.; Pieraccini, D. Ionic Liquids: Solvent Properties and Organic Reactivity. *J. Phys. Org. Chem.* **2005**, *18* (4), 275–297. <https://doi.org/10.1002/poc.863>.
- (12) Fredlake, C. P.; Crosthwaite, J. M.; Hert, D. G.; Aki, S. N. V. K.; Brennecke, J. F. Thermophysical Properties of Imidazolium-Based Ionic Liquids. *J. Chem. Eng. Data* **2004**, *49* (4), 954–964. <https://doi.org/10.1021/je034261a>.
- (13) Greaves, T. L.; Drummond, C. J. Protic Ionic Liquids: Properties and Applications. *Chem. Rev.* **2008**, *108* (1), 206–237. <https://doi.org/10.1021/cr068040u>.
- (14) Ngo, H. L.; LeCompte, K.; Hargens, L.; McEwen, A. B. Thermal Properties of Imidazolium Ionic Liquids. *Thermochim. Acta* **2000**, *357–358*, 97–102. [https://doi.org/10.1016/S0040-6031\(00\)00373-7](https://doi.org/10.1016/S0040-6031(00)00373-7).
- (15) Sato, T.; Masuda, G.; Takagi, K. Electrochemical Properties of Novel Ionic Liquids for Electric Double Layer Capacitor Applications. *Electrochimica Acta* **2004**, *49* (21), 3603–3611. <https://doi.org/10.1016/j.electacta.2004.03.030>.
- (16) Tokuda, H.; Tsuzuki, S.; Susan, Md. A. B. H.; Hayamizu, K.; Watanabe, M. How Ionic Are Room-Temperature Ionic Liquids? An Indicator of the Physicochemical Properties. *J. Phys. Chem. B* **2006**, *110* (39), 19593–19600. <https://doi.org/10.1021/jp064159v>.
- (17) Wilkes, J. Properties of Ionic Liquid Solvents for Catalysis. *J. Mol. Catal. Chem.* **2004**, *214* (1), 11–17. <https://doi.org/10.1016/j.molcata.2003.11.029>.

- (18) Zhang, S.; Sun, N.; He, X.; Lu, X.; Zhang, X. Physical Properties of Ionic Liquids: Database and Evaluation. *J. Phys. Chem. Ref. Data* **2006**, *35* (4), 1475–1517. <https://doi.org/10.1063/1.2204959>.
- (19) Krossing, I.; Slattery, J. M.; Daguene, C.; Dyson, P. J.; Oleinikova, A.; Weingärtner, H. Why Are Ionic Liquids Liquid? A Simple Explanation Based on Lattice and Solvation Energies. *J. Am. Chem. Soc.* **2006**, *128* (41), 13427–13434. <https://doi.org/10.1021/ja0619612>.
- (20) Fremantle, M. *An Introduction to Ionic Liquids*; RSC Publishing, 2010.
- (21) Zhang, S.; Lu, X.; Zhou, Q.; Li, X.; Zhang, X.; Li, S. *Ionic Liquids: Physicochemical Properties*; Elsevier, 2009.
- (22) Perez de los Rios, A.; Fernandez, F. J. H. *Ionic Liquids in Separation Technology*; Elsevier, 2014.
- (23) Wasserscheid, P.; Welton, T. *Ionic Liquids in Synthesis*; Wiley-VCH, 2003.
- (24) Huddleston, J. G.; Visser, A. E.; Reichert, W. M.; Willauer, H. D.; Broker, G. A.; Rogers, R. D. Characterization and Comparison of Hydrophilic and Hydrophobic Room Temperature Ionic Liquids Incorporating the Imidazolium Cation. *Green Chem.* **2001**, *3* (4), 156–164. <https://doi.org/10.1039/b103275p>.
- (25) Carda-Broch, S.; Berthod, A.; Armstrong, D. W. Solvent Properties of the 1-Butyl-3-Methylimidazolium Hexafluorophosphate Ionic Liquid. *Anal. Bioanal. Chem.* **2003**, *375* (2), 191–199. <https://doi.org/10.1007/s00216-002-1684-1>.
- (26) Liu, Y.; Zhao, E.; Zhu, W.; Gao, H.; Zhou, Z. Determination of Four Heterocyclic Insecticides by Ionic Liquid Dispersive Liquid–Liquid Microextraction in Water Samples. *J. Chromatogr. A* **2009**, *1216* (6), 885–891. <https://doi.org/10.1016/j.chroma.2008.11.076>.
- (27) Abulhassani, J.; Manzoori, J. L.; Amjadi, M. Hollow Fiber Based-Liquid Phase Microextraction Using Ionic Liquid Solvent for Preconcentration of Lead and Nickel from Environmental and Biological Samples Prior to Determination by Electrothermal Atomic Absorption Spectrometry. *J. Hazard. Mater.* **2010**, *176* (1–3), 481–486. <https://doi.org/10.1016/j.jhazmat.2009.11.054>.
- (28) Abdolmohammad-Zadeh, H.; Sadeghi, G. H. A Novel Microextraction Technique Based on 1-Hexylpyridinium Hexafluorophosphate Ionic Liquid for the Preconcentration of Zinc in Water and Milk Samples. *Anal. Chim. Acta* **2009**, *649* (2), 211–217. <https://doi.org/10.1016/j.aca.2009.07.040>.
- (29) Cao, X.; Ye, X.; Lu, Y.; Yu, Y.; Mo, W. Ionic Liquid-Based Ultrasonic-Assisted Extraction of Piperine from White Pepper. *Anal. Chim. Acta* **2009**, *640* (1–2), 47–51. <https://doi.org/10.1016/j.aca.2009.03.029>.
- (30) Cevasco, G.; Chiappe, C. Are Ionic Liquids a Proper Solution to Current Environmental Challenges? *Green Chem.* **2014**, *16* (5), 2375. <https://doi.org/10.1039/c3gc42096e>.
- (31) Zhu, S.; Wu, Y.; Chen, Q.; Yu, Z.; Wang, C.; Jin, S.; Ding, Y.; Wu, G. Dissolution of Cellulose with Ionic Liquids and Its Application: A Mini-Review. *Green Chem.* **2006**, *8* (4), 325. <https://doi.org/10.1039/b601395c>.
- (32) Abai, M.; Atkins, M. P.; Hassan, A.; Holbrey, J. D.; Kuah, Y.; Nockemann, P.; Oliferenko, A. A.; Plechkova, N. V.; Rafeen, S.; Rahman, A. A.; Ramli, R.; Shariff, S. M.; Seddon, K. R.; Srinivasan, G.; Zou, Y. An Ionic Liquid Process for Mercury Removal from Natural Gas. *Dalton Trans.* **2015**, *44* (18), 8617–8624. <https://doi.org/10.1039/C4DT03273J>.
- (33) Karadas, F.; Atilhan, M.; Aparicio, S. Review on the Use of Ionic Liquids (ILs) as Alternative Fluids for CO<sub>2</sub> Capture and Natural Gas Sweetening. *Energy Fuels* **2010**, *24* (11), 5817–5828. <https://doi.org/10.1021/ef1011337>.

- (34) Aghaie, M.; Rezaei, N.; Zendehboudi, S. A Systematic Review on CO<sub>2</sub> Capture with Ionic Liquids: Current Status and Future Prospects. *Renew. Sustain. Energy Rev.* **2018**, *96*, 502–525. <https://doi.org/10.1016/j.rser.2018.07.004>.
- (35) Valencia-Marquez, D.; Flores-Tlacuahuac, A.; Ricardez-Sandoval, L. Technoeconomic and Dynamical Analysis of a CO<sub>2</sub> Capture Pilot-Scale Plant Using Ionic Liquids. *Ind. Eng. Chem. Res.* **2015**, *54* (45), 11360–11370. <https://doi.org/10.1021/acs.iecr.5b02544>.
- (36) Valencia-Marquez, D.; Flores-Tlacuahuac, A.; Ricardez-Sandoval, L. A Controllability Analysis of a Pilot-Scale CO<sub>2</sub> Capture Plant Using Ionic Liquids. *AIChE J.* **2016**, *62* (9), 3298–3309. <https://doi.org/10.1002/aic.15371>.
- (37) Kidnay, A. J.; Parrish, W. R.; McCartney, D. G.; Parrish, W. R.; McCartney, D. G. *Fundamentals of Natural Gas Processing*; CRC Press, 2011. <https://doi.org/10.1201/b14397>.
- (38) Ding, J.; Zhou, D.; Spinks, G.; Wallace, G.; Forsyth, S.; Forsyth, M.; MacFarlane, D. Use of Ionic Liquids as Electrolytes in Electromechanical Actuator Systems Based on Inherently Conducting Polymers. *Chem. Mater.* **2003**, *15* (12), 2392–2398. <https://doi.org/10.1021/cm020918k>.
- (39) Liu, J.; Jiang, G.; Chi, Y.; Cai, Y.; Zhou, Q.; Hu, J.-T. Use of Ionic Liquids for Liquid-Phase Microextraction of Polycyclic Aromatic Hydrocarbons. *Anal. Chem.* **2003**, *75* (21), 5870–5876. <https://doi.org/10.1021/ac034506m>.
- (40) Lu, W.; Fadeev, A. G.; Qi, B.; Smela, E.; Mattes, B. R.; Ding, J.; Spinks, G. M.; Mazurkiewicz, J.; Zhou, D.; Wallace, G. G.; MacFarlane, D. R.; Forsyth, S. A.; Forsyth, M. Use of Ionic Liquids for  $\pi$ -Conjugated Polymer Electrochemical Devices. **2002**, 297, 6.
- (41) Park, S.; Kazlauskas, R. J. Improved Preparation and Use of Room-Temperature Ionic Liquids in Lipase-Catalyzed Enantio- and Regioselective Acylations. *J. Org. Chem.* **2001**, *66* (25), 8395–8401. <https://doi.org/10.1021/jo015761e>.
- (42) Parker, S. T.; Slinker, J. D.; Lowry, M. S.; Cox, M. P.; Bernhard, S.; Malliaras, G. G. Improved Turn-on Times of Iridium Electroluminescent Devices by Use of Ionic Liquids. *Chem. Mater.* **2005**, *17* (12), 3187–3190. <https://doi.org/10.1021/cm050314r>.
- (43) Suarez, P. A. Z.; Dullius, J. E. L.; Einloft, S.; De Souza, R. F.; Dupont, J. The Use of New Ionic Liquids in Two-Phase Catalytic Hydrogenation Reaction by Rhodium Complexes. *Polyhedron* **1996**, *15* (7), 1217–1219. [https://doi.org/10.1016/0277-5387\(95\)00365-7](https://doi.org/10.1016/0277-5387(95)00365-7).
- (44) Kulkarni, P. S.; Afonso, C. A. M. Deep Desulfurization of Diesel Fuel Using Ionic Liquids: Current Status and Future Challenges. **2010**, 11.
- (45) Abro, R.; Abdeltawab, A. A.; Al-Deyab, S. S.; Yu, G.; Qazi, A. B.; Gao, S.; Chen, X. A Review of Extractive Desulfurization of Fuel Oils Using Ionic Liquids. *RSC Adv* **2014**, *4* (67), 35302–35317. <https://doi.org/10.1039/C4RA03478C>.
- (46) Ibrahim, M. H.; Hayyan, M.; Hashim, M. A.; Hayyan, A. The Role of Ionic Liquids in Desulfurization of Fuels: A Review. *Renew. Sustain. Energy Rev.* **2017**, *76*, 1534–1549. <https://doi.org/10.1016/j.rser.2016.11.194>.
- (47) Chandra Srivastava, V. An Evaluation of Desulfurization Technologies for Sulfur Removal from Liquid Fuels. *RSC Adv* **2012**, *2* (3), 759–783. <https://doi.org/10.1039/C1RA00309G>.
- (48) Lin, Y.; Wang, F.; Zhang, Z.; Yang, J.; Wei, Y. Polymer-Supported Ionic Liquids: Synthesis, Characterization and Application in Fuel Desulfurization. *Fuel* **2014**, *116*, 273–280. <https://doi.org/10.1016/j.fuel.2013.08.014>.

- (49) Khan, N. A.; Hasan, Z.; Jhung, S. H. Ionic Liquids Supported on Metal-Organic Frameworks: Remarkable Adsorbents for Adsorptive Desulfurization. *Chem. - Eur. J.* **2014**, *20* (2), 376–380. <https://doi.org/10.1002/chem.201304291>.
- (50) Wu, J.; Gao, Y.; Zhang, W.; Tan, Y.; Tang, A.; Men, Y.; Tang, B. Adsorption Desulfurization Study with Ionic Liquid Compound ZrO<sub>2</sub>/PSMIMHSO<sub>4</sub>. *Appl. Petrochem. Res.* **2016**, *6* (4), 361–366. <https://doi.org/10.1007/s13203-016-0148-z>.
- (51) Bhutto, A. W.; Abro, R.; Gao, S.; Abbas, T.; Chen, X.; Yu, G. Oxidative Desulfurization of Fuel Oils Using Ionic Liquids: A Review. *J. Taiwan Inst. Chem. Eng.* **2016**, *62*, 84–97. <https://doi.org/10.1016/j.jtice.2016.01.014>.
- (52) Han, D.; Row, K. H. Recent Applications of Ionic Liquids in Separation Technology. *Molecules* **2010**, *15* (4), 2405–2426. <https://doi.org/10.3390/molecules15042405>.
- (53) Pohorecki, R.; Bridgwater, J.; Molzahn, M.; Gani, R.; Gallegos, C. *Chemical Engineering And Chemical Process Technology*; EOLSS Publications, 2010; Vol. II.
- (54) Seader, J. D.; Henley, E. J.; Roper, D. K. *Separation Processes Principles with Applications Using Process Simulators*; Wiley, 2016.
- (55) Kumar, A. A. P.; Banerjee, T. Thiophene Separation with Ionic Liquids for Desulphurization: A Quantum Chemical Approach. *Fluid Phase Equilib.* **2009**, *278* (1–2), 1–8. <https://doi.org/10.1016/j.fluid.2008.11.019>.
- (56) Domańska, U.; Laskowska, M. Measurements of Activity Coefficients at Infinite Dilution of Aliphatic and Aromatic Hydrocarbons, Alcohols, Thiophene, Tetrahydrofuran, MTBE, and Water in Ionic Liquid [BMIM][SCN] Using GLC. *J. Chem. Thermodyn.* **2009**, *41* (5), 645–650. <https://doi.org/10.1016/j.jct.2008.12.018>.
- (57) Domańska, U.; Królikowska, M. Measurements of Activity Coefficients at Infinite Dilution in Solvent Mixtures with Thiocyanate-Based Ionic Liquids Using GLC Technique. *J. Phys. Chem. B* **2010**, *114* (25), 8460–8466. <https://doi.org/10.1021/jp103496d>.
- (58) Domańska, U.; Karpińska, M.; Wlazło, M. Thermodynamic Study of Molecular Interaction-Selectivity in Separation Processes Based on Limiting Activity Coefficients. *J. Chem. Thermodyn.* **2018**, *121*, 112–120. <https://doi.org/10.1016/j.jct.2018.02.014>.
- (59) Królikowski, M.; Królikowska, M. The Study of Activity Coefficients at Infinite Dilution for Organic Solutes and Water in 1-Butyl-4-Methylpyridinium Dicyanamide, [B4MPy][DCA] Using GLC. *J. Chem. Thermodyn.* **2014**, *68*, 138–144. <https://doi.org/10.1016/j.jct.2013.09.007>.
- (60) Domańska, U.; Karpińska, M.; Zawadzki, M. Activity Coefficients at Infinite Dilution for Organic Solutes and Water in 1-Ethyl-1-Methylpyrrolidinium Lactate. *J. Chem. Thermodyn.* **2015**, *89*, 127–133. <https://doi.org/10.1016/j.jct.2015.05.014>.
- (61) Wlazło, M.; Gawkowska, J.; Domańska, U. Separation Based on Limiting Activity Coefficients of Various Solutes in 1-Allyl-3-Methylimidazolium Dicyanamide Ionic Liquid. *Ind. Eng. Chem. Res.* **2016**, *55* (17), 5054–5062. <https://doi.org/10.1021/acs.iecr.6b00942>.
- (62) Domańska, U.; Wlazło, M.; Karpińska, M. Activity Coefficients at Infinite Dilution of Organic Solvents and Water in 1-Butyl-3-Methylimidazolium Dicyanamide. A Literature Review of Hexane/Hex-1-Ene Separation. *Fluid Phase Equilib.* **2016**, *417*, 50–61. <https://doi.org/10.1016/j.fluid.2016.02.004>.

- (63) Domańska, U.; Redhi, G. G.; Marciniak, A. Activity Coefficients at Infinite Dilution Measurements for Organic Solutes and Water in the Ionic Liquid 1-Butyl-1-Methylpyrrolidinium Trifluoromethanesulfonate Using GLC. *Fluid Phase Equilib.* **2009**, 278 (1–2), 97–102. <https://doi.org/10.1016/j.fluid.2009.01.011>.
- (64) Domańska, U.; Lukoshko, E. V. Measurements of Activity Coefficients at Infinite Dilution for Organic Solutes and Water in the Ionic Liquid 1-Butyl-1-Methylpyrrolidinium Tricyanomethanide. *J. Chem. Thermodyn.* **2013**, 66, 144–150. <https://doi.org/10.1016/j.jct.2013.07.004>.
- (65) Domańska, U.; Paduszyński, K. Gas–Liquid Chromatography Measurements of Activity Coefficients at Infinite Dilution of Various Organic Solutes and Water in Tri-Iso-Butylmethylphosphonium Tosylate Ionic Liquid. *J. Chem. Thermodyn.* **2010**, 42 (6), 707–711. <https://doi.org/10.1016/j.jct.2010.01.004>.
- (66) Domańska, U.; Wlazło, M.; Karpińska, M.; Zawadzki, M. Separation of Binary Mixtures Hexane/Hex-1-Ene, Cyclohexane/Cyclohexene and Ethylbenzene/Styrene Based on Limiting Activity Coefficients. *J. Chem. Thermodyn.* **2017**, 110, 227–236. <https://doi.org/10.1016/j.jct.2017.03.004>.
- (67) Wlazło, M.; Marciniak, A.; Zawadzki, M.; Dudkiewicz, B. Activity Coefficients at Infinite Dilution and Physicochemical Properties for Organic Solutes and Water in the Ionic Liquid 4-(3-Hydroxypropyl)-4-Methylmorpholinium Bis(Trifluoromethylsulfonyl)-Amide. *J. Chem. Thermodyn.* **2015**, 86, 154–161. <https://doi.org/10.1016/j.jct.2015.02.024>.
- (68) Karpińska, M.; Wlazło, M.; Domańska, U. Separation of Binary Mixtures Based on Gamma Infinity Data Using [EMIM][TCM] Ionic Liquid and Modelling of Thermodynamic Functions. *J. Mol. Liq.* **2017**, 225, 382–390. <https://doi.org/10.1016/j.molliq.2016.11.081>.
- (69) Lukoshko, E.; Mutelet, F.; Domanska, U. Experimental and Theoretically Study of Interaction between Organic Compounds and Tricyanomethanide Based Ionic Liquids. *J. Chem. Thermodyn.* **2015**, 85, 49–56. <https://doi.org/10.1016/j.jct.2014.12.027>.
- (70) Domańska, U.; Karpińska, M. The Use of Ionic Liquids for Separation of Binary Hydrocarbons Mixtures Based on Gamma Infinity Data Measurements. *J. Chem. Thermodyn.* **2018**, 127, 95–105. <https://doi.org/10.1016/j.jct.2018.07.024>.
- (71) Wlazło, M.; Karpińska, M.; Domańska, U. A 1-Alkylcyanopyridinium-Based Ionic Liquid in the Separation Processes. *J. Chem. Thermodyn.* **2016**, 97, 253–260. <https://doi.org/10.1016/j.jct.2016.01.017>.
- (72) Domańska, U.; Królikowski, M.; Acree, W. E. Thermodynamics and Activity Coefficients at Infinite Dilution Measurements for Organic Solutes and Water in the Ionic Liquid 1-Butyl-1-Methylpyrrolidinium Tetracyanoborate. *J. Chem. Thermodyn.* **2011**, 43 (12), 1810–1817. <https://doi.org/10.1016/j.jct.2011.06.007>.
- (73) Domańska, U.; Marciniak, A. Activity Coefficients at Infinite Dilution Measurements for Organic Solutes and Water in the Ionic Liquid 4-Methyl-N-Butyl-Pyridinium Bis(Trifluoromethylsulfonyl)-Imide. *J. Chem. Thermodyn.* **2009**, 41 (12), 1350–1355. <https://doi.org/10.1016/j.jct.2009.06.011>.
- (74) Domańska, U.; Paduszyński, K. Measurements of Activity Coefficients at Infinite Dilution of Organic Solutes and Water in 1-Propyl-1-Methylpiperidinium Bis{(Trifluoromethyl)Sulfonyl}imide Ionic Liquid Using g.l.c. *J. Chem. Thermodyn.* **2010**, 42 (11), 1361–1366. <https://doi.org/10.1016/j.jct.2010.05.017>.
- (75) Domańska, U.; Królikowska, M.; Acree, W. E.; Baker, G. A. Activity Coefficients at Infinite Dilution Measurements for Organic Solutes and Water in

- the Ionic Liquid 1-Ethyl-3-Methylimidazolium Tetracyanoborate. *J. Chem. Thermodyn.* **2011**, *43* (7), 1050–1057. <https://doi.org/10.1016/j.jct.2011.02.012>.
- (76) Wlazło, M.; Marciniak, A. Activity Coefficients at Infinite Dilution and Physicochemical Properties for Organic Solutes and Water in the Ionic Liquid 4-(2-Methoxyethyl)-4-Methylmorpholinium Trifluorotris(Perfluoroethyl)Phosphate. *J. Chem. Thermodyn.* **2012**, *54*, 366–372. <https://doi.org/10.1016/j.jct.2012.05.017>.
- (77) Marciniak, A.; Wlazło, M. Activity Coefficients at Infinite Dilution and Physicochemical Properties for Organic Solutes and Water in the Ionic Liquid 4-(2-Methoxyethyl)-4-Methylmorpholinium Bis(Trifluoromethylsulfonyl)-Amide. *J. Chem. Thermodyn.* **2012**, *47*, 382–388. <https://doi.org/10.1016/j.jct.2011.11.021>.
- (78) Marciniak, A.; Wlazło, M. Activity Coefficients at Infinite Dilution and Physicochemical Properties for Organic Solutes and Water in the Ionic Liquid 1-(2-Methoxyethyl)-1-Methylpiperidinium Trifluorotris(Perfluoroethyl)Phosphate. *J. Chem. Thermodyn.* **2013**, *57*, 197–202. <https://doi.org/10.1016/j.jct.2012.08.016>.
- (79) Domańska, U.; Marciniak, A. Activity Coefficients at Infinite Dilution Measurements for Organic Solutes and Water in the Ionic Liquid Triethylsulphonium Bis(Trifluoromethylsulfonyl)Imide. *J. Chem. Thermodyn.* **2009**, *41* (6), 754–758. <https://doi.org/10.1016/j.jct.2008.12.005>.
- (80) Domańska, U.; Lukoshko, E. V.; Wlazło, M. Measurements of Activity Coefficients at Infinite Dilution for Organic Solutes and Water in the Ionic Liquid 1-Hexyl-3-Methylimidazolium Tetracyanoborate. *J. Chem. Thermodyn.* **2012**, *47*, 389–396. <https://doi.org/10.1016/j.jct.2011.11.025>.
- (81) Marciniak, A. Activity Coefficients at Infinite Dilution and Physicochemical Properties for Organic Solutes and Water in the Ionic Liquid 1-(3-Hydroxypropyl)Pyridinium Bis(Trifluoromethylsulfonyl)-Amide. *J. Chem. Thermodyn.* **2011**, *43* (10), 1446–1452. <https://doi.org/10.1016/j.jct.2011.04.018>.
- (82) Domańska, U.; Marciniak, A. Activity Coefficients at Infinite Dilution Measurements for Organic Solutes and Water in the Ionic Liquid 1-Butyl-3-Methylimidazolium Trifluoromethanesulfonate. *J. Phys. Chem. B* **2008**, *112* (35), 11100–11105. <https://doi.org/10.1021/jp804107y>.
- (83) Marciniak, A.; Wlazło, M. Activity Coefficients at Infinite Dilution Measurements for Organic Solutes and Water in the Ionic Liquid 1-Butyl-3-Methyl-Pyridinium Trifluoromethanesulfonate. *J. Chem. Eng. Data* **2010**, *55* (9), 3208–3211. <https://doi.org/10.1021/je1000582>.
- (84) Marciniak, A.; Wlazło, M. Activity Coefficients at Infinite Dilution and Physicochemical Properties for Organic Solutes and Water in the Ionic Liquid 1-(2-Methoxyethyl)-1-Methylpiperidinium Bis(Trifluoromethylsulfonyl)-Amide. *J. Chem. Thermodyn.* **2012**, *49*, 137–145. <https://doi.org/10.1016/j.jct.2012.01.019>.
- (85) Marciniak, A.; Wlazło, M. Activity Coefficients at Infinite Dilution and Physicochemical Properties for Organic Solutes and Water in the Ionic Liquid 1-(2-Hydroxyethyl)-3-Methylimidazolium Trifluorotris(Perfluoroethyl)Phosphate. *J. Chem. Thermodyn.* **2013**, *64*, 114–119. <https://doi.org/10.1016/j.jct.2013.05.008>.
- (86) Marciniak, A.; Wlazło, M. Activity Coefficients at Infinite Dilution and Physicochemical Properties for Organic Solutes and Water in the Ionic Liquid 1-(2-Methoxyethyl)-1-Methylpyrrolidinium Trifluorotris(Perfluoroethyl)Phosphate. *J. Chem. Thermodyn.* **2013**, *60*, 57–62. <https://doi.org/10.1016/j.jct.2013.01.007>.

- (87) Domańska, U.; Królikowski, M.; Acree, W. E.; Baker, G. A. Physicochemical Properties and Activity Coefficients at Infinite Dilution for Organic Solutes and Water in a Novel Bicyclic Guanidinium Superbase-Derived Protic Ionic Liquid. *J. Chem. Thermodyn.* **2013**, *58*, 62–69. <https://doi.org/10.1016/j.jct.2012.09.033>.
- (88) Paduszyński, K.; Domańska, U. Limiting Activity Coefficients and Gas–Liquid Partition Coefficients of Various Solutes in Piperidinium Ionic Liquids: Measurements and LSER Calculations. *J. Phys. Chem. B* **2011**, *115* (25), 8207–8215. <https://doi.org/10.1021/jp202010w>.
- (89) Marciniak, A.; Wlazło, M. Activity Coefficients at Infinite Dilution and Physicochemical Properties for Organic Solutes and Water in the Ionic Liquid 1-(2-Methoxyethyl)-1-Methylpyrrolidinium Bis(Trifluoromethylsulfonyl)-Amide. *J. Chem. Thermodyn.* **2012**, *54*, 90–96. <https://doi.org/10.1016/j.jct.2012.03.015>.
- (90) Paduszyński, K.; Domańska, U. Experimental and Theoretical Study on Infinite Dilution Activity Coefficients of Various Solutes in Piperidinium Ionic Liquids. *J. Chem. Thermodyn.* **2013**, *60*, 169–178. <https://doi.org/10.1016/j.jct.2013.01.005>.
- (91) Marciniak, A.; Wlazło, M. Activity Coefficients at Infinite Dilution, Physicochemical and Thermodynamic Properties for Organic Solutes and Water in the Ionic Liquid Ethyl-Dimethyl-(2-Methoxyethyl)Ammonium Trifluorotris-(Perfluoroethyl)Phosphate. *J. Chem. Thermodyn.* **2015**, *89*, 245–250. <https://doi.org/10.1016/j.jct.2015.05.022>.
- (92) Wlazło, M.; Marciniak, A.; Letcher, T. M. Activity Coefficients at Infinite Dilution and Physicochemical Properties for Organic Solutes and Water in the Ionic Liquid 1-Ethyl-3-Methylimidazolium Trifluorotris(Perfluoroethyl)Phosphate. *J. Solut. Chem.* **2015**, *44* (3–4), 413–430. <https://doi.org/10.1007/s10953-014-0274-0>.
- (93) Królikowski, M.; Królikowska, M.; Wiśniewski, C. Separation of Aliphatic from Aromatic Hydrocarbons and Sulphur Compounds from Fuel Based on Measurements of Activity Coefficients at Infinite Dilution for Organic Solutes and Water in the Ionic Liquid N,N-Diethyl-N-Methyl-N-(2-Methoxy-Ethyl)Ammonium Bis(Trifluoromethylsulfonyl)Imide. *J. Chem. Thermodyn.* **2016**, *103*, 115–124. <https://doi.org/10.1016/j.jct.2016.07.017>.
- (94) Ayad, A.; Mutelet, F.; Negadi, A.; Acree, W. E.; Jiang, B.; Lu, A.; Wagle, D. V.; Baker, G. A. Activity Coefficients at Infinite Dilution for Organic Solutes Dissolved in Two 1-Alkylquinuclidinium Bis(Trifluoromethylsulfonyl)Imides Bearing Alkyl Side Chains of Six and Eight Carbons. *J. Mol. Liq.* **2016**, *215*, 176–184. <https://doi.org/10.1016/j.molliq.2015.12.029>.
- (95) Wlazło, M.; Karpńska, M.; Domańska, U. Thermodynamics and Selectivity of Separation Based on Activity Coefficients at Infinite Dilution of Various Solutes in 1-Allyl-3-Methylimidazolium Bis{(Trifluoromethyl)Sulfonyl}imide Ionic Liquid. *J. Chem. Thermodyn.* **2016**, *102*, 39–47. <https://doi.org/10.1016/j.jct.2016.06.028>.
- (96) Domańska, U.; Papis, P.; Szydłowski, J. Thermodynamics and Activity Coefficients at Infinite Dilution for Organic Solutes, Water and Diols in the Ionic Liquid Choline Bis(Trifluoromethylsulfonyl)Imide. *J. Chem. Thermodyn.* **2014**, *77*, 63–70. <https://doi.org/10.1016/j.jct.2014.04.024>.
- (97) Domańska, U.; Marciniak, A. Activity Coefficients at Infinite Dilution Measurements for Organic Solutes and Water in the 1-Hexyloxymethyl-3-Methyl-Imidazolium and 1,3-Dihexyloxymethyl-Imidazolium Bis(Trifluoromethylsulfonyl)-Imide Ionic Liquids—The Cation Influence. *Fluid*



- Phase Equilib.* **2009**, 286 (2), 154–161.  
<https://doi.org/10.1016/j.fluid.2009.08.017>.
- (98) Domańska, U.; Karpńska, M.; Wiśniewska, A.; Dąbrowski, Z. Ammonium Ionic Liquids in Extraction of Bio-Butan-1-ol from Water Phase Using Activity Coefficients at Infinite Dilution. *Fluid Phase Equilib.* **2019**, 479, 9–16.  
<https://doi.org/10.1016/j.fluid.2018.09.024>.
- (99) Domańska, U.; Wlazło, M. Thermodynamics and Limiting Activity Coefficients Measurements for Organic Solutes and Water in the Ionic Liquid 1-Dodecyl-3-Methylimidazolium Bis(Trifluoromethylsulfonyl) Imide. *J. Chem. Thermodyn.* **2016**, 103, 76–85. <https://doi.org/10.1016/j.jct.2016.08.008>.
- (100) Domańska, U.; Wlazło, M.; Karpńska, M.; Zawadzki, M. High Selective Water/Butan-1-ol Separation on Investigation of Limiting Activity Coefficients with [P 8,8,8,8 ][NTf<sub>2</sub>] Ionic Liquid. *Fluid Phase Equilib.* **2017**, 449, 1–9.  
<https://doi.org/10.1016/j.fluid.2017.06.001>.
- (101) Sobota, M.; Dohnal, V.; Vrbka, P. Activity Coefficients at Infinite Dilution of Organic Solutes in the Ionic Liquid 1-Ethyl-3-Methyl-Imidazolium Nitrate. *J. Phys. Chem. B* **2009**, 113 (13), 4323–4332. <https://doi.org/10.1021/jp811041k>.
- (102) Blahut, A.; Sobota, M.; Dohnal, V.; Vrbka, P. Activity Coefficients at Infinite Dilution of Organic Solutes in the Ionic Liquid 1-Ethyl-3-Methylimidazolium Methanesulfonate. *Fluid Phase Equilib.* **2010**, 299 (2), 198–206.  
<https://doi.org/10.1016/j.fluid.2010.10.008>.
- (103) Domańska, U.; Królikowski, M. Measurements of Activity Coefficients at Infinite Dilution for Organic Solutes and Water in the Ionic Liquid 1-Ethyl-3-Methylimidazolium Methanesulfonate. *J. Chem. Thermodyn.* **2012**, 54, 20–27.  
<https://doi.org/10.1016/j.jct.2012.03.005>.
- (104) Blahut, A.; Dohnal, V. Interactions of Volatile Organic Compounds with the Ionic Liquid 1-Butyl-1-Methylpyrrolidinium Dicyanamide. *J. Chem. Eng. Data* **2011**, 56 (12), 4909–4918. <https://doi.org/10.1021/je200822w>.
- (105) Blahut, A.; Dohnal, V. Interactions of Volatile Organic Compounds with the Ionic Liquids 1-Butyl-1-Methylpyrrolidinium Tetracyanoborate and 1-Butyl-1-Methylpyrrolidinium Bis(Oxalato)Borate. *J. Chem. Thermodyn.* **2013**, 57, 344–354. <https://doi.org/10.1016/j.jct.2012.09.017>.
- (106) Órfão, E. F.; Dohnal, V.; Blahut, A. Infinite Dilution Activity Coefficients of Volatile Organic Compounds in Two Ionic Liquids Composed of the Tris(Pentafluoroethyl)Trifluorophosphate ([FAP]) Anion and a Functionalized Cation. *J. Chem. Thermodyn.* **2013**, 65, 53–64.  
<https://doi.org/10.1016/j.jct.2013.05.035>.
- (107) Blahut, A.; Dohnal, V.; Vrbka, P. Interactions of Volatile Organic Compounds with the Ionic Liquid 1-Ethyl-3-Methylimidazolium Tetracyanoborate. *J. Chem. Thermodyn.* **2012**, 47, 100–108. <https://doi.org/10.1016/j.jct.2011.09.028>.
- (108) Mutelet, F.; Butet, V.; Jaubert, J.-N. Application of Inverse Gas Chromatography and Regular Solution Theory for Characterization of Ionic Liquids. *Ind. Eng. Chem. Res.* **2005**, 44 (11), 4120–4127. <https://doi.org/10.1021/ie048806l>.
- (109) Ayad, A.; Mutelet, F.; Abumandour, E.-S.; Negadi, A. Activity Coefficients at Infinite Dilution of Organic Solutes in Methylphosphonate Based Ionic Liquids Using Gas-Liquid Chromatography. *J. Chem. Thermodyn.* **2015**, 86, 116–122.  
<https://doi.org/10.1016/j.jct.2015.02.023>.
- (110) Mafi, M.; Dehghani, M. R.; Mokhtarani, B. Liquid-Liquid Equilibrium Data for Extractive Desulfurization Using 1-Butyl-3-Methyl Imidazolium Thiocyanate, n-Alkane and Thiophene. *Fluid Phase Equilib.* **2018**, 456, 109–115.  
<https://doi.org/10.1016/j.fluid.2017.10.017>.

- (111) Mafi, M.; Dehghani, M. R.; Mokhtarani, B. Novel Liquid–Liquid Equilibrium Data for Six Ternary Systems Containing IL, Hydrocarbon and Thiophene at 25 °C. *Fluid Phase Equilib.* **2016**, *412*, 21–28. <https://doi.org/10.1016/j.fluid.2015.12.006>.
- (112) Alonso, L.; Arce, A.; Francisco, M.; Soto, A. Thiophene Separation from Aliphatic Hydrocarbons Using the 1-Ethyl-3-Methylimidazolium Ethylsulfate Ionic Liquid. *Fluid Phase Equilib.* **2008**, *270* (1–2), 97–102. <https://doi.org/10.1016/j.fluid.2008.06.012>.
- (113) Rodríguez-Cabo, B.; Arce, A.; Soto, A. Desulfurization of Fuels by Liquid–Liquid Extraction with 1-Ethyl-3-Methylimidazolium Ionic Liquids. *Fluid Phase Equilib.* **2013**, *356*, 126–135. <https://doi.org/10.1016/j.fluid.2013.07.028>.
- (114) Rodríguez-Cabo, B.; Soto, A.; Arce, A. Desulfurization of Fuel-Oils with [C2mim][NTf2]: A Comparative Study. *J. Chem. Thermodyn.* **2013**, *57*, 248–255. <https://doi.org/10.1016/j.jct.2012.08.031>.
- (115) Rodríguez-Cabo, B.; Francisco, M.; Soto, A.; Arce, A. Hexyl Dimethylpyridinium Ionic Liquids for Desulfurization of Fuels. Effect of the Position of the Alkyl Side Chains. *Fluid Phase Equilib.* **2012**, *314*, 107–112. <https://doi.org/10.1016/j.fluid.2011.10.017>.
- (116) Alonso, L.; Arce, A.; Francisco, M.; Rodríguez, O.; Soto, A. Liquid–Liquid Equilibria for Systems Composed by 1-Methyl-3-Octylimidazolium Tetrafluoroborate Ionic Liquid, Thiophene, and *n*-Hexane or Cyclohexane. *J. Chem. Eng. Data* **2007**, *52* (5), 1729–1732. <https://doi.org/10.1021/je700126z>.
- (117) Alonso, L.; Arce, A.; Francisco, M.; Soto, A. Phase Behaviour of 1-Methyl-3-Octylimidazolium Bis[Trifluoromethylsulfonyl]Imide with Thiophene and Aliphatic Hydrocarbons: The Influence of *n*-Alkane Chain Length. *Fluid Phase Equilib.* **2008**, *263* (2), 176–181. <https://doi.org/10.1016/j.fluid.2007.10.010>.
- (118) Kędra-Królik, K.; Fabrice, M.; Jaubert, J.-N. Extraction of Thiophene or Pyridine from *N*-Heptane Using Ionic Liquids. Gasoline and Diesel Desulfurization. *Ind. Eng. Chem. Res.* **2011**, *50* (4), 2296–2306. <https://doi.org/10.1021/ie101834m>.
- (119) Revelli, A.-L.; Mutelet, F.; Jaubert, J.-N. Extraction of Benzene or Thiophene from *n*-Heptane Using Ionic Liquids. NMR and Thermodynamic Study. *J. Phys. Chem. B* **2010**, *114* (13), 4600–4608. <https://doi.org/10.1021/jp911978a>.
- (120) Song, Z.; Zhang, J.; Zeng, Q.; Cheng, H.; Chen, L.; Qi, Z. Effect of Cation Alkyl Chain Length on Liquid-Liquid Equilibria of {ionic Liquids + Thiophene + Heptane}: COSMO-RS Prediction and Experimental Verification. *Fluid Phase Equilib.* **2016**, *425*, 244–251. <https://doi.org/10.1016/j.fluid.2016.06.016>.
- (121) Królikowski, M.; Walczak, K.; Domańska, U. Solvent Extraction of Aromatic Sulfur Compounds from *N*-Heptane Using the 1-Ethyl-3-Methylimidazolium Tricyanomethanide Ionic Liquid. *J. Chem. Thermodyn.* **2013**, *65*, 168–173. <https://doi.org/10.1016/j.jct.2013.05.048>.
- (122) Domańska, U.; Lukoshko, E. V.; Królikowski, M. Separation of Thiophene from Heptane with Ionic Liquids. *J. Chem. Thermodyn.* **2013**, *61*, 126–131. <https://doi.org/10.1016/j.jct.2013.01.033>.
- (123) Marciniak, A.; Wlazło, M. Ternary (Liquid + Liquid) Equilibria of {trifluorotris(Perfluoroethyl)Phosphate Based Ionic Liquids + Thiophene + Heptane}: Part 2. *J. Chem. Thermodyn.* **2015**, *86*, 196–201. <https://doi.org/10.1016/j.jct.2014.07.020>.
- (124) Marciniak, A.; Królikowski, M. Ternary (Liquid+liquid) Equilibria of {trifluorotris(Perfluoroethyl)Phosphate Based Ionic Liquids+thiophene+heptane}. *J. Chem. Thermodyn.* **2012**, *49*, 154–158. <https://doi.org/10.1016/j.jct.2012.01.026>.

- (125) Marciniak, A.; Królikowski, M. Ternary Liquid–Liquid Equilibria of Bis(Trifluoromethylsulfonyl)-Amide Based Ionic Liquids+thiophene+n-Heptane. The Influence of Cation Structure. *Fluid Phase Equilib.* **2012**, *321*, 59–63. <https://doi.org/10.1016/j.fluid.2012.02.019>.
- (126) Wlazło, M.; Ramjugernath, D.; Naidoo, P.; Domańska, U. Effect of the Alkyl Side Chain of the 1-Alkylpiperidinium-Based Ionic Liquids on Desulfurization of Fuels. *J. Chem. Thermodyn.* **2014**, *72*, 31–36. <https://doi.org/10.1016/j.jct.2013.12.029>.
- (127) Domańska, U.; Walczak, K.; Królikowski, M. Extraction Desulfurization Process of Fuels with Ionic Liquids. *J. Chem. Thermodyn.* **2014**, *77*, 40–45. <https://doi.org/10.1016/j.jct.2014.04.025>.
- (128) Kędra-Krolik, K.; Mutelet, F.; Moïse, J.-C.; Jaubert, J.-N. Deep Fuels Desulfurization and Denitrogenation Using 1-Butyl-3-Methylimidazolium Trifluoromethanesulfonate. *Energy Fuels* **2011**, *25* (4), 1559–1565. <https://doi.org/10.1021/ef200187y>.
- (129) Domańska, U.; Walczak, K.; Zawadzki, M. Separation of Sulfur Compounds from Alkanes with 1-Alkylcyanopyridinium-Based Ionic Liquids. *J. Chem. Thermodyn.* **2014**, *69*, 27–35. <https://doi.org/10.1016/j.jct.2013.09.032>.
- (130) Domańska, U.; Walczak, K. Ternary Liquid–Liquid Equilibria for Mixtures of {Ionic Liquid + Thiophene or Benzothiophene + Heptane} at T = 308.15 K. *J. Solut. Chem.* **2015**, *44* (3–4), 382–394. <https://doi.org/10.1007/s10953-014-0276-y>.
- (131) Arce, A.; Francisco, M.; Soto, A. Evaluation of the Polysubstituted Pyridinium Ionic Liquid [Hmmpy][Ntf2] as a Suitable Solvent for Desulfurization: Phase Equilibria. *J. Chem. Thermodyn.* **2010**, *42* (6), 712–718. <https://doi.org/10.1016/j.jct.2010.01.005>.
- (132) Alonso, L.; Arce, A.; Francisco, M.; Soto, A. Solvent Extraction of Thiophene from N-Alkanes (C7, C12, and C16) Using the Ionic Liquid [C8mim][BF4]. *J. Chem. Thermodyn.* **2008**, *40* (6), 966–972. <https://doi.org/10.1016/j.jct.2008.01.025>.
- (133) Cheruku, S. K.; Banerjee, T. Liquid–Liquid Equilibrium Data for 1-Ethyl-3-Methylimidazolium Acetate–Thiophene–Diesel Compound: Experiments and Correlations. *J. Solut. Chem.* **2012**, *41* (5), 898–913. <https://doi.org/10.1007/s10953-012-9840-5>.
- (134) Chikh Baelhadj, A.; Mutelet, F. Liquid–Liquid Equilibria for the Ternary Systems Dodecane + Toluene or Thiophene or Pyridine + 1-Ethyl-3-Methylimidazolium Methyl Sulfate. *J. Chem. Eng. Data* **2017**, *62* (6), 1749–1755. <https://doi.org/10.1021/acs.jced.6b00437>.
- (135) Alonso, L.; Arce, A.; Francisco, M.; Soto, A. (Liquid+liquid) Equilibria of [C8mim][NTf2] Ionic Liquid with a Sulfur-Component and Hydrocarbons. *J. Chem. Thermodyn.* **2008**, *40* (2), 265–270. <https://doi.org/10.1016/j.jct.2007.06.016>.
- (136) Francisco, M.; Arce, A.; Soto, A. Ionic Liquids on Desulfurization of Fuel Oils. *Fluid Phase Equilib.* **2010**, *294* (1–2), 39–48. <https://doi.org/10.1016/j.fluid.2009.12.020>.
- (137) Imidazolium-based ionic liquids | IoLiTec [https://iolitec.de/en/products/ionic\\_liquids/catalogue/imidazolium-based?sort\\_by=title&page=0](https://iolitec.de/en/products/ionic_liquids/catalogue/imidazolium-based?sort_by=title&page=0) (accessed Jun 17, 2020).
- (138) Wlazło, M.; Marciniak, A. Ternary Liquid–Liquid Equilibria of Trifluorotris(Perfluoroethyl)Phosphate Based Ionic

- Liquids+benzothiophene+heptane. *Fluid Phase Equilib.* **2014**, *361*, 54–59. <https://doi.org/10.1016/j.fluid.2013.10.028>.
- (139) Ahmed, O. U.; Mjalli, F. S.; Hadj-Kali, M. K.; Al-Wahaibi, T.; Al-Wahaibi, Y. Measurements and Prediction of Ternary Liquid–Liquid Equilibria for Mixtures of IL + Sulfur Compound + Hexadecane. *Fluid Phase Equilib.* **2016**, *421*, 16–23. <https://doi.org/10.1016/j.fluid.2016.03.014>.
- (140) Dharaskar, S. A.; Wasewar, K. L.; Varma, M. N.; Shende, D. Z.; Tadi, K. K.; Yoo, C. K. Synthesis, Characterization, and Application of Novel Trihexyl Tetradecyl Phosphonium Bis (2,4,4-Trimethylpentyl) Phosphinate for Extractive Desulfurization of Liquid Fuel. *Fuel Process. Technol.* **2014**, *123*, 1–10. <https://doi.org/10.1016/j.fuproc.2014.02.001>.
- (141) Dharaskar, S. A.; Wasewar, K. L.; Varma, M. N.; Shende, D. Z.; Yoo, C. Synthesis, Characterization and Application of 1-Butyl-3-Methylimidazolium Tetrafluoroborate for Extractive Desulfurization of Liquid Fuel. *Arab. J. Chem.* **2016**, *9* (4), 578–587. <https://doi.org/10.1016/j.arabjc.2013.09.034>.
- (142) Dharaskar, S. A.; Varma, M. N.; Shende, D. Z.; Yoo, C. K.; Wasewar, K. L. Synthesis, Characterization and Application of 1-Butyl-3 Methylimidazolium Chloride as Green Material for Extractive Desulfurization of Liquid Fuel. *Sci. World J.* **2013**, *2013*, 1–9. <https://doi.org/10.1155/2013/395274>.
- (143) Dharaskar, S. A.; Wasewar, K. L.; Varma, M. N.; Shende, D. Z. Imidazolium Ionic Liquid as Energy Efficient Solvent for Desulfurization of Liquid Fuel. *Sep. Purif. Technol.* **2015**, *155*, 101–109. <https://doi.org/10.1016/j.seppur.2015.05.032>.
- (144) Gao, L.; Wan, H.; Han, M.; Guan, G. Deep Desulfurization of Model Oil by Extraction with a Low-Viscosity Ionic Liquid [BMIM]SCN. *Pet. Sci. Technol.* **2014**, *32* (11), 1309–1317. <https://doi.org/10.1080/10916466.2011.653466>.
- (145) Gabrić, B.; Sander, A.; Cvjetko Bubalo, M.; Macut, D. Extraction of S- and N-Compounds from the Mixture of Hydrocarbons by Ionic Liquids as Selective Solvents. *Sci. World J.* **2013**, *2013*, 1–11. <https://doi.org/10.1155/2013/512953>.
- (146) Kianpour, E.; Azizian, S.; Yarie, M.; Zolfigol, M. A.; Bayat, M. A Task-Specific Phosphonium Ionic Liquid as an Efficient Extractant for Green Desulfurization of Liquid Fuel: An Experimental and Computational Study. *Chem. Eng. J.* **2016**, *295*, 500–508. <https://doi.org/10.1016/j.cej.2016.03.072>.
- (147) Hansmeier, A. R.; Meindersma, G. W.; de Haan, A. B. Desulfurization and Denitrogenation of Gasoline and Diesel Fuels by Means of Ionic Liquids. *Green Chem.* **2011**, *13* (7), 1907. <https://doi.org/10.1039/c1gc15196g>.
- (148) Taib, M. M.; Murugesan, T. Experimental Study on the Extractive Desulfurization of Model Fuel Using Hydroxyl Ammonium Ionic Liquids. *Asia-Pac. J. Chem. Eng.* **2012**, *7* (3), 469–473. <https://doi.org/10.1002/apj.542>.
- (149) Liu, C.; He, Q.; Zhang, Z.; Su, Y.; Xu, R.; Hu, B. Efficient Extractive Desulfurization of Fuel Oils Using N -Pyrrolidone/Alkylphosphate-Based Ionic Liquids. *Chin. J. Chem.* **2014**, *32* (5), 410–416. <https://doi.org/10.1002/cjoc.201400146>.
- (150) Domańska, U.; Wlazło, M. Effect of the Cation and Anion of the Ionic Liquid on Desulfurization of Model Fuels. *Fuel* **2014**, *134*, 114–125. <https://doi.org/10.1016/j.fuel.2014.05.048>.
- (151) Bui, T. T. L.; Nguyen, D. D.; Ho, S. V.; Nguyen, B. T.; Uong, H. T. N. Synthesis, Characterization and Application of Some Non-Halogen Ionic Liquids as Green Solvents for Deep Desulfurization of Diesel Oil. *Fuel* **2017**, *191*, 54–61. <https://doi.org/10.1016/j.fuel.2016.11.044>.

- (152) Ibrahim, J. J.; Gao, S.; Abdeltawab, A. A.; Al-Deyab, S. S.; Yu, L.; Yu, G.; Chen, X.; Yong, X. Extractive Desulfurization of Fuel Oils with Dicyano(Nitroso)Methanide-Based Ionic Liquids. *Sep. Sci. Technol.* **2015**, *50* (8), 1166–1174. <https://doi.org/10.1080/01496395.2014.960051>.
- (153) Chen, X.; Yuan, S.; Abdeltawab, A. A.; Al-Deyab, S. S.; Zhang, J.; Yu, L.; Yu, G. Extractive Desulfurization and Denitrogenation of Fuels Using Functional Acidic Ionic Liquids. *Sep. Purif. Technol.* **2014**, *133*, 187–193. <https://doi.org/10.1016/j.seppur.2014.06.031>.
- (154) Safa, M.; Mokhtarani, B.; Mortaheb, H. R. Deep Extractive Desulfurization of Dibenzothiophene with Imidazolium or Pyridinium-Based Ionic Liquids. *Chem. Eng. Res. Des.* **2016**, *111*, 323–331. <https://doi.org/10.1016/j.cherd.2016.04.021>.
- (155) Moghadam, F. R.; Azizian, S.; Kianpour, E.; Yarie, M.; Bayat, M.; Zolfigol, M. A. Green Fuel through Green Route by Using a Task-Specific and Neutral Phosphonium Ionic Liquid: A Joint Experimental and Theoretical Study. *Chem. Eng. J.* **2017**, *309*, 480–488. <https://doi.org/10.1016/j.cej.2016.10.026>.
- (156) Ren, T.-J.; Zhang, J.; Hu, Y.-H.; Li, J.-P.; Liu, M.-S.; Zhao, D.-S. Extractive Desulfurization of Fuel Oil with Metal-Based Ionic Liquids. *Chin. Chem. Lett.* **2015**, *26* (9), 1169–1173. <https://doi.org/10.1016/j.cclet.2015.05.023>.
- (157) Gao, H.; Xing, J.; Li, Y.; Li, W.; Liu, Q.; Liu, H. Desulfurization of Diesel Fuel by Extraction with Lewis-Acidic Ionic Liquid. *Sep. Sci. Technol.* **2009**, *44* (4), 971–982. <https://doi.org/10.1080/01496390802691232>.
- (158) Ufnalski, W. *Wprowadzenie Do Termodynamiki Chemicznej*; Oficyna Wydawnicza PW, 2008.
- (159) Prausnitz, J. M.; Lichtenthaler, R. N.; de Azevedo, E. G. *Molecular Thermodynamics of Fluid-Phase Equilibria*; Pearson Education, 1998.
- (160) Paduszyński, K. *Termodynamika Cieczy Jonowych - Badania Eksperymentalne Oraz Nowe Modele Matematyczne (Rozprawa Doktorska)*. Warsaw University of Technology 2013.
- (161) Lewis, G. N. The Law of Physico-Chemical Change. *Proc. Am. Acad. Arts Sci.* **1901**, *37* (3), 49. <https://doi.org/10.2307/20021635>.
- (162) Weinstock, J. J. Phase Equilibrium at Elevated Pressure in Ternary Systems of Ethylene and Water and Organic Liquids(PhD Dissertation). Princeton University 1952.
- (163) Swatoski, R. P.; Visser, A. E.; Reichert, W. M.; Broker, G. A.; Farina, L. M.; Holbrey, J. D.; Rogers, R. D. Solvation of 1-Butyl-3-Methylimidazolium Hexafluorophosphate in Aqueous Ethanol-a Green Solution for Dissolving “hydrophobic” Ionic Liquids. *Chem. Commun.* **2001**, No. 20, 2070–2071. <https://doi.org/10.1039/b106601n>.
- (164) Durski, M.; Naidoo, P.; Ramjugernath, D.; Domańska, U. Separation of Thiophene from Octane/Hexadecane with Ionic Liquids in Ternary Liquid-Liquid Phase Equilibrium. *Fluid Phase Equilib.* **2020**, *509*, 112467. <https://doi.org/10.1016/j.fluid.2020.112467>.
- (165) Gow, A. S. Calculation of Vapor-Liquid Equilibria from Infinite-Dilution Excess Enthalpy Data Using the Wilson or NRTL Equation. *Ind. Eng. Chem. Res.* **1993**, *32* (12), 3150–3161. <https://doi.org/10.1021/ie00024a028>.
- (166) Meindersma, G. W.; de Haan, A. B. Conceptual Process Design for Aromatic/Aliphatic Separation with Ionic Liquids. *Chem. Eng. Res. Des.* **2008**, *86* (7), 745–752. <https://doi.org/10.1016/j.cherd.2008.02.016>.
- (167) Davis, S. E.; Morton, S. A. Investigation of Ionic Liquids for the Separation of Butanol and Water. *Sep. Sci. Technol.* **2008**, *43* (9–10), 2460–2472. <https://doi.org/10.1080/01496390802122089>.

- (168) Sandler, S. I. Infinite Dilution Activity Coefficients in Chemical, Environmental and Biochemical Engineering. *Fluid Phase Equilib.* **1996**, *116* (1–2), 343–353. [https://doi.org/10.1016/0378-3812\(95\)02905-2](https://doi.org/10.1016/0378-3812(95)02905-2).
- (169) Eckert, C. A.; Newman, B. A.; Nicolaides, G. L.; Long, T. C. Measurement and Application of Limiting Activity Coefficients. *AIChE J.* **1981**, *27* (1), 33–40. <https://doi.org/10.1002/aic.690270107>.
- (170) Renon, H.; Prausnitz, J. M. Local Compositions in Thermodynamic Excess Functions for Liquid Mixtures. *AIChE J.* **1968**, *14* (1), 135–144. <https://doi.org/10.1002/aic.690140124>.
- (171) Walas, S. M. Activity Coefficients. In *Phase Equilibria in Chemical Engineering*; Elsevier, 1985; pp 165–244. <https://doi.org/10.1016/B978-0-409-95162-2.50012-9>.
- (172) Klamt, A. Conductor-like Screening Model for Real Solvents: A New Approach to the Quantitative Calculation of Solvation Phenomena. *J. Phys. Chem.* **1995**, *99* (7), 2224–2235. <https://doi.org/10.1021/j100007a062>.
- (173) *Encyclopedia of Applied Spectroscopy*; Andrews, D. L., Ed.; Wiley-VCH: Weinheim, Germany, 2009.
- (174) Jennings, W. *Gas Chromatography with Glass Capillary Columns*; Academic Press Inc., 1980.
- (175) Everett, D. H. Effect of Gas Imperfection on G.L.C. Measurements : A Refined Method for Determining Activity Coefficients and Second Virial Coefficients. *Trans. Faraday Soc.* **1965**, *61*, 1637. <https://doi.org/10.1039/tf9656101637>.
- (176) Cruickshank, A. J. B.; Gainey, B. W.; Hicks, C. P.; Letcher, T. M.; Moody, R. W.; Young, C. L. Gas-Liquid Chromatographic Determination of Cross-Term Second Virial Coefficients Using Glycerol. Benzene + Nitrogen and Benzene + Carbon Dioxide at 50°C. *Trans Faraday Soc* **1969**, *65* (0), 1014–1031. <https://doi.org/10.1039/TF9696501014>.
- (177) Letcher, T. M.; Harris, R. A.; Ramjugernath, D.; Raal, J. D. Activity Coefficients of Hydrocarbon Solutes at Infinite Dilution in Monoethanolamine from Gas–Liquid Chromatography. *J. Chem. Thermodyn.* **2001**, *33* (12), 1655–1662. <https://doi.org/10.1006/jcht.2000.0764>.
- (178) Belfer, A. J. *Neftekhimiya* **1972**, *12* (435).
- (179) Belfer, A. J.; Locke, D. C. Non-Steady-State Gas Chromatography for Activity Coefficient Measurements. *Anal. Chem.* **1984**, *56* (13), 2485–2489. <https://doi.org/10.1021/ac00277a050>.
- (180) Belfer, A. J.; Locke, D. C.; Landau, Isaac. Non-Steady-State Gas Chromatography Using Capillary Columns. *Anal. Chem.* **1990**, *62* (4), 347–349. <https://doi.org/10.1021/ac00203a007>.
- (181) Landau, I.; Belfer, A. J.; Locke, D. C. Measurement of Limiting Activity Coefficients Using Non-Steady-State Gas Chromatography. *Ind. Eng. Chem. Res.* **1991**, *30* (8), 1900–1906. <https://doi.org/10.1021/ie00056a034>.
- (182) Dohnal, V.; Ondo, D. Refined Non-Steady-State Gas–Liquid Chromatography for Accurate Determination of Limiting Activity Coefficients of Volatile Organic Compounds in Water. *J. Chromatogr. A* **2005**, *1097* (1–2), 157–164. <https://doi.org/10.1016/j.chroma.2005.08.015>.
- (183) Krummen, M.; Gruber, D.; Gmehling, J. Measurement of Activity Coefficients at Infinite Dilution in Solvent Mixtures Using the Dilutor Technique. *Ind. Eng. Chem. Res.* **2000**, *39* (6), 2114–2123. <https://doi.org/10.1021/ie990830p>.
- (184) Fowles, I. A.; Scott, R. P. W. A Vapour Dilution System for Detector Calibration. *J. Chromatogr.* **1963**, *11*, 1.

- (185) Leroi, J.-C.; Masson, J.-C.; Renon, H.; Fabries, J.-F.; Sannier, H. Accurate Measurement of Activity Coefficients at Infinite Dilution by Inert Gas Stripping and Gas Chromatography. *Ind. Eng. Chem. Process Des.* **1977**, *16* (1), 139–144. <https://doi.org/10.1021/i260061a609>
- (186) Krummen, M.; Gmehling, J. Measurement of Activity Coefficients at Infinite Dilution in N-Methyl-2-Pyrrolidone and N-Formylmorpholine and Their Mixtures with Water Using the Dilutor Technique. *Fluid Phase Equilib.* **2004**, *215* (2), 283–294. <https://doi.org/10.1016/j.fluid.2003.10.010>.
- (187) Kojima, K.; Zhang, S.; Hiaki, T. Measuring Methods of Infinite Dilution Activity Coefficients and a Database for Systems Including Water. *Fluid Phase Equilib.* **1997**, *131* (1–2), 145–179. [https://doi.org/10.1016/S0378-3812\(96\)03210-4](https://doi.org/10.1016/S0378-3812(96)03210-4).
- (188) Qureshi, M. S.; Uusi-Kyyny, P.; Richon, D.; Nikiforow, K.; Alopaeus, V. Measurement of Activity Coefficient at Infinite Dilution for Some Bio-Oil Components in Water and Mass Transfer Study of Bubbles in the Dilutor. *Fluid Phase Equilib.* **2015**, *392*, 1–11. <https://doi.org/10.1016/j.fluid.2015.01.010>.
- (189) Belting, P. C.; Rarey, J.; Gmehling, J.; Ceriani, R.; Chiavone-Filho, O.; Meirelles, A. J. A. Measurements of Activity Coefficients at Infinite Dilution in Vegetable Oils and Capric Acid Using the Dilutor Technique. *Fluid Phase Equilib.* **2014**, *361*, 215–222. <https://doi.org/10.1016/j.fluid.2013.10.035>.
- (190) Świątosławski, W. *Ebulliometric Measurements*; Reinhold Publishing Corporation: New York, 1945.
- (191) Gautreaux, M. F.; Coates, J. Activity Coefficients at Infinite Dilution. *AIChE J.* **1955**, *1* (4), 496–500. <https://doi.org/10.1002/aic.690010419>.
- (192) Scott, L. S. Determination of Activity Coefficients by Accurate Measurement of Boiling Point Diagram. *Fluid Phase Equilib.* **1986**, *26* (2), 149–163. [https://doi.org/10.1016/0378-3812\(86\)90003-8](https://doi.org/10.1016/0378-3812(86)90003-8).
- (193) Ebulliometer. *Wikipedia*; 2020.
- (194) Vrbka, P.; Dohnal, V. Limiting Activity Coefficient Measurements in Binary Mixtures of Dichloromethane and 1-Alkanols (C1–C4). *Fluid Phase Equilib.* **2016**, *411*, 59–65. <https://doi.org/10.1016/j.fluid.2015.11.037>.
- (195) Pavliček, J.; Bogdanić, G.; Wichterle, I. Ebulliometric Measurement of Total Pressure in the Binary Polystyrene + Butan-2-One System. *Fluid Phase Equilib.* **2016**, *424*, 41–43. <https://doi.org/10.1016/j.fluid.2015.09.028>.
- (196) Haidl, J.; Dohnal, V. Activity Coefficients of Water at Infinite Dilution in Common Oxygenated Solvents. *J. Chem. Eng. Data* **2020**, *65* (5), 2790–2797. <https://doi.org/10.1021/acs.jced.0c00108>.
- (197) Moodley, K.; Raal, J. D. Infinite Dilution Activity Coefficients for Systems of C2–C4 *n*-Alcohols in the Range of  $T = (303.15 \text{ to } 343.15) \text{ K}$ . *J. Chem. Eng. Data* **2020**, *65* (7), 3297–3305. <https://doi.org/10.1021/acs.jced.0c00101>.
- (198) Williams-Wynn, M. D.; Letcher, T. M.; Naidoo, P.; Ramjugernath, D. Activity Coefficients at Infinite Dilution of Organic Solutes in N-Formylmorpholine and N-Methylpyrrolidone from Gas–Liquid Chromatography. *J. Chem. Thermodyn.* **2013**, *61*, 154–160. <https://doi.org/10.1016/j.jct.2013.02.006>.
- (199) Williams-Wynn, M. D.; Letcher, T. M.; Naidoo, P.; Ramjugernath, D. Activity Coefficients at Infinite Dilution of Organic Solutes in Diethylene Glycol and Triethylene Glycol from Gas–Liquid Chromatography. *J. Chem. Thermodyn.* **2013**, *65*, 120–130. <https://doi.org/10.1016/j.jct.2013.05.011>.
- (200) Bahadur, I.; Govender, B. B.; Osman, K.; Williams-Wynn, M. D.; Nelson, W. M.; Naidoo, P.; Ramjugernath, D. Measurement of Activity Coefficients at Infinite Dilution of Organic Solutes in the Ionic Liquid 1-Ethyl-3-Methylimidazolium 2-(2-Methoxyethoxy) Ethylsulfate at  $T = (308.15, 313.15,$

- 323.15 and 333.15)K Using Gas+liquid Chromatography. *J. Chem. Thermodyn.* **2014**, *70*, 245–252. <https://doi.org/10.1016/j.jct.2013.10.017>.
- (201) Tumba, K.; Letcher, T.; Naidoo, P.; Ramjugernath, D. Activity Coefficients at Infinite Dilution of Organic Solutes in the Ionic Liquid Trihexyltetradecylphosphonium Hexafluorophosphate Using Gas–Liquid Chromatography at T=(313.15, 333.15, 353.15, and 363.15)K. *J. Chem. Thermodyn.* **2012**, *49*, 46–53. <https://doi.org/10.1016/j.jct.2012.01.004>.
- (202) Reddy, P.; Aslam Siddiqi, M.; Atakan, B.; Diedenhofen, M.; Ramjugernath, D. Activity Coefficients at Infinite Dilution of Organic Solutes in the Ionic Liquid PEG-5 Cocomonium Methylsulfate at T=(313.15, 323.15, 333.15, and 343.15)K: Experimental Results and COSMO-RS Predictions. *J. Chem. Thermodyn.* **2013**, *58*, 322–329. <https://doi.org/10.1016/j.jct.2012.10.024>.
- (203) Briggs, S. W.; Comings, E. W. Effect of Temperature on Liquid-Liquid Equilibrium: Benzene - Acetone - Water and Docosane - 1,6-Diphenylhexane - Furfural System. *Ind. Eng. Chem.* **1943**, *35* (4), 411–417.
- (204) Letcher, T. M.; Siswana, P. M.; van der Watt, P.; Radloff, S. Phase Equilibria for (an Alkanol + p-Xylene + Water) at 298.2 K. *J. Chem. Thermodyn.* **1989**, *21*, 1053–1060.
- (205) Rifai, I.; Durandet, J. *Rev Inst Fr. Pet.* **1962**, *17*, 1232. [https://doi.org/as given by Novak et al. \(1987\)](https://doi.org/as%20given%20by%20Novak%20et%20al.%20(1987)).
- (206) Benjamin, C. Y.; Ochi, K.; Momose, M.; Kojima, K. Determination of Mutual Solubilities in Aniline + n -Hexane and Furfural + Cyclohexane Systems by a Laser Light Scattering Technique. *Can. J. Chem. Eng.* **1993**, *71*, 982–985.
- (207) Ndlovu, M.; Eng, B. Development of a Dynamic Still for Measuring Low Pressure Vapour-Liquid-Liquid Equilibria. 302.
- (208) Raal, J. D.; Brouckaert, C. J. Vapour-Liquid and Liquid-Liquid Equilibria in the System Methyl Butenol - Water. *Fluid Phase Equilib.* **1992**, *74*, 253–270.
- (209) Narasigadu, C.; Naidoo, M.; Ramjugernath, D. Ternary Liquid–Liquid Equilibrium Data for the Water + Acetonitrile + {Butan-1-ol or 2-Methylpropan-1-ol} Systems at (303.2, 323.2, 343.2) K and 1 Atm. *J. Chem. Eng. Data* **2014**, *59* (11), 3820–3824. <https://doi.org/10.1021/je5007218>.
- (210) Mungar Ram, N.; Naidoo, P.; Letcher, T. M.; Ramjugernath, D. (Liquid + Liquid) Equilibria for Mixtures of Dodecane and Ethanol with Alkylsulfate-Based Ionic Liquids. *J. Chem. Thermodyn.* **2015**, *81*, 95–100. <https://doi.org/10.1016/j.jct.2014.09.009>.
- (211) Dong, M. W. *Modern HPLC for Practicing Scientists: Dong/Modern HPLC for Practicing Scientists*; John Wiley & Sons, Inc.: Hoboken, NJ, USA, 2006. <https://doi.org/10.1002/0471973106>.
- (212) Karger, B. L. HPLC: Early and Recent Perspectives. *J. Chem. Educ.* **1997**, *74* (1), 45. <https://doi.org/10.1021/ed074p45>.
- (213) Tamaoka, J.; Komagata, K. Determination of DNA Base Composition by Reversed-Phase High-Performance Liquid Chromatography. *FEMS Microbiol. Lett.* **1984**, *25* (1), 125–128. <https://doi.org/10.1111/j.1574-6968.1984.tb01388.x>.
- (214) Cavazzini, A.; Pasti, L.; Massi, A.; Marchetti, N.; Dondi, F. Recent Applications in Chiral High Performance Liquid Chromatography: A Review. *Anal. Chim. Acta* **2011**, *706* (2), 205–222. <https://doi.org/10.1016/j.aca.2011.08.038>.
- (215) Zhao, M.; Bada, J. L. Determination of  $\alpha$ -Dialkylamino Acids and Their Enantiomers in Geological Samples by High-Performance Liquid Chromatography after Derivatization with a Chiral Adduct of o-Phthaldialdehyde. *J Chromatogr A* **1995**, *9*.



- (216) Heymann, D.; Chibante, L. P. F.; Smalley, R. E. Determination of C<sub>60</sub> and C<sub>70</sub> Fullerenes in Geologic Materials by High-Performance Liquid Chromatography. *J. Chromatogr. A* **1995**, 689 (1), 157–163. [https://doi.org/10.1016/0021-9673\(94\)00941-2](https://doi.org/10.1016/0021-9673(94)00941-2).
- (217) Peng, G.; deGroot, F. M. F.; Haemaelaenen, K.; Moore, J. A.; Wang, X.; Grush, M. M.; Hastings, J. B.; Siddons, D. P.; Armstrong, W. H. High-Resolution Manganese x-Ray Fluorescence Spectroscopy. Oxidation-State and Spin-State Sensitivity. *J. Am. Chem. Soc.* **1994**, 116 (7), 2914–2920. <https://doi.org/10.1021/ja00086a024>.
- (218) Wobrauschek, P. Total Reflection X-Ray Fluorescence Analysis-a Review. **2007**, 12.
- (219) Oyedotun, T. D. T. X-Ray Fluorescence (XRF) in the Investigation of the Composition of Earth Materials: A Review and an Overview. *Geol. Ecol. Landsc.* **2018**, 2 (2), 148–154. <https://doi.org/10.1080/24749508.2018.1452459>.
- (220) Lasich, M.; Moodley, T.; Bhowanath, R.; Naidoo, P.; Ramjugernath, D. Liquid–Liquid Equilibria of Methanol, Ethanol, and Propan-2-Ol with Water and Dodecane. *J. Chem. Eng. Data* **2011**, 56 (11), 4139–4146. <https://doi.org/10.1021/je200646r>.
- (221) Schult, C. J.; Neely, B. J.; Robinson, R. L.; Gasem, K. A. M.; Todd, B. A. Infinite-Dilution Activity Coefficients for Several Solutes in Hexadecane and in n-Methyl-2-Pyrrolidone (NMP): Experimental Measurements and UNIFAC Predictions. *Fluid Phase Equilib.* **2001**, 179 (1–2), 117–129. [https://doi.org/10.1016/S0378-3812\(00\)00486-6](https://doi.org/10.1016/S0378-3812(00)00486-6).
- (222) Mutelet, F.; Revelli, A.-L.; Jaubert, J.-N.; Sprunger, L. M.; Acree, W. E.; Baker, G. A. Partition Coefficients of Organic Compounds in New Imidazolium and Tetralkylammonium Based Ionic Liquids Using Inverse Gas Chromatography. *J. Chem. Eng. Data* **2010**, 55 (1), 234–242. <https://doi.org/10.1021/je9003178>.
- (223) Revelli, A.-L.; Mutelet, F.; Jaubert, J.-N.; Garcia-Martinez, M.; Sprunger, L. M.; Acree, W. E.; Baker, G. A. Study of Ether-, Alcohol-, or Cyano-Functionalized Ionic Liquids Using Inverse Gas Chromatography. *J. Chem. Eng. Data* **2010**, 55 (7), 2434–2443. <https://doi.org/10.1021/je900838a>.
- (224) Narasigadu, C.; Naidoo, P.; Coquelet, C.; Richon, D.; Ramjugernath, D. A Novel Static Analytical Apparatus for Phase Equilibrium Measurements. *Fluid Phase Equilib.* **2013**, 338, 188–196. <https://doi.org/10.1016/j.fluid.2012.11.008>.
- (225) Casás, L. M.; Orge, B.; Ferreira, O. Liquid–Liquid Equilibria of Mixtures Containing Methyl Acetate + Methanol + Hexane or Heptane. *J. Chem. Eng. Data* **2008**, 53 (1), 89–93. <https://doi.org/10.1021/je700397g>.
- (226) Marino, G.; Orge, B.; Iglesias, M.; Tojo, J. Liquid–Liquid Equilibria of Acetone + Methanol + n-Alkane (C<sub>6</sub>–C<sub>8</sub>) at Different Temperatures. *J. Chem. Eng. Data* **2000**, 45 (3), 457–460. <https://doi.org/10.1021/je9901684>.
- (227) Matsuda, H.; Kurihara, K.; Ochi, K.; Kojima, K. Prediction of Liquid–Liquid Equilibria at High Pressure for Binary Systems Using EOS-GE Models: Methanol+hydrocarbon Systems. *Fluid Phase Equilib.* **2002**, 203 (1–2), 269–284. [https://doi.org/10.1016/S0378-3812\(02\)00188-7](https://doi.org/10.1016/S0378-3812(02)00188-7).
- (228) Orge, B.; Iglesias, M.; Rodríguez, A.; Canosa, J. M.; Tojo, J. Mixing Properties of (Methanol, Ethanol, or 1-Propanol) with (n-Pentane, n-Hexane, n-Heptane and n-Octane) at 298.15 K. *Fluid Phase Equilib.* **1997**, 133 (1–2), 213–227. [https://doi.org/10.1016/S0378-3812\(97\)00031-9](https://doi.org/10.1016/S0378-3812(97)00031-9).
- (229) Anderson, J. L.; Clark, K. D. Ionic Liquids as Tunable Materials in (Bio)Analytical Chemistry. *Anal. Bioanal. Chem.* **2018**, 410 (19), 4565–4566. <https://doi.org/10.1007/s00216-018-1125-4>.

- (230) Kermanioryani, M.; Abdul Mutalib, M. I.; Gonfa, G.; El-Harbawi, M.; Mazlan, F. A.; Lethesh, K. C.; Leveque, J.-M. Using Tunability of Ionic Liquids to Remove Methylene Blue from Aqueous Solution. *J. Environ. Chem. Eng.* **2016**, 4 (2), 2327–2332. <https://doi.org/10.1016/j.jece.2016.04.008>.
- (231) Jiang, S.; Hu, Y.; Wang, Y.; Wang, X. Viscosity of Typical Room-Temperature Ionic Liquids: A Critical Review. *J. Phys. Chem. Ref. Data* **2019**, 48 (3), 033101. <https://doi.org/10.1063/1.5090486>.
- (232) King, R. L.; Hiller, R. A.; Tatterson, G. B. Power Consumption in a Mixer. *AIChE J.* **1988**, 34 (3), 506–509. <https://doi.org/10.1002/aic.690340320>.
- (233) Zhao, K.; Cheng, Y.; Liu, H.; Yang, C.; Qiu, L.; Zeng, G.; He, H. Extractive Desulfurization of Dibenzothiophene by a Mixed Extractant of N,N-Dimethylacetamide, N,N-Dimethylformamide and Tetramethylene Sulfone: Optimization by Box–Behnken Design. *RSC Adv.* **2015**, 5 (81), 66013–66023. <https://doi.org/10.1039/C5RA12305D>.
- (234) Zhu, J.; Lu, X.; Zhao, D.; Dong, Z.; Ji, J. Role of Cosolvents in Enhancing the Performance of ILs for Extraction of Linolenic Acid from Tallow Seed Oil. *J. Mol. Liq.* **2017**, 242, 308–313. <https://doi.org/10.1016/j.molliq.2017.07.013>.
- (235) Tang, Q.; Zhang, J.; Wu, Y.; Wang, Y.; Liu, Z. An Experimental Study of Immiscible Liquid–Liquid Dispersions in a Pump–Mixer of Mixer–Settler. *Chin. J. Chem. Eng.* **2020**, 28 (1), 33–45. <https://doi.org/10.1016/j.cjche.2019.07.022>.
- (236) Diab, S.; Gerogiorgis, D. I. Technoeconomic Mixed Integer Nonlinear Programming (MINLP) Optimization for Design of Liquid-Liquid Extraction (LLE) Cascades in Continuous Pharmaceutical Manufacturing of Atropine. 20.
- (237) Ammonium Based Ionic Liquids | Sigma-Aldrich | Sigma-Aldrich <https://www.sigmaaldrich.com/chemistry/chemistry-products.html?TablePage=16255867> (accessed Nov 10, 2020).
- (238) Pyridinium - Ionic Liquids <https://www.sigmaaldrich.com/chemistry/chemistry-products.html?TablePage=16256019> (accessed Nov 10, 2020).
- (239) ReagentPlus® Solvent Grade Products - ACS and Reagent Grade Solvents <https://www.sigmaaldrich.com/chemistry/solvents/products.html?TablePage=14577692> (accessed Nov 10, 2020).
- (240) Iolitec - Ionic Liquids Technologies <https://iolitec.de/en> (accessed Nov 10, 2020).
- (241) DLD Scientific <https://www.dldscientific.co.za/> (accessed Nov 28, 2020).

## Appendix A

This appendix presents the comparison of the experimentally obtained values of the activity coefficients at infinite dilution with the literature data [<sup>221</sup>] for the system of hexadecane and five solutes. The maximum % error between the literature and experimental data is  $\pm 2.5\%$ .

**Table A-1** The literature and the experimental activity coefficients at infinite dilution  $\gamma_{13}^{\infty}$  for the solutes in hexadecane at different temperatures - test system.

Solute	T/K					
	323.15		333.15		343.15	
	lit.	this work	lit.	this work	lit.	this work
hexane	0.860	0.875	0.867	0.888	0.824	0.835
1-hexene	0.855	0.847	0.878	0.870	0.816	0.811
cyclohexane	0.739	0.750	0.757	0.769	0.704	0.699
benzene	0.932	0.916	0.933	0.918	0.876	0.854
toluene	0.941	0.922	0.948	0.930	0.870	0.884

## Appendix B

Appendix B shows the results of the temperature calibration of thermocouples used to determine the temperature of the systems during the LLE study.

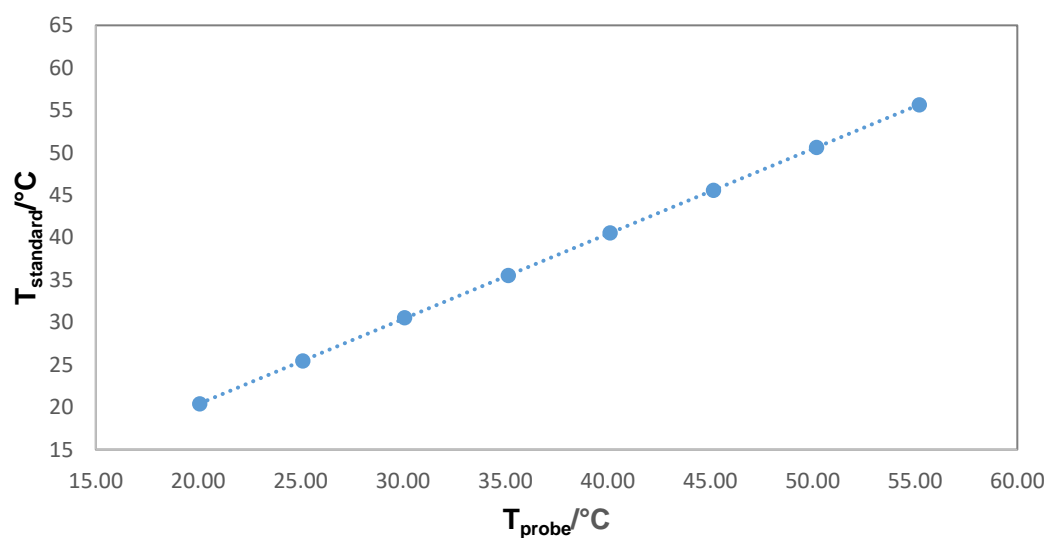


**Fig. B-1** Calibration curve for the temperature probe 1 used during the LLE measurements. The calibration curve linear equation is  $y = 1.0021x + 0.3223$  with coefficient of determination  $R^2 = 1$ .

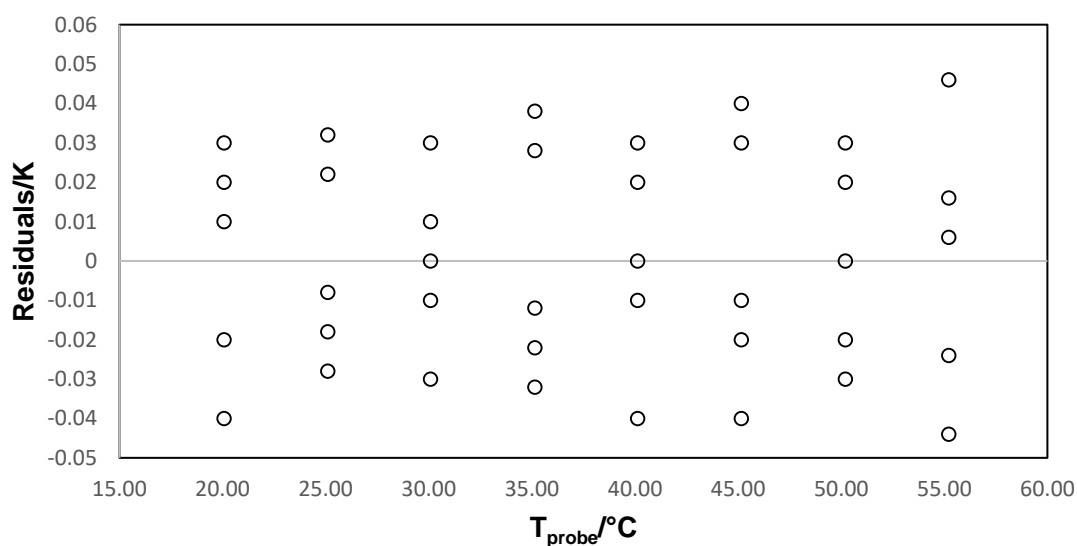


**Fig. B-2** Residuals for the calibration of the temperature probe calibration. The standard error for the calibration was 0.005.

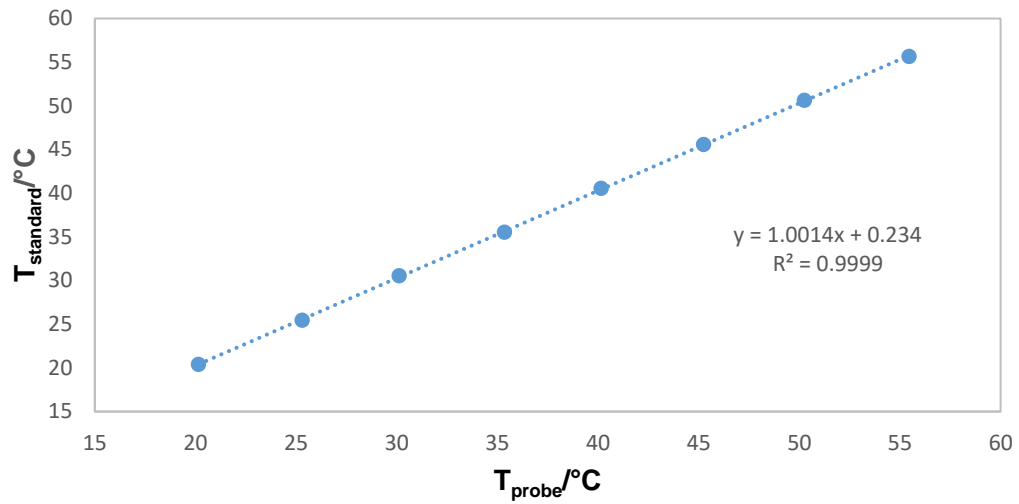


**Fig. B-3** Calibration curve for the temperature probe 2 used during the LLE measurements. The calibration curve linear equation is  $y = 1.0014x + 0.234$  with coefficient of determination  $R^2 = 0.9999$ .

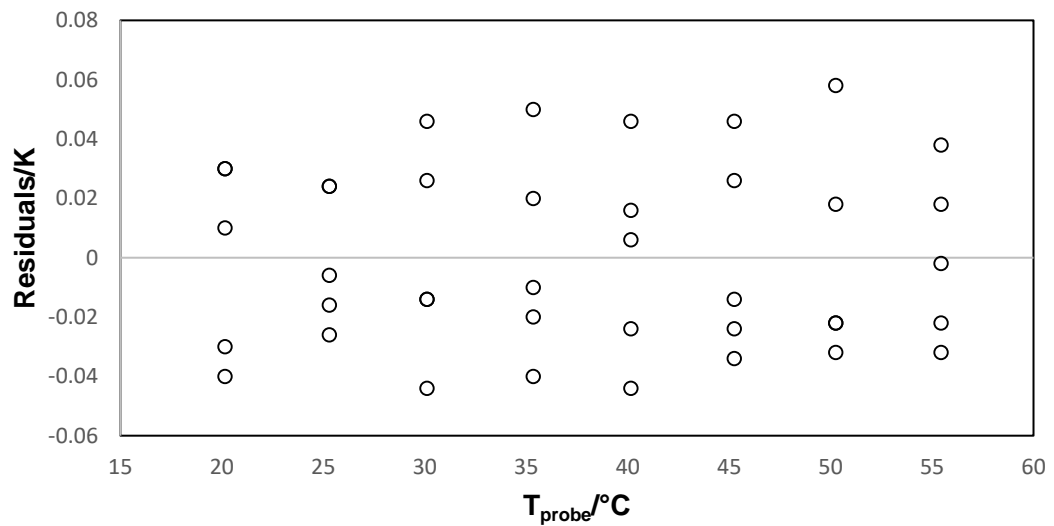


**Fig. B-4** Residuals for the calibration of the temperature probe calibration. The standard error for the calibration was 0.005.

## Appendix C

Appendix C presents the LLE measurements of the test system of heptane and methanol, which were performed in the  $T = 298.15$  K to  $T = 323.15$  K temperature range. The experimental results were compared with literature data [224,225,227]. Fig. C-1 shows data for the methanol rich phase, while fig. C-2 shows data for the heptane rich phase. The maximum % error between the literature and experimental data is  $\pm 10\%$ .

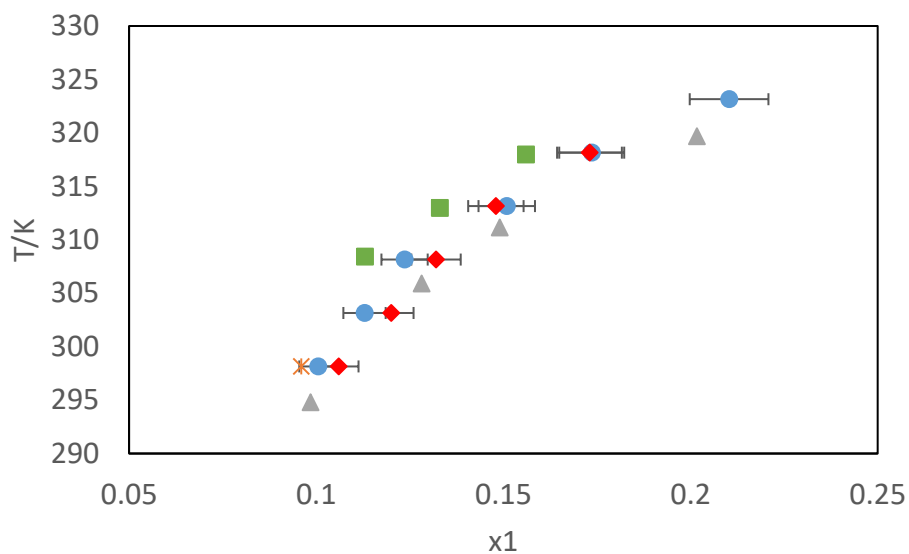


**Fig. C-1** Plot of the molar fraction of heptane ( $x_1$ ) versus  $T/K$  for {heptane (1) + methanol (2)} binary system – methanol rich phase. ● Experiment 1; ♦ Experiment 2; ▲ Matsuda [227], ■ Narasigadu [224], × Casas [225].

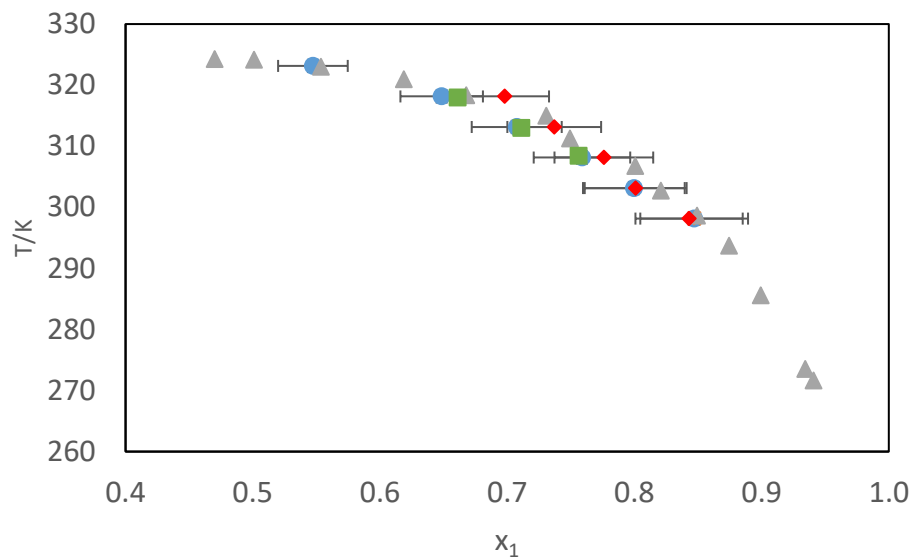


**Fig. C-2** Plot of the molar fraction of heptane ( $x_1$ ) versus T/K for {heptane (1) + methanol (2)} binary system – heptane rich phase. ● Experiment 1; ♦ Experiment 2; ▲ Matsuda [227], ■ Narasigadu [224], × Casas [225].

## Appendix D

Appendix D presents table which summarizes all of the uncertainties included in this work.

**Table D-1** Standard uncertainties estimations.

Source of uncertainty	Deviation estimated
GLC	
Activity coefficient at infinite dilution uncertainty ( $\gamma_{13}^{\infty}$ )	5%
(Gas + liquid) partition coefficient uncertainty ( $K_L$ )	5%
Temperature uncertainty ( $T$ )	0.01 K
Pressure uncertainty ( $P$ )	1 kPa
LLE	
Mass balance and impurity uncertainty ( $x_i$ )	0.005
Correlation of $x_i$ calibration ( $x_i$ )	0.005
Selectivity uncertainty ( $S$ )	0.005
Partition coefficient uncertainty ( $\beta$ )	0.005
Temperature uncertainty for LLE cells ( $T$ )	0.1 K
Temperature uncertainty for GC method ( $T$ )	0.01 K
Pressure uncertainty ( $P$ )	1 kPa